SYNTHESIS AND BIOLOGICAL EVALUATION OF SMALL MOLECULES AS INHIBITORS OF WEST NILE VIRUS NS2B-NS3 PROTEASE

SANJAY SAMANTA

(B.Sc, Calcutta University and M.Sc, IIT-Guwahati)

A THESIS SUBMITTED

FOR THE DEGREE OF DOCTOR OF PHILOSOPHY

DEPARTMENT OF CHEMISTRY

NATIONAL UNIVERSITY OF SINGAPORE

2012

Acknowledgements

Completing a Ph.D. is one of my life's greatest experiences. I have been honored over these last four years to have had the opportunity to meet some truly inspiring people. Coming in touch with them during my time at NUS has given me a new perspective about the complexities of both life and science. First and foremost I want to express my sincere gratitude to my supervisor, Associate Professor Lam Yulin, for welcoming me into her laboratory and for providing me constant help, guidance, inspiration, constructive criticism and encouragement to complete my thesis successfully. Also, I would like to thank Dr. Taian Cui for giving me a chance of a collaborative work in his laboratory.

I would like to thank laboratory officers in CMMAC, Department of Chemistry, Mdm Han Yanhui, Ms. Tan Geok Kheng, Ms. Hong Yimian, Mdm Wong Lai Kwai, Mdm Lai Hui Ngee, Dr. Liu Qiping and Dr. Wu Ji'En for their assistance and technical support. I really appreciate all of their support throughout the course of my Ph.D studies.

I extend my appreciation to all of my past and present colleagues in the laboratory, Dr. Gao Yaojun, Dr. Kong Kah Hoe, Dr. Che Jun, Dr. Fang Zhanxiong, Dr. Wong Ling Kai, William Lin Xijie, Woen Susanto, Hadhi Wijaya, Ang Wei Jie, Poh Zhong Wei, Ng Cheng Yang, Ran Jiangkun, for their help and encouragement during my research. In addition, I would like to thank Ms. Ang Cuixia of Singapore Polytechnic for her support and technical help.

No word would be sufficient to express my deep gratitude to my parents and other members of my family for their moral support. I would also like thank my friends, Amarenduda, Ananya, Aniruddha, Animesh, Goutam, Nirmalya, Rajkumar, Sandipda, Tanay, Tapan, Vamsikrishna and many others, in Singapore and overseas, who have given me the real flavor of life are gratefully acknowledged.

Finally, I thank National University of Singapore for awarding me a research scholarship to pursue my doctorate degree.

Thesis Declaration

The work described in this thesis is the original work, performed independently under the supervision of Prof. Lam Yulin, (in the laboratory S5-03-19), Chemistry Department, National University of Singapore, between 05 May 2009 and 03 August 2012. The content of this thesis has not been submitted for a degree at this or any other university before.

Sanjay Samanta 21 August, 2012

Name	Signature	Date

TABLE OF CONTENTS

SUMMARY

The West Nile Virus (WNV), a member of the Flaviviridae family, is a reemerging pathogen causing outbreaks in multiple continents. In recent years, clinical symptoms resulting from WNV have worsened in severity, with an increased frequency in neuroinvasive diseases among the elderly. Since, there are presently no successful antiviral therapies and vaccines for human use against WNV, continual efforts to develop new chemotherapeutics against this virus are highly desired. The viral NS2B-NS3 protease is a promising target for viral inhibition due to its importance in viral replication and its unique substrate preference. The overall goal of this thesis was to identify potent small molecule inhibitors against full-length NS2B-NS3 protease. For the design of WNV NS2B-NS3 protease inhibitors, initially, a library of 110 compounds was screened against viral protease assay by high throughput screening (HTS). The ‘‘hit’’ compounds were further sorted out by cytotoxicity test and the non-toxic compounds were chosen for library synthesis and biological evaluation based on structural activity relationship (SAR) study.

In chapter 2, a WNV NS2B-NS3 protease inhibitor with a 9,10-dihydro-3H,4aH-1,3,9,10a-tetraaza-phenanthren-4-one scaffold was selected as a non-peptidic “hit” compound. Optimization of this initial “hit” by solution-phase synthesis of a focussed library of compounds with this scaffold for screening led to the identification of a novel, uncompetitive inhibitor (**2-1a40**, IC_{50} = 5.41±0.45 μM) of the WNV NS2B-NS3 protease. Molecular docking of this chiral compound onto the WNV protease indicates that the S-enantiomer of **2-1a40** appears to interfere with the productive interactions of the NS2B cofactor with the NS3 protease domain and is a preferred isomer for the inhibition of the WNV NS3 protease.

In chapter 3, we have optimized another “hit” through a facile synthesis of a focused library of compounds with a 2-{6-[2-(5-phenyl-4H-[1,2,4]triazol-3-ylsulfanyl)acetylamino]benzothiazol-2-ylsulfanyl}acetamide scaffold. Screening of these compounds led to the identification of a novel, uncompetitive inhibitor (**3-1a24**, IC_{50} = 3.35±0.15 μM) of the WNV NS2B-NS3 protease. Molecular docking of **3-1a24** onto the WNV protease indicated that the compound interferes with the productive interactions of the NS2B cofactor with the NS3 protease domain and is an allosteric inhibitor of the WNV NS2B-NS3 protease.

Finally, in chapter 4 we have synthesized a focused library of compounds based on the 4-benzoyl-3-hydroxy-1-(5-mercapto-1,3,4-thiadiazol-2-yl)-5-phenyl-1H-pyrrol-2(5H)-one scaffold and their SAR study resulted in the identification of a novel racemate inhibitor (**4-1a16**, IC_{50} = 6.1±1.9 μM) of the WNV NS2B-NS3 protease. In addition, chiral separation led to a highly potent uncompetitive inhibitor **(-)-4-1a16** of WNV protease (IC_{50} = 2.2±0.7 μM) and *in silico* docking study suggested that the inhibitor **(R)-4-1a16** interferes with the productive interactions of NS2B cofactor with the NS3 protease as an allosteric inhibitor. In addition, docking studies indicated that the R-enantiomer is the preferred isomer for the inhibition of the WNV NS2B-NS3 protease which is in agreement with our experimental inhibition result obtained for **(-)-4-1a16**.

LIST OF TABLES

LIST OF FIGURES

LIST OF SCHEMES

LIST OF ABBREVIATIONS

AMC	7-amino-4-methylcoumarin
AcOH	acetic acid
AFP	acute flacid paralysis
aq.	aqueous
Arg	arginine
Ar	aromatic
Asp	aspartic acid
BHK21	baby hamster kidney cells
Bz	benzyl
calcd	calculated
C	capside
CDC	Center for Disease Control
CNS	central nervous system
δ	chemical shift in ppm
m-CPBA	3-chloroperoxybenzoic acid
cpd	compound
conc.	concentrated
J	coupling constant
cryoEM	cryo-electron microscopy
^{o}C	degree Celsius
DENV	dengue virus
DBU	1,8-diazabicycloundec-7-ene
DDQ	2,3-dichloro-5,6-dicyano-1,4-benzoquinone
DCM	dichloromethane
Et_2O	diethylether
DIAD	Diisopropyl azodicarboxylate
DMA	dimethyl acetamide
DMSO	dimethylsulfoxide
d	doublet
dd	doublet of doublets

dt	doublet of triplets
EI	electron ionization
ESI	electrospray ionization
equiv.	equivalent
EtOH	Ethanol
Et	ethyl
EtOAc	ethyl acetate
Glu	glutamic acid
Gly	glycine
g	gram
HCV	hepatitis C virus
HRMS	high resolution mass spectroscopy
HPLC	high-performance liquid chromatography
h	hour
HCl	hydrochloric acid
K_i	inhibition constant
IC_{50}	inhibitory concentration
Ile	isoleucine
kcal	kilocalories
kJ	kilojoules
Leu	leucine
LC	liquid chromatography
Lys	lysine
MS	mass spectroscopy
max	maximum
Me	methyl
K_m	Michaelis constant
µM	micromolar
MW	microwave
mg	miligram
mL	millilitre
MOE	Molecular Operating Environment
DMF	N,N-dimethylformamide

nm	nanometre
NS	non-structural
nPr	n-propyl
n	number
%	percentage
Ph	phenyl
Phe	phenylalanine
KOH	potassium hydroxide
prM	precursor membrane
Pro	proline
PDB	protein data bank
q	quartet
RFU	relative fluorescence units
RSD	relative standard deviation
rt	room temperature
RPMI	Roswell Park Memorial Institute
s	singlet
NaOEt	sodium ethoxide
Na_2SO_4	sodium sulphate
SAR	structure-activity relationship
H_2SO_4	sulfuric acid
THF	tetrahydrofuran
TLC	thin layer chromatography
Thr	threonine
TBEV	tick-borne encephalitis viruses
TEA	triethylamine
TFA	trifluoroacetic acid
TMSCl	trimethylsilylchloride
t	triplet
Trp	tryptophan
UV	ultraviolet
Val	valine
v	velocity

H_2O	water
W	watt
WNV	West Nile Virus
YFV	yellow fever virus

LIST OF PUBLICATIONS

1) Yaojun Gao**, Sanjay Samanta**, Yulin Lam; Synthesis, *In Vitro* Evaluation and Docking Studies of (-)-4-Benzoyl-3-hydroxy-1-(5-mercapto-1,3,4-thiadiazol-2-yl)-5-phenyl-1H-pyrrol-2(5H)-ones as Potent Inhibitor of WNV NS2B-NS3 Protease (**In preparation**).

2) Sanjay Samanta, Ting Liang Lim, Yulin Lam; Synthesis and the biological evaluation of 2-{6-[2-(5-phenyl-4H-[1,2,4]triazol-3-ylsulfanyl)acetylamino] benzothiazol-2-ylsulfanyl}acetamides as potential anti-West Nile Virus agents, **2012 (Submitted).**

3) Sanjay Samanta, Taian Cui, Yulin Lam; Discovery, Synthesis and *In Vitro* Evaluation of West Nile Virus Protease Inhibitor Based on the 9,10-Dihydro-3H,4aH-1,3,9,10a-tetraaza-phenanthren-4-one Scaffold; *ChemMedChem*, **2012**, *7*, 1210-1216.

4) Benedict Yan, Ee Xuan Yau, **Sanjay Samanta**, Chee Wee Ong and Kol Jia Yong, *et al.* Clinical and therapeutic relevance of PIM1 kinase in gastric cancer; *Gastric Cancer* **2012**, *15*, 188-197.

LIST OF CONFERENCES ATTENDED

1) **Sanjay Samanta**, Taian Cui, Yulin Lam; Synthesis And Biological Evaluation of Small Molecules as Inhibitors of West Nile Virus NS2B-NS3 Protease, **Twelfth Tetrahedron Symposium, 21-24th June 2011, Spain.**
2) **Sanjay Samanta**, Lim Ting Liang, Yulin Lam; Synthesis and Biological Evaluation of West Nile Virus inhibitors; **243rd ACS National Meeting, 25-29th March 1012, San Diego, CA**. (Document ID: 10226, post ID: 172).

Chapter 1: Introduction

1.1 Introduction

The reemergence of the West Nile Virus (WNV), a neurotropic Flavivirus, is a mosquito-borne pathogen that is causing outbreaks in multiple continents[1]. The more commonly known species of WNV are such as dengue virus (DENV), yellow fever virus (YFV), hepatitis C virus (HCV) and tick-borne encephalitis viruses (TBEV), etc. This virus is a major cause of infectious disease in human and other animals. Till date, vaccines are available for YFV, JEV, and TBEV; however there have been no successful antiviral therapies and vaccines for human use against WNV.[2,3] The WNV was first isolated and identified as a distinct pathogen from a feverish woman in Uganda's West Nile district and subsequently was associated with sporadic cases of disease as well as major outbreaks in Africa, Europe, the Middle East, west and central Asia.[4,5] Since 1999, when the first WNV outbreak occurred in the city of New York , the Center for Disease Control (CDC) has reported that more than thirty thousand people were infected, resulting in 1263 fatalities cases in the United State of America alone.[6] The clinical manifestation of WNV in human was found to vary significantly from being asymptomatic to developing a mild febrile syndrome termed "West Nile fever" or a neuroinvasive disease termed "West Nile meningitis or encephalitis". Approximately 80% of WNV infected patients are asymptomatic, 20% develop West Nile fever and less than 1% develop severe neurological manifestations.[7] The symptoms of West Nile fever in human include an abrupt onset of fever, headache, fatigue, variable malaise, anorexia, nausea, myalgia, lymphadenopathy and a non-pruritic generalized maculapapular rash. Additional non-neurological manifestations that may develop in West Nile fever patients include

hepatitis, pancreatitis, myocarditis, rhabdomyolysis, orchitis and ocular manifestations. Neurological manifestations of WNV infection include meningitis, encephalitis, acute flacid paralysis (AFP)/poliomyelitis, Parkinsonism, pharyngitis, conjunctivitis, coma, and seizure/status epilepticus.[8] Despite the growing public health concern associated with WNV infection, thus current treatment is supportive care only. *In vitro* and animal model studies have provided important clues to the possible novel therapies against WNV. However, the development of effective therapeutics that diminishes disease may be difficult, as patients with the most severe disease often have underlying immune deficits and present to clinical attention relatively late in the course of the disease. Among the challenges will be the development of therapeutics that efficiently cross into the central nervous system (CNS), clear virus from infected neurons, and have a beneficial effect on patient outcome.[9] In this chapter, we provide a comprehensive review of WNV, describe its transmission, life cycle, molecular virology, viral proteins, drug target, existing inhibitors and identification of "hit" compound by HTS. The focus, however, will be on the WNV non-structural (NS) NS2B-NS3 protease and its inhibitors, which represents the basis of this thesis.

1.2 Viral transmission

Infection is transmitted primarily by mosquitoes, although the role of tick and other hematophagous insects as vectors cannot be excluded. The majority of the clinical cases are found in human or horse to maintain with an infection cycle (Figure 1.1) involving birds and mosquito.[10] However, the ecology of transmission between primary vectors and vertebrate hosts is complicated. The mosquito must feed on an

infected amplifying host bird, to serve as an effective vector. Birds with high viremia, i.e. containing WNV concentrations of sufficiently high levels in their blood are effective hosts for WNV amplification and transmission.[11a] In addition, bird migration provides a potential basis for viral transport over large distances and has been

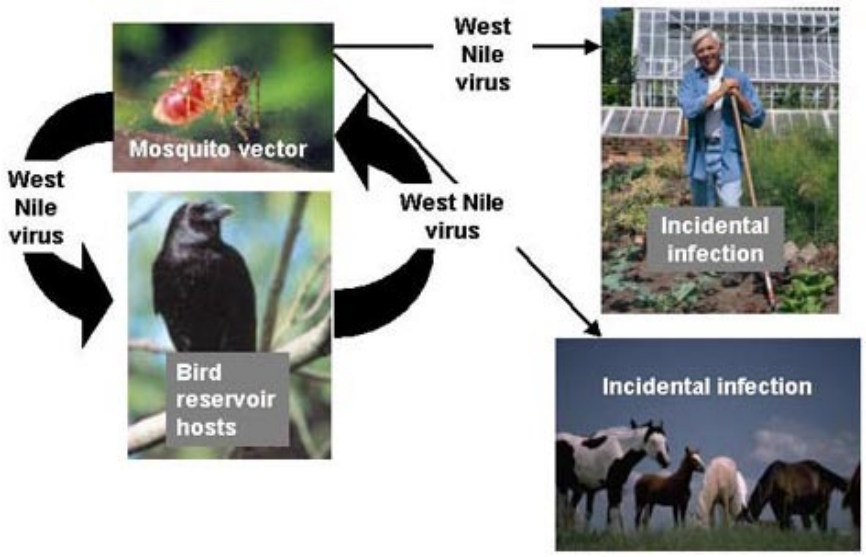

Figure 1.1 WNV transmission cycle[11b]

proposed as an explanation for the seasonal recurrence of WNV infections in temperate zones where winter precludes mosquito activity. The *Culex* mosquito is caught up most commonly worldwide and postulated to have major contribution to spread out in the New York City outbreak.[6] However, *Aedes*, *Anopheles*, *Minomyia*, and *Mansonia* mosquitoes may also serve as transmission vector.

1.3 Molecular virology of WNV

1.3.1 West Nile virion morphology and composition

West Nile virion is a small virus particle of approximately 500 Å in diameters and is composed of an icosahedral nucleocapsid (NC) that is ~25 nm in diameter. The

consists a single-strand positive-sense RNA genome of 11000-12000 nucleotides long and is capped by virus capside (C) protein which is also surrounded by lipid bilayer and 180 copies of two glycoproteins.[12] The envelop (E) protein and membrane (M) or its precursor (prM) protein are embedded on the NC.[13] In addition, advance cryo-electron microscopy (cryoEM) data suggested many important structural feature of West Nile virion at the level of atomic resolution (Figure 1.2).[14] The E protein is the major viral surface protein and the major antigenic determinant. It mediates binding and fusion during virus entry into host cells. The E protein is arranged in a head-to-

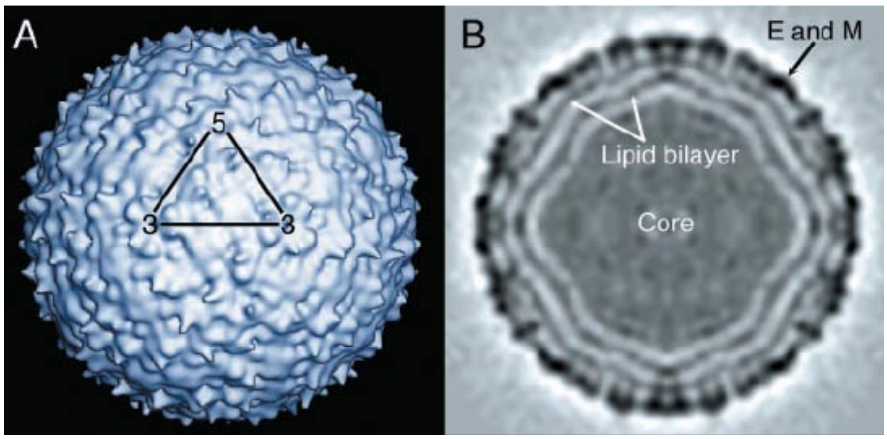

Figure 1.2 A 17 Å structure of West Nile Virus determined by cryo-EM. (**A**) A surface shaded view of the virus with one asymmetric unit of the icosahedron shown by the triangle. The 5-fold and 3-fold icosahedral symmetry axes are labeled. (**B**) A central cross section showing the concentric layers of density.[14]

tail homo dimer conformation that lies parallel to the lipid bilayer on the virus surface. It also known from cryo-EM that flavivirus employs a fusion mechanism in which the distal β barrels domain II of the glycoprotein E are inserted into the cellular membrane.[15] On the other hand, the M protein is produced from the proteolytic processing of a prM precursor protein. The prM precursor protects the E protein from fusing with intracellular membranes as the virion transits through the secretory

pathway. The immature prM-E virus particles are larger in size (~60 nm) compared to the mature M-E virions (~50 nm). The larger particle size is due to the prM-E heterodimer protruding from the virus surface resulting in a spiky appearance compared to the smooth outer surface observed in the M-E mature virion.[16]

1.3.2 The WNV life cycle

Cellular and molecular biology studies have elucidated the basic mechanism of action of WNV in host cells. This virus can replicate in various types of cell cultures from a wide variety of avian, mammalian, amphibian, and insect species.[17] In the life cycle of WNV, the E protein first attaches to the surface of a host cell (Figure 1.3) at an unknown host receptor and subsequently enters the cell by receptor-mediated endocytosis. At lower pH region of endosome triggers an irreversible trimerisation of the E protein results in fusion of the viral and cell membrane.[18] The fusion covered by the pr portion of prM protein and protected from premature fusion with cell membranes.[19,20] The lysosome enters after fusion of E protein and the virus has a self signal that it is inside a cell. The NC is released into the cytoplasm and single strand positive sense RNA dissociates from its C protein, once the genome is released into the cytoplasm, the RNA is translated into a single polyprotein.[21,22] The amino terminal end of the polyprotein includes the three structural components of the virus, while the rest forms the seven different NS proteins are processed co- and post-translationally by viral and host proteases. The genome replication occurs on intracellular membranes and initially immature particles are formed in the lumen of the endoplasmic reticulum (ER). The particle contains prM-E proteins, lipid membrane and NC cannot induce host-cell fusion to make them non-infectious. Subsequent, cleavage of the prM-E heterodimer occurs in the trans-Golgi network (TGN) by furin, the E protein changes conformation lying parallel on the virus surface.[23a] However,

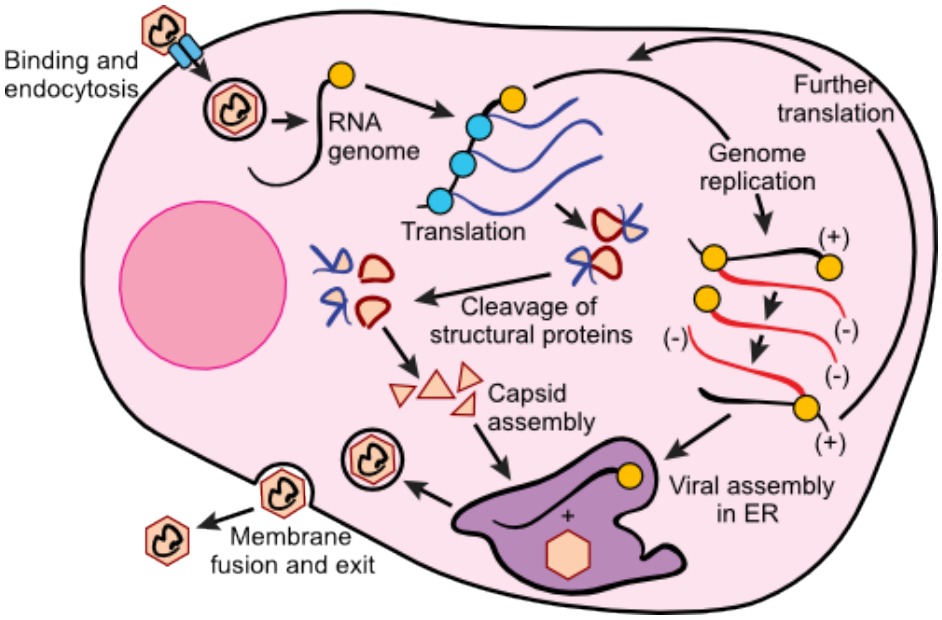

Figure 1.3 The life cycle of West Nile Virus (Diagram from the microbial world).[23b] Replication of WNV occurs in the cytoplasm. The interesting feature of its replication is the synthesis of a single polyprotein and its subsequent digestion.

the remains associated to the E protein, preventing membrane fusion during virion release at the host cell surface.[24] When the virion enters the extracellular milieu, the pr protein dissociates from the E protein and allowing for membrane fusion to occur in the next replication cycle .[24] The particle only contains the glycoproteins and membrane in ER is known as subviral particle also cleaved by furin. However, the lack of C protein and genomic RNA make them non-infectious.[25] Mature virus and sub-viral particles are subsequently released from the host cell by exocytosis.

1.3.3 WNV poly protein processing

The WNV contain a ~10.8-kb single-stranded positive-sense RNA genome which has 3' and 5' untranslated region (UTR) and an open reading frame (ORF) translates into a large polyprotein of about 350 kD that is processed to individual flavivirus proteins which are arranged in the genome with the order of UTR-5'-C-prM-E-NS1-NS2A-

NS2B-NS3-NS4A-NS4B-NS5-3'-UTR (Figure 1.4).[26] The 5' UTR is about 120 nucleotides in length and 3' UTR comprises about 500 nucleotides. As can be seen, the ORF encodes a total of 10 viral proteins: three structural proteins (C, M and E) are forming the new virion and seven NS proteins are expressed in the infected cells which are requires for viral replication. All of the flavivirus NS proteins emerge to be directly or indirectly involved in viral RNA synthesis. Still, the functions of the WNV NS proteins have not been completely characterized. However, little is known about the interactions between the various viral NS proteins and the host cell proteins that may also be required for the formation of active viral RNA replication complexes.[21,27] Processing of the polyprotein is believed to occur in the viral induced membranous structures which are continuous with the rough ER known as convoluted membranes/paracrystalline (CM/PC) arrays.[28] A host signal peptidase located within the lumen of the ER cleaves the junctions C-prM, prM-E, E-NS1, and NS4A-NS4B[29,30] while cleavage at the NS1-NS2A junction takes place in the lumen of the ER by an unknown protease.[31] The cleavage of prM to generate mature M is carried out by the host proteases furin, in the Golgi during export of virions through the secretory pathway.[32] The virus encoded NS2B-NS3 protease cleaves the remaining junctions of NS2A-NS2B, NS2B-NS3, NS3-NS4A and NS4B-NS5 and also cleaves sites at the C-terminus of the C protein and the C-terminus of NS4A.[26,33,34] Cleavage at all of these sites has been shown to be essential for replication of Flaviviruses, highlighting the vital role of NS2B-NS3protease.[33,35,36] Many of the NS proteins are believed to associate with the viral RNA to form a complex which carries out replication of the genomic RNA within membranous structures referred to as vesicle packets (VPs). The replication complex is composed of NS5 function as RNA dependent RNA polymerase (RdRp) and methyltransferase, NS3 function as RNA

Figure 1.4 Schematic representations of flavivirus genome organization and polyprotein processing. Top, the flaviviral genome with the structural and NS proteins coding region, the 5' UTR with 5' cap structure and the 3' UTR with the potential 3' secondary structure are shown. Below, the mature flavivaral proteins generated after processing of polyprotein are demonstrated. The dotted line boxes are represent the structural proteins C, prM and E, with solid line boxes represents the NS proteins and corresponding cleavage site with various protease are indicated.[37a]

helicase, RNA triphosphatase and nucleotide triphosphatase, function of NS1 protein as unknown yet, suspected to play a structural role in helping to anchor the replication complex to membrane of the VPs and NS2A, NS4A and NS4B proteins putatively involved in protein-protein interactions and membrane association.[28,37b,38] In addition, the 5'm7GpppAmp cap structure is synthesized by the RNA triphosphatase activity of NS3[39] and methylated by the methyltransferase activity of NS5.[40]

The capsid protein

The WNV capsid protein is encoded at the 5' end of the genome which is about 11 kD, highly rich in basic amino acid residues and a large number of positively charged residues, which are distributed throughout the protein.[41,42] The hydrophobic carboxylic terminal of the protein serves as a signal sequence for the translocation of prM across the membrane of the endoplasmic reticulum (ER). Cleavage of the carboxylic terminus of the capsid protein is catalyzed by the viral NS2B-NS3 protease complex on the cytoplasmic side of the ER membrane, while the C-prM junction on the lumenal side is cleaved by host signal peptidase.[43] Analysis of the purified capsid protein from *E.coli* revealed its largely α-helical structure in the dimmeric form.[44] However, its dimmer formation mechanism is not elucidated yet, but interaction with RNA can induced isolated ca proteipsidn to assemble into NC like particle.[45]

The prM/M protein

The mature membrane protein is about 26 kD and while it was about 34 kD before cleaved from its precursor prM. The N-terminal region of prM has 1-3 N-linked glycosylation sites, as well as six conserved, disulfide-linked cysteine residues. The C-terminal region of prM contains two transmembrane domains which help to secure prM and M in the ER membranes, and may assist in the heterodimerization of prM and E. Besides providing structural support for E in the immature virion, prM also protects E from undergoing conformational changes during the transit of immature virions through acidic compartments of the trans-Golgi network.[20] Furin-mediated cleavage of virion-associated prM to release the pr fragment occurs in the Golgi and leads to the rearrangement of E trimers into the homodimers seen in mature virion structures.[46]

The envelop (E) protein

The E protein is about 53 kD and the major portion on the surface of flavivirus virions. This protein is primarily responsible for facilitating entry into the cell during infection, by binding to an unknown receptor protein and mediating the fusion of viral and host membranes.[18] The native form of E is composed of three domains. Domain I is located at the N-terminus and contains the most conserved sequence, which has been hypothesized to be part of the flavivirus receptor-binding site.[47] Domain II contains a putative fusion peptide, which mediates insertion into the host membrane during virus entry, and domain III, which is located at the carboxylic terminus of the E protein contains a hydrophobic domain which serves as a signal sequence for the translocation of NS1 into the lumen of the ER during polyprotein translation.[46,48,49]

The NS1 protein

Nonstructural glycoprotein protein 1 (NS1) is about 46 kD and has been shown to exist as a dimmer.[50] This is the only flaviviral NS protein known to be glycosylated which contains two or three N-linked glycosylation sites and 12 conserved cysteines that form disulfide bonds.[46,51,52] The pattern of disulfide pairing has been recently solved. The N-terminal end of NS1 is cleaved from the E protein by host signal peptidase, while the NS1/NS2a junction is cleaved by an unknown host protease.[49,53] Although the majority of NS1 is retained in infected cells, it is also detected at the cell surface where it is slowly secreted.[22] NS1 has an important nuclear role in RNA replication, with a large deletion in the NS1 gene was shown to be deficient in RNA replication. Even, mutation of the N-linked glycosylation sites in NS1 can lead to dramatic defects in RNA replication and virus production. However, its exact function in viral RNA replication is not known yet.[54,55]

The NS2A protein

NS2A is a small hydrophobic protein of about 24kD and contains a serine protease-dependent cleavage site, which results in the release of a C-terminal truncated NS2A product of about 22 kD (NS2Aα).[36] Previously, many research group have been shown that a mutation in the carboxylic terminal cleavage site of NS2A resulted in a failure to yield infectious virus in spite of normal viral RNA replication presenting the importance of this protein and suggesting that this protein may be involved in virus assembly.[56] The NS2A/NS2B junction is cleaved by the viral serine protease.[31]

The NS2B protein

The NS2B is membrane associated another small hydrophobic protein of about 14kD and encodes three membrane domains, two of them located at the N-terminal and third one located at the carboxylic terminal. This protein has been shown to exist in complex with and functions as the cofactor for the viral serine protease NS3.[57,58] The conserved hydrophilic domain of NS2B is essential for its cofactor activity, whereas the hydrophobic regions of NS2B are required for co-translational insertion of the NS2B-NS3 precursor into ER membranes and for the interaction between NS3 and NS2B.[59,60] The NS2B/NS3 junction is cleaved by viral serine protease. Mutation of conserved residues in NS2B can have dramatic effects on auto proteolytic cleavage and trans cleavage activities.

The NS3 protein

NS3 is a (~70 kD) multifunctional protein with both protease and helicase functions. However, NS3 is not an active protease until its N-terminal region comprises the protease domain to forms a stable complex with NS2B. The N-terminal third of NS3 encodes a serine protease that is a member of the trypsin super-family which forms

the catalytic domain of the NS2B-NS3 protease complex.[35,61] This protease auto catalytically cleaves itself from the polyprotein and also cleaves at multiple other sites in the polyprotein like NS2A/NS2B, NS2B/NS3, NS3/NS4A and NS4B/NS5; carboxylic termini of mature capsid protein and NS4A.[62] The C-terminal region of NS3 protease encodes domains with homology to the super family II of RNA helicases and NTPases.[39,63] Additionally, the NS3 protein has been shown to act as an RNA 5' triphosphatase, dephosphorylating the 5' end of the genome prior to cap addition.[64] Collectively, these functions establish NS3 as a protein that is essential to the replication cycle of flaviviruses.

The NS4A and NS4B proteins

NS4A and NS4B are small hydrophobic proteins with a size of 16 and 27 kD, respectively. The C-terminus of NS4A is generated by a combination of host signal peptidase and viral serine protease cleavage[33]. Genetic studies indicated that NS4A interacts with NS1 and that interaction is important for RNA replication[65]. Furthermore, NS4A has been shown to colocalize with double-stranded RNA and VPs within the replication complex, suggesting a role for NS4A in RNA replication[66]. On the other hand, the NS4B have been detected in reticular structures and its hydrophobic characters help to associate with membrane. It has been reported that, NS4B initially appears as a 30 kD protein which post-translationally modified to 28 kD; however, its post-translational modification is not known. In addition, NS4B colocalization with the membrane-bound viral replication complexes, but the exact role of NS4B has yet to be determined.

The NS5 protein

The NS5 is largest and multifunctional proteins among the all other flavivirus proteins and very well conserved protein of about 103 kD that is cleaved from the polyprotein by viral serine protease.[67] It contains a Gly-Asp-Asp peptide (GDD) motif, which is present in all RdRp, which was demonstrated for recombinant dengue type 1 virus NS5 expressed in E. coli.[68] The N-terminal region of this protein shows homology to methyltransferase domains[40] and mutagenesis studies of the C-terminal region of GDD motif of Kunjin virus completely abolished viral replication.[69,70] Several groups have shown that NS5 is phosphorylated *in vivo*, and have detected the presence of some NS5 in the nucleus of infected cells.[38,71,72] However, the significance of this localization is not currently understood.

1.4 WNV drug target

In order for a biomolecule to be selected as a drug target, two essential pieces of information are required. The first, evidence is that modulation of the target will produce therapeutic value. This knowledge may come from disease linkage studies that show an association between mutations in the biological target and certain disease state. The second is that the target is "druggable", that means it is capable to bind a molecule and this fact could be modulated its activity.

As can be seen, the two components NS2B-NS3 viral serine protease activity plays an important role in flaviviral polyprotein processing and interference of its function has been shown to be stop in viral replication. In addition, site-directed mutagenesis studies also have shown that mutation of essential catalytic residues at NS3 protease

cleavage sites lead to a halt in viral infectivity, indicating its importance in the WNV life cycle.[73] This mode of substrate recognition is conserved among other flaviviral proteases but not in the host cellular enzymes,[62] indicating the possibility of designing inhibitors selective for flaviviral proteases without adversely affecting normal cellular functions. Thus, the biological importance of the NS2B-NS3 complex (NS2B-NS3pro) in the activation of viral proteins coupled with unique substrate preference make it an attractive target for selective viral inhibition. Two possible strategies for inhibiting the Flavivirus NS2B-NS3protease are either blocking interactions with its substrate or blocking the essential association between NS3protease and its cofactor NS2B. Based on sequence and structure pattern analysis, WNV NS3 protease is a tripsine-like serine protease which form a catalytic triade with His51, Asp75 and Ser135 amino acid residues (Figure 1.5a) and this triade is located at the active site of the two component protease. This viral serine protease recognizes and cleaves to the C-terminal side of two highly conserved consecutive amino acid residues (R and K) at the P1 and P2 positions. This unusual specificity does not share by other host protease suggesting that inhibitor designed to recognize this site may also be highly specific. However, the charged nature of the interactions of such basic residues makes the design of nonpeptidic inhibitors extremely challenging. Recently, the crystal structure coordinate (pdb id: 2fp7) of the WNV NS2B-NS3 protease have been published by Erbel *et al.*[74] and further inspection of the X-ray crystal structure revealed the important information about the nature of the binding pockets. Active site mainly consist of four binding pocket, these are S1, S2, S3, and S4 (Figure 1.5a). The S1 pocket is well defined hydrophobic due to the presence of two tyrosine side chains (NS3: Tyr150, Tyr161) forming the bottom and edge of the pocket, this pocket also

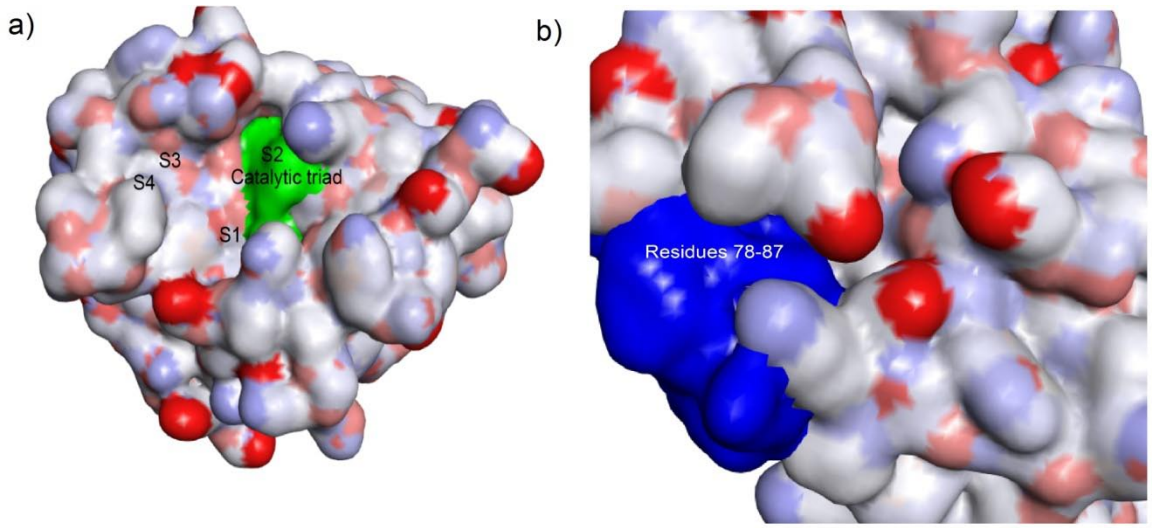

Figure 1.5 Crystal structure of WNV NS2B-NS3 protease (2fp7).[74] (a) represents the substrate binding site with binding pockets S1, S2, S3 and S4; catalytic triad in green color. (b) Potential target sites for blocking cofactor association residues 78-87 with NS3 protease (blue).

offer some opportunity to form hydrogen bond between substrate/inhibitor-protease via the protein back bone atom of NS3 (Tyr130, Pro131, Ser135 and Gly151). The S2 pocket also well define but it is much narrow compared to S1. This pocket contains lot of amino acid residues those can act as a hydrogen bond acceptor and donor, these are NS2B (Gly83, Asn84 and Phe85) and NS3 (His51, Glu74, Asp75 and Asn152). In contrast to pocket S1 and S2, the pocket S3 is relatively wide and shallow. One side of this pocket lined with hydrophobic side chains NS3 (Val154 and Ile155) and other side of the pocket include NS2B (Phe85, Gln86 and Leu87) and NS3 (Gly153). Lastly, binding region of S4 pocket entirely covered by the residue Ile155. The residue predicted to be in the pocket at the active site by Fairlie *et al.*[62] These informations help to design or modification of an inhibitor which will be interact with active site of two component viral protease by competing with substrate.

In alternative strategy, the blocking of association between NS2B and NS3 proteins which affects the productive interaction of NS2B-binding cavity with NS3 protease domain to increase NS3 protease catalytic activity[75,73] and remains to be rigorously tested. In addition, it may avoid the problems facing development of substrate based competitive inhibitors for the active site. Likewise other flaviviral serine protease, human serine protease has largely conserved active site which could be accessible to the specificity and potency of the inhibitors. Therefore, inhibitor interference with the productive conformation of the NS2B cofactor is also a superior drug discovery strategy compared with targeting of the active site of the NS2B-NS3 protease[27] Earlier studies have shown that the integration of residues 78-87 of NS2B (Figure 1.5b) into the protease-cofactor complex affected the formation of the catalytic active sites. Deletion or mutagenesis of these residues produced an inert enzyme. Therefore, the region on the NS3 protease, where key interactions with the NS2B cofactor (residue 78-87) occur, is important for the NS2B-NS3 protease activity and particularly attention is paying to this region for developing allosteric inhibitors. Alternatively, the residue Trp62 from NS2B also has been shown to be essential for protease activity along with the surrounding residues NS2B59-62. This region binds into a deep hydrophobic trench in NS3, which could be targeted by small aromatic, drug-like compounds. However, because this region of the NS2B cofactor remains tightly associated in substrate-bound and substrate-free crystal structures, it is unidentified if an allosteric inhibitor would be capable of binding with high enough affinity to interrupt strong hydrophobic interactions of NS2B and NS3 protein.

The WNV NS5 protein contains a MTase domain involved in RNA capping and an RdRp domain essential for virus replication. The essential role of NS5 in flavivirus replication makes it an attractive antiviral target.[76] Thus, the structure of the full-

length molecule is required to provide a more accurate model for functional analysis and drug design. While recent studies have elucidated separate crystal structures for the MTase and RdRp domains of WNV NS5[77,78] and apparent instability of the full-length recombinant protein during purification precluded crystallization of the entire molecule. A possible solution to this dilemma is co-purification and co-crystallization of NS5 in the presence of a monoclonal antibody (mAb) that binds to both MTase and RdRp domains and stabilizes the full-length protein.

1.5 Strategies for the identification of novel inhibitors of WNV NS2B-NS3 protease

Each step of the WNV life cycle present a potential target for antiviral intervention. Three approaches are commonly taken to identify WNV NS2B-NS3 protease inhibitors; 1) Structure-based rational design 2) Biochemical enzyme based screening and 3) Genetic system-based screening.

1.5.1 Structure-based rational design

The traditional methods of drug discovery is rely on trial and error testing of chemical substances on cultured cells or animals, and matching the apparent effects to treatments, rational drug design begins with a hypothesis that modulation of a specific biological target may have therapeutic value. The atomic structures of many flavivirus proteins and domains have been solved. This structural information makes the rational design of inhibitors possible.

From our above discussion, it is clear that WNV NS2B-NS3 protease and NS5 protein are the most promising targets in drug discovery and recently, their crystal structure has been published with or without ligand. The two X-ray structures of NS2B-NS3

protease with different inhibitors have similar conformations and are therefore appropriate for structure based drug design. The two component protease adopts a chymotrypsin-like fold with two six-stranded β-barrels and details of the nature and shape of the active side pockets are already described in the section of drug target. Among the reported peptides inhibitors of NS2B-NS3 protease, the preferred amino acids at the nonprime part of the protease active site are arginine at the P1 position and arginine or lysine at the P2 position[79] underlining the role of electrostatic interactions with the negatively charged S1 and S2 pockets. Most of the reported active compounds are with charged moieties or the guanidino group being the most frequently used. Even, five non-peptidic compounds reported by Ganesh *et al.*[80] have guanidine moieties. Ekonomiuk *et al.*[81] group introduced thiourea moiety instead of guannidin and they found to shown moderate activity against viral protease.

The N-terminal region of NS5 encodes an MTase, which is required to methylate the cap guanine N7 and the ribose 2'-OH of the first nucleotide during cap formation. A virtual screening, using NS5 MTase structure, revealed a compound that inhibited DENV 2'-O cap methylation with an IC_{50} value of 60 μM.[82] The study used *S*-adenosylmethionine (SAM), the methyl donor, as a starting molecule to search for analogs that could specifically dock into the SAM-binding pocket of the DENV-2 MTase. Since the SAM molecule bound in the same pocket donates methyl groups to both N7 and 2'-O positions during cap methylations[83], the identified compound is expected to inhibit N7 methylation of the viral RNA cap. A SAM analog in which the transferring methyl group is replaced by an amino group, inhibits both N7 and 2'-O methylations of the WNV RNA cap, with an IC_{50} value of approximately 14 μM.

1.5.2 Biochemical enzyme based screening

For enzyme-based assays, the advantage is that the identified compounds possess known targets and major disadvantage is that cellular uptake and non-specific binding of the compound, two potential problems for many inhibitors, are not evaluated within the assay. Previous discussion suggests that the two component NS2B-NS3 serine protease and NS5 are important enzymes of the viral replication are ideal target for antiviral screening. Therefore, NS2B-NS3 protease assay is a fluorogenic peptide substrate-based assay (Figure 1.6) has been widely used in high throughput screening (HTS) technique.[84,85] This method uses a small peptide substrate coupled to a highly fluorescent dye 7-amino-4-methylcoumarin (AMC), whose fluorescence is quenched while linked to

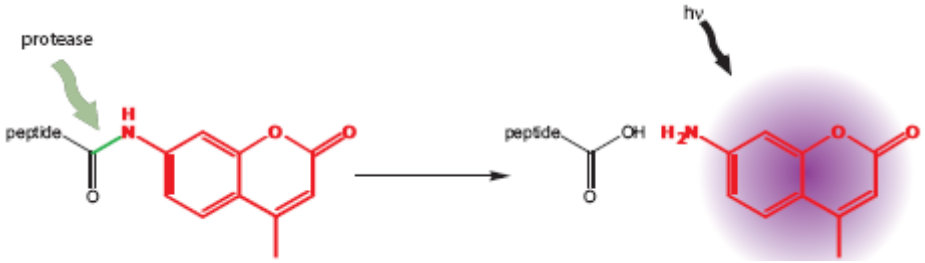

Figure 1.6 Schematic representation of fluorogenic substrate (Pyr-RTKR-AMC) cleavage by WNV NS2B-NS3 protease.

the un-cleaved peptide substrate. Upon protease-mediated cleavage, the fluorescent dye is released from the peptide, thus producing an increase in fluorescence intensity. The enzyme-based assays can potentially be developed for identify inhibitors of Flavivirus MTase. A scintillation proximity assay (SPA) could be developed for HTS, to search for MTase inhibitors. SPA is a radioactive homogeneous technology that relies upon the fact that the energy emitted from a radioisotope will only travel a

limited distance in an aqueous environment. When a radioisotope-labeled molecule binds to the microsphere beads, the radioisotope is brought into close proximity to the scintillant, and effective energy transfer from the particle occurs, resulting in light emission. When the radioisotope remains free in solution, it is too distant from the scintillant; the particle dissipates its energy into the aqueous medium and remains undetected. Because the flavivirus MTase specifically requires viral RNA for cap methylation, the RNA substrate should contain the 5 terminal stem-loop of genomic RNA. The 5 viral RNA should be biotin-labeled. Upon transfer of the 3H-labeled methyl group from SAM to RNA cap, the biotin-labeled RNA can be captured on the streptavidin SPA beads and measured with a scintillation counter.

1.5.3 Genetic cell based assay

The cell-based assays have two major advantages: more than one target and step are analyzed during replication and the uptake of compounds into cells is required, which represents a more authentic therapeutic environment. Inhibitors identified through cell-based assays have had a higher success rate in subsequent animal experiments. Since most flavivirus infections cause cytopathogenic effect (CPE), the traditional cell-based screening assay involves viral infection of cultured cells and monitoring of inhibition through measurement of CPE or quantification of viral RNA by reverse transcription polymerase chain reaction (RT-PCR).[86,87] Unfortunately, these assays are labor-intensive and lack sensitivity. Thus, while informative, they are not ideal for screening large compound libraries.

1.6 Current inhibitors of WNV NS2B-NS3 protease

The WNV infection is a major public health threat. As no effective therapy is currently available for clinical treatment of this infection, many research groups have focused on the development of antiviral therapies using recent advances in the structural and molecular biology of flavivirus. Efforts on inhibitor development against the WNV NS2B-NS3 protease have thus far focused mainly on natural or modified natural peptidic ocompounds and only a few non-peptidic compounds have been reported. A number of compounds have been reported to inhibit WNV protease or viral replication in cell culture and few have shown *in vivo* efficacy.

1.6.1 Peptide inhibitors

The substrate-based peptide inhibitors of NS2B-NS3 protease were first described by Leung *et al.*[88] with a K_i vlues at micromolar concentration for Dengue 2 (DEN2). These inhibitors were designed based on native substrate (Ac-EVKKQR-pNA) sequences P6-P1 and cleavable amide group replaced with an α-keto amide (Table 1.1, cpd **1-1**) transition state isosteric. Subsequent removal of α-keto amide group (Table 1-1, cpd **1-2**) and simultaneously replacement of the carboxylic terminus carboxylic acid with aldehyde group shows slightly better inhibition (Table 1.1, cpd **1-3**).[89] Since, substrate-based peptide inhibitors with aldehyde as a warhead showed better inhibitory activity compare to the equivalent inhibitor α-keto amide, the inhibition of the NS2B-NS3 protease by aldehyde inhibitors have been investigated in details by a number of research groups. The truncation of the substrate based inhibitor to a tetra-peptide, tri-peptide or di-peptide were result in loosing inhibition potency by di-peptides against WNV NS2B-NS3 protease. However, Knox's group[90] reported a series of inhibitors related to the benzoyl-norleucine-lysine-arginine-arginine

aldehyde (Bz-Nle-KRR-H) tetra-peptide (Table 1.1, cpds **1-4** to **1-9**) containing a fixed basic amino acid residue (K) at third position enhanced inhibitory activity. Their biological activity found against the WNV NS2B-NS3 protease ranged from 1.9 to 262 µM (K_i) suggesting a good lead compound for generating a broad spectrum of inhibitors. The modeling study of this class of peptides was supported to bind at the active site of WNV NS2B- NS3 protease complex. This shows a general trend that S1 and S2 pockets of the protease are the key peptide recognition sites. The peptide inhibitor having side chain residue of capable for both σ-stacking and hydrogen bonding is favourable at the S1 pocket, while a positively charged

Table 1.1 Summary of peptidic inhibitors of DENV and WNV NS2B-NS3 proteases

Cpd	Peptide	DEN2 K_i (µM)	WNV K_i (µM)
1-1	Ac-FAAGKR-αketo-SL-NH2	47	-
1-2	Ac-FAAGKR-NH2	26	-
1-3	Ac-FAAGRR-H	16	-
1-4	Bz-Nle-KRR-H	5.8	4.1
1-5	Bz-Nle-KKR-H	41	1.9
1-6	Bz-Nle-KRA-H	193	4.6
1-7	Bz-Nle-KAR-H	>500	262
1-8	Bz-Nle-KRF-H	16	110
1-9	Bz-Nle-KFR-H	41	108
1-10	Phenylacetyl-KKR-H	-	9
1-11	4-phenyl-phenacetyl-KKR-H	-	6
1-12	3-methoxy-phenacetyl-KKR-H	-	11
1-13	NH_2- (hexa-D-R-NH_2)	-	0.478

1-14	NH_2- (hepta-D-R-NH_2)	-	0.041
1-15	NH_2- (octa-D-R-NH_2)	-	0.17
1-16	NH_2- (nona-D-R-NH_2)	-	0.006
1-17	NH_2- (deca-D-R-NH_2)	-	0.002
1-18	NH_2- (undeca-D-R-NH_2)	-	0.001
1-19	NH_2- (dodeca-D-R-NH_2)	-	0.001
1-20	4-phenylphenacetyl-KK-agtamine	-	2.05

residue is preferred in the S2 pocket. In addition, *in silico* studies suggested that aldehyde inhibitors bind to the substrate-binding cleft by forming a covalent bond with the catalytic Ser135. While the true level of inhibition by the actual aldehyde form of such inhibitors may be underestimated. Fairlie and coworkers[62] have reasoned that aldehyde inhibitors containing arginine residue at P1 show only modest activity against flavivirus NS3 protease, as they are in equilibrium with their hydrate or hemi-aminal cyclic form in aqueous form and only about 5% of the active free aldehyde remain to interact with the active site serine hydroxyl group. On the basis of diverse tetra-peptide aldehyde inhibitors a range of tri-peptide aldehyde have converted into aldehyde derivatives (Table 1.1, cpds **1-10** to **1-12**) to prospectively inhibit the protease. The space at the N-terminus of these peptides (X) was examined to test whether substituent at this position could enhance interaction with enzyme. The smallest and most potent inhibitors was found from this series is a cationic tripeptides with non-peptidic caps at the N-terminus and aldehyde at the C-terminus. One of the compound (Table 1.1, cpd **1-11**) from these series of peptide inhibitors shows high inhibition potency with K_i value of 6 nM and stable in serum.[91] The incorporation of multiple D-Arginine residues into amide inhibitors (Table 1.1, cpds **1-13** to **1-19**) has

been shown to enhance inhibitor potency against WNV NS2B-NS3 protease.[92] The level of inhibition was found to be improved 500-fold by increasing the number of D-Arg residues from 7 to 12. It is unlikely that the enzyme has specificity for binding to multiple arginine residues outside of the P2-P1 recognition site and another explanation is that multiple arginine residues have a cumulative effect on the association at S1 and S2. The D-arginine-based 9-12-mer peptides are potent inhibitors of WNV NS2B-NS3 protease with a range of K_i values from 1 to 6 nM. Most of the peptide inhibitors of the NS2B-NS3 protease involved covalent inhibitors that compete with the substrate for the catalytic site. Such peptide-based covalent inhibitors have their C-terminal carboxyl group chemically modified into aldehyde 'warheads'. This popular aldehyde functional group and peptide aldehydes have been shown to inhibit the WNV NS2B-NS3 protease at sub-micromolar potencies. However, warhead peptidomimetics have several undesirable characteristics, including lack of selectivity over other trypsin-like proteases due to their high reactivity and low chemical stability, curtailing their potential for drug development. Therefore, Lim *et al*.[93] investigated peptidomimetics without aldehyde warheads if could inhibit the WNV NS2B-NS3 protease and they found agmatine peptidomimetic (Table 1.1, cpd **1-20**) was shown to be a competitive inhibitor with a binding affinity of K_i value is 2.05 μM and specific to inhibit WNV NS2B-NS3 protease. The inhibitor does not bind covalently to the catalytic serine in the active site but instead employ hydrophobic and/or electrostatic interactions to compete with the natural substrate for the active site. Such inhibitors should be less reactive and hence more 'druggable' compared to warhead inhibitors.

Although the *in vitro* results were fruitful, a major disadvantage of peptidic inhibitors is their short physiologic half life, as peptides are easily cleaved and inactivated in the

body. In addition, most of the peptide inhibitors are highly charged and interacting with WNV protease by electrostatic interaction; such charged peptides are highly prohibited to penetrate the cell membrane. Also, a high drug clearance rate *in vivo* will consequently lead to diminished therapeutic effects. Thus, there is a need to explore the inhibitory effects of non-peptidic compounds, which has been attempted by very few groups till date.

1.6.2 Nonpeptidic inhibitors

The degradation problem of peptide based inhibitors of proteases has been overcome in a number of ways, including the generation of macrocyclic inhibitors by covalent linkages. Such inhibitors retain the high potency and selectivity of peptide inhibitors while the macrocycle makes the peptide components more resistant to degradation. However, such a compound would most likely only be a tool for probing the effects of protease inhibition *in vivo*, rather than being a drug candidate. In comparison to the peptidic inhibitors, only a few nonpeptidic inhibitors are reported to show satisfactory inhibition against the WNV NS2B-NS3 protease. Besides peptide inhibitors, small molecules are one of the major tools for drug discovery. Small molecule drugs in the human body behave like a foreign molecule, which is found in an organism but does not normally produced. Attempts to deal with such types of small molecules have many advantages: a number of drugs are excreted from the human body intact and an ideal drug should leave the body after it completes its mission. However, most small molecules need to be modified structurally to facilitate excretion Modifications of small molecules are relatively more affordable than macromolecules. In addition, small molecules differ with respect to distribution, metabolism, serum half-life, typical dosing regimen, toxicity, species reactivity, antigenicity, clearance mechanisms, and drug-drug docking studies on compound **1-22** and **1-23** showed that

the amide oxygen of the indole ring in compound **1-22** and oxygen from phosphonic acid group form a strong hydrogen bond with Ser135 which is located at the active

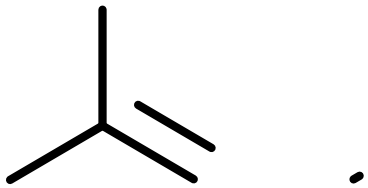

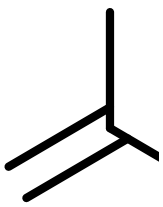

Figure 1.7 Non-peptidic inhibitors of WNV NS2B-NS3 protease and their inhibition potencies.

site and that might be reason of showing better inhibition than compound **1-21**. The small molecule inhibitor of the WNV NS2B-NS3 protease with thiourea moiety has been identified by automatic fragment-based docking of about 12000 compounds.[81] High-throughput docking into the active site of the WNV protease and binding free energy evaluation were identified compound **1-24** (Figure 1.7) to shows moderate inhibitory activity. The thiourea moiety of symmetrical inhibitor (Figure 1.7, cpd **1-24**) was found to interact with S1 and S2 pocket through hydrogen bonding. Beside the rational designed inhibitors of WNV NS2B-NS3 protease, some inhibitors of this protease were identified by high throughput screening which provides a powerful complement to structural based rational design of small molecule inhibitors of protease. In the WNV NS2B-NS3 protease assay, Mueller *et al.*[94] identified 8-hydroxyquinoline (8-HQ) derivatives compound **1-25** and **1-26** (Figure 1.7) which showed ~~s~~ competitive inhibition with K_i values of 3.2 µM and 3.4 µM respectively. These two inhibitors identified from initial screening of 32337 molecules after applying the Lipinski's rule of five.[95] Further structural activity relation (SAR) study on scaffold 8-HQ assisted to find out more potent inhibitor (Figure 1.7, cpd **1-27**) of WNV protease[96]. In addition, the 1-oxo-1,2,3,4-tetrahydroisoquinoline and 1-oxo-1,2-dihydroisoquinoline scaffolds were utilized in the design libraries of compounds for screening against WNV protease. Exploratory studies have led to the identification of a WNV protease inhibitor a 1-oxo-1,2-dihydroisoquinoline-based derivative which could potentially serve as a launching pad for a hit-to-lead optimization campaign[97]. One of the inhibitors (Figure 1.7, cpd **1-28**) from the abovementioned scaffold showed moderate inhibition against WNV protease with IC_{50} value of 30 µM. A HTS study of more than 65000 compounds at the National Institutes of Health identified several sulfonyl pyrazolyl derivatives of novel, uncompetitive inhibitory activity.

Scaffold 5-amino-1-(phenylsulfonyl)-1H-pyrazol-3-yl (Figure 1.7, cpds **1-29** and **1-30**) appears to interfere with the productive interactions of the NS2B cofactor with NS3 protease domain. These compounds showed relatively high potencies (IC_{50} <200 nM) against recombinant NS2B-NS3 protease *in vitro* and gave clues to block productive interactions. However, this class of compound was relatively unstable in aqueous buffer solutions and degraded completely in hours, therefore they were unsuitable for inhibitory effects at physiological conditions.[98] Further attempts to improve the stability of these compounds via addition of electronegative groups on the aromatic ring to shield the hydrolytically sensitive ester group and isosteric replacement of the ester moiety (Figure 1.7, cpd **1-31**) led to slight increases in their half life in aqueous buffer but with compromises to their inhibitory potencies.[99] Based on the structural requirements important for potency and stability of sulfonyl pyrazolyl derivatives, further modification on the corresponding 1-benzyl-3-methyl-1H-pyrazol-5-yl derivatives (Figure 1.7, cpd **1-32**) showed relatively better stability in aqueous buffer but with compromises to their inhibition activity with compare to 5-amino-1-(phenylsulfonyl)-1H-pyrazol-3-yl. The small molecule interference with the productive interaction of the NS2B cofactor with NS3protease could be a superior drug discovery strategy when compared with targeting of the conserved active site of the flaviviral proteinase. In addition, to investigating the assumption, a focused structure-based approach was employed to identify the allosteric small molecule inhibitors of NS2B-NS3pro. Using high throughput *in silico* docking, a diverse set of 275000 molecules from NCI compound library were virtually screened and found to show potenteial (Figure 1.7, cpds **1-33** and **1-34)** activity against the protease. However, these compounds are too toxic to baby hamsterm (BHK21) to carry out further screening. Therefore, based on current research progress, there is much room

for further studies on the development of potential inhibitor molecules of WNV protease.

1.7 Identification of “hit” compound by HTS

Historically, most drugs have been derived from natural products, but there has been a shift away from their use with the increasing predominance of molecular approaches to drug discovery. Nevertheless, their structural diversity makes them a valuable source of novel lead compounds against newly discovered therapeutic targets. In the preliminary WNV NS3 protease inhibition assay, a collection of 110 compounds from our in-house compound library which have a history of antimicrobial, antiviral and anticancer activities were screened at 100 μM using high throughput screening (HTS)

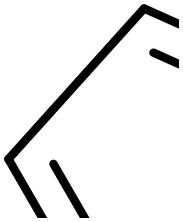

Figure 1.8 Structures and IC_{50} values of initial ‘‘hit’’ compounds against WNV NS2B-NS3 protease confirmed in the HTS.

technique to filter out the potential inhibitors. This initial screening provided a rapid identification of compounds that show potential ability to inhibit WNV NS3 protease. Eight compounds were found to exhibit detectable inhibition ability towards the WNV NS2B-NS3 protease. These compounds were further refined by cell cytotoxicity assays. This resulted in the identification of six compounds (Figure 1.8) as lead compounds. To optimize the potency of these compounds, a library of structurally diverse analogues of selected three scaffolds (Figure 1.8, **2-1a**, **3-1a** and **4-1a**) were synthesized for biological evaluation of their inhibitory activities. The compound **2-1a1**, was of primary interest to us because, to our knowledge, this is the first zwitterion-type inhibitor identified and we reasoned that such an entity together with its surrounding amino groups could function like highly charged peptidyl recognition components to provide favourable binding interactions. To provide access to structurally diverse analogues of compound **2-1a1** for biological evaluation of their inhibitory activities, a focused library of **2-1a1** analogues were synthesized by modifying a literature procedure. Similarly, structurally diverse analogues of compound **3-1a1** and **4-1a1** were synthesised and evaluated for their biological property by SAR study.

1.8 Purpose of this research work

The main aim of this project was to identify novel and potent small molecule inhibitors of WNV NS2B-NS3 protease which will be stable under physiological condition and are non-cytotoxic to normal cells. In Section 1.1 we have highlighted the details on how WNV infection has been expanding rapidly over the past years and the growing public health concerns associated with this viral infection. Till date, there

is neither safe antiviral therapy nor vaccine available for human use against the WNV. The most potent small molecule inhibitor of WNV NS2B-NS3 protease was found to be unstable under physiological conditions and degraded within one hour in aqueous buffer. Attempts to increase the compound's stability without compromising its activity have proven to be unsatisfactory. Therefore, a more specific aim of this project based on the screen a library of small molecules having better therapeutics indices via high throughput screening technique to identify ''hit'' compounds. Further, evaluation of selected scaffold from these initial ''hit'' compounds by SAR study with changing at diverse position through different functional group that would have better inhibition activity and their kinetics study to see the mode of interactions. Finally, a docking study was performed to rationalize the inhibition and kinetics result as well as to identify the possible binding sites of compound on the WNV NS2B-NS3 protease.

Chapter 2

Discovery, Synthesis and *In Vitro* Evaluation of West Nile Virus Protease Inhibitor Based on the 9,10-Dihydro-3H,4aH-1,3,9,10a-tetraaza-phenanthren-4-one Scaffold

2.1 Synthesis of analogues of the lead compound

To provide access to structurally diverse analogues of compound **2-1a1** for biological evaluation of their inhibitory activities, a focused library of **2-1a1** analogues were synthesized by modifying a literature procedure.[100,101] The general strategy for the synthesis of compound **2-1a** is shown in Scheme 2.1. A warm, aqueous solution of chloral hydrate and sodium sulfate were reacted with an acidic solution of the respective aniline **2-3** followed by aqueous hydroxylamine at 90 ^{o}C to give isonitrosoacetanilide[102] **2-4** which precipitated upon cooling from the reaction mixture in 80-95% yield. Polychronopoulos *et al.*[103] had reported the cyclization of **2-4** with ~68 equiv. of concentrated H_2SO_4. However in our hands, this large amount of concentrated H_2SO_4 hindered the precipitation for isatin **2-5**. We explored the reaction using a reduced amount of concentrated H_2SO_4 and found that with 46 equiv. of concentrated H_2SO_4, the cyclization reaction proceeded equally readily and the crude **2-5** which precipitated easily could be used in the next step of the reaction without purification. Compound **2-5** was subsequently reacted under reflux with thiosemicarbazide in 10% aqueous KOH[100] to yield intermediate **2-6** which was precipitated from the reaction mixture at pH 5 as a yellow solid. Intermediate **2-6** was treated with the respective benzyl bromide derivatives and then acidified with glacial acetic acid to pH 5-6 to yield compound **2-7** as a pure yellow solid. Reaction of

compound **2-7** with various aldehydes in the presence of catalytic amounts of glacial acetic acid provided racemic **2-1a** which could be further oxidized with 2,3-dichloro-5,6-dicyano-1,4-benzoquinone (DDQ) at room temperature[104] to the corresponding compound **2-2a**.

Scheme 2.1 Synthesis of compounds **2-1a** and **2-2a**

Reagents and conditions: a) $Cl_3CCH(OH)_2$, Na_2SO_4, HCl, H_2O, $NH_2OH.HCl$, 90 ^oC, 2.5 h (80-95% yield); b) conc H_2SO_4, 60 ^oC to 80 ^oC, 45 min; c) $NH_2NHCSNH_2$, 10% aq. KOH, 115 ^oC, 1h, then acidify to pH 5 (52-70% yield); d) $ArCH_2Br$, EtOH-10% aq KOH mixture, rt, 4h (80-90% yield); e) R^2CHO, glacial acetic acid, EtOH, reflux 10-15 min (50-90% yield); f) DDQ, CH_2Cl_2, 0 ^oC to rt, 4h (70-85% yield).

2.2 Structure-activity relation studies

A representative set of 69 analogues of compound **2-1a** and 3 analogues of compound **2-2a** were synthesized and tested in a WNV assay at 100 µM concentration to filter

out potential inhibitors. Potential inhibitors were determined by their ability to inhibit the NS2B-NS3 protease activity by at least 50%. The effects of these compounds were then evaluated at different concentrations and the IC_{50} values of each compound were calculated using the Graphpad Prism software (Table 2.1). The K_m value for the fluorogenic peptide substrate Pyr-RTKR-AMC for WNV NS2B-NS3 protease was determined, using the protocol from the SensoLyte® 440 West Nile Virus Protease Assay Kit, to be 3.45±0.41 μM.

In the structure-activity relation (SAR) studies, R^2 was first changed from 2-(3-chlorophenyl)-furan-5-yl to various alkyl, aromatic or heteroaromatic groups whilst keeping R^1 and Ar unchanged (Table 2.1, cpds **2-1a2** to **2-1a32**). Replacing the 2-(3-chlorophenyl)-furan-5-yl group in **2-1a1** with a 2-(4-nitrophenyl)-furan-5-yl, 2-(4-bromophenyl)-furan-5-yl or 2-(4-chlorophenyl)-furan-5-yl moiety gave comparatively better inhibition (Table 2.1, cpds **2-1a3** to **2-1a5**), indicating that a 4-substituted phenyl group plays an important role in the compound's inhibitory activity. In addition, when R^2 is a phenyl group (Table 2.1, cpd **2-1a9**), the inhibitory activity was also much better than compound **2-1a1**. Since having a phenyl group also made the compound more drug-like,[95] we carried out further SAR studies of this novel type of scaffold. Aromatic rings carrying an electron-donating or electron-withdrawing group at different positions of the phenyl ring were synthesized (Table 2.1, cpds **2-1a13** to **2-1a32**) and the screening results showed that the presence of a *p*-chloro, *p*-bromo or *p*-thiomethyl substituent on the phenyl ring (Table 2.1, cpds **2-1a21** to **2-1a23**) significantly amplified the compound's inhibition activity.

Next, we proceeded to tune the R^1 group of the two strongest lead compounds, *i.e.* **2-1a21** and **2-1a23**, by first replacing H with an electron-withdrawing group, such as a halide. This did not provide any improvement in the inhibitory activities of the two

Table 2.1. IC_{50} values of compounds[a] **2-1a** and **2-2a**

Cpd	R^1	R^2	Ar	IC_{50} (μM)
2-1a2	H	2-(2-chlorophenyl)-furan-5-yl	C_6H_5	72.84±6.00
2-1a3	H	2-(4-chlorophenyl)-furan-5-yl	C_6H_5	13.56±0.53
2-1a4	H	2-(4-bromophenyl)-furan-5-yl	C_6H_5	29.41±3.97
2-1a5	H	2-(4-nitrophenyl)-furan-5-yl	C_6H_5	10.05±1.34
2-1a6	H	ethyl	C_6H_5	NA[b]
2-1a7	H	thiophene-2-yl	C_6H_5	45.06±2.85
2-1a8	H	5-methylfuran-2-yl	C_6H_5	49.17±5.51
2-1a9	H	phenyl	C_6H_5	27.33±5.81
2-1a10	H	quinoline-3-yl	C_6H_5	11.02±0.78
2-1a11	H	pyridine-3-yl	C_6H_5	>100
2-1a12	H	pyridine-2-yl	C_6H_5	>100
2-1a13	H	2-methylphenyl	C_6H_5	20.46±1.47
2-1a14	H	2-chlorophenyl	C_6H_5	29.99±2.52
2-1a15	H	2-(methylthio)phenyl	C_6H_5	>100
2-1a16	H	3-phenoxyphenyl	C_6H_5	NA
2-1a17	H	3-carboxyphenyl	C_6H_5	>100
2-1a18	H	3-chlorophenyl	C_6H_5	NA
2-1a19	H	3-nitrophenyl	C_6H_5	11.39±0.31
2-1a20	H	4-fluorophenyl	C_6H_5	45.22±3.28
2-1a21	H	4-chlorophenyl	C_6H_5	7.66±0.91
2-1a22	H	4-bromophenyl	C_6H_5	9.39±1.00
2-1a23	H	4-(methylthio)phenyl	C_6H_5	6.28±1.39
2-1a24	H	4-methoxyphenyl	C_6H_5	NA
2-1a25	H	4-nitrophenyl	C_6H_5	NA
2-1a26	H	3-methyl-4-hydroxyphenyl	C_6H_5	>100
2-1a27	H	2-chloro-4-hydroxyphenyl	C_6H_5	>100
2-1a28	H	3,4-dichlorophenyl	C_6H_5	>100
2-1a29	H	4-hydroxy-3-nitrophenyl	C_6H_5	>100
2-1a30	H	4-fluoro-3-nitrophenyl	C_6H_5	35.72±3.77
2-1a31	H	4-bromo-3-nitrophenyl	C_6H_5	18.73±0.99
2-1a32	H	3,5-dibromophenyl	C_6H_5	>100
2-1a33	F	4-bromophenyl	C_6H_5	>100
2-1a34	F	4-chlorophenyl	C_6H_5	>100
2-1a35	F	4-(methylthio)phenyl	C_6H_5	23.91±7.37
2-1a36	F	3-nitrophenyl	C_6H_5	>100
2-1a37	Cl	phenyl	C_6H_5	>100
2-1a38	Cl	4-chlorophenyl	C_6H_5	16.28±2.56
2-1a39	Cl	4-(methylthio)phenyl	C_6H_5	>100
2-1a40	Me	4-chlorophenyl	C_6H_5	5.41±0.45
2-1a41	Me	4-(methylthio)phenyl	C_6H_5	10.70±0.72
2-1a42	Me	2-(4-chlorophenyl)-furany5-yl	C_6H_5	8.21±0.28
2-1a43	Me	phenyl	C_6H_5	>100
2-1a44	Me	2-(4-nitrophenyl)-furan-5-yl	C_6H_5	>100

2-1a45	Me	4-bromophenyl	C_6H_5	>100
2-1a46	Me	3-nitrophenyl	C_6H_5	>100
2-1a47	Me	4-bromo-3-nitrophenyl	C_6H_5	>100
2-1a48	Et	4-chlorophenyl	C_6H_5	NA
2-1a49	Et	4-(methylthio)phenyl	C_6H_5	NA
2-1a50	H	phenyl	4-$MeOC_6H_4$	NA
2-1a51	H	3-nitrophenyl	4-$MeOC_6H_4$	NA
2-1a52	H	4-chlorophenyl	4-$MeOC_6H_4$	8.47±2.54
2-1a53	H	4-(methylthio)phenyl	4-$MeOC_6H_4$	5.56±0.10
2-1a54	H	4-chlorophenyl	4-BrC_6H_4	>100
2-1a55	H	4-(methylthio)phenyl	4-BrC_6H_4	>100
2-1a56	H	4-chlorophenyl	3-BrC_6H_4	>100
2-1a57	H	4-(methylthio)phenyl	3-BrC_6H_4	11.15±1.32
2-1a58	H	4-chlorophenyl	4-ClC_6H_4	>100
2-1a59	H	4-(methylthio)phenyl	4-ClC_6H_4	6.20±0.15
2-1a60	H	4-chlorophenyl	3-ClC_6H_4	23.35±5.05
2-1a61	H	4-(methylthio)phenyl	3-ClC_6H_4	11.14±2.42
2-1a62	H	4-chlorophenyl	4-FC_6H_4	>100
2-1a63	H	4-(methylthio)phenyl	4-FC_6H_4	13.29±1.55
2-1a64	H	4-chlorophenyl	3-FC_6H_4	>100
2-1a65	H	4-(methylthio)phenyl	3-FC_6H_4	13.80±2.69
2-1a66	H	4-chlorophenyl	4-CNC_6H_4	>100
2-1a67	H	4-(methylthio)phenyl	4-CNC_6H_4	>100
2-1a68	Me	4-chlorophenyl	4-$MeOC_6H_5$	14.56±1.03
2-1a69	Me	4-(methylthio)phenyl	4-$MeOC_6H_5$	11.92±1.32
2-2a1	Me	4-chlorophenyl	C_6H_5	NA
2-2a2	Me	4-(methylthio)phenyl	C_6H_5	NA
2-2a3	Et	4-(methylthio)phenyl	C_6H_5	NA

[a] Data represent concentrations required to inhibit WNV NS2B–NS3 protease activity by 50% and are the mean±SE of triplicate experiments; compounds used are ≥98% pure. [b] NA: no activity.

compounds (Table 2.1 cpds **2-1a33** to **2-1a39**). However, if R^1 was changed to an electron-donating methyl group (Table 2.1, cpds **2-1a40** to **2-1a47**), a slight enhancement in the inhibition of WNV NS2B–NS3 protease was observed in one of the two compounds (Table 2.1 cpd **2-1a40**). However, increasing the size of the alkyl group by replacing the methyl substituent with an ethyl group resulted in a total loss of inhibitory activity in the two compounds (Table 2.1 cpds **2-1a48** to **2-1a49**).

To explore the effect of the Ar group on the biological activity of the compound, we replaced to the phenyl ring of the Ar group with a phenyl group containing either an electron-donating and electron-withdrawing substituent (Table 2.1 cpds **2-1a50** to **2-1a69**). The best inhibition was observed in compound **2-1a53** which contains a 4-methoxyphenyl group on the Ar position and a 4-(methylthio)phenyl moiety at the R^2 position. In addition, the inhibitory activity of compound **2-1a52** was comparably to **2-1a21**. Finally, we synthesized compounds **2-1a68** and **2-1a69** to analyze the combined effects of the preferred substituents on R^1, R^2 and Ar. However, the inhibitory activities of compounds **2-1a68** and **2-1a69** were weaker than compounds **2-1a23**, **2-1a40** or **2-1a53**, the three strongest candidates identified from our earlier screening efforts.

Considering that the compounds tested thus far were always racemate compounds, we proceeded to investigate the influence of stereochemistry on the compounds' biological activities. However, attempts to separate the R- and S- enantiomers of **2-1a23**, **2-1a40** and **2-1a53** using our own column available in lab and collaboration Diacel Japan with various methods proved futile as a single peak was constantly observed in the chiral HPLC analysis. In addition, removal of the chiral centre by DDQ oxidation gave a new scaffold **2a** which was completely inactive as inhibitors to WNV NS2B-NS3 protease (Table 2.1, cpds **2-2a1** to **2-2a3**). Thus compounds **2-1a23**, **2-1a40** and **2-1a53** were used for subsequent *in vitro* evaluations. The stabilities of compounds **2-1a23**, **2-1a40** and **2-1a53** at 37 °C in pH 8 buffer were determined by analyzing the amount of compound remaining with time using LCMS-IT-TOF detection. Quantization of the compounds was determined by Shimadzu's LC solution software. Compounds **2-1a23**, **2-1a40** and **2-1a53** showed excellent stability in a pH 8 buffer after 72 h.

Next we evaluated the cytotoxicities of compounds **2-1a23**, **2-1a40** and **2-1a53** against baby hamster kidney fibroblasts (BHK21 cells) for incubation times of 48 and 72 h.

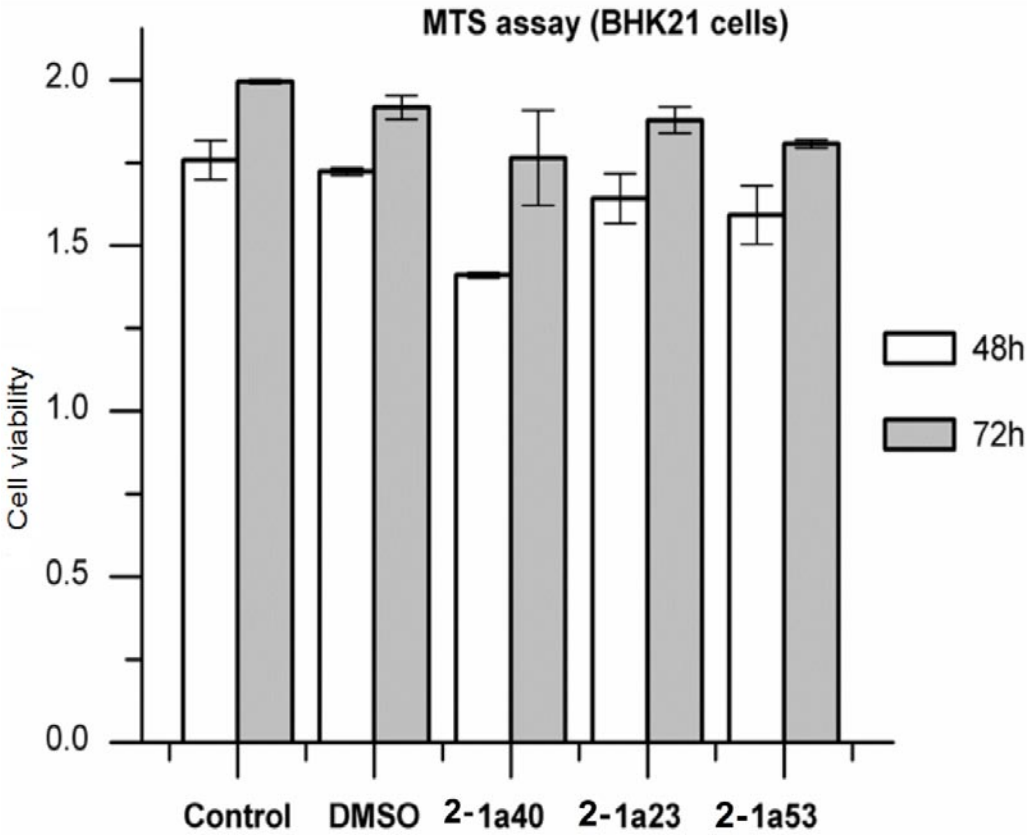

Figure 2.1 MTS assay results obtained at incubation times of 48 ( ) and 72 h ( ) with the BHK21 cell line. Compounds were added at a final concentration of 50 µM.

Vehicular control, dimethyl sulfoxide (DMSO), was also included to serve as control as the test compounds were dissolved in DMSO. The amount of DMSO used in the assay was controlled at 0.2% of the total volume. This is to ensure that DMSO does not result in cytotoxicity of cells. From the results obtained (Figure 2.1), compounds **2-1a23**, **2-1a40** and **2-1a53** were shown to be non-cytotoxic to BHK21 cells. To determine the mode of inhibition of the WNV NS2B-NS3 protease activity by compound **2-1a40**, we followed the kinetics of inhibition using Pyr-RTKR-AMC as

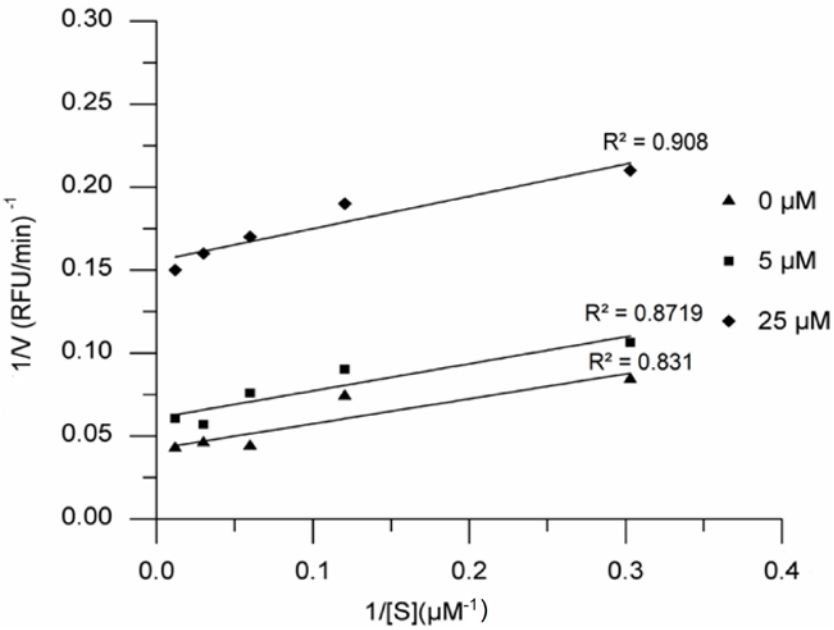

Figure 2.2 Uncompetitive inhibition of **2-1a40** with WNV NS2B-NS3 protease**.** WNV protease assays were performed at various concentrations of **2-1a40** (0, 5.0 and 25 µM) and substrate concentrations (3.3, 8.3, 16.7, 33.3, 83.3 µM). Double reciprocal plots of 1/V versus 1/[S] for **2-1a40** at each inhibitor concentration were plotted using the OriginPro 8.

substrate. This provided a substrate concentration dependent inhibition of the NS2B-NS3 protease activity (Figure 2.2). Lineweaver-Burk analysis of the initial velocities suggested that the inhibition by **2-1a40** was uncompetitive with respect to the substrate that possesses a K_i value of 4.47±0.37 µM. Uncompetitive inhibition by the compound **2-1a24**, due to the absence of charge on the inhibitor that prefers active site of the protease.

2.3 Docking analysis

The crystal structure of the WNV NS2B-NS3 protease in complex with peptide Bz-Nle-Lys-Arg-Arg-H (pdb 2fp7) has been reported earlier.[74] To identify the potential

binding site of compound **2-1a40** on the NS2B-NS3 protease, *in silico* docking studies were performed by using these crystal structure coordinates. Since compound **2-1a40** is an uncompetitive inhibitor of the WNV NS2B-NS3 protease, we focused our analysis on regions beyond the substrate binding sites. Earlier studies have shown that the integration of residues 78-87 of NS2B into the protease-cofactor complex affected the formation of the catalytic active sites.[74,75,105] Deletion or mutagenesis of these residues produced an inert enzyme. Therefore the region on the NS3 protease where key interactions with the NS2B cofactor (residue 78-87) occur is important for the NS2B-NS3 protease activity and particular attention was paid to this region during our docking studies.

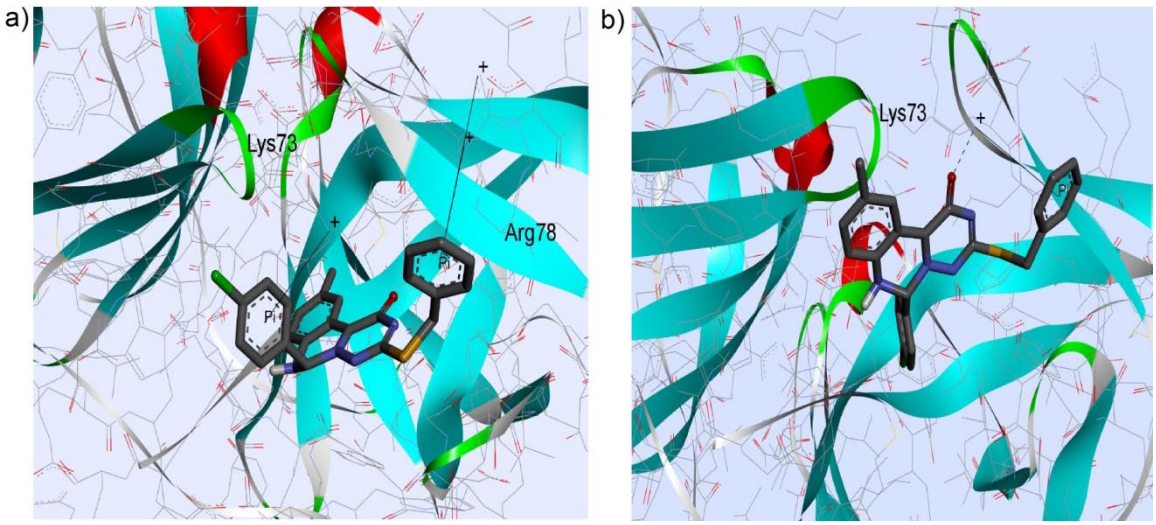

Figure 2.3 Molecular docking of compound **2-1a40** onto WNV NS2B-NS3 protease. The WNV protease crystal structure coordinates (pdb 2fp7)[74] were used for the molecular docking. The NS2B-NS3 protease and the enantiomers of compound **2-1a40** are shown as a wireframe and flat ribbon model generated using Discovery Studio 3.1 client. (a) S-enantiomer; (b) R-enantiomer.

Since compound **2-1a40** contains a chiral centre, the R- and S- enantiomers were separately analyzed for their interactions with the WNV NS2B-NS3 protease. Our

docking analysis predicted that the binding energies of the S- and R- enantiomers with the WNV NS2B-NS3 protease were similar (S-enantiomer: -8.10 kcal/mol; R-enantiomer: -8.22 kcal/mol). Amino acid residues that are in close proximity (less than 5 Å) to the atoms of the S-enantiomers include Arg78, Leu79 and Phe85 of NS2B; Ser71, Lys73, Glu74, Arg76, Lys88, Pro119, Glu120, Ile123, Ala164, Ile165 and Gln167 of the NS3 protease. Amino acid residues that are in close proximity (less than 5 Å) to the atoms of the R-enantiomers are Val77, Arg78 and Leu79 of NS2B; Lys88, Thr118, Glu120, Ile123 and Gln167 of the NS3 protease. The guanidine group in Arg78 of the NS2B cofactor binds strongly with the Ar group of the S-enantiomer via π-cation type of interactions. Strong π-cation type of interaction was also observed between the 4-chlorophenyl moiety of the S-enantiomer and Lys73 on the NS3 protease (Figure 2.3a). On the other hand, the R-enantiomer could potentially form hydrogen bond with residue Lys73 on the NS3 protease as well as π-cation interaction with the same residue. However we did not observe any strong interaction between the R-enantiomer and the key residues from the NS2B binding cavity (Figure 2.3b). This indicates that the S-enantiomer more strongly interferes with the productive interactions of the NS2B cofactor with the NS3 protease domain and is a preferred isomer for the inhibition of the WNV NS3 protease.

2.4 Conclusion

This study reports an *in vitro* assay for the WNV NS2B-NS3 protease that yielded a lead inhibitor with a 9,10-dihydro-3H,4aH-1,3,9,10a-tetraaza-phenanthren-4-one scaffold. Refinement of this initial “hit” by synthesizing and evaluating a focussed library of 9,10-dihydro-3H,4aH-1,3,9,10a-tetraaza-phenanthren-4-one compounds

provided an analogue (S)-**2-1a40** that showed low micromolar inhibition of the WNV NS2B-NS3 protease. Compound (S)-**2-1a40** inhibited the interaction between the NS2B cofactor and the NS3 proteases in an uncompetitive manner.

2.5 Experimental Section

2.5.1 Chemistry

All chemical reagents and anhydrous solvent were obtained from Aldrich, Merck, Lancaster or Fluka and used without further purification. Flash chromatography was performed with silica (Merck, 70-230 mesh) whilst TLC was carried out on pre-coated plates (Merck silica gel 60, F254) and visualized with UV light. Purity of the final compound was determined by HPLC using a Shimadzu LCMS-IT-TOF system with a Phenomenex C18 column (50 mm x 3.0 mm, 5 μm). Purity of the compound was checked at 254 nm and integration was obtained with Shimadzu LCMS solution software. ^{1}H and ^{13}C NMR spectra were recorded using $CDCl_3$, acetone-d_6, or DMSO-d_6 as solvents and tetramethylsilane (TMS) as internal reference on a Bruker AMX500 or a Bruker ACF 300 Fourier transform spectrometer. The following abbreviations were used to explain the multiplicities: s (singlet), d (doublet), t (triplet), dd (doublet of doublet), q (quatrate), and m (multiplet). The number of protons (n) for a given resonance was indicated as nH. Mass spectrometry was performed on a Finnigan/MAT LCQ mass spectrometer using electron spray (ESI) ionization.

General procedure for the synthesis of 2-4: Chloral hydrate (3.84 g, 23.2 mmol) and Na_2SO_4 (60 g, 422 mmol) were dissolved in water (20 mL) in a 500 mL beaker

and warmed to 35 °C. A warm solution of the commercial available aniline or its derivatives **2-3** (21.5 mmol) in water (6 mL) and an aqueous solution of concentrated HCl (1.83 mL, 22 mmol) were added (a white precipitate of the aniline sulfate was formed) followed by a warm solution of hydroxylamine hydrochloride (4.72 g, 67.94 mmol) in water (8.25 mL). The mixture was heated at 90 °C for 2.5 h and then allowed to cool to 50 °C before filtering. The pale cream solid obtained was washed by stirring with water (100 mL), filtered and dried overnight at 50 °C to give the corresponding isonitrosoacetanilide **2-4** in 80-95% yield.

General procedure for the synthesis of 2-5: Concentrated sulfuric acid (18 mL, 337.68 mmol) was heated in a 250-mL beaker to 60 °C. The respective dried compound **2-4** (7.3 mmol) was added in portion with stirring over 30 min so that the temperature did not exceed 65 °C. The mixture was then heated to 80 °C for 15 min, allowed to cool to 70 °C, and cooled on ice-cold water. The solution was then poured very slowly into ice and allowed to stand until a reddish precipitate of isatine ***2*-5** was formed. The crude solid **2-5** was filtered and used in the next step without further purification.

General procedure for the synthesis of 2-6: The respective compound **2-5** (10.2 mmol) was dissolved in 10 % aqueous KOH (10 mL, 45.5 mmol) and then treated with thiosemicarbazide (985 mg, 10.7 mmol). The reaction mixture was heated at 115 ^{o}C for 1h, cooled to room temperature and then poured over ice. Acidification of the reaction mixture to ~pH 5 with glacial acetic acid provided yellow fluffy precipitate which was filtered, washed copiously with water, dried in air and then in a vacuum oven (at 50 °C) to afford a yellow solid **2-6** in 60-78% yield. Purification of compound **2-6** by column chromatography gave the pure product is 52-70%.

General procedure for the synthesis of 2-7: The respective crude compound **2-6** (6 mmol) was dissolved in a mixture of ethanol (12 mL) and 10 % aq. KOH (18 mL, 27.3 mmol) was treated with a solution of benzylbromide or benzylbromide derivative (6 mmol) and allowed to stir over night. Thereafter, the reaction mixture was diluted with ether (100 mL) and water (70 mL). The ether layer was separated and the aqueous layer was washed with ether (3x100 mL) and then poured over ice. Upon careful, dropwise addition of glacial acetic acid with vigorous shaking at 0-4 °C, yellow precipitate formed. This precipitate was filtered, washed with water (3x30 mL) and dried in a vacuum oven (at 50 °C) to provide compound **2-7** in 80-90% yield.

General procedure for the synthesis of 2-1a: To a suspension of the respective compound **2-7** (0.32 mmol) in anhydrous ethanol (6 mL) was added glacial acetic acid (25 µL, 0.42 mmol) followed by the respective aldehyde (0.42 mmol, 1.3 equiv.). The reaction mixture was refluxed for 10-15 min resulting in a dark-reddish solution. Upon cooling to room temperature, orange-yellow solid **2-1a** precipitated from the solution. Sometimes the hot reaction mixture contained insoluble particles which were removed by filtering the reaction mixture under hot condition. The filtrate was then cooled to room temperature to provide the crude solid compound **2-1a**. The crude product was recrystallized with ethanol, filtered and washed with cold ethanol (2x3 mL). In a few cases, the product was purified by column chromatography then dried in a vacuum oven at 50 °C. Compound **2-1a** was obtained in 50-90% yield.

General procedure for the synthesis of 2-2a: The respective compound **2-1a** (0.16 mmol) was dissolved in CH_2Cl_2 (10 mL) and the reaction mixture was kept at 0 °C followed by the slow addition of DDQ (0.2 mmol). After the addition of DDQ, the temperature of the reaction mixture was allowed to rise to room temperature and was kept at this temperature for 4 hours. During this time, the time reaction was monitored

by TLC. When the reaction was completed, the reaction mixture was extracted with a CH_2Cl_2/H_2O mixture. The organic layer was concentrated, purified by column chromatography using a ethyl acetate/hexane (starting from 1:4 to 1:1) solvent system and dried under vacuum at 50 °C temperature to yield compound **2-2a** in 70-85% yield.

2.5.2 Biology

All the compounds were tested against the WNV NS2B-NS3 protease using the SensoLite® 440 WNV protease assay kit (Catalog # 72079) and the active recombinant WNV protease (Calalog # 72081) which were purchased from Anaspec (USA). This protease assay kit uses a fluorogenic peptide Pyr-RTKR-AMC as substrate. Eight different substrate concentrations ranging from 1 to 80 μM were incubated in 96-well plates with 0.3μg/mL recombinant WNV protease at 37 °C in the buffer provided. The increase in fluorescence intensity was monitored using an Infinite F200 microplate reader (Tecan, Switzerland) at an excitation wavelength of 354 nm (±10 nm) and emission wavelength of 442 nm (±15 nm). The initial velocity was determined from the linear portion of the progress curve, and the value of K_m was determined using the Michaelis-Menten equation, i.e. $v = V_{max}[S] / ([S] + K_m)$ to be 3.45±0.41 μM. Triplicate measurements were taken at each data point and the data were reported as mean±SE. In the preliminary WNV NS2B-NS3 protease inhibition assay, compounds **2-1a** and **2-2a** were screened at a fixed concentration of 100 μM to filter out potential inhibitors. Compounds which showed more than 50% inhibition were further investigated for their IC_{50} determination.

Determination of IC_{50}: For the IC_{50} calculations, recombinant WNV protease concentration of 0.3 μg/mL and seven different concentrations of the inhibitor ranging

from 10 nM to 100μM were used. For each experiment, the protease was pre-incubated with the inhibitor at 37 ^{o}C for 15 min in separate wells and the enzyme kinetics was initiated by adding substrate Pyr-RTKR-AMC to a final concentration 16.7 μM. The increase in fluorescence intensity was monitored continuously using an Infinite F200 microplate reader at an excitation wavelength of 354 nm and emission wavelength at 442 nm. Fluorescence values obtained from the positive control (no inhibitor) were considered as 100% complex formation and those values obtained in the presence of inhibitors were calculated as the percentage of inhibition of the control. Duplicate measurements were obtained at each data point. The IC_{50} values were calculated using a sigmoidal dose-response using the Graphpad prism 3.0 software (San Diego, USA). Duplicate measurements were recorded as the mean±SE.

Determination of inhibition mechanism: Two different inhibitor concentrations and a no-inhibitor control (0 to 25 μM) were each assayed at five substrate concentrations ranging from 3.3 to 83.3 μM. In each assay, the enzyme and inhibitor were incubated at 37 °C for 15 min, followed by the addition of the substrate to start the kinetic measurement. The rate of substrate cleavage (v) was monitored using the F200 microplate reader. To illustrate the inhibition mechanism, 1/V versus 1/[S] was plotted for at each inhibitor concentration using OriginPro 8.

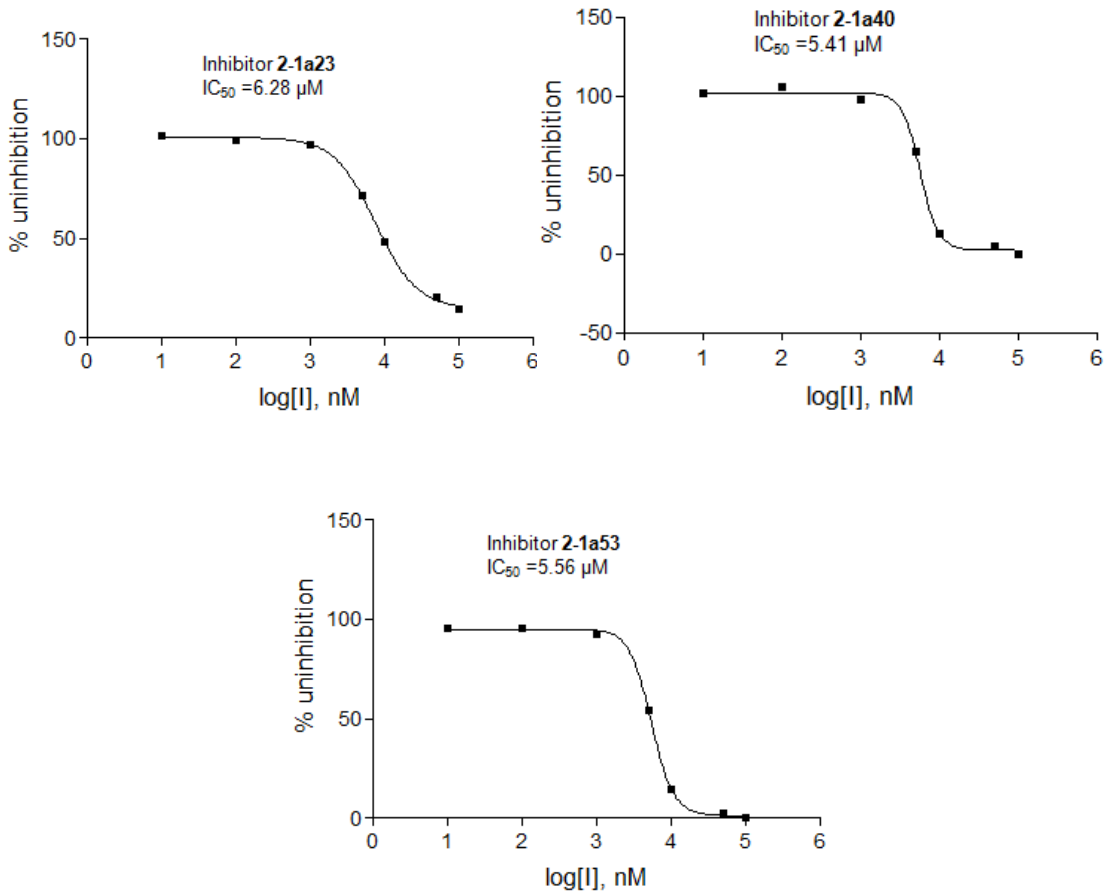

Figure 2.4 Un-inhibition curves of compound **2-1a23**, **2-1a40** and **2-1a53**

MTS Assay

The baby hamster kidney fibroblast (BHK21) cells were cultured in Roswell Park Memorial Institute (RPMI) 1640 medium containing 10% fetal bovine serum (FBS). The 1500 cells were placed in each well of three 96-well plates with a cell density of $1.66x10^4$ cells/mL and incubated for 24 h at 37 °C with 5% CO_2. Thereafter, the compound of interest or DMSO was added into each well at 50 µM. Wells containing plain DMSO served as a vehicular control. The plate was then placed in the incubator for 48 and 72 h of incubation at 37 °C with 5% CO_2. At the end of each individual incubation time point, MTS reagent solution (20µL) was added into each sample well. The plate was then incubated again in the dark for 2 h, gently shaken using a vortemp

machine for 5 min to ensure equal mixing and absorbance at 492 nm was taken using a spectrometer.

2.5.3 *In silico* studies

Molecular docking simulations were performed with the AutoDock4 program. Both enantiomers of compound **2-1a40** were constructed in ChemBio 3D Ultra 11.0 by minimizing the energy. The active site of the WNV protease was prepared using the crystal structure of the WNV NS2B-NS3 protease in complex with peptide Bz-Nle-Lys-Arg-Arg-H (pdb 2fp7).[18] The structure was stripped of all water molecules and bound ligand. Hydrogen atom was added to all polar atoms of the protein followed by the addition of Gasteiger-Marsili charges. AutoDock simulations were performed using the Lamarckian Genetic Algorithms (GA) subroutine at default settings for GA population size, crossover rate, mutation rate, and starting with fully randomized ligand position, orientation and conformation. Fifty GA runs were performed for the inhibitor-enzyme pair and results were analyzed using Discovery Studio 3.1 client.

2.6 ^{1}H and ^{13}C NMR data of all compounds synthesized and crystal structure of 2-1a43 and 2-2a1

^{1}H and ^{13}C NMR data of compound 2-4:

(E)-2-(Hydroxyimino)-N-phenylacetamide (2-4a) as a light brown solid (Yield: 83%): ^{1}H NMR (500 MHz, Acetone-d_6): δ = 11.73 (s, 1H), 9.66 (s, 1H), 8.21-8.19 (m, 2H), 8.01 (d, *J* = 3.8 Hz, 1H), 7.79-7.76 (m, 2H), 7.56-7.53 (m, 2H). ^{13}C NMR (125 MHz, Acetone-d_6): δ = 160.9, 144.6, 138.8, 129.2, 124.4, 120.4, 120.3. HRMS-ESI *m/z* [M - H] calcd for $C_8H_7N_2O_2$: 163.0513, found: 163.0514.

(E)-N-(4-Fluorophenyl)-2-(hydroxyimino)acetamide(2-4b) as a light brown solid (Yield: 95%): ^{1}H NMR (500 MHz, Acetone-d_6): δ = 11.25 (s, 1H), 9.28 (s, 1H), 7.75-7.71 (m, 2H), 7.50 (s, 1H), 7.06-7.03 (m, 2H). ^{13}C NMR (125 MHz, Acetone-d_6): δ = 160.3, 159.9, 158.1, 144.2, 134.7, 121.8, 121.7, 115.2, 115.0. HRMS-ESI m/z [M + Na] calcd for $C_8H_7FN_2O_2$ Na: 205.0384, found: 205.0388.

(E)-N-(4-Chlorophenyl)-2-(hydroxyimino)acetamide (2-4c) as a brown solid (Yield: 84%): ^{1}H NMR (500 MHz, Acetone-d_6): δ = 9.41 (s, 1H), 7.75-7.72 (m, 2H) 7.51 (s, 1H), 7.29-7.27 (m, 2H). ^{13}C NMR (125 MHz, Acetone-d_6): δ = 161.2, 144.5, 137.9, 129.2, 128.9, 122.0, 121.9. HRMS-ESI m/z [M - H] calcd for $C_8H_6ClN_2O_2$: 197.0123, found: 197.0118.

(E)-2-(Hydroxyimino)-N-p-tolylacetamide (2-4d) as a brown solid (Yield: 89%): ^{1}H NMR (500 MHz, Acetone-d_6): δ = 9.19 (s, 1H), 7.57 (d, *J* = 3.2 Hz, 2H), 7.51 (s, 1H), 7.07 (d, *J* = 3.2 Hz, 2H), 2.22 (s, 3H). ^{13}C NMR (125 MHz, Acetone-d_6): δ = 160.8, 144.5, 136.2, 133.8, 129.5, 120.3, 120.2, 20.4. HRMS-ESI m/z [M + H] calcd for $C_9H_{11}N_2O_2$: 179.0815 found: 179.0819.

(E)-N-(4-ethylphenyl)-2-(hydroxyimino)acetamide (2-4e) as a brown solid (Yield: 92%): ^{1}H NMR (500 MHz, Acetone-d_6): δ = 11.20 (s, 1H), 9.11 (s, 1H), 7.65 (d, *J* = 8.15 Hz, 2H), 7.53 (s, 1H), 7.16 (d, *J* = 8.8 Hz, 2H) 2.62-2.58 (q, *J* = 7.5 Hz, 2H), 1.17 (t, *J* = 8.8 Hz, 2H) ^{13}C NMR (125 MHz, Acetone-d_6): δ = 160.0, 144.3, 139.8, 136.1, 127.9, 119.9, 119.8, 27.9, 15.2. HRMS-ESI m/z [M + H] calcd for $C_{10}H_{12}N_2O_2$:193.0972, found: 193.0978

.

^{1}H and ^{13}C NMR data of compound 2-6:

6-(2-Aminophenyl)-3-thioxo-3,4-dihydro-1,2,4-triazin-5(2H)-one (2-6a). The crude product was purified using flash chromatography (EtOAc/hexane =1:3) to afford as a yellow solid (Yield: 52%). ^{1}H NMR (500 MHz, DMSO-d_6): δ =13.37 (s, 1H), 7.32 (d, *J* = 7.55 Hz, 1H), 7.09 (t, *J* = 7.55 Hz, 1H), 6.68 (d, *J* = 8.2 Hz, 1H), 6.53 (t, *J* = 7.55 Hz, 1H), 5.53 (s, 2H). ^{13}C NMR (125 MHz, DMSO-d_6): δ = 172.0, 151.9, 146.7, 146.3, 129.6, 129.3, 114.4, 113.9, 113.8. HRMS-ESI *m/z* [M - H] calcd for $C_8H_8N_4OS$: 219.0346, found: 219.0352.

6-(2-Amino-5-fluorophenyl)-3-thioxo-3,4-dihydro-1,2,4-triazin-5(2H)-one (2-6b). The crude product was purified using flash chromatography (EtOAc/hexane =1:3) to afford as a yellow solid (Yield: 58%). ^{1}H NMR (500 MHz, DMSO-d_6): δ =13.50 (s, 2H), 7.27-7.25 (dd, *J* = 10.7 Hz, 1H), 7.00-6.96 (m, 1H), 6.70-6.67 (q, *J* = 5.05 Hz, 1H), 5.51 (s, 2H). ^{13}C NMR (125 MHz, DMSO-d_6): δ = 173.1, 153.9, 152.8, 152.1, 146.4, 143.9, 117.5, 117.2, 116.5, 116.4, 116.3, 116.1, 114.7, 114.6. HRMS-ESI *m/z* [M - H] calcd for $C_9H_7FN_4OS$: 237.0252, found: 237.0253.

6-(2-Amino-5-chlorophenyl)-3-thioxo-3,4-dihydro-1,2,4-triazin-5(2H)-one (2-6c). The crude product was purified using flash chromatography (EtOAc/hexane =1:3) to afford as a yellow solid (Yield: 66%). ^{1}H NMR (300 MHz, DMSO-d_6): δ = 7.43 (d, *J* = 3.6 Hz, 1H), 7.11-7.09 (m, 1H), 6.79 (d, *J* = 14.5 Hz, 1H), 5.73 (s, 2H). ^{13}C NMR (75 MHz, DMSO-d_6): δ 173.2, 153.3, 145.3, 144.8, 128.7, 117.1, 116.0, 115.5. HRMS-ESI *m/z* [M - H] calcd for $C_9H_6ClN_4OS$: 252.9956, found: 252.9950.

6-(2-Amino-5-methylphenyl)-3-thioxo-3,4-dihydro-1,2,4-triazin-5(2H)-one (2-6d). The crude product was purified using flash chromatography (EtOAc/hexane =1:3) to

afford as a yellow solid (Yield: 66%). ^{1}H NMR (300 MHz, DMSO-d_6): δ = 7.13 (s, 1H), 7.43 (m, 1H), 6.59 (d, *J* = 8.15 Hz, 1H), 2.13 (s, 3H). ^{13}C NMR (75 MHz, DMSO-d_6): δ = 172.4, 152.6, 146.5, 143.9, 130.0, 129.6, 122.3, 114.8, 114.3, 19.0. HRMS-ESI *m/z* [M - H] calcd for $C_{11}H_{10}N_4OS$: 235.0648, found: 235.0651.

6-(2-Amino-5-ethylphenyl)-3-thioxo-3,4-dihydro-1,2,4-triazin-5(2H)-one (2-6e). The crude product was purified using flash chromatography (EtOAc/hexane =1:4) to afford as a yellow solid (Yield: 70%). ^{1}H NMR (500 MHz, DMSO-d_6): δ = 13.48 (s, 1H), 13.09 (s, 1H), 7.15 (s, 1H), 6.96 (d, *J* = 8.2 Hz, 1H), 6.62 (, *J* = 8.2 Hz, 1H), 5.30 (s, 2H), 2.46-2.41 (q, *J* = 7.55 Hz, 2H), 1.10 (t, *J* = 7.55 Hz, 3H) ^{13}C NMR (125 MHz, DMSO-d_6): δ 172.9, 153.4, 152.8, 147.8, 145.1, 129.9, 129.3, 115.6, 114.8, 27.1, 15.8. HRMS-ESI *m/z* [M - H] calcd for $C_{11}H_{13}N_4OS$: 249.0805, found: 249.0808.

^{1}H and ^{13}C NMR data of compound 2-7:

6-(2-Aminophenyl)-3-(benzylthio)-1,2,4-triazin-5(2H)-one (2-7a) as a yellow solid (Yield: 83%). ^{1}H NMR (500 MHz, DMSO-d_6): δ =7.45 (d, *J* = 7.55 Hz, 3H), 7.36-7.28 (m, 6H), 7.11 (t, *J* = 8.2 Hz, 1H), 6.74 (d, *J* = 8.2 Hz, 1H), 6.58 (d, *J* = 6.9 Hz, 3H), 4.46 (s, 2H). ^{13}C NMR (125 MHz, DMSO-d_6): δ = 146.5, 135.9, 129.8, 129.2, 128.1, 127.6, 127.5, 127.3, 126.5, 125.9, 115.2, 114.9, 114.2, 31.9. HRMS-ESI *m/z* [M - H] calcd for $C_{16}H_{13}N_4OS$: 309.0816, found: 309.0821.

6-(2-Amino-5-fluorophenyl)-3-(benzylthio)-1,2,4-triazin-5(2H)-one (2-7b) as a yellow solid (Yield: 80%). ^{1}H NMR (500 MHz, DMSO-d_6): δ = 7.47-7.29 (m, 6H), 7.01 (s, 1H), 6.75 (s, 1H), 4.46 (s, 2H). ^{13}C NMR (125 MHz, DMSO-d_6): δ = 161.1, 158.2, 153.1, 151.3, 147.4, 143.2, 135.8, 128.1, 127.6, 126.5, 116.3, 116.2, 115.9,

115.8, 115.5, 115.3, 31.9. HRMS-ESI *m/z* [M - H] calcd for $C_{16}H_{12}FN_4OS$: 327.0721, found: 327.0728.

6-(2-Amino-5-chlorophenyl)-3-(benzylthio)-1,2,4-triazin-5(2H)-one (2-7c) as a yellow solid (Yield: 87%). ^{1}H NMR (500 MHz, DMSO-d_6): δ = 7.61 (d, *J* = 2.5 Hz, 1H), 7.44 (d, *J* = 6.95 Hz, 2H), 7.34-7.26 (m, 3H), 7.12-7.10 (dd, *J* = 2.55 Hz and 6.3 Hz, 1H), 6.74 (d, *J* = 8.2 Hz, 1H), 4.43 (s, 2H). ^{13}C NMR (125 MHz, DMSO-d_6): δ 163.0, 159.7, 148.5, 146.5, 137.2, 129.8, 129.3, 129.0, 128.5, 127.3, 118.2, 117.9, 117.2, 32.9. HRMS-ESI *m/z* [M - H] calcd for $C_{16}H_{12}ClN_4OS$: 343.0426, found: 343.0438.

6-(2-Amino-5-methylphenyl)-3-(benzylthio)-1,2,4-triazin-5(2H)-one (2-7d) as a yellow solid (Yield: 90%). ^{1}H NMR (500 MHz, DMSO-d_6): δ = 7.47-7.25 (m, 6H), 6.93 (d, *J* = 13.45 Hz, 1H), 6.65 (d, *J* = 13.7 Hz, 1H), 4.45 (s, 2H), 2.16 (s, 3H). ^{13}C NMR (125 MHz, DMSO-d_6): δ = 161.1, 158.6, 148.9, 144.0, 136.0, 129.9, 129.8, 128.0, 127.5, 126.4, 122.7, 115.9, 115.2, 31.9, 19.0. HRMS-ESI *m/z* [M + H] calcd for $C_{17}H_{17}N_4OS$: 325.1118, found: 325.1113.

6-(2-Amino-5-ethylphenyl)-3-(benzylthio)-1,2,4-triazin-5(2H)-one (2-7e) as a yellow solid (Yield: 85%). ^{1}H NMR (500 MHz, DMSO-d_6): δ = 7.45 (d, *J* = 7.55 Hz, 2H), 7.36-7.25 (m, 4H), 6.98 (d, *J* = 8.2 Hz, 1H), 6.67 (d, *J* = 8.85 Hz, 1H), 4.46 (s, 2H), 2.48-2.43 (q, *J* = 7.55 Hz, 2H), 1.10 (t, *J* = 7.55 Hz 3H). HRMS-ESI *m/z* [M + H] calcd for $C_{18}H_{19}N_4OS$: 339.1274, found: 339.1284.

6-(2-Aminophenyl)-3-(4-methoxybenzylthio)-1,2,4-triazin-5(2H)-one (2-7f) as a yellow solid (Yield: 86%). ^{1}H NMR (500 MHz, DMSO-d_6): δ = 7.55 (s, H), 7.37 (d, *J* = 8.2 Hz, 2H), 7.14-7.12 (m, 1H), 6.91-6.89 (m, 3H), 6.74 (d, *J* = 8.8 Hz, 1H), 4.41

(s, 2H), 3.74 (s, 3H). ^{13}C NMR (125 MHz, DMSO-d_6): δ 158.7, 146.5, 130.3, 129.8, 129.7, 128.4, 128.1, 118.2, 117.3, 117.0, 113.9, 113.8, 113.7, 55.1, 32.7.

^{1}H and ^{13}C NMR data of compounds 2-1a and 2-2a:

3-(Benzylthio)-6-(5-(2-chlorophenyl)furan-2-yl)-6,7-dihydro-[1,2,4]triazino[1,6-c]quinazolin-5-ium-1-olate (2-1a2) as an orange-yellow solid (Yield: 50%). ^{1}H NMR (500 MHz, DMSO-d_6): δ = 8.93 (d, *J* = 7.55 Hz, 1H), 8.45 (d, *J* = 3.15 Hz, 1H), 7.51-7.19 (m, 10H), 7.06-6.96 (m, 4H) 6.66 (d, *J* = 3.8 Hz, 1H), 4.35-4.26 (m, 2H). ^{13}C NMR (125 MHz, DMSO-d_6): δ = 170.3, 160.8, 150.2, 148.5, 144.7, 137.6, 134.7, 134.6, 130.7, 129.9, 129.5, 129.2, 128.9, 128.3, 127.8, 127.5, 127.4, 127.0, 119.2, 115.4, 112.4, 112.3, 111.5, 71.3, 33.4. HRMS-ESI *m/z* [M - H] calcd for $C_{27}H_{18}ClN_4O_2S$: 497.0844, found: 497.0839.

3-(Benzylthio)-6-(5-(4-chlorophenyl)furan-2-yl)-6,7-dihydro-[1,2,4]triazino[1,6-c]quinazolin-5-ium-1-olate (2-1a3) as an orange-yellow solid (Yield: 57%). ^{1}H NMR (500 MHz, DMSO-d_6): δ = 8.92 (d, *J* = 13.4 Hz, 1H), 8.44 (s, 1H), 7.52-7.21(m, 11H), 7.07-6.96 (m, 4H), 6.62 (s, 1H), 4.35-4.23 (m, 2H).^{13}C NMR (125 MHz, DMSO-d_6): δ =170.4, 160.9, 152.8, 146.3, 144.8, 137.7, 134.7, 134.6, 134.6, 132.5, 129.9, 128.9, 128.4, 128.2, 127.1, 125.1, 119.3, 115.4, 112.9, 112.4, 107.3, 71.3, 33.5. HRMS-ESI *m/z* [M + H] calcd for $C_{27}H_{20}ClN_4O_2S$: 499.0990 found: 499.0993.

3-(Benzylthio)-6-(5-(4-bromophenyl)furan-2-yl)-6,7-dihydro-[1,2,4]triazino[1,6-c]quinazolin-5-ium-1-olate (2-1a4) as an orange-yellow solid (Yield: 54%). ^{1}H NMR (300 MHz, DMSO-d_6): δ = 8.83 (d, *J* = 8.16 Hz, 1H), 8.45 (d, *J* = 3.51 Hz,

1H), 7.46-7.06 (m, 11H), 6.89 (t, *J* = 7.59 Hz, 2H), 4.34-4.22 (m, 2H). ^{13}C NMR (75 MHz, DMSO-d_6): δ = 170.3, 163.4, 161.5, 161.0, 144.7, 137.6, 134.9, 132.2, 132.1, 130.0, 128.9, 128.8, 128.4, 127.1, 76.0, 33.5. HRMS-ESI *m/z* [M + H] calcd for $C_{27}H_{20}BrN_4O_2S$: 543.0485, found: 543.0493 and HRMS (ESI, $C_{27}H_{19}{}^{81}BrN_4O_2S$ + H) calcd: 545.0464, found: 545.0469.

3-(Benzylthio)-6-(5-(4-nitrophenyl)furan-2-yl)-6,7-dihydro-[1,2,4]triazino[1,6-c]quinazolin-5-ium-1-olate (2-1a5) as an orange-yellow solid (Yield: 52%). ^{1}H NMR (500 MHz, DMSO-d_6): δ = 8.93 (d, *J* = 7.6 Hz, 1H), 7.48 (d, *J* = 3.15 Hz, 1H), 8.36 (d, *J* = 8.8 Hz, 2H), 8.24-8.13 (m, 2H), 7.49 (t, *J* = 7.55 Hz, 1H), 7.37 (d, *J* = 7.55 Hz, 2H), 7.28-7.21 (m, 3H), 7.11 (d, *J* = 8.2 Hz, 2H), 6.93 (t, *J* = 7.55 Hz, 1H), 4.33-4.23 (m, 2H). HRMS-ESI *m/z* [M +Na] calcd for $C_{27}H_{19}N_5O_4SNa$: 532.5010, found: 532.1065.

3-(Benzylthio)-6-ethyl-6,7-dihydro-[1,2,4]triazino[1,6-c]quinazolin-5-ium-1-olate (2-1a6). The crude product was purified using flash chromatography (EtOAc/hexane =1:4) to afford as an orange-yellow solid (Yield: 62%). ^{1}H NMR (300 MHz, DMSO-d_6): δ = 8.87-8.84 (d, *J* = 7.23 Hz, 1H), 7.84 (d, *J* = 3.3 Hz, 1H), 7.40-7.33 (m, 3H), 7.26-7.21 (m, 3H), 6.96-6.85 (m, 2H), 5.54-5.48 (m, 2H), 1.85-1.71 (m, 2H), 0.86 (t, *J* = 7.39 Hz, 3H). ^{13}C NMR (75 MHz, DMSO-d_6): δ = 170.4, 161.2, 144.2, 137.9, 134.7, 134.1, 130.1, 129.1, 128.5, 127.3, 118.8, 115.7, 112.4, 77.3, 33.6, 23.8, 9.7. HRMS-ESI *m/z* [M + H] calcd for $C_{19}H_{19}N_4OS$: 351.1274, found: 351.1279.

3-(Benzylthio)-6-(thiophen-2-yl)-6,7-dihydro-[1,2,4]triazino[1,6-c]quinazolin-5-ium-1-olate (2-1a7) as an orange-yellow solid (Yield: 66%). ^{1}H NMR (500 MHz, DMSO-d_6): δ = 8.88 (d, *J* = 7.6 Hz 1H), 8.52 (d, *J* = 3.2 Hz, 1H), 7.52-7.43 (m, 4H), 7.32-7.23 (m, 3H), 7.15 (d, *J* = 3.75 Hz, 1H), 7.09-7.08 (m, 2H), 6.96-6.94 (m,

2H), 4.38-4.30 (m, 2H). ^{13}C NMR (125 MHz, DMSO-d_6): δ = 170.5, 160.8, 144.2, 138.5, 137.6, 134.9, 133.7, 129.9, 128.9, 128.4, 127.9, 127.8, 127.1, 126.8, 119.4, 115.8, 111.9, 73.7, 33.5. HRMS-ESI *m/z* [M + H] calcd for $C_{21}H_{17}N_4OS_2$: 405.0838, found: 405.0844.

3-(Benzylthio)-6-(5-methylfuran-2-yl)-6,7-dihydro-[1,2,4]triazino[1,6-c]quinazolin-5-ium-1-olate (2-1a8) as an orange-yellow solid (Yield: 60%). ^{1}H NMR (300 MHz, DMSO-d_6): δ = 8.91-8.88 (d, *J* = 8.19 Hz, 1H), 8.37 (s, 1H), 7.49-7.24 (m, 6H), 7.04-6.84 (m, 3H), 6.26 (d, *J*= 2.94 Hz, 1H), 6.02 (s, 1H), 4.35-4.23 (m, 2H), 2.15 (s, 3H). ^{13}C NMR (75 MHz, DMSO-d_6): δ = 170.2, 160.9, 153.4, 146.4, 144.7, 137.7, 134.7, 134.2, 129.9, 128.9, 128.4, 127.1, 119.1, 115.2, 112.0, 111.7, 106.8, 71.6, 33.4, 13.2. HRMS-ESI *m/z* [M + H] calcd for $C_{22}H_{19}N_4O_2Sd$: 403.1223, found: 403.1234.

3-(Benzylthio)-6-phenyl-6,7-dihydro-[1,2,4]triazino[1,6-c]quinazolin-5-ium-1-olate (2-1a9) as an orange-yellow solid (Yield: 68%). ^{1}H NMR (500 MHz, DMSO-d_6): δ = 8.83-8.82 (d, *J* = 6.9 Hz, 1H), 8.5-8.4 (d, *J* = 3.8 Hz, 1H), 7.42-7.24 (m, 10H), 7.08-7.7.06 (d, *J* = 8.15 Hz, 1H), 6.90-6.86 (m, 2H), 4.34-4.24 (m, 2H). ^{13}C NMR (125 MHz, DMSO-d_6): δ = 170.3, 161.0, 144.8, 137.6, 135.9, 134.8, 134.4, 129.9, 129.2, 128.9, 128.6, 128.3, 127.1, 126.3, 119.0, 115.4, 112.0, 76.4, 33.5. HRMS-ESI *m/z* [M +H] calcd for $C_{23}H_{19}N_4OS$: 399.1274, found: 399.1274.

3-(Benzylthio)-6-(quinolin-3-yl)-6,7-dihydro-[1,2,4]triazino[1,6-c]quinazolin-5-ium-1-olate (2-1a10) as an orange-yellow solid (Yield: 55%). ^{1}H NMR (300 MHz, DMSO-d_6): δ = 8.99 (s, 1H), 8.88-8.86 (d, *J* = 8.22 Hz, 1H), 8.53-8.52(d, *J* = 2.64 Hz, 1H), 8.27 (s, 1H), 8.03-7.96 (m, 2H), 7.79 (t, *J* = 7.08 Hz, 1H), 7.64-7.61 (m, 1H), 7.44 (t, *J* = 1.29 Hz, 1H), 7.28-7.07 (m, 7H), 6.92 (t, *J* = 8.07 Hz, 1H), 4.29-4.16

(m, 2H). ^{13}C NMR (125 MHz, DMSO-d_6): δ = 170.3, 161.0, 149.1, 147.5, 144.6, 137.5, 135.0, 134.7, 134.4, 130.5, 130.2, 128.8, 128.6, 128.4, 128.2, 127.3, 127.0, 126.6, 119.4, 115.6, 112.5, 75.4, 33.4. HRMS-ESI *m/z* [M + H] calcd for $C_{26}H_{20}N_5OS$: 450.1383, found: 450.1369.

3-(Benzylthio)-6-(pyridin-3-yl)-6,7-dihydro-[1,2,4]triazino[1,6-c]quinazolin-5-ium-1-olate (2-1a11). as an orange-yellow solid (Yield: 68%). ^{1}H NMR (300 MHz, DMSO-d_6): δ = 8.87-8.84 (d, *J* = 8.04 Hz, 1H), 8.57-8.46(m, 3H), 7.70 (d, *J* = 7.89 Hz, 1H), 7.49-6.90 (m, 10H), 4.32-4.20 (m, 2H). ^{13}C NMR (125 MHz, DMSO-d_6): δ = 170.9, 161.5, 150.9, 148.3, 145.0, 138.0, 135.5, 135.3, 135.2, 130.6, 129.5, 129.4, 129.0, 128.9, 127.6, 120.0, 116.1, 112.7, 75.6, 34.0. HRMS-ESI *m/z* [M + H] calcd for $C_{22}H_{18}N_5OS$: 400.1227, found: 400.1217.

3-(Benzylthio)-6-(pyridin-2-yl)-6,7-dihydro-[1,2,4]triazino[1,6-c]quinazolin-5-ium-1-olate (2-1a12). as an orange-yellow solid (Yield: 87%).. ^{1}H NMR (500 MHz, DMSO-d_6): δ = 8.85 (d, *J* = 8.2, Hz, 1H), 8.53 (d, *J* = 3.8 Hz, 1H), 8.42 (d, *J* = 4.4 Hz, 1H), 7.85-7.81 (m, 1H), 7.52 (d, *J* = 7.6 Hz, 1H), 7.39-7.33 (m, 4H), 7.27-7.21 (m, 3H), 6.96 (t, *J* = 10.1 Hz, 2H), 6.96 (t, *J* = 7.55 Hz, 1H), 4.35-4.24 (m, 2H). ^{13}C NMR (125 MHz, DMSO-d_6): δ = 170.1, 161.2, 154.6, 148.9, 144.0, 137.7, 137.4, 135.3, 134.5, 129.8, 128.9, 128.3, 127.1, 124.4, 119.0, 115.5, 112.6, 76.8, 33.4. HRMS-ESI *m/z* [M + H] calcd for $C_{22}H_{18}N_5OS$: 400.1227, found: 400.1214.

3-(Benzylthio)-6-o-tolyl-6,7-dihydro-[1,2,4]triazino[1,6-c]quinazolin-5-ium-1-olate (2-1a13). as an orange-yellow solid (Yield: 77%). ^{1}H NMR (500 MHz, DMSO-d_6): δ = 8.93 (d, *J* = 8.2 Hz, 1H), 8.13 (s, 1H), 7.43-7.16 (m, 11H), 6.97-6.85 (m, 3H), 4.10-4.02 (m, 2H). ^{13}C NMR (125 MHz, DMSO-d_6): δ =169.8, 161.1, 145.5, 137.7, 137.1, 135.8, 134.5, 133.1, 131.1, 130.1, 129.6, 128.8, 128.3, 127.4, 127.0,

126.1, 118.9, 115.2, 112.4, 75.5, 33.3, 19.3. HRMS-ESI *m/z* [M + H] calcd for $C_{24}H_{21}N_4OS$: 413.1431, found: 413.1435.

3-(Benzylthio)-6-(2-chlorophenyl)-6,7-dihydro-[1,2,4]triazino[1,6-c]quinazolin-5-ium-1-olate (2-1a14) as an orange-yellow solid (Yield: 74%). ^{1}H NMR (500 MHz, DMSO-d_6): δ = 8.94 (d, *J* = 7.6 Hz, 1H), 8.23 (d, *J* = 1.9 Hz, 1H), 7.59 (d, *J* = 8.2 Hz, 1H), 7.49-7.36 (m, 4H), 7.22-7.20 (m, 5H), 6.98-6.92 (m, 3H), 4.13-4.04 (m, 2H). ^{13}C NMR (75 MHz, DMSO-d_6): δ = 170.0, 160.9, 144.9, 137.6, 136.1, 134.7, 132.6, 132.5, 131.5, 130.2, 130.1, 129.3, 128.8, 128.3, 127.7, 127.0, 119.1, 115.2, 112.1, 75.1, 33.3. HRMS-ESI *m/z* [M + H] calcd for $C_{23}H_{18}ClN_4OS$: 433.0884, found: 433.0872.

3-(Benzylthio)-6-(2-(methylthio)phenyl)-6,7-dihydro-[1,2,4]triazino[1,6-c]quinazolin-5-ium-1-olate (2-1a15) as an orange-yellow solid (Yield: 71%). ^{1}H NMR (500 MHz, DMSO-d_6): δ = 8.95 (d, *J* = 8.2 Hz, 1H), 8.16 (d, *J* = 1.85 Hz, 1H), 7.53 (d, *J* = 7.55 Hz, 1H), 7.47-7.41 (m, 2H), 7.37 (d, *J* = 7.55 Hz, 1H), 7.26-7.17 (m, 6H), 6.96-6.91 (m, 3H), 4.12-4.04 (m, 2H). ^{13}C NMR (125 MHz, DMSO-d_6): δ = 169.9, 160.9, 145.0, 138.2, 137.7, 135.9, 134.6, 133.3, 130.4, 130.2, 128.8, 128.1, 127.0125.7, 119.1, 115.3, 112.2, 75.7, 33.3, 16.6. HRMS-ESI *m/z* [M + H] calcd for $C_{24}H_{21}N_4OS_{2:}$ 445.1151 found: 445.1151.

3-(Benzylthio)-6-(3-phenoxyphenyl)-6,7-dihydro-[1,2,4]triazino[1,6-c]quinazolin-5-ium-1-olate (2-1a16) as an orange-yellow solid (Yield: 79%). ^{1}H NMR (500 MHz, DMSO-d_6): δ = 8.83 (d, *J* = 8.2 Hz, 1H), 8.46 (d, *J* = 3.15 Hz, 1H), 7.47-6.89 (m, 18H), 4.33-4.25 (m, 2H). ^{13}C NMR (125 MHz, DMSO-d_6): δ = 170.3, 160.9, 156.9, 155.7, 144.7, 138.0, 137.6, 134.9, 134.4, 130.5, 130.1, 129.9, 128.9, 128.4, 127.1,

123.8, 121.0, 119.1, 118.9, 118.8, 116.2, 115.4, 112.1, 76.0, 33.5. HRMS-ESI *m/z* [M + H] calcd for $C_{29}H_{23}N_4O_2S$: 491.1536, found: 491.1532.

3-(Benzylthio)-6-(3-carboxyphenyl)-6,7-dihydro-[1,2,4]triazino[1,6-c]quinazolin-5-ium-1-olate (2-1a17) as an orange-yellow solid (Yield: 73%). ^{1}H NMR (300 MHz, DMSO-d_6): δ = 8.83 (d, *J* = 7.59 Hz, 1H), 8.54 (s, 1H), 7.97-7.90 (m, 2H), 7.49-7.24 (m, 8H), 7.02-6.89 (m, 3H), 4.33-4.21 (m, 2H). ^{13}C NMR (75 MHz, DMSO-d_6): δ = 170.3, 166.6, 160.9, 144.7, 137.5, 136.4, 134.9, 134.5, 131.2, 130.8, 130.1, 130.0, 129.1, 128.8, 128.3, 127.4, 127.0, 119.1, 115.5, 112.1, 76.1, 33.4. HRMS-ESI *m/z* [M + H] calcd for $C_{24}H_{19}N_4O_3S$: 443.1172, found: 443.1168.

3-(Benzylthio)-6-(3-chlorophenyl)-6,7-dihydro-[1,2,4]triazino[1,6-c]quinazolin-5-ium-1-olate (2-1a18) as an orange-yellow solid (Yield: 69%). ^{1}H NMR (500 MHz, DMSO-d_6): δ = 8.81 (d, *J* = 7.96 Hz, 1H), 8.48 (d, *J* = 3.51 Hz, 1H), 7.49-7.21 (m, 10H), 7.14 (d, *J* = 8.16 Hz, 1H), 6.93-6.81 (m, 2H), 4.34-2.21 (m, 2H). ^{13}C NMR (75 MHz, DMSO-d_6): δ = 170.3, 160.9, 144.5, 138.3, 137.6, 134.8, 134.6, 133.3, 130.6, 130.0, 129.3, 128.8, 128.3, 127.0, 126.4, 125.2, 119.2, 115.5, 112.1, 75.8, 33.4. HRMS-ESI *m/z* [M + H] calcd for $C_{23}H_{18}ClN_4OS$: 433.0884, found: 433.0879.

3-(Benzylthio)-6-(3-nitrophenyl)-6,7-dihydro-[1,2,4]triazino[1,6-c]quinazolin-5-ium-1-olate (2-1a19) as an orange-yellow solid (Yield: 63%). ^{1}H NMR (500 MHz, DMSO-d_6): δ = 8.84 (d, *J* = 8.2 Hz, 1H), 8.58 (d, *J* = 3.15 Hz, 1H), 8.22 (t, *J* = 13.85 Hz, 2H), 7.73-7.63 (m, 2H), 7.49 (t, *J* = 7.55 Hz, 1H), 7.37 (d, *J* = 7.55 Hz, 2H), 7.28-7.21 (m, 3H), 7.11 (d, *J* = 8.2 Hz, 2H), 6.93 (t, *J* = 7.55 Hz, 1H), 4.33-4.23 (m, 2H).^{13}C NMR (125 MHz, DMSO-d_6): δ = 169.5, 159.9, 146.8, 143.4, 137.0, 136.5, 134.0, 133.7, 132.1, 129.4, 129.1, 127.8, 127.3, 126.1, 123.2, 120.7, 118.5, 114.6,

111.2, 74.6, 32.5. HRMS-ESI *m/z* [M + H] calcd for $C_{23}H_{18}N_5O_3S$: 444.1125, found: 444.1127.

3-(Benzylthio)-6-(4-fluorophenyl)-6,7-dihydro-[1,2,4]triazino[1,6-c]quinazolin-5-ium-1-olate (2-1a20) as an orange-yellow solid (Yield: 79%). ^{1}H NMR (300 MHz, DMSO-d_6): δ = 8.92 (d, *J* = 8.16 Hz, 1H), 8.44 (d, *J* = 2.34 Hz, 1H), 7.57-7.21 (m, 9H), 7.07-6.95 (m, 3H), 6.61(d, *J*= 3.51 Hz, 1H), 4.35-4.23 (m, 2H). ^{13}C NMR (75 MHz, DMSO-d_6): δ = 170.3, 163.4, 161.5, 161.0, 144.7, 137.6, 134.9, 134.4, 132.1, 132.1, 130.0, 128.9, 128.9, 128.8, 128.4, 127.1, 119.2, 115.7, 115.5, 112.1, 76.0, 33.5. HRMS-ESI *m/z* [M + H] calcd for $C_{23}H_{18}FN_4OS$: 417.1180, found: 417.1168.

3-(Benzylthio)-6-(4-chlorophenyl)-6,7-dihydro-[1,2,4]triazino[1,6-c]quinazolin-5-ium-1-olate (2-1a21) as an orange-yellow solid (Yield: 76%). ^{1}H NMR (500 MHz, Acetone-d_6): δ = 9.05-9.01 (dd, *J* = 5.8 Hz and 1.47 Hz, 1H), 7.60-7.16 (m, 10H), 7.01-6.98 (m, 1H), 6.96-6.37 (m, 1H), 6.31 (d, *J* = 13.8 Hz, 1H), 4.42-4.28 (m, 2H). ^{13}C NMR (125 MHz, DMSO-d_6): δ = 170.3, 160.9, 144.5, 137.5, 134.9, 134.8, 134.0, 130.0, 128.8, 128.6, 128.4, 128.3, 127.0, 119.2, 115.5, 112.1. HRMS-ESI *m/z* [M + H] calcd for $C_{23}H_{18}ClN_4OS$: 433.0884, found: 433.0886.

3-(Benzylthio)-6-(4-bromophenyl)-6,7-dihydro-[1,2,4]triazino[1,6-c]quinazolin-5-ium-1-olate (2-1a22) as an orange-yellow solid (Yield: 86%). ^{1}H NMR (500 MHz, DMSO-d_6): δ = 8.83-8.82 (m, 1H), 8.48 (d, *J* = 3.8 Hz, 1H), 7.55-7.53 (m, 2H), 7.47-7.44 (m, 1H), 7.37 (d, *J* = 6.95 Hz, 2H), 7.30-7.23 (m, 5H), 7.06 (d, *J* = 8.15 Hz, 1H), 6.90-6.88 (m, 2H), 4.34-4.24 (m, 2H). ^{13}C NMR (125 MHz, DMSO-d_6): δ = 170.3, 160.9, 144.5, 137.6, 135.3, 134.9, 134.4, 131.6, 130.0, 128.9, 128.7, 128.4, 127.1, 122.7, 119.2, 115.5, 112.1, 75.9, 33.5. HRMS-ESI *m/z* [M + H] calcd for

$C_{23}H_{18}BrN_4OS$ 477.0379, found: 477.0379 and HRMS-ESI *m/z* [M + H] calcd for $C_{23}H_{18}{}^{81}BrN_4OS$: 479.0359 found: 479.0366.

3-(Benzylthio)-6-(4-(methylthio)phenyl)-6,7-dihydro-[1,2,4]triazino[1,6-c]quinazolin-5-ium-1-olate (2-1a23) as an orange-yellow solid (Yield: 71%). ^{1}H NMR (300 MHz, DMSO-d_6): δ = 8.84-8.81 (d, *J* = 8.16 Hz, 1H), 8.45 (d, *J* = 3.51 Hz, 1H), 7.46-7.21 (m, 11H), 7.06 (d, *J* = 8.19 Hz, 1H), 6.89-6.85 (m, 2H), 4.37-4.24 (m, 2H), 2.42 (s, 3H). ^{13}C NMR (125 MHz, DMSO-d_6): δ = 169.2, 159.9, 143.7, 138.9, 136.6, 133.8, 133.3, 131.2, 128.9, 127.86, 127.3, 126.0, 125.8, 124.6, 118.0, 114.4, 111.0, 75.2, 32.4, 13.2. HRMS-ESI *m/z* [M + H] calcd for $C_{24}H_{21}N_4OS_2$: 445.1151, found: 445.1132.

3-(Benzylthio)-6-(4-methoxyphenyl)-6,7-dihydro-[1,2,4]triazino[1,6-c]quinazolin-5-ium-1-olate (2-1a24) as an orange-yellow solid (Yield: 51%). ^{1}H NMR (300 MHz, DMSO-d_6): δ = 8.84-8.82 (d, *J* = 7.89 Hz, 1H), 8.5 (d, *J* = 3.51 Hz, 1H), 7.48-7.22 (m, 7H), 7.07 (d, *J* = 8.19 Hz, 1H), 6.92-6.80 (m, 5H), 4.37-4.24 (m, 2H), 3.66 (s, 3H). ^{13}C NMR (125 MHz, DMSO-d_6): δ = 170.2, 160.9, 159.2, 144.8, 137.6, 137.5, 134.8, 134.4, 129.9, 129.9, 128.8, 128.3, 115.4, 114.1, 112.5, 112.0, 76.3, 55.0, 33.4. HRMS-ESI *m/z* [M + H] calcd for $C_{24}H_{21}N_4O_2S$: 429.1380, found: 429.1382.

3-(Benzylthio)-6-(4-nitrophenyl)-6,7-dihydro-[1,2,4]triazino[1,6-c]quinazolin-5-ium-1-olate (2-1a25) as an orange-yellow solid (Yield: 85%). ^{1}H NMR (300 MHz, DMSO-d_6): δ = 8.81 (d, *J* = 7.89 Hz, 1H), 8.6 (d, *J* = 3.51 Hz, 1H), 8.17 (d, *J* = 8.76 Hz), 7.57-7.23 (m, 8H), 7.11-7.07 (m, 2H), 6.90 (t, *J* = 7.29 Hz, 1H), 4.37-4.24 (m, 2H). ^{13}C NMR (75 MHz, DMSO-d_6): δ =170.5, 160.8, 147.9, 144.2, 142.9, 137.5, 134.9, 134.6, 130.0, 128.8, 128.3, 127.9, 127.1, 123.7, 119.4, 115.7, 112.2, 75.6, 33.5. HRMS-ESI *m/z* [M + H] calcd for $C_{23}H_{18}N_5O_3S$: 444.1125, found: 444.1119.

3-(Benzylthio)-6-(4-hydroxy-3-methylphenyl)-6,7-dihydro-[1,2,4]triazino[1,6-c]quinazolin-5-ium-1-olate (2-1a26) as an orange-yellow solid (Yield: 72%). ^{1}H NMR (500 MHz, DMSO-d_6): δ = 9.61 (s, 1H), 8.86 (d, *J* = 8.15 Hz, 1H), 8.34 (d, *J* = 2.5 Hz, 1H), 7.46-7.24 (m, 6H), 7.04 (d, *J* = 7.6 Hz, 2H), 6.93-6.87 (m, 2H), 6.72-6.68 (m, 2H), 4.33-4.22 (m, 2H), 2.03 (s, 3H). ^{13}C NMR (125 MHz, DMSO-d_6): δ = 170.1, 161.1, 156.4, 137.7, 134.7, 134.2, 129.9, 128.9128.8, 128.3, 127.0, 125.9, 125.2, 124.1, 118.8, 115.2, 114.4, 111.9, 76.8, 33.4, 16.0. HRMS-ESI *m/z* [M + H] calcd for $C_{24}H_{21}N_4O_2S$: 429.1380, found: 429.1394.

3-(Benzylthio)-6-(2-chloro-4-hydroxyphenyl)-6,7-dihydro-[1,2,4]triazino[1,6-c]quinazolin-5-ium-1-olate (2-1a27) as an orange-yellow solid (Yield: 70%). ^{1}H NMR (500 MHz, DMSO-d_6): δ = 10.30 (s, 1H), 8.92 (d, *J* = 7.55 Hz, 1H), 8.16 (s, 1H), 7.44-7.21 (m, 7H), 6.95-6.77 (m, 5H), 4.14-4.06 (m, 2H). HRMS-ESI *m/z* [M + Na] calcd for $C_{23}H_{17}ClN_4O_2SNa$: 471.0653 found: 471.0639.

3-(Benzylthio)-6-(3,4-dichlorophenyl)-6,7-dihydro-[1,2,4]triazino[1,6-c]quinazolin-5-ium-1-olate (2-1a28) as an orange-yellow solid (Yield: 68%). ^{1}H NMR (500 MHz, DMSO-d_6): δ = 8.83 (d, *J* = 6.95 Hz, 1H), 8.44 (d, *J* = 3.15 Hz, 1H), 7.61-7.6 (m, 2H), 7.49-7.45 (m, 1H), 7.36-7.23 (m, 6H), 7.06 (d, *J* = 8.15 Hz, 1H), 6.93-6.90 (m, 2H), 4.32-4.21 (m, 2H). ^{13}C NMR (125 MHz, DMSO-d_6): δ = 170.3, 160.9, 137.6, 136.8, 134.9, 134.7, 132.1, 131.4, 130.9, 130.1, 128.8, 128.4, 127.1, 127.0, 119.4, 115.5, 112.2, 75.4, 33.5. HRMS-ESI *m/z* [M + H] calcd for $C_{23}H_{17}Cl_2N_4OS$: 467.0495, found: 467.0484.

3-(Benzylthio)-6-(4-hydroxy-3-nitrophenyl)-6,7-dihydro-[1,2,4]triazino[1,6-c]quinazolin-5-ium-1-olate (2-1a29) as an orange-yellow solid (Yield: 57%). ^{1}H NMR (300 MHz, DMSO-d_6): δ = 11.33 (s, 1H), 8.84 (d, *J* = 8.19 Hz, 1H), 8.40 (d, *J*

= 2.91 Hz, 1H), 7.90 (d, *J* = 2.04 Hz, 1H), 7.50-7.22 (m, 7H), 7.11-7.05 (m, 2H), 6.94-6.85 (m, 2H), 4.32-4.19 (m, 2H). ^{13}C NMR (75 MHz, DMSO-d_6): δ = 170.2, 160.9, 152.8, 144.6, 137.6, 136.4, 134.8, 134.5, 133.3, 130.1, 128.8, 128.3, 127.0, 126.6, 124.0, 119.5, 119.3, 115.4, 112.1, 75.6, 33.4. HRMS-ESI *m/z* [M + H] calcd for $C_{23}H_{18}N_5O_4S$: 460.1074, found: 460.1073.

3-(Benzylthio)-6-(4-fluoro-3-nitrophenyl)-6,7-dihydro-[1,2,4]triazino[1,6-c]quinazolin-5-ium-1-olate (2-1a30) as an orange-yellow solid (Yield: 59%). ^{1}H NMR (500 MHz, DMSO-d_6): δ = 8.85 (d, *J* = 1.3 Hz, 1H), 8.83 (d, *J* = 1.3 Hz, 1H), 8.50 (d, *J* = 3.15 Hz, 1H), 8.17-8.15 (m, 1H), 7.73-7.70 (m, 1H), 7.58-7.54 (m, 1H), 7.507.46 (m,1H), 7.37-7.35 (m, 2H), 7.29-7,20 (m, 3H), 7.09-7.08 (d, *J* = 8.2 Hz, 1H), 7.02 (d, *J* = 3.15 Hz, 1H) 4.31-4.22 (m, 2H). ^{13}C NMR (125 MHz, DMSO-d_6): δ = 170.4,160.9, 155.9, 153.8, 144.2, 137.5, 136.8, 136.6, 134.9, 134.8, 134.7, 134.6, 133.3, 133.2, 128.8, 128.3, 127.0, 124.9, 119.5, 119.0, 118.9, 115.6, 112.2, 75.1, 33.5. HRMS-ESI *m/z* [M + H] calcd for $C_{23}H_{17}FN_5O_3S$: 462.1031, found: 462.1029.

3-(Benzylthio)-6-(4-bromo-3-nitrophenyl)-6,7-dihydro-[1,2,4]triazino[1,6-c]quinazolin-5-ium-1-olate (2-1a31) as an orange-yellow solid (Yield: 67%). ^{1}H NMR (500 MHz, DMSO-d_6): δ = 8.84 (d, *J* = 8.2 Hz, 1H), 8.49 (d, *J* = 8.2 Hz, 1H), 8.03 (d, *J* = 1.9 Hz, 1H), 7.9 (d, *J* = 8.2 Hz, 1H), 7.54-7.47 (m, 2H), 7.36 (d, *J* = 7.55 Hz, 2H), 7.30-7.24 (m, 3H), 7.06 (d, *J* = 8.2 Hz, 1H), 7.00 (d, *J* = 3.15 Hz, 1H), 6.94 (t, *J* = 8.15 Hz, 1H), 4.33-4.22 (m, 2H).^{13}C NMR (125 MHz, DMSO-d_6): δ = 170.4, 160.9, 149.5, 144.1, 137.5, 137.4, 135.0, 134.8, 131.9, 130.2, 128.8, 128.3, 127.0, 124.0, 119.5, 115.7, 114.1, 112.3, 75.3, 33.5. HRMS-ESI *m/z* [M + H] calcd for $C_{23}H_{17}{}^{79}BrN_5O_3S$: 522.0230, found: 522.0221 and HRMS-ESI *m/z* [M + H] calcd for $C_{23}H_{17}{}^{81}BrN_5O_3S$: 524.0210 found: 524.0208.

3-(Benzylthio)-6-(3,5-dibromophenyl)-6,7-dihydro-[1,2,4]triazino[1,6-c]quinazolin-5-ium-1-olate (2-1a32) as an orange-yellow solid (Yield: 65%). ^{1}H NMR (500 MHz, DMSO-d_6): δ = 8.84 (d, *J* = 8.15, Hz, 1H), 8.42 (d, *J* = 3.15 Hz, 1H),7.86 (s, 1H), 7.56 (s, 2H), 7.47 (m, 1H), 7.35-7.23 (m, 5H), 7.06 (d, *J* = 8.2 Hz, 1H), 6.93 (m, 2H), 4.31-4.19 (m, 2H). ^{13}C NMR (125 MHz, DMSO-d_6): δ = 170.2, 160.9, 144.4, 140.2, 137.7, 135.0, 134.9, 130.2, 128.9, 128.8, 128.3, 127.1, 122.6, 119.5, 115.4, 112.2, 75.2, 33.4. HRMS-ESI *m/z* [M - H] calcd for $C_{23}H_{15}Br_2N_4OS$: 552.9339, found: 552.9341, HRMS-ESI *m/z* [M - H] calcd for $C_{23}H_{15}Br^{81}BrN_4OS$: 554.9318, found: 554.9318, HRMS-ESI *m/z* [M - H] calcd for $C_{23}H_{15}{}^{81}Br_2N_4OS$: 556.9298, found: 556.9390.

3-(Benzylthio)-6-(4-bromophenyl)-10-fluoro-6,7-dihydro-[1,2,4]triazino[1,6-c]quinazolin-5-ium-1-olate (2-1a33) as an orange-yellow solid (Yield: 84%). ^{1}H NMR (500 MHz, DMSO-d_6): δ = 8.62 (d, *J* = 8.85 Hz, 1H), 8.38 (s, 1H), 7.55-7.11 (m, 11H), 6.91 (s, 1H), 4.33-4.24 (m, 2H). ^{13}C NMR (125 MHz, DMSO-d_6): δ = 171.0, 160.9, 155.9, 154.0, 141.1, 137.5, 134.9, 133.4, 131.6, 128.8, 128.7, 128.3, 127.0, 122.7, 122.5, 122.3, 117.4, 117.3, 114.9, 114.7, 112.7, 112.6, 76.4, 33.5. HRMS-ESI *m/z* [M - H] calcd for $C_{23}H_{15}BrFN_4OS$: 493.0139 found: 493.0150 and HRMS-ESI *m/z* [M - H] calcd for $C_{23}H_{15}{}^{81}BrFN_4OS$: 495.0119 found: 495.0136.

3-(Benzylthio)-6-(4-chlorophenyl)-10-fluoro-6,7-dihydro-[1,2,4]triazino[1,6-c]quinazolin-5-ium-1-olate (2-1a34) as an orange-yellow solid (Yield: 62%). ^{1}H NMR (500 MHz, DMSO-d_6): δ = 8.63-8.60 (m, 1H), 8.38 (d, *J* = 3.8 Hz, 1H), 7.44-7.22 (m, 10H), 7.11-7.09 (dd, *J* = 5.05 and 3.8 Hz, 1H) 6.93 (d, *J* = 3.8 Hz, 1H), 4.33-4.23 (m, 2H). ^{13}C NMR (125 MHz, DMSO-d_6): δ = 171.0, 160.9, 155.9, 154.0, 141.1, 137.4, 134.5, 134.1, 133.3, 128.8, 128.6, 128.5, 128.3, 127.0, 122.5, 122.3,

117.4, 117.3, 114.9, 114.6, 112.7, 112.6, 76.4, 33.5. HRMS-ESI *m/z* [M +Na] calcd for $C_{23}H_{16}ClFN_4OSNa$: 473.0610, found: 473.0614.

3-(Benzylthio)-10-fluoro-6-(4-(methylthio)phenyl)-6,7-dihydro-[1,2,4]triazino[1,6-c]quinazolin-5-ium-1-olate (2-1a35) as an orange-yellow solid (Yield: 66%). ^{1}H NMR (500 MHz, DMSO-d_6): δ = 8.61 (d, *J* = 8.85 Hz, 1H), 8.36 (s, 1H), 7.39-7.21 (m, 10H), 7.10 (m, 1H) 6.86 (d, *J* = 2.55 Hz, 1H), 4.34-4.25 (m, 2H), 2.41 (s, 3H). ^{13}C NMR (125 MHz, DMSO-d_6): δ = 170.9, 160.9, 155.8, 153.9, 141.3, 140.0, 137.5, 133.2, 131.9, 128.9, 128.4, 127.1, 127.0, 125.6, 122.5, 122.3, 117.3, 117.2, 114.8, 114.6, 112.5, 76.7, 33.5, 14.2. HRMS-ESI *m/z* [M +Na] calcd for $C_{24}H_{19}FN_4OS_2Na$: 485.0877, found: 485.0881.

3-(Benzylthio)-10-fluoro-6-(3-nitrophenyl)-6,7-dihydro-[1,2,4]triazino[1,6-c]quinazolin-5-ium-1-olate (2-1a36) as an orange-yellow solid (Yield: 78%). ^{1}H NMR (500 MHz, DMSO-d_6): δ = 8.62 (d, *J* = 10.1 Hz, 1H), 8.48 (s, 1H), 8.25-8.20 (m, 2H), 7.74-7.62 (m, 2H) 7.40-7.10 (m, 8H), 4.31-4.21 (m, 2H). ^{13}C NMR (125 MHz, DMSO-d_6): δ 171.0, 160.9, 156.0, 155.9, 154.1, 147.8, 140.9, 137.6, 137.4, 133.7, 133.2, 130.3, 128.8, 128.3, 124.2, 122.6, 122.4, 121.8, 117.5, 117.4, 115.0, 114.8, 112.8, 112.7, 76.0, 33.5. HRMS-ESI *m/z* [M - H] calcd for $C_{23}H_{15}FN_5O_3S$: 460.0885, found: 460.0888.

3-(Benzylthio)-10-chloro-6-phenyl-6,7-dihydro-[1,2,4]triazino[1,6-c]quinazolin-5-ium-1-olate (**2-1a37**) as an orange-yellow solid (Yield: 73%). ^{1}H NMR (500 MHz, DMSO-d_6): δ = 8.88 (d, *J* = 2.55 Hz, 1H), 8.63 (d, *J* = 3.15 Hz, 1H), 7.49-7.23 (m, 11H), 7.1 (d, *J* = 3.8 Hz, 1H), 6.94 (d, *J* = 3.15 Hz, 1H), 4.34-4.24 (m, 2H). ^{13}C NMR (125 MHz, DMSO-d_6): δ = 170.9, 160.9, 143.5, 137.5, 135.6, 134.2, 133.2, 129.4,

128.8, 128.7, 128.3, 127.1, 126.4, 122.5, 117.2, 112.9, 76.7, 33.5. HRMS-ESI *m/z* [M - H] calcd for $C_{23}H_{16}ClN_4OS$: 431.0739, found: 431.0750.

3-(Benzylthio)-10-chloro-6-(4-chlorophenyl)-6,7-dihydro-[1,2,4]triazino[1,6-c]quinazolin-5-ium-1-olate (**2-1a38**) as an orange-yellow solid (Yield: 57%). ^{1}H NMR (500 MHz, DMSO-d_6): δ = 8.87 (d, *J* = 2.55 Hz, 1H), 8.61 (d, *J* = 3.15 Hz, 1H), 7.50 (d, *J* = 2.55 Hz, 1H), 7.48 (d, *J* = 3.5 Hz, 2H), 7.43-7.24 (m, 7H), 7.08 (d, *J* = 8.5 Hz, 1H), 6.95 (d, *J* = 3.15 Hz, 1H), 4.33-4.23 (m, 2H). ^{13}C NMR (125 MHz, DMSO-d_6): δ = 170.9, 160.9, 143.3, 137.5, 134.6, 134.3, 134.2, 133.4, 131.1, 128.9, 128.7, 128.5, 128.4, 127.1, 122.7, 117.2, 113.0, 76.1, 33.5. HRMS-ESI *m/z* [M - H] calcd for $C_{23}H_{15}Cl_2N_4OS$: 465.0349 found: 465.0361.

3-(Benzylthio)-10-chloro-6-(4-(methylthio)phenyl)-6,7-dihydro-[1,2,4]triazino[1,6-c]quinazolin-5-ium-1-olate (**2-1a39**) as an orange-yellow solid (Yield: 74%). ^{1}H NMR (500 MHz, DMSO-d_6): δ = 8.86 (d, *J* = 3.25 Hz, 1H), 8.5-8.4 (d, *J* = 4.35 Hz, 1H), 7.51 (d, *J* = 3.55 Hz, 1H), 7.47 (d, *J* = 3.55 Hz, 2H), 7.39-7.24 (m, 7H), 7.07 (d, *J* = 14.5 Hz, 1H), 6.88 (d, *J* = 3.2 Hz, 1H) , 4.35-4.23 (m, 2H) 2.41 (s, 3H). ^{13}C NMR (125 MHz, DMSO-d_6): δ = 170.9, 160.9, 143.5, 140.2, 137.5, 143.3, 133.2, 131.9, 128.9, 128.5, 128.3, 127.1, 126.9, 125.5, 122.5, 117.1, 112.9, 76.5, 33.5, 14.2. HRMS-ESI *m/z* [M + H] calcd for $C_{24}H_{20}ClN_4OS_2$: 479.0762, found: 479.0742.

3-(Benzylthio)-6-(4-chlorophenyl)-10-methyl-6,7-dihydro-[1,2,4]triazino[1,6-c]quinazolin-5-ium-1-olate (2-1a40) as an orange-yellow solid (Yield: 79%). ^{1}H NMR (300 MHz, DMSO-d_6): δ = 8.64 (s, 1H), 8.29 (d, *J* = 3.8 Hz, 1H), 7.40-7.38 (m, 4H), 7.30-7.24 (m, 6H), 6.99 (d, *J* = 8.2 Hz, 1H), 6.87 (d, *J* = 3.8 Hz, 1H), 4.34-4.24 (m, 2H), 2.22 (s, 3H). ^{13}C NMR (125 MHz, DMSO-d_6): δ = 169.3, 159.9, 141.3,

136.6, 135.0, 133.9, 133.3, 132.9, 128.5, 127.9, 127.6, 127.0, 126.0, 114.7, 111.4, 75.0, 32.5, 19.4. HRMS-ESI *m/z* [M + H] calcd for $C_{24}H_{20}ClN_4OS$: 447.1041, found: 447.1042.

3-(Benzylthio)-10-methyl-6-(4-(methylthio)phenyl)-6,7-dihydro-[1,2,4]triazino[1,6-c]quinazolin-5-ium-1-olate (2-1a41) as an orange-yellow solid (Yield: 72%). ^{1}H NMR (300 MHz, DMSO-d_6): δ = 8.63 (s, 1H), 8.27 (s, 1H), 8.39 (d, *J* = 7.6 Hz, 1H), 7.29 (d, *J* = 5.7 Hz, 2H), 7.26-7.19 (m, 8H), 6.98 (d, *J* = 8.2 Hz, 1H), 6.80 (d, *J* = 3.15 Hz, 1H), 4.35-4.25 (m, 2H), 2.24 (s, 3H), 2.22 (s, 3H). ^{13}C NMR (125 MHz, DMSO-d_6): δ = 170.7, 161.5, 143.1, 140.3, 138.1, 136.5, 134.6, 132.8, 129.9, 129.4, 128.8, 128.4, 127.6, 127.3, 126.1, 116.1, 112.8, 76.9, 34.0, 20.9, 14.7. HRMS-ESI *m/z* [M + H] calcd for $C_{25}H_{23}N_4OS_2$: 459.1308, found: 459.1306.

3-(Benzylthio)-6-(5-(4-chlorophenyl)furan-2-yl)-10-methyl-6,7-dihydro-[1,2,4]triazino[1,6-c]quinazolin-5-ium-1-olate (2-1a42) as an orange-yellow solid (Yield: 64%). ^{1}H NMR (300 MHz, DMSO-d_6): δ = 8.74 (s, 1H), 8.28 (s, 1H), 7.46-7.27 (m, 9H), 6.96 (m, 3H), 6.59 (s, 1H), 4.30 (s, 2H), 2.31 (s, 3H). HRMS-ESI *m/z* [M + H] calcd for $C_{28}H_{22}ClN_4O_2S$: 513.1147 found: 513.1124.

3-(Benzylthio)-10-methyl-6-phenyl-6,7-dihydro-[1,2,4]triazino[1,6-c]quinazolin-5-ium-1-olate (2-1a43) as an orange-yellow solid (Yield: 58%). ^{1}H NMR (300 MHz, DMSO-d_6): δ = 8.65 (s, 1H), 8.31 (d, *J* = 3.8 Hz, 1H), 7.40-7.24 (m, 11H), 6.99 (d, *J* = 8.85 Hz, 1H), 6.86 (d, *J* = 3.15 Hz, 1H), 4.36-4.25 (m, 2H), 2.22 (s, 3H). ^{13}C NMR (125 MHz, DMSO-d_6): δ = 169.2, 159.9, 141.6, 136.6, 134.9, 133.2, 128.4, 128.1, 127.9127.6, 127.3, 126.8, 126.1, 125.3, 114.7, 111.3, 75.6, 32.5, 19.4. HRMS-ESI *m/z* [M - H] calcd for $C_{24}H_{21}N_4OS$: 411.1285 found: 411.1286.

Crystal data of compound 2-1a43: Chemical formula = $C_{24}H_{20}N_4OS$, FW = 412.50, monoclinic, space group C2/c, a = 25.0003(14) A˚ , b = 7.7488(4) A˚ , c = 24.1800(14) Å, V = 4078.0(4)A˚^{3}, Z = 8, T = 223 (2) K, $d_{(calcd)}$ = 1.344 Mg.m^{-3}, F (000) = 1728.The final R value was R1 = 0.0516 and wR2 = 0.1301 with $I > 2s(I)$.

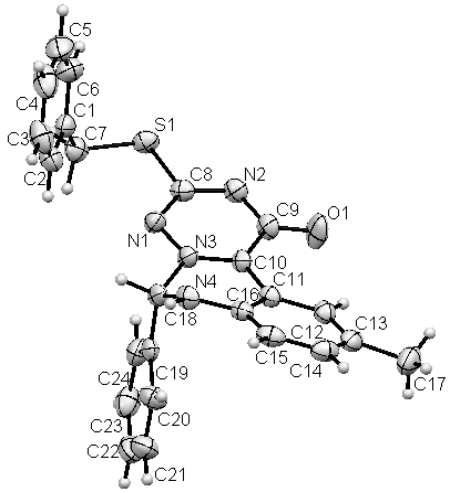

3-(Benzylthio)-10-methyl-6-(5-(4-nitrophenyl)furan-2-yl)-6,7-dihydro-[1,2,4]triazino[1,6-c]quinazolin-5-ium-1-olate (2-1a44) as an orange-yellow solid (Yield: 69%). ^{1}H NMR (500 MHz, DMSO-d$_6$): δ = 8.74 (s, 1H), 8.34-8.11 (m, 3H), 7.71 (d, J = 7.55 Hz, 2H), 7.40-7.22 (m, 8H), 6.99 (d, J = 8.2 Hz, 2H), 6.67 (s, 1H) 4.34-4.25 (m, 2H), 2.29 (s, 3H). ^{13}C NMR (125 MHz, DMSO-d$_6$): δ = 170.4, 160.9, 151.8, 159.0, 146.3, 142.5, 137.7, 135.9, 135.1, 134.6, 129.5, 128.9, 128.4, 127.1, 124.4, 124.2, 115.7, 113.4, 112.6, 110.8, 71.7, 33.5, 20.5. HRMS-ESI *m/z* [M - H] calcd for $C_{28}H_{20}N_5O_4S$: 522.1241 found: 522.1243.

3-(Benzylthio)-6-(4-bromophenyl)-10-methyl-6,7-dihydro-[1,2,4]triazino[1,6-c]quinazolin-5-ium-1-olate (2-1a45) as an orange-yellow solid (Yield: 90%). ^{1}H NMR (500 MHz, DMSO-d$_6$): δ = 8.63 (s, 1H), 8.34-8.11 (m, 3H), 7.71 (d, J= 7.55 Hz, 2H), 7.40-7.22 (m, 8H), 6.99 (d, J= 8.2 Hz, 2H), 6.67 (s, 1H) 4.34-4.25 (m, 2H), 2.29 (s, 3H). ^{13}C NMR (125 MHz, DMSO-d$_6$): δ =170.3, 160.9, 142.4, 137.6, 136.1,

135.4, 134.3, 131.6, 129.5, 128.9, 128.6, 128.4, 128.1, 127.1, 122.6, 115.7, 112.4, 76.1, 33.5, 20.4. HRMS-ESI *m/z* [M - H] calcd for $C_{24}H_{18}BrN_4OS$: 491.0536 found: 491.0534.

3-(Benzylthio)-10-methyl-6-(3-nitrophenyl)-6,7-dihydro-[1,2,4]triazino[1,6-c]quinazolin-5-ium-1-olate (2-1a46) as a orange-yellow solid (Yield: 61%). ^{1}H NMR (300 MHz, DMSO-d_6): δ = 8.65 (s, 1H), 8.39 (d, *J* = 3.2 Hz, 1H), 8.22-8.18 (m, 2H), 7.70-7.61 (m, 2H), 7.38-7.21 (m, 6H), 7.05-7.02 (m, 2H), 4.33-4.23 (m, 2H), 2.23 (s, 3H). ^{13}C NMR (125 MHz, DMSO-d_6): δ = 170.3, 160.8, 147.8, 142.1, 138.0, 137.5, 136.1, 134.5, 133.0, 130.3, 129.5, 128.8, 128.3,4, 128.3, 127.0, 124.1, 121.6, 115.8, 112.4, 75.7, 33.5, 20.4. HRMS-ESI *m/z* [M + H] calcd for $C_{24}H_{20}N_5O_3S$: 458.1281 found: 458.1274.

3-(Benzylthio)-6-(4-bromo-3-nitrophenyl)-10-methyl-6,7-dihydro-[1,2,4]triazino[1,6-c]quinazolin-5-ium-1-olate (2-1a47) as an orange-yellow solid (Yield: 82%). ^{1}H NMR (300 MHz, DMSO-d_6): δ = 8.65 (s, 1H), 8.30 (d, *J* = 3.75 Hz, 1H), 8.00 (d, *J* = 1.9 Hz, 1H), 7.87 (d, *J* = 8.2 Hz, 1H), 7.51-7.49 (m, 1H), 7.37-7.23 (m, 6H), 7.00-6.96 (m, 2H), 4.32-4.21 (m, 2H), 2.23 (s, 3H). ^{13}C NMR (125 MHz, DMSO-d_6): δ = 170.3, 160.9, 149.5, 141.9, 137.5, 137.4, 135.9, 134.9, 134.8, 131.8, 129.9, 128.8, 128.4, 128.3, 127.1, 123.9, 115.9, 114.0, 112.6, 75.4, 33.5, 20.4. HRMS-ESI *m/z* [M + H] calcd for $C_{24}H_{19}BrN_5O_3S$: 536.0386 found: 536.0371 and HRMS (ESI, $C_{24}H_{18}BrN_5O_3S$ + H) calcd: 538.0366 found: 538.0345.

3-(Benzylthio)-6-(4-chlorophenyl)-10-ethyl-6,7-dihydro-[1,2,4]triazino[1,6-c]quinazolin-5-ium-1-olate (2-1a48). The crude product was purified using flash chromatography (EtOAc/hexane =1:4) to afford as an orange-yellow solid (Yield: 80%): ^{1}H NMR (500 MHz, DMSO-d_6): δ = 8.69 (t, *J* = 19.6 Hz, 1H), 8.33-8.26 (m,

1H), 7.44-7.24 (m, 11H), 7.06-6.96 (m, 1H), 6.91-6.83 (m, 1H), 4.34-4.22 (m, 2H), 2.22 (s, 3H). ^{13}C NMR (125 MHz, DMSO-d_6): δ 169.3, 159.9, 141.3, 136.6, 135.0, 133.9, 133.3, 132.9, 128.5, 127.9, 127.6, 127.0, 126.0, 114.7, 111.4, 75.0, 32.5, 19.4. HRMS-ESI *m/z* [M + H] calcd for $C_{25}H_{22}ClN_4OS$: 461.1197, found: 461.1207.

3-(Benzylthio)-10-ethyl-6-(4-(methylthio)phenyl)-6,7-dihydro-[1,2,4]triazino[1,6-c]quinazolin-5-ium-1-olate (2-1a49). The crude product was purified using flash chromatography (EtOAc/hexane =1:4) to afford as an orange-yellow solid (Yield: 75%): ^{1}H NMR (500 MHz, DMSO-d_6): δ = 8.80 (s, 1H), 8.38 (d, *J*= 3.15 Hz, 1H), 7.59-7.29 (m, 11H), 7.10 (d, *J* = 3.2 Hz, 1H), 6.91 (d, *J* = 3.15 Hz, 1H), 4.45-4.35 (m, 2H), 2.65-2.59 (q, *J* = 7.55 Hz, 2H), 1.24 (t, *J* = 7.6 Hz, 3H). ^{13}C NMR (125 MHz, DMSO-d_6): δ = 170.1, 160.9, 142.7, 139.8, 137.6, 134.8, 134.2, 134.1, 132.3, 128.8, 128.3, 126.9, 126.8, 125.6, 115.6, 112.2, 76.3, 33.5, 27.4, 14.2. HRMS-ESI *m/z* [M + H] calcd for $C_{26}H_{25}N_4OS_2$: 473.1464, found: 473.1476.

3-(4-Methoxybenzylthio)-6-phenyl-6,7-dihydro-[1,2,4]triazino[1,6-c]quinazolin-5-ium-1-olate (2-1a50) as an orange-yellow solid (Yield: 67%). ^{1}H NMR (500 MHz, DMSO-d_6): δ = 8.83 (d, *J* = 3.2 Hz, 1H), 8.48 (d, *J* = 3.15 Hz), 7.47-7.29 (m, 8H), 7.07 (d, *J*= 3.2 Hz, 1H), 6.91-6.84 (m, 4H), 4.29-4.20 (m, 2H), 3.72 (s, 3H HRMS-ESI *m/z* [M - H] calcd for $C_{2419}N_4O_2S$: 427.1234 found: 427.1228.

3-(4-Methoxybenzylthio)-6-(3-nitrophenyl)-6,7-dihydro-[1,2,4]triazino[1,6-c]quinazolin-5-ium-1-olate (2-1a51) as an orange-yellow solid (Yield: 63%). ^{1}H NMR (500 MHz, DMSO-d_6): δ = 8.84 (d, *J* = 7.6 Hz, 1H), 8.58 (s, 1H) 8.24-8.21 (m, 2H), 7.73-7.65 (m, 2H), 7.49 (d, *J* = 6.35 Hz, 1H), 7.28 (d, *J*= 6.35 Hz, 2H), 7.10 (d, *J*= 3.8 Hz, 2H), 6.94-6.81 (m, 3H), 4.27-4.17 (m, 2H), 3.71 (s, 3H). ^{13}C NMR (125 MHz, DMSO-d_6): δ = 171.1, 161.4, 158.9, 148.3, 144.9, 138.5, 135.5, 135.1, 130.9,

130.6, 130.5, 129.7, 124.7, 122.2, 119.9, 116.1, 114.2, 112.7, 76.1, 55.5, 33.6. HRMS-ESI *m/z* [M - H] calcd for $C_{24}H_{20}N_5O_4S$: 472.1085 found: 472.1086.

6-(4-Chlorophenyl)-3-(4-methoxybenzylthio)-6,7-dihydro-[1,2,4]triazino[1,6-c]quinazolin-5-ium-1-olate (2-1a52) as an orange-yellow solid (Yield: 76%).^{1}H NMR (500 MHz, DMSO-d_6): δ = 8.84 (d, *J* = 8.2 Hz, 1H), 8.47 (d, *J* = 3.75 Hz, 1H), 7.47-7.29 (m, 7H), 7.07 (d, *J* = 8.2 Hz, 2H), 6.92-6.83 (m, 4H), 4.29-4.19 (m, 2H), 3.72 (s, 3H). ^{13}C NMR (125 MHz, DMSO-d_6): δ = 171.0, 161.4, 158.9, 145.0, 135.4, 135.4, 134.9, 134.5, 130.6, 130.5, 129.7, 129.2, 128.9, 119.7, 116.0, 114.3, 112.6, 76.4, 55.5, 33.6. HRMS-ESI *m/z* [M - H] calcd for $C_{24}H_{18}ClN_4O_2S$: 461.0844, found: 461.0865.

3-(4-Methoxybenzylthio)-6-(4-(methylthio)phenyl)-6,7-dihydro-[1,2,4]triazino[1,6-c]quinazolin-5-ium-1-olate (2-1a53) as an orange-yellow solid (Yield: 71%). ^{1}H NMR (500 MHz, DMSO-d_6): δ = 8.83 (d, *J* = 3.2 Hz, 1H), 8.45 (s, 1H) 7.46 (t, *J* = 7.55 Hz, 1H), 7.31 (d, *J*= 8.15 Hz, 2H), 7.21 (d, *J*= 6.35 Hz, 4H), 7.06 (d, *J*= 3.2 Hz, 1H), 6.90-6.83 (m, 4H), 4.30-4.20 (m, 2H), 3.72 (s, 3H), 2.41 (s, 3H). ^{13}C NMR (125 MHz, DMSO-d_6): δ = 170.9, 161.5, 158.9, 145.2, 140.5, 135.3, 134.8, 132.8, 132.8, 130.6, 130.5, 129.8, 127.4, 126.1, 119.6, 115.9, 114.3, 112.6, 76.7, 55.5, 33.6, 14.7. HRMS-ESI *m/z* [M - H] calcd for $C_{25}H_{21}N_4O_2S_2$: 473.1111, found: 473.1117.

3-(4-Bromobenzylthio)-6-(4-chlorophenyl)-1-oxo-6,7-dihydro-1H-[1,2,4]triazino[1,6-c]quinazolin-5-ium-4(2)-ide (2-1a54) as an orange-yellow solid (Yield: 88%). ^{1}H NMR (500 MHz, DMSO-d_6): δ = 8.83 (s, 1H), 8.50 (s, 1H), 7.74 – 6.69 (m, 12H), 4.25 (m, 2H). ^{13}C NMR (125 MHz, DMSO-d_6): δ = 170.07, 160.93, 144.62, 137.45, 134.95, 134.86, 134.55, 134.07, 131.17, 131.06, 130.07, 128.67,

128.40, 120.17, 119.22, 115.54, 112.09, 75.88, 32.77. HRMS-ESI *m/z* [M - H] calcd for $C_{23}H_{15}BrClN_4OS$ - H) calcd: 508.9844, found: 508.9830, HRMS-ESI *m/z* [M - H] calcd for $C_{23}H_{15}{}^{81}BrClN_4OS$: 510.9823, found: 510.9809.

3-(4-Bromobenzylthio)-6-(4-(methylthio)phenyl)-1-oxo-6,7-dihydro-1H-[1,2,4]triazino[1,6-c]quinazolin-5-ium-4(2)-ide (2-1a55) as an orange-yellow solid (Yield: 81%). ^{1}H NMR (500 MHz, DMSO-d_6): δ = 8.83 (s, 1H), 8.47 (s, 1H), 7.26 (dd, *J* = 136.3, 49.0 Hz, 10H), 6.86 (d, *J* = 16.5 Hz, 2H), 4.26 (m, 2H), 2.40 (s, 3H). ^{13}C NMR (125 MHz, DMSO-d_6): δ = 169.99, 160.97, 144.81, 140.02, 137.51, 134.91, 134.41, 132.20, 131.18, 131.05, 130.03, 126.90, 125.56, 120.16, 119.06, 115.46, 112.02, 76.23, 32.78, 14.24. HRMS-ESI *m/z* [M - H] calcd for $C_{24}H_{18}BrClN_4OS_2$: 521.0111, found: 521.0113, HRMS-ESI *m/z* [M - H] calcd for $C_{24}H_{18}{}^{81}BrClN_4OS_2$: 523.0090, found: 523.0090.

3-(3-Bromobenzylthio)-6-(4-chlorophenyl)-1-oxo-6,7-dihydro-1H-[1,2,4]triazino[1,6-c]quinazolin-5-ium-4(2)-ide (2-1a56) as an orange-yellow solid (Yield: 57%). ^{1}H NMR (500 MHz, DMSO): δ = 8.86 (s, 1H), 8.62-6.93 (m, 12H), 8.54 (s, 1H), 4.33 (s, 1H). ^{13}C NMR (125 MHz, DMSO-d_6): δ = 170.04, 160.95, 144.64, 140.85, 134.94, 134.55, 134.06, 131.49, 130.46, 129.94, 128.68, 128.39, 127.96, 121.53, 119.23, 115.54, 112.10, 75.89, 32.74. HRMS-ESI *m/z* [M - H] calcd for $C_{23}H_{15}BrClN_4OS$ - H) calcd: 508.9844, found: 508.9842, HRMS-ESI *m/z* [M - H] calcd for $C_{23}H_{15}{}^{81}BrClN_4OS$ calcd: 510.9823, found: 510.9819.

3-(3-Bromobenzylthio)-6-(4-(methylthio)phenyl)-1-oxo-6,7-dihydro-1H-[1,2,4]triazino[1,6-c]quinazolin-5-ium-4(2)-ide (2-1a57) as an orange-yellow solid (Yield: 60%). ^{1}H NMR (500 MHz, DMSO-d_6): δ = 8.84 (s, 1H), 8.49 (s, 1H), 8.11 – 6.40 (m, 12H), 4.30 (m, 2H), 2.40 (s, 3H). ^{13}C NMR (125 MHz, DMSO-d_6): δ =

169.96, 160.98, 144.84, 140.90, 139.99, 134.92, 134.41, 132.19, 131.49, 130.47, 129.95, 127.98, 126.90, 125.62, 121.53, 119.07, 115.46, 112.04, 76.24, 32.74, 14.25. HRMS-ESI *m/z* [M - H] calcd for $C_{24}H_{18}BrClN_4OS_2$: 521.0111, found: 521.0114, HRMS-ESI *m/z* [M - H] calcd for $C_{24}H_{18}{}^{81}BrClN_4OS_2$: 523.0090, found: 523.0093.

3-(4-Chlorobenzylthio)-6-(4-chlorophenyl)-1-oxo-6,7-dihydro-1H-[1,2,4]triazino[1,6-c]quinazolin-5-ium-4(2)-ide (2-1a58) as an orange-yellow solid (Yield: 84%). ^{1}H NMR (500 MHz, DMSO-d_6): δ = 8.80 (d, *J* = 6.9 Hz, 1H), 8.47 (s, 1H), 7.58 – 7.15 (m, 9H), 7.04 (d, *J* = 6.8 Hz, 1H), 6.88 (s, 2H), 4.25 (m, 2H). ^{13}C NMR (125 MHz, DMSO-d_6): δ = 170.10, 160.95, 144.65, 137.05, 134.97, 134.91, 134.59, 134.08, 131.68, 130.75, 130.09, 128.71, 128.43, 128.29, 119.25, 115.56, 112.11, 75.89, 32.71. HRMS-ESI *m/z* [M - H] calcd for $C_{23}H_{15}Cl_2N_4OS$: 465.0349, found: 465.0355.

3-(4-Chlorobenzylthio)-6-(4-(methylthio)phenyl)-1-oxo-6,7-dihydro-1H-[1,2,4]triazino[1,6-c]quinazolin-5-ium-4(2)-ide (2-1a59) as an orange-yellow solid (Yield: 73%). ^{1}H NMR (500 MHz, DMSO-d_6): δ = 8.82 (s, 1H), 8.46 (s, 1H), 7.69 – 6.54 (m, 12H), 4.28 (m, 2H), 2.41 (s, 3H). ^{13}C NMR (125 MHz, DMSO-d_6): δ = 170.01, 160.95, 144.82, 140.01, 137.09, 134.91, 134.44, 132.23, 131.65, 130.72, 130.02, 128.28, 126.91, 125.58, 119.07, 115.46, 112.03, 76.23, 32.70, 14.22. HRMS-ESI *m/z* [M - H] calcd for $C_{24}H_{18}ClN_4OS_2$: 477.0616, found: 477.0612.

3-(3-Chlorobenzylthio)-6-(4-chlorophenyl)-1-oxo-6,7-dihydro-1H-[1,2,4]triazino[1,6-c]quinazolin-5-ium-4(2)-ide (2-1a60) as an orange-yellow solid (Yield: 71%). ^{1}H NMR (500 MHz, DMSO-d_6): δ = 8.83 (s, 1H), 8.50 (s, 1H), 7.38 (dd, *J* = 51.0, 31.1 Hz, 10H), 7.07 (s, 1H), 6.91 (s, 2H), 4.29 (m, 2H). ^{13}C NMR (125 MHz, DMSO-d_6): δ = 170.04, 160.95, 144.65, 140.61, 134.96, 134.86, 134.58,

134.06, 132.90, 130.19, 130.08, 128.69, 128.65, 128.40, 127.60, 127.06, 119.24, 115.54, 112.11, 75.89, 32.76. HRMS-ESI *m/z* [M - H] calcd for $C_{23}H_{15}Cl_2N_4OS$: 465.0349, found: 465.0345.

3-(3-Chlorobenzylthio)-6-(4-(methylthio)phenyl)-1-oxo-6,7-dihydro-1H-[1,2,4]triazino[1,6-c]quinazolin-5-ium-4(2)-ide (2-1a61) as an orange-yellow solid (Yield: 75%). ^{1}H NMR (500 MHz, DMSO-d_6): δ = 8.83 (s, 1H), 8.47 (s, 1H), 7.60 – 6.98 (m, 11H), 6.86 (d, *J* = 19.3 Hz, 2H), 4.30 (m, 2H), 2.40 (s, 3H). ^{13}C NMR (125 MHz, DMSO-d_6): δ = 170.46, 161.47, 145.34, 141.14, 140.49, 135.42, 134.93, 133.40, 132.69, 130.70, 130.51, 129.14, 128.11, 127.56, 127.39, 126.11, 119.57, 115.95, 112.53, 76.73, 33.25, 14.73. HRMS-ESI *m/z* [M - H] calcd for $C_{24}H_{18}ClN_4OS_2$: 477.0616, found: 477.0617.

6-(4-Chlorophenyl)-3-(4-fluorobenzylthio)-1-oxo-6,7-dihydro-1H-[1,2,4]triazino[1,6-c]quinazolin-5-ium-4(2)-ide (2-1a62) as an orange-yellow solid (Yield: 62%). ^{1}H NMR (500 MHz, DMSO-d_6): δ = 8.84 (s, 1H), 8.51 (s, 1H), 7.18 (dd, *J* = 181.4, 64.2 Hz, 12H), 4.28 (m, 2H). ^{13}C NMR (125 MHz, DMSO-d_6): δ = 170.26, 162.24, 160.99, 160.30, 144.62, 134.92, 134.54, 134.09, 134.02, 130.88, 130.82, 130.07, 128.69, 128.44, 119.24, 115.56, 115.18, 115.01, 112.14, 75.93, 32.70. HRMS-ESI *m/z* [M - H] calcd for $C_{23}H_{15}ClFN_4OS$: 449.0645, found: 449.0635.

3-(4-Fluorobenzylthio)-6-(4-(methylthio)phenyl)-1-oxo-6,7-dihydro-1H-[1,2,4]triazino[1,6-c]quinazolin-5-ium-4(2)-ide (2-1a63) as an orange-yellow solid (Yield: 80%). ^{1}H NMR (500 MHz, DMSO-d_6): δ = 8.84 (s, 1H), 8.45 (s, 1H), 7.14 (dd, *J* = 103.2, 70.5 Hz, 12H), 4.29 (d, *J* = 10.2 Hz, 2H), 2.41 (s, 3H). ^{13}C NMR (125 MHz, DMSO-d_6): δ = 170.19, 162.89, 161.01, 159.66, 144.80, 140.04, 134.89, 134.42, 134.09, 132.28, 130.91, 130.80, 130.02, 126.94, 125.64, 119.10, 115.50,

115.25, 114.97, 112.09, 76.30, 32.71, 14.26. HRMS-ESI *m/z* [M - H] calcd for $C_{24}H_{18}FN_4OS_2$: 461.0912, found: 461.0924.

6-(4-Chlorophenyl)-3-(3-fluorobenzylthio)-1-oxo-6,7-dihydro-1H-[1,2,4]triazino[1,6-c]quinazolin-5-ium-4(2)-ide (2-1a64) as an orange-yellow solid (Yield: 82%). ^{1}H NMR (500 MHz, DMSO-d_6): δ = 8.82 (d, *J* = 8.3 Hz, 1H), 8.48 (s, 1H), 7.56 – 7.16 (m, 8H), 7.07 (t, *J* = 8.0 Hz, 2H), 6.98 – 6.79 (m, 2H), 4.30 (m, 2H). ^{13}C NMR (125 MHz, DMSO-d_6): δ = 170.08, 163.61, 160.94, 160.38, 144.62, 140.90, 140.80, 134.94, 134.89, 134.58, 134.06, 130.30, 130.19, 130.06, 128.67, 128.41, 124.95, 119.24, 115.75, 115.55, 115.46, 114.05, 113.77, 112.12, 75.91, 32.87. HRMS-ESI *m/z* [M - H] calcd for $C_{23}H_{15}ClFN_4OS$: 449.0645, found: 449.0639.

3-(3-Fluorobenzylthio)-6-(4-(methylthio)phenyl)-1-oxo-6,7-dihydro-1H-[1,2,4]triazino[1,6-c]quinazolin-5-ium-4(2)-ide (2-1a65) as an orange-yellow solid (Yield: 71%). ^{1}H NMR (500 MHz, DMSO-d_6): δ = 8.83 (s, 1H), 8.47 (s, 1H), 7.74 – 6.67 (m, 12H), 4.32 (m, 2H), 2.40 (s, 3H). ^{13}C NMR (125 MHz, DMSO-d_6): δ = 170.00, 162.96, 160.98, 144.82, 140.90, 140.84, 139.99, 134.90, 134.41, 132.22, 130.28, 130.22, 130.01, 126.90, 125.60, 124.99, 119.06, 115.70, 115.53, 115.45, 113.99, 113.83, 112.04, 76.23, 32.85, 14.22. HRMS-ESI *m/z* [M - H] calcd for $C_{24}H_{18}FN_4OS_2$: 461.0912, found: 461.0923.

6-(4-Chlorophenyl)-3-(4-cyanobenzylthio)-1-oxo-6,7-dihydro-1H-[1,2,4]triazino[1,6-c]quinazolin-5-ium-4(2)-ide (2-1a66) as an orange-yellow solid (Yield: 71%). ^{1}H NMR (500 MHz, DMSO-d_6): δ = 8.82 (d, *J* = 8.2 Hz, 1H), 8.46 (d, *J* = 3.4 Hz, 1H), 7.72 (d, *J* = 8.1 Hz, 2H), 7.58 (d, *J* = 8.1 Hz, 2H), 7.46 (t, *J* = 7.5 Hz, 1H), 7.40 (d, *J* = 8.5 Hz, 2H), 7.06 (d, *J* = 8.2 Hz, 1H), 6.89 (dd, *J* = 10.1, 5.6 Hz, 2H), 4.35 (m, 2H). ^{13}C NMR (125 MHz, DMSO-d_6): δ = 169.76, 160.86, 144.62,

144.10, 134.96, 134.80, 134.65, 134.07, 132.16, 130.04, 129.80, 128.64, 128.39, 119.23, 118.69, 115.54, 112.07, 109.74, 75.89, 33.02. HRMS-ESI *m/z* [M - H] calcd for $C_{24}H_{15}ClN_5OS$: 456.0691, found: 456.0700.

3-(4-Cyanobenzylthio)-6-(4-(methylthio)phenyl)-1-oxo-6,7-dihydro-1H-[1,2,4]triazino[1,6-c]quinazolin-5-ium-4(2)-ide (2-1a67) as an orange-yellow solid (Yield: 65%). ^{1}H NMR (500 MHz, DMSO-d_6): δ = 8.82 (d, *J* = 7.6 Hz, 1H), 8.44 (s, 1H), 7.72 (d, *J* = 7.3 Hz, 2H), 7.58 (d, *J* = 7.2 Hz, 2H), 7.45 (d, *J* = 7.1 Hz, 1H), 7.17 (d, *J* = 8.0 Hz, 4H), 7.06 (d, *J* = 7.6 Hz, 1H), 6.88 (t, *J* = 7.0 Hz, 1H), 6.81 (s, 1H), 4.36 (m, 2H), 2.41 (s, 3H). ^{13}C NMR (125 MHz, DMSO-d_6): δ 169.67, 160.87, 144.80, 144.16, 140.02, 134.91, 134.49, 132.16, 129.99, 129.79, 126.88, 125.55, 119.04, 118.70, 115.44, 111.98, 109.71, 76.22, 33.02, 14.20. HRMS-ESI *m/z* [M - H] calcd for $C_{25}H_{18}N_5OS_2$: 469.1031, found: 469.0959.

6-(4-Chlorophenyl)-3-(4-methoxybenzylthio)-10-methyl-1-oxo-6,7-dihydro-1H-[1,2,4]triazino[1,6-c]quinazolin-5-ium-4(2)-ide (2-1a68) as an orange-yellow solid (Yield: 68%). ^{1}H NMR (500 MHz, DMSO-d_6): δ = 8.64 (s, 1H), 8.31 (s, 1H), 7.64 – 7.15 (m, 7H), 7.07 – 6.73 (m, 4H), 4.24 (m, 2H), 3.72 (s, 3H), 2.22 (s, 3H). ^{13}C NMR (125 MHz, DMSO-d_6): δ = 170.45, 160.97, 158.39, 142.36, 136.03, 135.02, 134.25, 133.95, 130.12, 129.49, 129.21, 128.67, 128.34, 128.08, 115.77, 113.80, 112.39, 76.06, 55.01, 33.15, 20.41. HRMS-ESI *m/z* [M - H] calcd for $C_{25}H_{20}ClN_4O_2S$ calcd: 475.1001, found: 475.1003.

3-(4-Methoxybenzylthio)-10-methyl-6-(4-(methylthio)phenyl)-1-oxo-6,7-dihydro-1H-[1,2,4]triazino[1,6-c]quinazolin-5-ium-4(2)-ide (2-1a69) as an orange-yellow solid (Yield: 76%). ^{1}H NMR (500 MHz, DMSO-d_6): δ = 8.63 (s, 1H), 8.28 (s, 1H), 7.45 – 7.08 (m, 7H), 6.99 (d, *J* = 7.9 Hz, 1H), 6.83 (d, *J* = 7.8 Hz, 3H), 4.25 (m, 2H),

3.72 (s, 3H), 2.40 (s, 3H), 2.22 (s, 3H). ^{13}C NMR (125 MHz, DMSO-d_6): δ = 170.37, 161.00, 158.39, 142.55, 139.85, 135.99, 134.12, 132.36, 130.12, 129.44, 129.28, 127.90, 126.85, 125.61, 115.68, 113.81, 112.32, 76.39, 55.02, 33.15, 20.41, 14.22. HRMS-ESI *m/z* [M - H] calcd for $C_{26}H_{23}N_4O_2S_2$: 487.1268, found: 487.1277.

3-(Benzylthio)-10-methyl-6-(4-chlorophenyl)-[1,2,4]triazino[1,6-c]quinazolin-5-ium-1-olate (2-2a1) as a yellow solid (Yield: 82%). ^{1}H NMR (500 MHz, DMSO): δ = 9.83 (s, 1H), 8.11 (d, *J* = 8.2 Hz, 1H), 8.00 (dd, *J* = 8.2Hz and 1.25 Hz, 1H), 7.94-7.92 (m, 2H), 7.65-7.63 (m, 2H), 7.25-7.21 (m, 3H), 7.15-7.14 (m, 2H), 4.16 (s, 1H), 2.65 (s, 3H), 2.54 (m, 3H). ^{13}C NMR (125 MHz, DMSO-d_6): δ = 169.5, 162.0, 149.5, 143.5, 141.6, 137.6, 135.2, 135.1, 132.3, 131.8, 128.7, 128.3, 128.1, 127.9, 127.1, 127.0, 119.7, 33.4, 21.8. HRMS-ESI *m/z* [M + H] calcd for $C_{24}H_{18}ClN_4OS$: 445.0884 found: 445.0900.

Crystal data of compound 2-2a1:

Chemical formula = $C_{24}H_{17}ClN_4O_{1.25}S$, FW = 448.93, monoclinic, space group P2(1)/c, *a* = 12.3523(19) A˚ , *b* = 8.2615(13) A˚ , c = 20.944(3*)* Å, V = 2106.6(6)A˚^{3}, *Z* = 4, *T* =

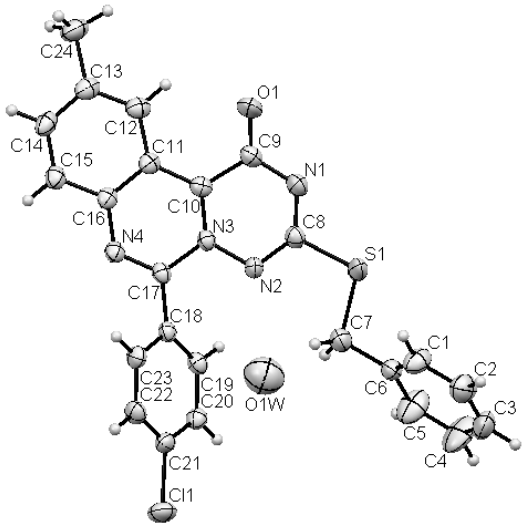

223 (2) K, $d_{(calcd)}$ = 1.416 Mg.m^{-3}, *F* (000) = 928.The final *R* value was *R*1 = 0.0538 and w*R*2 = 0.1309 with $I > 2s(I)$. A small residual peak was treated as partially occupied water (25%). H atoms of the waters were not located.

3-(Benzylthio)-10-methyl-6-(4-(methylthio)phenyl)-[1,2,4]triazino[1,6-c]quinazolin-5-ium-1-olate (2-2a2). as a yellow solid (Yield: 70%). ^{1}H NMR (500 MHz, DMSO-d_6): δ = 9.79 (s, 1H), 8.05 (d, *J* = 8.2 Hz, 1H), 8.00 (d, *J* = 1.85 Hz, 1H), 7.90-7.89 (m, 2H), 7.44-7.42 (m, 2H), 7.26-7.16 (m, 5H), 4.19 (s, 2H), 2.63 (s, 3H), 2.54 (m, 3H). ^{13}C NMR (125 MHz, DMSO-d_6): δ = 169.5, 162.2, 150.1, 143.5, 142.0, 141.3, 137.7, 137.5, 135.1, 131.1, 128.9, 128.8, 128.3, 127.9, 127.0, 124.4, 119.5, 33.4, 21.9, 14.2 . HRMS-ESI *m/z* [M + H] calcd for $C_{25}H_{21}N_4OS_2$: 457.1151 found: 457.1161.

3-(Benzylthio)-10-ethyl-6-(4-(methylthio)phenyl)-[1,2,4]triazino[1,6-c]quinazolin-5-ium-1-olate (2-2a3). as a yellow solid (Yield: 85%). ^{1}H NMR (500 MHz, DMSO-d_6): δ = 9.86 (s, 1H), 8.13-8.10 (m, 2H), 7.88 (d, *J* = 8.15 Hz, 2H), 7.43 (d, *J* = 8.85 Hz, 2H), 7.26-7.16 (m, 5H), 4.21 (s, 2H), 2.97-2.92 (q, *J* = 7.55 Hz, 2H), 2.53 (s, 3H), 1.33 (t, *J* = 8.2 Hz, 3H) . ^{13}C NMR (125 MHz, DMSO-d_6): δ = 169.4, 162.3, 150.2, 147.2, 143.8, 141.9, 137.6, 136.5, 135.3, 131.1, 128.9, 128.8, 128.3, 128.2, 127.0, 125.9, 124.4, 119.6, 33.4, 28.8, 15.4, 14.2. HRMS-ESI *m/z* [M + H]$^{+}$: calcd for $C_{26}H_{23}N_4OS_2$: 471.1308 found: 471.1309.

Chapter 3

Synthesis and the Biological Evaluation of 2-{6-[2-(5-Phenyl-4H-[1,2,4]triazol-3-ylsulfanyl)acetylamino]benzothiazol-2-ylsulfanyl}acetamides as Potential Anti-West Nile Virus Agents

3.1 Synthesis of analogues of the lead compound

To optimize the potency of scaffold **3-1a**, a library of structurally diverse analogues of compound **3-1a1** was synthesized for biological evaluation of their inhibitory activities. To the best of our knowledge, the synthesis of compound **3-1a** has not been reported earlier. To develop a synthetic strategy to prepare compound **3-1a** expediently, we carried out a retrosynthetic analysis of the compound (Figure 3.1). Disconnection of compound **3-1a** at the amide and C-S bonds gave 4 fragments: triazole **3-2a**, amino benzothiazole (or benzoimidazole) -2-thione **3-3**, amine **3-4** and bromoacetyl bromide.

Figure 3.1 Retrosynthesis of compound **3-1a**.

Compound **3-2a** was prepared from the respective benzoic acid **3-5** (Scheme 3.1a) by first treating it with either (i) methanol and concentrated H_2SO_4 under microwave irradiation for 15 min, or (ii) oxalyl chloride and DMF at room temperature for 2.5 h[106] to provide the respective methyl ester **3-6a** or acyl chloride **3-6b** in good yields. Li and coworkers[107] have previously reported that reacting compound **3-6a** (R^1=H) with hydrazine hydrate in ethanol under overnight reflux gave benzohydrazide **3-7** in 83% yield. To shorten the reaction time, we explored refluxing compound **3-6a** with neat hydrazine hydrate. The reaction was completed within 20 min and the benzohydrazide **3-7** that formed precipitated from the cold reaction mixture in good yield. Conversion of **3-7** to compound **3-8** was adapted from an earlier reported procedure where the reaction was performed on the surface of silica gel under

Scheme 3.1 Synthesis of compound **3-2a**

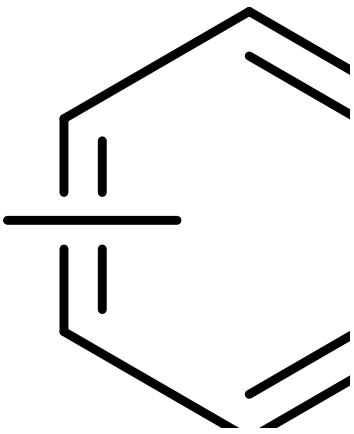

microwave irradiation.[108] However, we found that treating compound **3-7** with alkylisothiocyanate under microwave irradiation at 130 ^{o}C and in the absence of silica gel gave compound **3-8** in higher yields (76-86%). It is worth noting that when $R^1 \neq NH_2$, compound **3-8** could be obtained directly from acyl chloride **3-6b** by reacting it with thiosemicarbazide at room temperature.[109] With compound **3-8** in our hands, we proceeded with the cyclization reaction in sodium hydroxide solution under microwave irradiation at 150 ^{o}C. The reaction was completed in 3 min (versus 1h under conventional reflux) to provide 1,2,4-triazole-5(4H)-thione **3-2a** in good yield. We have also synthesized compound **3-2a12** from **3-2a6** by reducing the nitro group with iron and concentrated HCl (Scheme 3.1b).

Scheme 3.2 Synthesis of compound **3-3**

Compound **3-3** was prepared by first treating 2-aminothiophenol or o-phenylenediamine **3-9** with CS_2 in the presence of KOH under microwave irradiation to provide intermediate **3-10** (Scheme 3.2). Nitration of compound **3-10** followed by reduction of the nitro group with iron powder and concentration HCl afforded compound **3-3** in moderately good yield.

Compounds **3-2**, **3-3** and various commercially available amines or anilines **3-4** were coupled as shown in Scheme 3.3. Compound **3-4** was treated with bromoacetyl bromide to yield compound **3-12** which was then reacted with the thiolate anion, generated *in situ* from the reaction of compound **3-3** with KOH, to provide compound **3-13**. Subsequent coupling of the amino group on **3-13** with another molecule of bromoacetyl bromide gave intermediate **3-14** which precipitated readily from the

Scheme 3.3 Synthesis of compound **3-1a**

reaction mixture. Finally, regioselective coupling of compound **3-2a** with compound **3-14** under basic conditions gave compound **3-1a** in moderately good yield.

3.2 Structure-activity relation studies

A representative set of 40 analogues of compound **3-1a** were synthesized and tested in a WNV assay at 50 μM concentration to identify potential inhibitors. Inhibitors

exhibiting more than 50% inhibition were further evaluated for their effects at different concentrations and the IC_{50} values of each compound were calculated using the Graphpad Prism software (Table 3.1). The fluorogenic peptide Pyr-RTKR-AMC was used as a substrate for the WNV NS2B-NS3 protease and the K_m value was determined, using the protocol from the SensoLyte® 440 West Nile Virus Protease Assay Kit, to be 3.45±0.41 μM.

In our preliminary SAR studies, we examined the effects of substituents on the inhibitory activity of the compound by varying the X, R^1, R^2 and R^5 groups of compound **3-1a1** (Table 3.1, cpds **3-1a2** to **3-1a10**). However, these changes did not provide any significant improvement in the activity. Hence, we proceeded to screen the inhibitory activity of the unsubstituted compound by changing both R^1 and R^2 on compound **3-1a1** to H (Table 3.1, cpd **3-1a11**). To our delight, an enhancement in the inhibition of the WNV NS2B-NS3 protease was observed, indicating that the 5-phenyl-1,2,4-triazole group plays an important role in the compound's inhibitory

Table 3.1 IC_{50} values of compound **3-1a**[a]

Cpd	R^1	R^2	X	R^3	n	R^4	R^5	IC_{50} (μM)
3-1a2	*p*-NH_2	Me	S	H	1	H	F	45.67±6.40
3-1a3	*p*-NH_2	Me	S	H	1	H	OMe	>50
3-1a4	*p*-NH_2	Me	NH	H	1	H	H	NA[b]
3-1a5	*p*-NH_2	Me	NH	H	1	H	F	NA
3-1a6	*p*-NH_2	Et	S	H	1	H	H	NA
3-1a7	*p*-NH_2	Et	S	H	1	H	F	NA
3-1a8	H	Me	S	H	1	H	H	>50
3-1a9	H	Me	S	H	1	H	F	>50
3-1a10	H	Et	S	H	1	H	H	NA
3-1a11	H	H	S	H	1	H	H	14.27±2.51
3-1a12	H	H	S	H	1	H	F	29.28±3.62
3-1a13	H	H	S	H	1	H	OMe	>50
3-1a14	H	H	S	H	1	H	Me	>50
3-1a15	H	H	NH	H	1	H	H	NA
3-1a16	H	H	NH	H	1	H	F	NA
3-1a17	H	H	NH	H	1	H	OMe	NA

3-1a18	H	H	S	Me	1	H	H	NA
3-1a19	H	H	S	H	0	H	H	>50
3-1a20	H	H	S	H	0	H	F	>50
3-1a21	H	H	S	H	0	H	Cl	10.93±2.58
3-1a22	H	H	S	H	0	H	OMe	8.79±0.23
3-1a23	H	H	S	H	0	H	Me	7.13±0.87
3-1a24	H	H	S	H	0	H	Et	3.35±0.15
3-1a25	H	H	S	H	0	H	*n*-Pr	4.15±0.63
3-1a26	H	H	S	H	0	F	H	>50
3-1a27	H	H	S	H	0	Cl	H	>50
3-1a28	H	H	S	H	0	OMe	H	29.44±4.78
3-1a29	H	H	S	H	0	Et	H	>50
3-1a30	H	H	NH	H	0	H	Et	NA
3-1a31	H	Me	S	H	0	H	Et	NA
3-1a32	*p*-NH_2	H	S	H	0	H	Et	>50
3-1a33	*p*-NO_2	H	S	H	0	H	Et	>50
3-1a34	*p*-OH	H	S	H	0	H	Et	>50
3-1a35[c]	cyclohexyl	H	S	H	0	H	Et	>50
3-1a36[d]	*n*-Pr	H	S	H	0	H	Et	NA
3-1a37	*o*-Me	H	S	H	0	H	Et	5.63±1.44
3-1a38[e]	pyridine-4-yl	H	S	H	0	H	Et	>50
3-1a39	*p*-NH_2	Me	S	H	0	H	Et	20.06±3.59
3-1a40[f]	H	H	S	H	0	-	-	29.76±2.8

[a] Data represent the concentrations required to inhibit the WNV NS2B-NS3 protease activity by 50% and are the mean±SE of triplicate experiments; compounds used are ≥95% pure. [b] NA: no activity. [c] Phenyl group containing R^1 was replaced by a cyclohexyl ring. [d] Phenyl group containing R^1 was replaced by a n-propyl group. [e] Phenyl group containing R^1 was replaced by a pyridine-4-yl ring. [f] Phenyl group containing R^4 and R^5 was replaced by a cyclohexyl ring.

activity. Further modifications by varying the X and R^5 groups on compound **3-1a11** (Table 3.1, cpds **3-1a12** to **3-1a18**) resulted in a loss of the inhibitory activity. Next we proceeded to explore the effect of the methylene linker. Analogues of **3-1a11** were synthesized with various aniline derivative **3-4** (Table 3.1, cpds **3-1a19** to **3-1a29**) and the screening results showed that the presence of alkyl substituent on R^5 (Table 3.1, cpds **3-1a23** to **3-1a25**) significantly amplified the compound's inhibition activity. The best inhibition was observed in compound **3-1a24** which contains an ethyl group

at the para-position (=R^5) of the phenyl ring. Further tuning of compound **3-1a24** by varying the substituents on X, R^1 and R^2 (Table 3.1, cpds **3-1a30** to **3-1a39**) did not result in further improvement of the inhibitory activity, confirming the importance of the 5-phenyl-1,2,4-triazole and benzothiazole fragments in the compound's inhibitory activity. In addition, replacing the phenyl ring with a cyclohexyl moiety (Table 3.1, cpd **3-1a40**) provided a compound with modest inhibition against the WNV NS2B-NS3 protease.

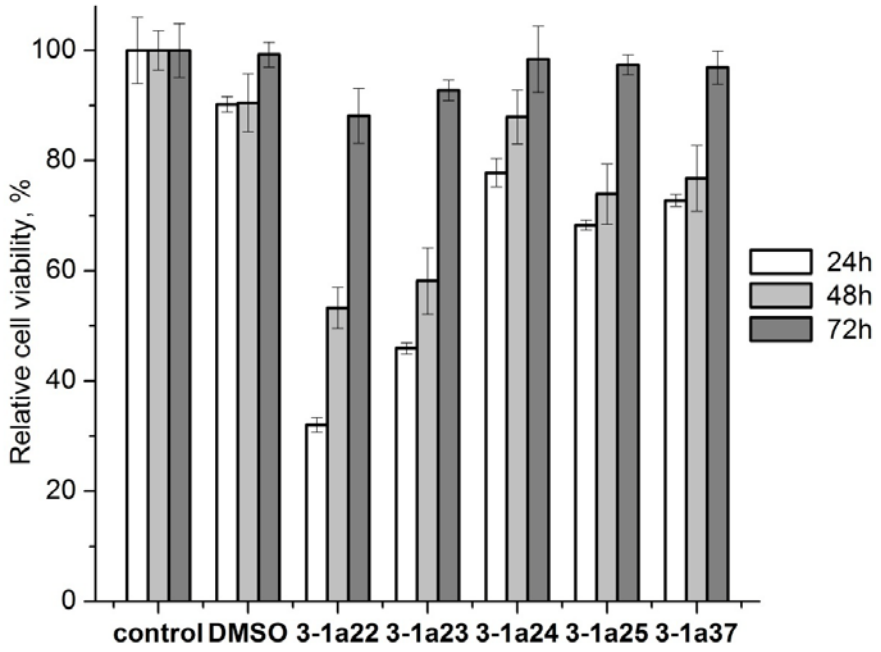

Figure 3.2 MTS assay results obtained at incubation times of 24 ( ), 48 ( ) and 72 h ( ) with the BHK21 cell line. Compounds were added at a final concentration of 25 µM.

The stabilities of compounds **3-1a22**, **3-1a23**, **3-1a24**, **3-1a25** and **3-1a37** in the assay buffer (pH 8) were determined by analyzing the amount of compound remaining with time using LCMS-IT-TOF detection. Quantization of the compounds was determined by Shimadzu's LCsolution software. Compounds **3-1a22**, **3-1a23**, **3-1a24**, **3-1a25** and **3-1a37** showed excellent stability in a pH 8 buffer after 72 h at 37 ^{o}C without any

degradation. Next, we evaluated the cytotoxicities of compounds **3-1a22**, **3-1a23**, **3-1a24**, **3-1a25** and **3-1a37** against baby hamster kidney fibroblast (BHK21) cells at different incubation timings. Vehicular control, dimethyl sulfoxide (DMSO), was also included to serve as control as the test compounds were dissolved in DMSO. The amount of DMSO used in the assay was controlled at 0.2% of the total volume. This is to ensure that DMSO does not result in cytotoxicity of cells. From the results obtained (Figure 3.2), the three strongest candidates identified from our earlier SAR

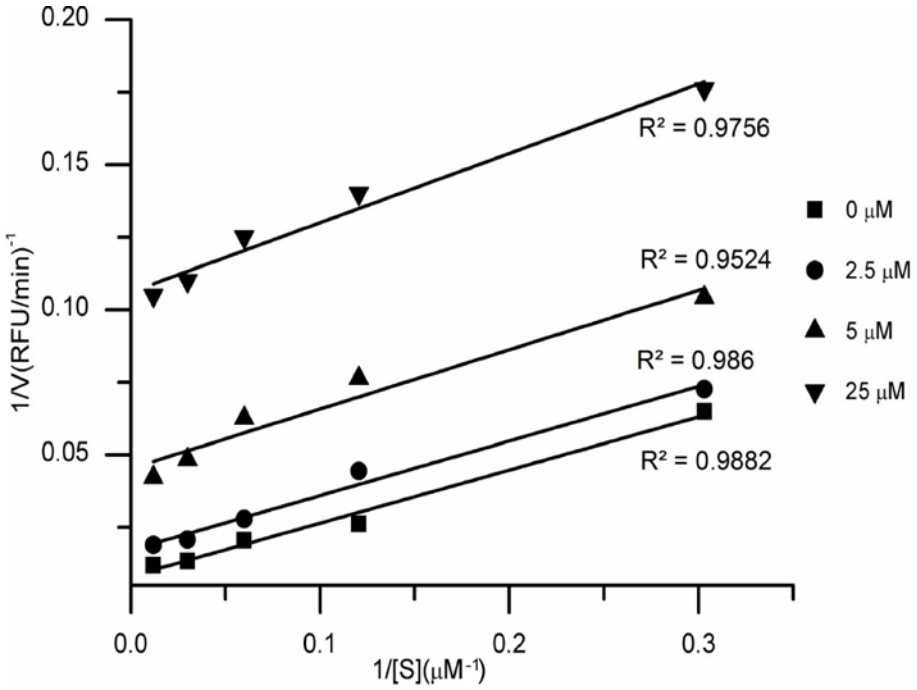

Figure 3.3 Uncompetitive inhibition of **3-1a24** with WNV NS2B-NS3 protease: WNV protease assays were performed at various concentrations of **3-1a24** (0, 2.5, 5.0 and 25μM) and substrate (3.3, 8.3, 16.7, 33.3, 83.3μM). Double reciprocal plots of 1/V versus 1/[S] for **3-1a24** at each inhibitor concentration were plotted using the OriginPro 8.

studies, compounds **3-1a24**, **3-1a25** and **3- 1a37** were also shown to be non-cytotoxic to BHK21 cells with compound **3-1a24** being the least toxic of the three compounds.

To determine the inhibition mode of compound **3-1a24**, we followed the kinetics of inhibition using Pyr-RTKR-AMC as substrate. Lineweaver-Burk analysis (Figure 3.3) of the initial velocities of this substrate concentration-dependent inhibition of the NS2B-NS3 protease activity suggested that the inhibition by compound **3-1a24** was uncompetitive with respect to the substrate with a K_i value of 2.77±0.13 μM. Uncompetitive inhibition by the compound **3-1a24**, due to the absence of charge on the inhibitor that prefers active site of the protease.

3.3 Docking analysis

A docking study was performed to rationalize the inhibition and kinetics result as well as to identify the possible binding sites of compound on the WNV NS2B-NS3 protease. The crystal structure of the WNV NS2B-NS3 protease in complex with peptide Bz-Nle-Lys-Arg-Arg-H (pdb 2fp7) has been reported earlier.[74] To identify the potential binding site of compound **3-1a24** on the NS2B-NS3 protease, *in silico* docking studies was performed with Molecular Operating Environment (MOE) using these crystal structure coordinates. Since compound **3-1a24** is an uncompetitive inhibitor of the WNV NS2B-NS3 protease, we focused our analysis on regions beyond the substrate binding sites. Earlier studies have shown that the integration of residues 78-87 of NS2B into the protease-cofactor complex affected the formation of the catalytic active sites.[74,75,105] Deletion or mutagenesis of these residues produced an inert enzyme. Therefore, the region on the NS3 protease where key interactions with the NS2B cofactor (residue 78-87) occur is important for the NS2B-NS3 protease activity and particularly attention was paid to this region during our docking studies. The best docked pose for compound **3-1a24** and the WNV NS2B-NS3 protease is

shown in Figure 3.4. The docking analysis predicted two strong π-cation type interactions between the guanidine group in Arg78 of the NS2B cofactor and the phenyl ring directly attached to triazole. Arg78 was also observed to form a hydrogen

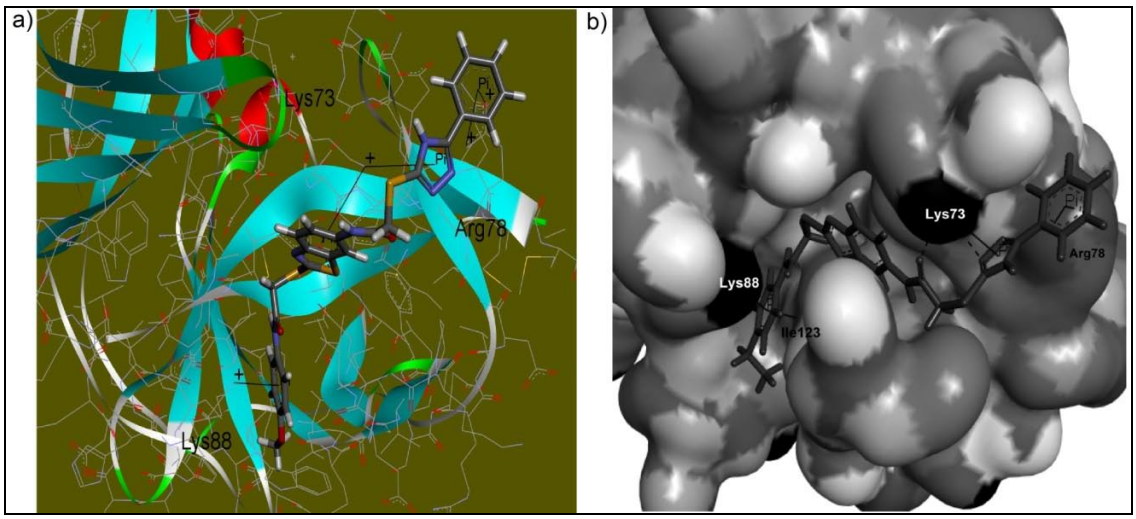

Figure 3.4 Molecular docking of compound **3-1a24** onto WNV NS2B-NS3 protease. The WNV protease crystal structure coordinates (pdb 2fp7)[74] were used for the molecular docking. a) The NS2B-NS3 protease is shown as a wireframe and flat ribbon model and the inhibitor is shown as a stick model; b) surface representation of NS2B-NS3 protease shows the electrostatic potential where blue represents positive, white represents neutral and red represents negative electrostatic potential. Docked inhibitor is shown in stick model. All views were generated using Discovery Studio 3.1 client.

bonding with the triazole nitrogen. Since the interaction of Arg78 with a ligand interferes with the productive interaction of the NS2B cofactor with the catalytic active site in the NS3 protease, these bonding interactions between compound **3-1a24** and Arg78 are important factors contributing to the compound's inhibitory potency. Other interactions present involve the phenyl ring containing R^4 and R^5 which is attracted to Lys88 and Ile123 of NS3 via strong π-cation and π-π type bonding respectively and the strong π-π bonding between the triazole ring in compound **3-1a24**

with Lys73 from NS3 protease. At the same time, the nitrogen atom on triazole and the oxygen atom on the amide group directly linked to benzothiazole of **3-1a24** were observed to interact with Lys73 of NS3 via hydrogen bonding. Amino acid residues that are in close proximity (less than 5 Å) to atoms of compound **3-1a24** include Arg78, Leu79, Asp80, Asp81 and Phe85 of NS2B and Lys73, Glu74, Arg76, Lys88, Trp89, Gly91, Val115, Pro119, Glu120, Glu122, Ile123, Gly124 and Ile147 of NS3. These results support our experimental inhibition assay data that compound **3-1a24** is an allosteric inhibitor of the WNV NS2B-NS3 protease.

3.4 Conclusion

In this study, we have identified a lead compound **3-1a1** with moderate inhibitory activity against the WNV NS2B-NS3 protease. Refinement of this initial "hit" by synthesizing a focused library of **3-1a1** derivatives for SAR studies provided compound **3-1a24** which inhibited the interaction of the NS2B cofactor and the NS3 protease in low micromolar concentration (IC_{50} = 3.35±0.15 μM) and in an uncompetitive manner. Compound **3-1a24** is stable under physiological condition and is non-cytotoxic to baby hamster kidney fibroblast cells. Further studies are presently ongoing to further develop compound **3-1a24** as a potential antiviral therapeutic.

3.5 Experimental section

3.5.1 Chemistry

All chemical reagents and anhydrous solvent were obtained from Aldrich, Merck, Lancaster or Fluka and used without further purification. Flash chromatography was

performed with silica (Merck, 70-230 mesh) whilst TLC was carried out on pre-coated plates (Merck silica gel 60, F254) and visualized with UV light. Final compounds were purified on a Gilson preparative HPLC system with a Waters C_{18} column (250 x 10.0 mm, 5 μm). Purity of the compound was determined by analytical HPLC using a Shimadzu LCMS-IT-TOF system with a Phenomenex C18 column (50 mm x 3.0 mm, 5 μm). Purity of the compound was checked at 254 nm and integration was obtained with Shimadzu LCMS solution software. ^{1}H and ^{13}C NMR spectra were recorded using $CDCl_3$, acetone-d_6, or DMSO-d_6 as solvents and tetramethylsilane (TMS) as an internal reference on a Bruker AMX500 or a Bruker ACF300 Fourier transform spectrometer. The following abbreviations were used to explain the multiplicities: s (singlet), d (doublet), t (triplet), dd (doublet of doublet), q (quartet), and m (multiplet). The number of protons (n) for a given resonance was indicated as nH. Mass spectrometry was performed on a Finnigan/MAT LCQ mass spectrometer using electron spray ionization (ESI) or electron impact (EI)

General procedure for the synthesis of 3-6a (L=OMe)

To a solution of the corresponding benzoic acid **3-5** (3.9 mmol) in methanol (15 mL) was added concentrated H_2SO_4 (0.39 mmol). The reaction mixture was microwave irradiated at 130 °C (with the heating program starting at 150 W) for 15 min. Thereafter, the reaction mixture was concentrated and saturated $NaHCO_3$ was added slowly at room temperature until no more bubbling occurred. The reaction mixture was then extracted with EtOAc (20x3 mL) and the combined organic layer was dried over Na_2SO_4, concentrated and purified via a short column chromatography using EtOAc/hexane (2:3 or 1:49) as the eluent. The product obtained was dried overnight in a vacuum oven at 50 °C to provide compound **3-6a** in 86-95% yield.

General procedure for the synthesis of 3-6b (L=Cl)

To a solution of the corresponding benzoic acid **3-5** (9.0 mmol) in CH_2Cl_2 (30 mL) was added oxalyl chloride (27.5 mmol) and DMF (2 drops) at 0 °C. The mixture was allowed to stir at room temperature for 2.5 h. After which, the reaction mixture was concentrated and the crude product obtained was used directly for the next reaction.

General procedure for the synthesis of 3-7

To the corresponding methyl benzoate **3-6a** (3 mmol) was added hydrazine hydrate (5 mL, 100 mmol). The reaction mixture was stirred and heated under reflux for 20 min. Thereafter, the reaction mixture was cooled to room temperature and then to -15 °C for 10 min. The precipitate that formed was filtered and washed with ice-cold water (3 mL). After which, the crude product **3-7** was dried overnight in a vacuum oven at 50 °C and used for the next reaction. The crude yield of **3-7** was 82-90%.

General procedure for the synthesis of 3-8 (R^2=Me or Et)

The corresponding benzohydrazide **3-7** (3.6 mmol) was added to a solution of alkyl isothiocyanate (3.96 mmol) in THF (12 mL). The mixture was irradiated under microwave at 130 °C (with the heating program starting at 150 W) for 8 min. Thereafter the reaction mixture was concentrated and extracted with EtOAc/H_2O. The combined organic layer was dried over Na_2SO_4, concentrated and purified by column chromatography using EtOAc/hexane (starting from 3:7 to 3:2) as the eluent. The product obtained was dried overnight in a vacuum oven at 50 °C to provide compound **3-8** in 76-86% yield.

General procedure for the synthesis of 3-8 (R^2=H)

Commercially available acid chloride (9.0 mmol) or crude product **3-6b** (L = Cl, 9.0 mmol) was added slowly to a mixture of thiosemicarbazide (19.6 mmol) in THF (20 mL) at 0 ^oC. The reaction mixture was stirred at room temperature for 1.5 h. Thereafter, the reaction mixture was concentrated and the residue was triturated with water. The product which precipitated from the reaction mixture was filtered, washed with water and dried overnight under vacuum at 50 °C to yield product **3-8** in 60-87% yield. This product was directly used for the next reaction.

General procedure for the synthesis of 3-2a

To compound **3-8** (3.4 mmol) was added NaOH (2 M, 15 mL) and the reaction mixture was irradiated under microwave at 150 °C (with the heating program starting at 150 W) for 3 min. Thereafter, the solution was neutralized with acetic acid, and extracted with EtOAc (3x15 mL). The combined organic layer was dried over Na_2SO_4, concentrated, and purified by flash column chromatography using EtOAc/hexane (starting with EtOAc/hexane = 1:5 and then changing to EtOAc/hexane = 1:2) as the eluent. The product was dried overnight under vacuum at 50 °C to provide compound **3-2a** in 71-94% yield.

Synthesis of 3-(4-aminophenyl)-1H-1,2,4-triazole-5(4H)-thione 3-2a12

To a mixture of iron powder (10 mmol) in 80% aqueous ethanol (5 mL) was added concentrated HCl (1 mmol) and the reaction mixture was stirred in a warm (40 °C) water bath. Thereafter 3-(4-nitrophenyl)-1H-1,2,4-triazole-5(4H)-thione **3-2a6** (R^1 = NO_2, 2 mmol) was added portionwise and the resulting reaction mixture was stirred and heated under reflux for 45 min. After which ethanol was removed on a rotavapor

and the residual reaction mixture was adjusted to ~pH 13 with NaOH. The reaction mixture was then filtered by suction filtration and the filtrate was adjusted to pH 5 with glacial acetic acid. The precipitate which formed was filtered and purified by flash column chromatography using EtOAc/hexane (starting with EtOAc/hexane = 1:1 and then changing to EtOAc/hexane = 2:1) as eluent. The product obtained was dried overnight under vacuum at 50 °C to yield compound **3-2a12** in 61% yield.

General procedure for the synthesis of 3-10

To a mixture of KOH (5.5 mmol) in 80% aqueous ethanol (7.5 mL) was added carbon disulfide (5.5 mmol) and the reaction mixture was stirred at room temperature for 15 min. Thereafter, the corresponding phenylamine **3-9** (5 mmol) was added and the reaction mixture was irradiated under microwave at 130 °C (with the heating program starting at 150 W) for 15 min and then cooled to room temperature. After which, the reaction mixture was diluted with water (10 mL), adjusted to pH 5 with glacial acetic acid and cooled to 0 °C for 1h to complete the crystallization. The shiny precipitate that formed was filtered and dried overnight under vacuum at 50 °C to yield compound **3-10** in 85-94 % yield.

General procedure for the synthesis of 3-11

The corresponding azole derivative **3-10** (3.0 mmol) was slowly dissolved in concentrated H_2SO_4 (1.4 mL, 25.7 mmol) with cooling at 0 ^oC to -5 ^oC. Thereafter, a mixture of fuming HNO_3 (0.4 mL, 9.6 mmol) and concentrated H_2SO_4 (0.3 mL, 5.6 mmol) was added dropwise and the reaction mixture was stirred for 1 h at 0 ^oC to -5 ^oC then poured into ice. The precipitate that formed was filtered and dissolved in a minimum volume of 25% aqueous ammonia solution. The resultant solution was heated at 50 ^oC and filtered under suction. The filtrate was cooled to 0 ^oC and adjusted

to pH 2 with 6M HCl. The precipitate that formed was filtered and purified by flash column chromatography using EtOAc/hexane (starting with EtOAc/hexane = 1:2 and then changing to EtOAc/hexane = 1:1) as eluent. The product was dried overnight under vacuum at 50 °C and compound **3-11** was obtained in 48-65% yield.

General procedure for the synthesis of 3-3

The procedure is similar to that used for the synthesis of **3-2b12**. However the precipitate which formed was purified by flash column chromatography using EtOAc/hexane (starting with EtOAc/hexane = 2:3 and then changing to EtOAc/hexane = 2:1) as eluent. The product was dried overnight under vacuum at 50 °C and compound **3-3** was obtained in 67-74% yield.

General procedure for the synthesis of 3-12

To a mixture of bromoacetyl bromide (5.3 mmol) in acetonitrile (50 mL) at 0 ^{o}C was added dropwise the corresponding amine or aniline **3-4** (4.4 mmol). After addition, the mixture was stirred at room temperature for 1 h. Acetonitrile was removed by rotary evaporation and the residue was extracted with an EtOAc/H_2O solvent system. The combined organic layer was concentrated and purified by flash column chromatography using EtOAc/hexane (starting with EtOAc/hexane = 1:10 and then changing to EtOAc/hexane = 3:10) as eluent. The product was dried overnight under vacuum at 50 °C and compound **3-12** was obtained in 68-87% yield.

General procedure for the synthesis of 3-13

Compound **3-3** (0.3 mmol) was dissolved in a mixture of KOH (0.6 mmol) in 60% aqueous ethanol (20 mL). Thereafter, the corresponding intermediate **3-12** (0.3 mmol) was added and the reaction mixture was stirred for 1h at room temperature. When the

reaction had completed (monitored by TLC), ethanol was removed by rotary evaporation and the residual mixture was neutralized with dilute acetic acid followed by extraction with EtOAc (3x15 mL). The combined organic layer was concentrated and purified using a short silica column with EtOAc/hexane (starting with EtOAc/hexane = 3:10 and then changing to EtOAc/hexane = 1:4) as eluent. The semi-pure product obtained was dried under high vacuum at room temperature and used for next step of the reaction.

General procedure for the synthesis of 3-14

To the corresponding intermediate **3-13** (4.4 mmol) in CH_2Cl_2 (30 mL) at 0 ^oC was added bromoacetyl bromide (5.3 mmol) dropwise. After addition, the reaction mixture was stirred at room temperature for 1 h. The product which precipitated from the reaction mixture was filtered, washed with CH_2Cl_2 (3x15 mL) and dried overnight under vacuum at 50 °C to provide compound **3-14** in 73-86 % yield.

General procedure for the synthesis of 3-1a

The corresponding triazole compound **3-2a** (0.22 mmol) was dissolved in a mixture of KOH (0.66 mmol) in 60% aqueous ethanol (16 mL). The corresponding intermediate **3-14** (0.22 mmol) was added and the reaction mixture was stirred for 2 h at room temperature. Thereafter, ethanol was removed by rotary evaporation and the residual mixture was neutralized with dilute acetic acid followed by extraction with EtOAc/H_2O. The combined organic layer was concentrated and purified by reverse phase HPLC using solvent A with 0.1% TFA in water, and solvent B was 0.1% TFA in acetonitrile as the mobile phase. Detection was conducted at 254nm, the mobile phase was a gradient with solvent B increasing from 15% to 95% over 30 min and a flow rate of 8.0ml/min. Fractions containing the pure product were combined,

concentrated and dried overnight under vacuum at 50 °C to give compound **3-1a** in 56-83 % yield.

3.5.2 Biology

All the compounds used in the biological testing were at least 95% pure. Compounds were tested against the WNV NS2B-NS3 protease using the SensoLite® 440 WNV protease assay kit (Catalog # 72079) and the active recombinant WNV protease (Calalog # 72081) which were purchased from Anaspec (USA). This protease assay kit uses a fluorogenic peptide Pyr-RTKR-AMC as substrate. Eight different substrate concentrations ranging from 1 μM to 80 μM were incubated in 96-well plates with 0.3 μg/mL recombinant WNV protease at 37 °C in the assay buffer provided. The increase in fluorescence intensity was monitored using an Infinite F200 microplate reader (Tecan, Switzerland) at an excitation wavelength of 354 nm (±10 nm) and emission wavelength of 442 nm (±15 nm). The initial velocity was determined from the linear portion of the progress curve, and the value of K_m was determined using the Michaelis-Menten equation, i.e. $v = V_{max}$ [S] / ([S] + K_m) to be 3.45±0.41 μM. Triplicate measurements were taken at each data point and the data were reported as mean±SE. In the preliminary WNV NS2B-NS3 protease inhibition assay, analogues of **3-1a** were screened at a fixed concentration of 50 μM to filter out potential inhibitors. Compounds which showed more than 50% inhibition were further investigated for their IC_{50} determination.

Determination of IC_{50}

For the IC_{50} calculations, recombinant WNV protease concentration of 0.3 μg/mL and seven different concentrations of the inhibitor ranging from 10 nM to 50 μM were used. For each experiment, the protease was pre-incubated with the inhibitor at 37 ^{o}C

for 15 min in separate wells and the enzyme kinetics was initiated by adding substrate Pyr-RTKR-AMC to a final concentration 16.7 µM. The increase in fluorescence intensity was monitored continuously using an Infinite F200 microplate reader at an excitation wavelength of 354 nm and emission wavelength at 442 nm. Fluorescence values obtained from the positive control (no inhibitor) were considered as 100%

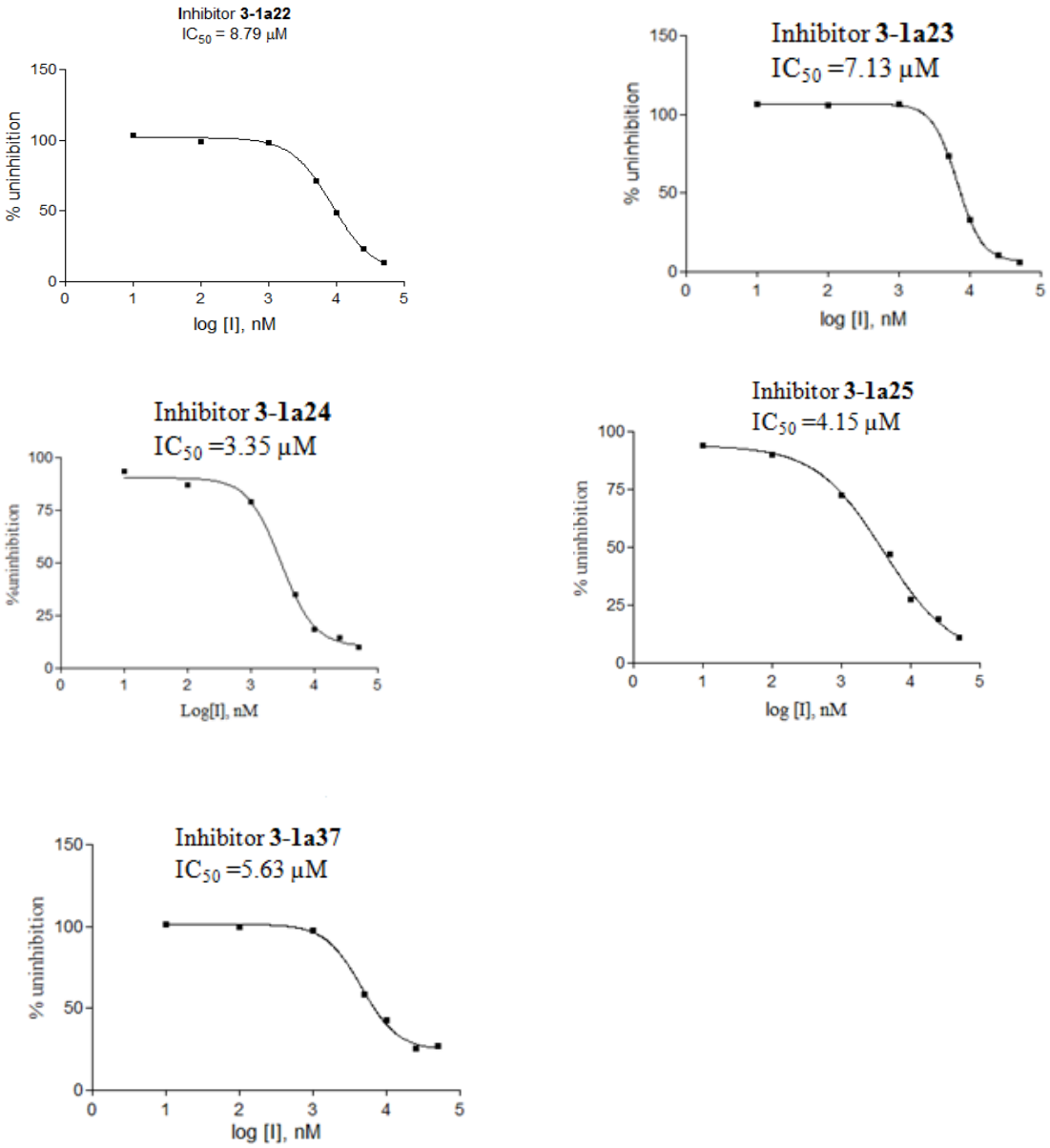

Figure 3.5 Un-inhibition curve of compounds **3-1a22**, **3-1a23**, **3-1a24**, **3-1a25** and **3-1a37**

complex formation and those values obtained in the presence of inhibitors were calculated as the percentage of inhibition of the control. Triplicate measurements were obtained at each data point. The IC_{50} values were calculated using a sigmoidal dose-response using the Graphpad prism 3.0 software (San Diego, USA). Triplicate measurements were recorded as the mean ± SE.

Determination of inhibition mechanism

Three different inhibitor (**3-1a24)** concentrations and a no-inhibitor control (0 to 25 μM) were each assayed at five substrate concentrations ranging from 3.3 μM to 83.3 μM. In each assay, the enzyme and inhibitor were incubated at 37 °C for 15 min, followed by the addition of the substrate to start the kinetic measurement. The rate of substrate cleavage (v) was monitored using the F200 microplate reader. To illustrate the inhibition mechanism, 1/V versus 1/[S] was plotted for at each inhibitor concentration using OriginPro8.

MTS Assay

The baby hamster kidney fibroblast (BHK21) cells were cultured in Roswell Park Memorial Institute (RPMI) 1640 medium containing 10% fetal bovine serum (FBS). The 1500 cells were placed in each well of three 96-well plates with a cell density of $1.66x10^4$ cells/mL and incubated for 24 h at 37 °C with 5% CO_2. Thereafter, the compound of interest or DMSO was added into each well at 25 μM. Wells containing plain DMSO served as a vehicular control. The plate was then placed in the incubator for 24, 48 and 72 h of incubation at 37 °C with 5% CO_2. At the end of each individual incubation time point, MTS reagent solution (20 μL) was added into each sample

well. The plate was then incubated again in the dark for 2 h, gently shaken using a vortemp machine for 5 min to ensure equal mixing and absorbance at 492 nm was taken using a spectrometer.

3.5.3 Docking

All docking studies were performed using the Molecular Operating Environment (MOE 2009.10) software system designed by the Chemical Computing Group. The program operated under the 'Windows Vista' operating system installed on an Intel Core™2 Duo PC with a 2.4 MHz processor and 4.0 GB RAM. Docked compound was built using the MOE builder and subjected to energy minimization with the MMFF94x force field. The active site of the WNV protease was prepared using the crystal structure of the WNV NS2B-NS3 protease in complex with peptide Bz-Nle-Lys-Arg-Arg-H (pdb 2fp7). The structure was stripped of all water molecules and bound ligand followed by the addition of valance hydrogen atoms to the protein. By keeping in mind the amino acid residues in NS2B which are responsible for the activation of the catalytic triad, the active site in NS2B-NS3 was identified using the Alpha site finder tool. Docking simulations were performed at default settings with placement at triangle matcher, rescoring at London DG, refinement at force field and the geometry of resulting complex was studied using the Discovery Studio 3.1 client.

3.6 ^{1}H and ^{13}C NMR data of all compounds synthesized

^{1}H and ^{13}C NMR data of compound 3-6a

Methyl 4-aminobenzoate (3-6a1) light brown solid (Yield: 86%): ^{1}H NMR (300 MHz, DMSO-d_6) δ 7.63 (dt, J = 8.7 Hz, 2.5 Hz, 2H), 6.56 (dt, J = 8.7 Hz, 2.5 Hz,

2H), 5.95 (s, 2H), 3.72 (s, 3H); ^{13}C NMR (75 MHz, DMSO-d_6) δ 166.4, 153.5, 131.0, 115.7, 112.7, 51.1. HRMS (ESI) $[M + H]^+$: calcd for $C_8H_{10}NO_2$: 152.0706; found 152.0706.

Methyl benzoate (3-6a2) colorless liquid (Yield: 95%). 1H NMR (300 MHz, $CDCl_3$) δ 8.10 – 7.98 (m, 2H), 7.62 – 7.49 (m, 1H), 7.49 – 7.37 (m, 2H), 3.91 (s, 3H); 13C NMR (75 MHz, $CDCl_3$) δ 167.36, 133.14, 130.44, 129.82, 128.60, 52.31. HRMS (EI) [M]: calcd for $C_8H_8NO_2$: 136.0524; found 136.0525.

^{1}H and ^{13}C NMR data of compound 3-8

2-(4-Aminobenzoyl)-N-methylhydrazinecarbothioamide (3-8a) white solid (Yield: 76%): ^{1}H NMR (500 MHz, $CDCl_3$) δ 9.84 (s, 1H), 9.11 (s, 1H), 7.89 (d, *J* = 3.6 Hz, 1H), 7.63 (d, *J* = 8.4 Hz, 2H), 6.56 (d, *J* = 8.6 Hz, 2H), 5.70 (s, 2H), 2.87 (d, *J* = 4.2 Hz, 3H); ^{13}C NMR (125 MHz, $CDCl_3$) δ 182.90, 166.57, 152.71, 129.95, 119.32, 112.92, 31.39. HRMS (ESI) $[M + H]^+$: calcd for $C_9H_{11}N_4OS$: 223.0659; found 223.0653.

2-(4-Aminobenzoyl)-N-ethylhydrazinecarbothioamide (3-8b) as a white solid (Yield: 81%): ^{1}H NMR (300 MHz, DMSO-d_6) δ 9.81 (s, 1H), 9.04 (s, 1H), 7.93 (d, *J* = 4.9 Hz, 1H), 7.63 (d, *J* = 8.6 Hz, 2H), 6.56 (d, *J* = 8.6 Hz, 2H), 5.70 (s, 2H), 3.46 (dt, *J* = 13.5, 6.8 Hz, 2H), 1.05 (t, *J* = 7.1 Hz, 3H); ^{13}C NMR (125 MHz, DMSO-d_6) δ 181.79, 166.50, 152.72, 129.96, 119.35, 112.89, 38.91, 15.00. HRMS (ESI) $[M + H]^+$: HRMS (ESI) $[M - H]^-$: calcd for $_{10}H_{13}N_4OS$: 237.0816; found 237.0808.

2-benzoyl-N-methylhydrazinecarbothioamide (3-8c) white solid (Yield: 80%): ^{1}H NMR (500 MHz, DMSO-d_6) δ 10.34 (s, 1H), 9.32 (s, 1H), 8.05 (d, *J* = 3.1 Hz, 1H),

7.93 (d, *J* = 7.7 Hz, 2H), 7.59 (t, *J* = 7.2 Hz, 1H), 7.50 (t, *J* = 7.6 Hz, 2H), 2.89 (s, 3H); ^{13}C NMR (125 MHz, DMSO-d_6) δ 182.32, 165.93, 132.46, 131.80, 128.20, 127.79, 30.92. HRMS (ESI) $[M + H]^+$: calcd for $C_9H_{10}N_3OS$: 208.0550; found 208.0543.

2-benzoyl-N-ethylhydrazinecarbothioamide (3-8d) white solid (Yield: 86%): ^{1}H NMR (500 MHz, DMSO-d_6) δ 10.32 (s, 1H), 9.24 (s, 1H), 8.10 (s, 1H), 7.92 (d, *J* = 7.5 Hz, 2H), 7.57 (t, *J* = 7.3 Hz, 1H), 7.49 (t, *J* = 7.6 Hz, 2H), 3.49 – 3.45 (m, 2H), 1.06 (t, *J* = 7.0 Hz, 3H); ^{13}C NMR (125 MHz, DMSO-d_6) δ 181.34, 166.05, 132.52, 131.92, 128.32, 127.89, 38.60, 14.56. HRMS (ESI) $[M - H]^-$: calcd for $C_{10}H_{12}N_3OS$: 222.0707; found 222.0702.

^{1}H and ^{13}C NMR data of compound 3-2a

3-(4-Aminophenyl)-4-methyl-1H-1,2,4-triazole-5(4H)-thione (3-2a1) white solid (Yield: 94%): ^{1}H NMR (500 MHz, DMSO-d_6) δ 13.65 (s, 1H), 7.36 (d, *J* = 7.3 Hz, 2H), 6.66 (d, *J* = 7.4 Hz, 2H), 5.67 (s, 2H), 3.50 (s, 3H).^{13}C NMR (125 MHz, DMSO-d_6) δ 166.86, 152.14, 150.96, 129.41, 113.36, 112.35, 31.62. HRMS (ESI) $[M - H]^-$: calcd for $C_9H_{10}N_4S$: 205.0553; found 205.0544.

3-(4-Aminophenyl)-4-ethyl-1H-1,2,4-triazole-5(4H)-thione (3-2a2) white solid (Yield: 90%). ^{1}H NMR (500 MHz, DMSO-d_6) δ 13.65 (s, 1H), 7.29 (d, *J* = 8.2 Hz, 2H), 6.66 (d, *J* = 8.2 Hz, 2H), 5.67 (s, 2H), 4.01 (q, *J* = 6.9 Hz, 2H), 1.16 (t, *J* = 6.9 Hz, 3H); ^{13}C NMR (75 MHz, DMSO-d_6) δ 166.3, 151.9, 151.0, 129.4, 113.6, 112.4, 39.0, 13.4. HRMS (ESI) $[M + H]^+$: calcd for $C_{10}H_{13}N_4S$: 221.0855; found 221.0848.

4-Methyl-3-phenyl-1H-1,2,4-triazole-5(4H)-thione (3-2a3) white solid (Yield: 90%): ^{1}H NMR (500 MHz, DMSO-d_6) δ 12.53 (s, 1H), 7.64 – 7.58 (m, 2H), 7.57 – 7.49 (m, 3H), 3.65 (s, 3H);^{13}C NMR (125 MHz, DMSO-d_6) δ 168.20, 152.44, 131.33, 129.41, 128.76, 125.88, 32.50. HRMS (ESI) $[M - H]^-$: calcd for $C_9H_8N_3S$: 190.0444; found 190.0437.

4-Ethyl-3-phenyl-1H-1,2,4-triazole-5(4H)-thione (3-2a4) white solid (Yield: 90%). ^{1}H NMR (500 MHz, DMSO-d_6) δ 12.55 (s, 1H), 7.58 – 7.50 (m, 5H), 4.15 (q, J = 7.0 Hz, 2H), 1.33 (t, J = 7.0 Hz, 3H); ^{13}C NMR (125 MHz, DMSO-d_6) δ 167.2, 151.9, 131.0, 129.1, 128.5, 125.8, 40.0, 13.8. HRMS (ESI) $[M - H]^-$: calcd for $C_{10}H_{10}N_3S$: 204.0601; found 204.0592.

3-Phenyl-1H-1,2,4-triazole-5(4H)-thione (3-2a5) white solid (Yield: 82%). ^{1}H NMR (500 MHz, DMSO-d_6) δ 13.67 (br, 2H), 7.91 – 7.89 (m, 2H), 7.52 – 7.49 (m, 3H); ^{13}C NMR (125 MHz, DMSO-d_6) δ 167.1, 150.2, 130.1, 129.1, 125.7, 125.5. HRMS (ESI) $[M - H]^-$: calcd for $C_8H_6N_3S$: 176.0288; found 176.0286.

3-(4-Nitrophenyl)-1H-1,2,4-triazole-5(4H)-thione (3-2a6) yellow solid (Yield: 78%). ^{1}H NMR: (300 MHz, DMSO-d_6) δ 13.94 (br, 2H), 8.34 (d, J = 8.7 Hz, 2H), 8.13 (d, J = 8.7 Hz, 2H); ^{13}C NMR (75 MHz, DMSO-d_6) δ 167.7, 148.6, 148.2, 131.2, 126.8, 124.4. HRMS (ESI) $[M - H]^-$: calcd for $C_8H_5N_4O_2S$: 221.0139; found 221.0130.

3-(4-Hydroxyphenyl)-1H-1,2,4-triazole-5(4H)-thione (3-2a7) as a white solid (Yield: 80%). ^{1}H NMR (300 MHz, DMSO-d_6) δ 13.46 (s, 1H), 10.07 (s, 1H), 7.73 (d, J = 8.4 Hz, 2H), 6.86 (d, J = 8.4 Hz, 2H); ^{13}C NMR (75 MHz, DMSO-d_6) δ 166.5, 159.6, 150.5, 127.5, 116.4, 115.9. HRMS (ESI) $[M - H]^-$: calcd for $C_8H_6N_3OS$: 192.0237; found 192.0245.

3-o-Tolyl-1H-1,2,4-triazole-5(4H)-thione (3-2a8) white solid (Yield: 85%): ^{1}H NMR (300 MHz, DMSO-d_6) δ 7.70 (d, J = 7.6 Hz, 1H), 7.54 – 7.22 (m, 3H), 2.55 (s, 3H). ^{13}C NMR (75 MHz, DMSO-d_6) δ 168.05, 150.57, 137.25, 131.28, 130.23, 128.67, 126.00, 125.00, 20.18.HRMS (ESI) [M – H]$^-$: calcd for $C_9H_8N_3S$, 190.0444; found 190.0441.

3-Propyl-1H-1,2,4-triazole-5(4H)-thione (3-2a9) white solid (Yield: 71%): ^{1}H NMR (500 MHz, DMSO-d_6) δ 13.13 (d, J = 57.3 Hz, 1H), 2.49 (d, J = 6.6 Hz, 1H), 1.62 (d, J = 6.5 Hz, 2H), 0.88 (s, 3H).^{13}C NMR (75 MHz, DMSO-d_6) δ 165.92, 152.34, 26.90, 19.80, 13.28. HRMS (ESI) [M – H]$^-$: calcd for $C_5H_8N_3S$: 142.0444; found 142.0438.

3-Cyclohexyl-1H-1,2,4-triazole-5(4H)-thione (3-2a10) white solid (Yield: 83%): ^{1}H NMR (500 MHz, DMSO-d_6) δ 13.12 (d, J = 56.9 Hz, 2H), 2.57 (s, 1H), 2.02 – 1.54 (m, 5H), 1.53 – 1.08 (m, 5H).^{13}C NMR (75 MHz, DMSO-d_6) δ 165.87, 156.12, 34.60, 29.86, 25.21, 25.04. HRMS (ESI) [M – H]$^-$: calcd for $C_8H_{12}N_3S$: 182.0757; found 182.0755.

3-(Pyridin-4-yl)-1H-1,2,4-triazole-5(4H)-thione (3-2a11) white solid (Yield: 76%): ^{1}H NMR (500 MHz, DMSO-d_6) δ 8.60 (d, J = 5.2 Hz, 1H), 7.81 (d, J = 5.2 Hz, 1H).^{13}C NMR (125 MHz, DMSO-d_6) δ 169.01, 154.45, 150.05, 137.69, 119.58. HRMS (ESI) [M – H]$^-$: calcd for $C_7H_5N_4S$: 177.0240; found 177.0235.

3-(4-Aminophenyl)-1H-1,2,4-triazole-5(4H)-thione (3-2a12) light gray solid (Yield: 61%). ^{1}H NMR: (300 MHz, DMSO-d_6) δ 13.36 (br, 1H), 13.32 (br, 1H), 7.56 (d, J = 8.6 Hz, 2H), 6.60 (d, J = 8.6 Hz, 2H), 5.64 (s, 2H); ^{13}C NMR (75 MHz, DMSO-d_6) δ 166.0, 151.0 (2C), 127.0, 113.5, 112.3. HRMS (ESI) [M – H]$^-$: calcd for $C_8H_7N_4S$: 191.0397; found 191.0392.

^{1}H and ^{13}C NMR data of compound 3-10

Benzo[d]thiazole-2(3H)-thione (3-10a) white solid (Yield: 94%). ^{1}H NMR (500 MHz, DMSO-d_6) δ 13.75 (s, 1H), 7.68 (d, J = 7.6 Hz, 1H), 7.40 – 7.26 (m, 3H).^{13}C NMR (125 MHz, DMSO-d_6) δ 189.90, 141.28, 129.40, 127.23, 124.30, 121.83, 112.50. HRMS (ESI) [M-H]$^-$: calcd for $C_7H_4NS_2$: 165.9791; found 165.9785.

1H-Benzo[d]imidazole-2(3H)-thione (3-10b) light brown solid (Yield: 85%): ^{1}H NMR (300 MHz, $CDCl_3$) δ 11.35 (s, 1H), 7.29 – 7.20 (m, 2H), 7.20 – 7.11 (m, 2H); ^{13}C NMR (75 MHz, $CDCl_3$) δ 169.78, 132.45, 122.42, 109.33; HRMS (ESI) [M-H]$^-$: calcd for $C_7H_5N_2S$: 149.0179; found 149.0179.

^{1}H and ^{13}C NMR data of compound 3-11

6-Nitrobenzo[d]thiazole-2(3H)-thione (3-11a) yellow solid (Yield: 48%): ^{1}H NMR (500 MHz, DMSO-d_6) δ 8.35 (d, J = 2.5 Hz, 1H), 8.08 (dd, J = 9.2, 2.5 Hz, 1H), 7.38 (s, 2H), 6.90 (d, J = 9.2 Hz, 1H).^{13}C NMR (125 MHz, DMSO-d_6) δ 154.47, 135.13, 132.10, 127.31, 113.80, 109.92, 102.38. HRMS (ESI) [M-H]$^-$: calcd for $C_7H_3N_2O_2S$: 210.9641; found 210.9633.

5-Nitro-1H-benzo[d]imidazole-2(3H)-thione (3-11b) yellow solid (Yield: 65%): ^{1}H NMR (300 MHz, Acetone-d_6) δ 11.87 (s, 2H), 8.41 – 7.78 (m, 2H), 7.38 (d, J = 8.7 Hz, 1H). ^{13}C NMR (75 MHz, Acetone-d_6) δ 172.90, 143.36, 137.29, 132.39, 118.84, 108.92, 104.73.HRMS (ESI) [M-H]$^-$: calcd for $C_7H_4N_3O_2S$: 194.0030; found 194.0024.

^{1}H and ^{13}C NMR data of compound 3-3

6-Aminobenzo[d]thiazole-2(3H)-thione (3-3a) brown solid (Yield: 74%). ^{1}H NMR (500 MHz, DMSO-d_6) δ 13.37 (s, 1H), 7.01 (d, J = 8.2 Hz, 1H), , 6.76 (s, 1H), 6.63 (d, J = 8.2 Hz, 1H), 5.27 (s, 2H); ^{13}C NMR (125 MHz, DMSO-d_6): δ 184.8, 145.4, 130.9, 129.8, 113.0, 112.0, 103.7. HRMS (ESI) $[M + H]^+$: calcd for $C_7H_7N_2S_2$: 183.0045; found 183.0041.

5-Amino-1H-benzo[d]imidazole-2(3H)-thione (3-3b) brown solid (Yield: 67%). ^{1}H NMR (500 MHz, DMSO-d_6) δ 12.02 (s, 1H), 11.99 (s, 1H), 6.80 (d, J = 9.5 Hz, 1H), 6.39 (t, J = 4.7 Hz, 2H), 4.92 (s, 2H); ^{13}C NMR (125 MHz, DMSO-d_6): δ 165.2, 144.2, 132.6, 122.9, 109.0 (2C), 93.6. HRMS (ESI) $[M - H]^-$: calcd for $C_7H_6N_3S$: 164.0288; found 164.0281.

^{1}H and ^{13}C NMR data of compound 3-12

N-Benzyl-2-bromoacetamide (3-12a) white solid (Yield: 72%). ^{1}H NMR (500 MHz, $CDCl_3$) δ 7.39 – 7.28 (m, 5H), 4.49 (d, J = 5.7 Hz, 2H), 3.93 (s, 2H); ^{13}C NMR (125 MHz, $CDCl_3$) δ 165.4, 137.3, 128.9, 127.8, 127.7 44.2, 29.1. [^{1}H and ^{13}C NMR matching with reported values][110]

2-Bromo-N-(4-fluorobenzyl)acetamide (3-12b) white solid (Yield: 77%). ^{1}H NMR (500 MHz, Acetone-d_6): δ 7.98 (s, 1H), 7.38 – 7.34 (m, 2H), 7.10 – 7.05 (m, 2H), 4.42 (d, J = 6.3 Hz, 1H), 3.93 (s, 2H); ^{13}C NMR (125 MHz, Acetone-d_6) δ 167.5, 163.5 (d, J = 242.9 Hz, 1C), 136.7 (d, J = 2.7 Hz, 1C), 131.0 (d, J = 8.3 Hz, 1C), 116.5 (d, J = 22.0 Hz, 1C), 43.9, 30.2. HRMS (ESI) $[M - H]^-$: calcd for C_9H_8BrFNO: 243.9779; found 243.9773.

2-Bromo-N-(4-methoxybenzyl)acetamide (3-12c) white solid (Yield: 76%). ^{1}H NMR (500 MHz, DMSO-d_6) δ 10.22 (s, 1H), 7.49 (d, J = 8.8 Hz, 2H), 6.89 (d, J = 8.8 Hz, 2H), 4.38 (d, J = 5.7 Hz, 2H), 4.00 (s, 2H), 3.72 (s, 3H); ^{13}C NMR (125 MHz, DMSO-d_6) δ 164.2, 155.6, 131.7, 120.7, 113.9, 55.1,42.2, 30.4. [^{1}H and ^{13}C NMR matching with reported values][111]

2-Bromo-N-(4-methylbenzyl)acetamide (3-12d) white solid (Yield: 72%). ^{1}H NMR (500 MHz, DMSO-d_6) δ 8.71 (s, 1H), 7.16 – 7.14 (m, 4H), 4.25 (d, J = 5.7 Hz, 2H), 3.90 (s, 2H), 2.28 (s, 3H); ^{13}C NMR (125 MHz, DMSO-d_6) δ 166.4, 136.5, 136.2, 129.3, 127.8, 42.8, 29.9, 21.1. HRMS (ESI) [M – H]$^-$: calcd for $C_{10}H_{11}BrNO$: 240.0030; found 240.0024

N-Benzyl-2-bromo-N-methylacetamide (3-12e) white solid (Yield: 72%). ^{1}H NMR (500 MHz, DMSO-d_6) δ 8.71 (s, 1H), 7.16 – 7.14 (m, 4H), 4.25 (d, J = 5.7 Hz, 2H), 3.90 (s, 2H), 2.28 (s, 3H); ^{13}C NMR (125 MHz, DMSO-d_6) δ 166.4, 136.5, 136.2, 129.3, 127.8, 42.8, 29.9, 21.1. HRMS (ESI) [M – H]$^-$: calcd for $C_{10}H_{11}BrNO$: 240.0030; found 240.0021.

2-Bromo-N-phenylacetamide (3-12f) white solid (Yield: 80%). ^{1}H NMR (500 MHz, $CDCl_3$) δ 8.18 (s, 1H), 7.52 (d, J = 7.6 Hz, 2H), 7.35 (t, J = 8.2 Hz, 2H), 7.17 (t, J = 7.6 Hz, 1H), 4.01 (s, 2H); ^{13}C NMR (125 MHz, $CDCl_3$) δ 163.4, 136.9, 129.1, 125.2, 120.0, 29.4. HRMS (ESI) [M – H]$^-$: calcd for C_8H_7BrNO: 211.9717; found 211.9713

2-Bromo-N-(4-chlorophenyl)acetamide (3-12g) white solid (Yield: 84%). ^{1}H NMR (300 MHz, DMSO-d_6) δ 10.51 (s, 1H), 7.61 (d, J = 8.9 Hz, 2H), 7.38 (t, J = 8.9 Hz, 2H), 4.03 (s, 2H); ^{13}C NMR (75 MHz, DMSO-d_6) δ 164.9, 137.5, 128.8, 127.4, 120.8, 30.3. HRMS (ESI) [M – H]$^-$: calcd for $C_8H_6BrClNO$: 245.9327; found 245.9317.

2-Bromo-N-(4-fluorophenyl)acetamide (3-12h) white solid (Yield: 76%). ^{1}H NMR (300 MHz, DMSO-d_6) δ 10.43 (s, 1H), 7.60 (dd, J = 5.1 Hz, 8.8 Hz, 2H), 7.16 (t, J = 8.8 Hz, 2H), 4.02 (s, 2H); ^{13}C NMR (125 MHz, DMSO-d_6) δ 164.7, 158.3 (d, J = 240.1 Hz,1C), 134.9 (d, J = 1.8 Hz, 1C), 121.1 (d, J = 7.3 Hz, 1C), 115.4 (d, J = 22.0 Hz, 1C), 30.2. HRMS (ESI) [M – H]$^-$: calcd for C_8H_6BrFNO: 229.9622; found 229.9628.

2-Bromo-N-(4-methoxyphenyl)acetamide (3-12i) white solid (Yield: 68%). ^{1}H NMR (500 MHz, DMSO-d_6) δ 10.22 (s, 1H), 7.49 (d, J = 8.8 Hz, 2H), 6.89 (d, J = 8.8 Hz, 2H), 4.00 (s, 2H), 3.72 (s, 3H); ^{13}C NMR (125 MHz, DMSO-d_6) δ 164.2, 155.6, 131.7, 120.7, 113.9, 55.1, 30.4. HRMS (ESI) [M – H]$^-$: calcd for $C_9H_9BrNO_2$: 241.9822; found 241.9812.

2-Bromo-N-p-tolylacetamide (3-12j) white solid (Yield: 83%): ^{1}H NMR (500 MHz, DMSO-d_6) δ 10.26 (s, 1H), 7.47 (d, J = 8.3 Hz, 2H), 7.13 (d, J = 8.1 Hz, 2H), 4.02 (s, 2H), 2.25 (s, 3H); ^{13}C NMR (125 MHz, DMSO-d_6) δ 167.42, 163.44, 135.05, 131.77, 128.16, 118.19, 29.38, 19.40. HRMS (ESI) [M – H]$^-$: calcd for C_9H_9BrNO: 225.9873; found 225.9866.

2-Bromo-N-(4-ethylphenyl)acetamide (3-12k) brown solid (Yield: 77%). ^{1}H NMR (500 MHz, DMSO-d_6) δ 10.28 (s, 1H), 7.48 (d, J = 8.2 Hz, 2H), 7.15 (d, J = 8.2 Hz, 2H), 4.02 (s, 2H), 2.55 (q, J = 7.6 Hz, 2H), 1.15 (t, J = 7.6 Hz, 3H); ^{13}C NMR (125 MHz, DMSO-d_6) δ 164.5, 139.2, 136.2, 128.0, 119.3, 30.4, 27.6, 15.6. HRMS (ESI) [M – H]$^-$: calcd for $C_{10}H_{11}BrNO$: 240.0030; found 240.0020.

2-Bromo-N-(4-propylphenyl)acetamide (3-12l) white solid (Yield: 87%): ^{1}H NMR (500 MHz, $CDCl_3$) δ 8.15 (s, 1H), 7.45 (d, J = 8.3 Hz, 2H), 7.18 (d, J = 8.3 Hz, 2H), 4.03 (s, 2H), 2.69 – 2.47 (m, 2H), 1.76 – 1.47 (m, 2H), 0.95 (t, J = 7.3 Hz, 3H).^{13}C

NMR (125 MHz, $CDCl_3$) δ 163.30, 139.84, 134.56, 129.05, 120.15, 77.29, 77.03, 76.78, 37.46, 29.52, 24.51, 13.72. HRMS (ESI) $[M - H]^-$: calcd for $C_{11}H_{13}BrNO$: 254.0186; found 254.0184.

2-Bromo-N-cyclohexylacetamide (3-12m) white solid (Yield: 82%). ^1H NMR (300 MHz, DMSO-d_6) δ 8.15 (s, 1H), 3.79 (s, 2H), 3.51 – 3.48 (m, 1H), 1.74 – 1.64 (m, 4H), 1.56 – 1.53 (m, 1H), 1.28 – 1.13 (m, 5H); ^{13}C NMR (75 MHz, DMSO-d_6): δ 164.9, 48.0, 32.0, 29.8, 25.1, and 24.4. HRMS (ESI) $[M + H]^+$: calcd for $C_8H_{15}BrNO$: 220.0332; found 220.0333.

2-Bromo-N-(3-chlorophenyl)acetamide (3-12n) white solid (Yield: 85%): ^1H NMR (500 MHz, DMSO-d_6) δ 9.67 (s, 1H), 7.87 (t, J = 1.8 Hz, 1H), 7.32 (t, J = 8.1 Hz, 1H), 7.12 (dd, J = 8.3, 1.4 Hz, 1H), 4.04 (s, 2H).^{13}C NMR (125 MHz, DMSO-d_6) δ 164.17, 139.25, 133.08, 129.40, 123.00, 118.40, 116.87, 29.37. HRMS (ESI) $[M + H]^+$: calcd for $C_8H_6ClBrNO$: 245.9327; found 245.9320.

2-Bromo-N-(3-fluorophenyl)acetamide (3-12o) white solid (Yield: 78%). ^1H NMR (300 MHz, DMSO-d_6) δ 10.60 (s, 1H), 7.58 (d, J = 11.4 Hz, 1H), 7.40 – 7.28 (m, 2H), 6.91 (dt, J = 1.8 Hz, 8.0 Hz, 1H), 4.05 (s, 2H); ^{13}C NMR (75 MHz, DMSO-d_6) δ 165.1, 162.1 (d, J = 241.9 Hz, 1C), 140.3 (d, J = 10.8 Hz, 1C), 130.5 (d, J = 9.2 Hz, 1C), 115.0, 110.3 (d, J = 21.1 Hz, 1C), 106.0 (d, J = 26.5 Hz, 1C), 30.2. HRMS (ESI) $[M - H]^-$: calcd for C_8H_6BrFNO: 229.9622; found 229.9612.

2-Bromo-N-(3-ethylphenyl)acetamide (3-12p) golden brown gel (Yield: 79%): ^1H NMR (500 MHz, $CDCl_3$) δ 8.17 (s, 1H), 7.38 (d, J = 8.0 Hz, 2H), 7.29 (dd, J = 8.7, 6.7 Hz, 1H), 7.04 (d, J = 7.5 Hz, 1H), 4.05 (s, 2H), 2.68 (q, J = 7.6 Hz, 2H), 1.26 (t, J = 7.6 Hz, 3H); ^{13}C NMR (125 MHz, DMSO-d_6) δ 163.75, 135.37, 134.48, 129.08,

127.10, 126.4, 123.22, 30.14, 24.6, 14.27. HRMS (ESI) [M – H]⁻: calcd for $C_{10}H_{11}BrNO$: 240.0030; found 240.0019.

2-Bromo-N-(3-methoxyphenyl)acetamide (3-12q) white solid (Yield: 76%). ^{1}H NMR (500 MHz, DMSO-d_6) δ 10.34 (s, 1H), 7.27 (t, *J* = 2.2 Hz, 1H), 7.23 (t, *J* = 8.2 Hz, 1H), 7.12 (d, *J* = 8.8 Hz, 1H), 6.67 (dd, *J* = 2.6 Hz, 8.2 Hz, 1H), 4.02 (s, 2H), 3.73 (s, 3H); ^{13}C NMR (125 MHz, DMSO-d_6) δ 164.7, 159.5, 139.7, 129.6, 111.5, 109.2, 105.0, 55.0, 30.4. HRMS (ESI) [M – H]⁻: calcd for $C_9H_9BrNO_2$: 241.9822; found 241.9817.

^{1}H and ^{13}C NMR data of compound 3-14:

N-Benzyl-2-(6-(2-bromoacetamido)benzo[d]thiazol-2-ylthio)acetamide (3-14a) white solid (Yield: 81%). ^{1}H NMR (500 MHz, DMSO-d_6) δ 10.67 (s, 1H), 8.81 (t, *J* = 5.5 Hz, 1H), 8.37 (d, *J* = 0.8 Hz, 1H), 7.78 (d, *J* = 8.8 Hz, 1H), 7.56 (d, *J* = 8.8 Hz, 1H), 7.34 – 7.15 (m, 5H), 4.32 (d, *J* = 5.9 Hz, 2H), 4.19 (s, 2H), 4.09 (s, 2H).^{13}C NMR (125 MHz, DMSO-d_6) δ 166.40, 164.94, 164.85, 149.00, 138.97, 135.48, 135.41, 128.20, 127.11, 126.78, 121.13, 118.61, 111.62, 42.52, 36.54, 30.33. HRMS (ESI) [M – H]⁻: calcd for $C_{18}H_{15}BrN_3O_2S_2$: 447.9795; found 447.9789.

2-Bromo-N-(2-(2-(4-fluorobenzylamino)-2-oxoethylthio)benzo[d]thiazol-6-yl)acetamide (3-14b) white solid (Yield: 76%): ^{1}H NMR (500 MHz, DMSO-d_6) δ 10.73 (s, 1H), 8.85 (t, *J* = 5.5 Hz, 1H), 8.38 (s, 1H), 7.76 (d, *J* = 8.8 Hz, 1H), 7.58 (d, *J* = 8.7 Hz, 1H), 7.28 (dd, *J* = 7.7, 5.9 Hz, 2H), 7.07 (t, *J* = 8.7 Hz, 2H), 4.29 (d, *J* = 5.7 Hz, 2H), 4.18 (s, 2H), 4.12 (d, *J* = 14.1 Hz, 2H).^{13}C NMR (125 MHz, DMSO-d_6) δ 166.51, 165.01, 164.84, 162.14, 160.21, 149.02, 135.51, 135.25, 135.23, 129.17,

129.11, 121.17, 118.67, 115.04, 114.87, 111.64, 41.88, 36.59, 30.39. HRMS (ESI) [M – H]$^-$: calcd for $C_{18}H_{14}BrFN_3O_2S_2$: 465.9700; found 465.9701.

2-Bromo-N-(2-(2-(4-methoxybenzylamino)-2-oxoethylthio)benzo[d]thiazol-6-yl)acetamide (3-14c) white solid (Yield: 86%): ^{1}H NMR (500 MHz, DMSO-d_6) δ 10.71 (s, 1H), 9.18 (s, 1H), 8.75 (t, *J* = 5.6 Hz, 1H), 8.39 (d, *J* = 0.9 Hz, 1H), 7.76 (d, *J* = 8.8 Hz, 1H), 7.57 (dd, *J* = 8.8, 1.4 Hz, 1H), 7.15 (d, *J* = 8.3 Hz, 2H), 6.80 (d, *J* = 8.5 Hz, 2H), 4.23 (d, *J* = 5.7 Hz, 2H), 4.16 (s, 2H), 4.10 (s, 2H), 3.69 (s, 3H).^{13}C NMR (125 MHz, DMSO-d_6) δ 166.25, 164.97, 164.85, 158.21, 149.01, 135.51, 135.46, 130.89, 128.51, 121.18, 118.60, 113.62, 111.59, 55.05, 42.02, 36.62, 30.37. HRMS (ESI) [M – H]$^-$: calcd for $C_{19}H_{17}BrN_3O_3S_2$: 477.9900; found 477.9907.

N-Benzyl-2-(6-(2-bromoacetamido)-1H-benzo[d]imidazol-2-ylthio)acetamide (3-14d) white solid (Yield: 75%): ^{1}H NMR (500 MHz, DMSO-d_6) δ 10.71 (s, 1H), 8.84 (s, 1H), 8.38 (s, 1H), 7.78 (d, *J* = 8.7 Hz, 1H), 7.58 (d, *J* = 8.6 Hz, 1H), 7.43 – 7.12 (m, 5H), 4.32 (d, *J* = 5.6 Hz, 2H), 4.19 (s, 2H), 4.11 (s, 2H). ^{13}C NMR (125 MHz, DMSO-d_6) δ 166.45, 164.99, 149.03, 139.00, 135.51, 135.46, 128.24, 127.14, 126.82, 121.16, 118.63, 111.63, 42.56, 36.58, 30.38. HRMS (ESI) [M – H]$^-$: calcd for $C_{18}H_{16}BrN_4O_2S$: 431.0183; found 431.0186.

2-Bromo-N-(2-(2-(4-fluorobenzylamino)-2-oxoethylthio)-1H-benzo[d]imidazol-6-yl)acetamide (3-14e) white solid (Yield: 74%): ^{1}H NMR (300 MHz, DMSO-d_6) δ 10.83 (s, 1H), 8.94 (d, *J* = 5.8 Hz, 1H), 8.21 (s, 1H), 7.90 – 7.43 (m, 2H), 7.14 (dd, *J* = 33.9, 25.7 Hz, 5H), 4.21 (m, 6H).^{13}C NMR (75 MHz, DMSO-d_6) δ 166.20, 165.16, 162.82, 159.61, 149.86, 136.10, 134.92, 134.88, 133.16, 129.35, 129.24, 117.26, 115.16, 114.87, 113.79, 102.86, 42.01, 35.86, 30.34. HRMS (ESI) [M – H]$^-$: calcd for $C_{18}H_{15}BrFN_4O_2S$: 449.0089; found 449.0089.

N-Benzyl-2-(6-(2-bromoacetamido)benzo[d]thiazol-2-ylthio)-N-methylacetamide (3-14f) white solid (Yield: 73%). ^{1}H NMR (500 MHz, DMSO-d_6) δ 10.61 (s, 1H), 10.33 (s, 1H), 8.38 (d, *J* = 1.9 Hz, 1H), 7.79 (d, *J* = 8.8 Hz, 1H), 7.54 – 7.48 (m, 3H), 7.14 (d, J = 8.2 Hz, 2H), 4.36 (s, 2H), 4.07 (s, 2H), 2.54 (q, *J* = 7.6 Hz, 2H), 1.14 (t, *J* = 7.6 Hz, 3H); ^{13}C NMR (125 MHz DMSO-d_6) δ 164.9 (2C), 164.8, 149.0, 139.0, 136.4, 135.5, 135.4, 127.9, 121.1, 119.2, 118.6, 111.6, 37.7, 30.3, 27.5, 15.6. HRMS (ESI) $[M - H]^-$: calcd for $C_{19}H_{17}BrN_3O_2S_2$: 461.9951; found 461.9956.

2-Bromo-N-(2-(2-(4-methylbenzylamino)-2-oxoethylthio)benzo[d]thiazol-6-yl)acetamide (3-14g) white solid (Yield: 80%). ^{1}H NMR (500 MHz, DMSO-d_6) δ 10.68 (s, 1H), 8.86 – 8.66 (m, 1H), 8.47 – 8.26 (m, 1H), 7.76 (d, *J* = 8.7 Hz, 1H), 7.56 (d, *J* = 8.7 Hz, 1H), 7.09 (dd, *J* = 32.6, 7.6 Hz, 4H), 4.26 (d, *J* = 5.6 Hz, 2H), 4.17 (s, 2H), 4.10 (s, 2H), 2.24 (s, 3H); ^{13}C NMR (125 MHz, DMSO-d_6) δ 166.29, 164.93, 164.84, 149.00, 135.90, 135.83, 135.48, 135.41, 128.75, 127.14, 121.13, 118.60, 111.59, 42.30, 36.58, 30.33, 20.64. HRMS (ESI) $[M - H]^-$: calcd for $C_{19}H_{17}BrN_3O_2S_2$: 461.9951; found 461.9953.

2-Bromo-N-(2-(2-(4-methoxybenzylamino)-2-oxoethylthio)-1H-benzo[d]imidazol-6-yl)acetamide (3-14h) white solid (Yield: 83%). ^{1}H NMR (500 MHz, DMSO) δ 10.74 (s, 1H), 8.81 (t, *J* = 5.6 Hz, 1H), 8.19 (s, 1H), 7.64 (d, *J* = 8.8 Hz, 1H), 7.48 (dd, *J* = 8.7, 1.0 Hz, 1H), 7.14 (d, *J* = 8.4 Hz, 2H), 6.82 (d, *J* = 8.5 Hz, 2H), 4.22 (d, *J* = 5.4 Hz, 4H), 4.11 (s, 2H) 3.71 (s, 3H).^{13}C NMR (126 MHz, DMSO) δ 166.61, 165.53, 158.79, 150.30, 136.27, 131.06, 129.09, 117.41, 114.35, 114.16, 103.49, 55.56, 42.65, 36.27, 30.82.

2-Bromo-N-(2-(2-oxo-2-(phenylamino)ethylthio)benzo[d]thiazol-6-yl)acetamide (3-14i) white solid (Yield: 84%). ^{1}H NMR (300 MHz, DMSO-d_6) δ 10.78 (s, 1H),

10.52 (s, 1H), 8.40 (s, 1H), 7.76 (d, *J* = 8.7 Hz, 1H), 7.59 (t, *J* = 6.9 Hz, 3H), 7.29 (t, *J* = 7.7 Hz, 2H), 7.03 (t, *J* = 7.2 Hz, 1H), 4.39 (s, 2H), 4.12 (s, 2H).^{13}C NMR (75 MHz, DMSO-d_6) δ 165.33, 165.06, 164.89, 149.03, 138.86, 135.58, 135.54, 128.89, 123.68, 121.22, 119.28, 118.73, 111.68, 37.88, 30.47. HRMS (ESI) [M – H]$^-$: calcd for $C_{17}H_{13}BrN_3O_2S_2$: 433.9638; found 433.9638.

2-Bromo-N-(2-(2-(4-chlorophenylamino)-2-oxoethylthio)benzo[d]thiazol-6-yl)acetamide (3-14j) white solid (Yield: 81%). ^{1}H NMR (500 MHz, DMSO-d_6) δ 11.01 – 10.43 (m, 1H), 8.39 (s, 1H), 8.00 – 7.31 (m, 6H), 4.40 (s, 2H), 4.09 (s, 2H). HRMS (ESI) [M – H]$^-$: calcd for $C_{17}H_{12}BrClN_3O_2S_2$: 467.9248; found 467.9248.

2-Bromo-N-(2-(2-(4-fluorophenylamino)-2-oxoethylthio)benzo[d]thiazol-6-yl)acetamide (3-14k) white solid (Yield: 75%). ^{1}H NMR: (300 MHz, DMSO-d_6): δ 10.64 (s, 1H), 10.49 (s, 1H), 8.38 (d, *J* = 3.6 Hz, 1H), 7.78 (d, *J* = 8.7 Hz, 1H), 7.63 – 7.51 (m, 3H), 7.16 (t, *J* = 8.9 Hz, 2H), 4.36 (s, 2H), 4.07 (s, 2H); ^{13}C NMR (75 MHz, DMSO-d_6): δ 165.9, 165.8, 165.5, 158.8 (d, *J* = 239.9 Hz, 1C), 149.5, 135.8 (d, *J* = 17.6 Hz, 1C), 135.3, 135.3, 121.8 (d, *J* = 8.2 Hz, 1C), 121.7, 119.4, 115.9 (d, *J* = 22.0 Hz, 1C), 112.3, 37.9, 30.5. HRMS (ESI) [M – H]$^-$: calcd for $C_{17}H_{12}BrFN_3O_2S_2$: 451.9544; found 451.9548.

2-Bromo-N-(2-(2-(4-methoxyphenylamino)-2-oxoethylthio)benzo[d]thiazol-6-yl)acetamide (3-14l) white solid (Yield: 74%). ^{1}H NMR (500 MHz, DMSO-d_6) δ 10.61 (s, 1H), 10.27 (s, 1H), 8.38 (d, *J* = 1.9 Hz, 1H), 7.79 (d, *J* = 8.2 Hz, 1H), 7.54 – 7.49 (m, 3H), 6.89 (d, J = 8.8 Hz, 2H), 4.34 (s, 2H), 4.07 (s, 2H), 3.71 (s, 3H); ^{13}C NMR (125 MHz DMSO-d_6) δ 164.9, 164.8, 164.6,155.4, 149.0, 135.5, 135.4, 131.8, 121.1, 120.7, 118.6, 113.9, 111.6, 55.1, 37.6, 30.3. HRMS (ESI) [M – H]$^-$: calcd for $C_{18}H_{15}BrN_3O_3S_2$: 463.9744; found 463.9746.

2-Bromo-N-(2-(2-oxo-2-(p-tolylamino)ethylthio)benzo[d]thiazol-6-yl)acetamide (3-14m) white solid (Yield: 74%). ^{1}H NMR (500 MHz, DMSO-d_6) δ 10.60 (s, 1H), 10.32 (s, 1H), 8.38 (s, 1H), 7.78 (d, *J* = 8.3 Hz, 1H), 7.53 – 7.46 (m, 3H), 7.11 (d, J = 7.5 Hz, 2H), 4.36 (s, 2H), 4.08 (s, 2H), 2.24 (s, 3H); ^{13}C NMR (125 MHz DMSO-d_6) δ 164.89, 164.83, 148.96, 136.22, 135.47, 135.38, 132.52, 129.16, 121.13, 119.15, 118.63, 111.86, 37.7, 30.29, 20.41. HRMS (ESI) [M – H]$^-$: calcd for $C_{18}H_{15}BrN_3O_2S_2$: 447.9781; found 447.9781.

2-Bromo-N-(2-(2-(4-ethylphenylamino)-2-oxoethylthio)benzo[d]thiazol-6-yl)acetamide (3-14n) white solid (Yield: 78%). ^{1}H NMR (500 MHz, DMSO-d_6) δ 10.61 (s, 1H), 10.33 (s, 1H), 8.38 (d, *J* = 1.9 Hz, 1H), 7.79 (d, *J* = 8.8 Hz, 1H), 7.54 – 7.48 (m, 3H), 7.14 (d, J = 8.2 Hz, 2H), 4.36 (s, 2H), 4.07 (s, 2H), 2.54 (q, *J* = 7.6 Hz, 2H), 1.14 (t, *J* = 7.6 Hz, 3H); ^{13}C NMR (125 MHz DMSO-d_6) δ 164.9, 164.8, 149.0, 139.0, 136.4, 135.5, 135.4, 127.9, 121.1, 119.2, 118.6, 111.6, 37.7, 30.3, 27.5, 15.6. HRMS (ESI) [M-H]$^-$: cald for $C_{19}H_{17}BrN_3O_2S_2$: 461.9951; found 461.9935.

2-Bromo-N-(2-(2-oxo-2-(4-propylphenylamino)ethylthio)benzo[d]thiazol-6-yl)acetamide (3-14o) white solid (Yield: 85%). ^{1}H NMR (500 MHz, DMSO-d_6) δ 10.70 (s, 1H), 10.39 (s, 1H), 8.40 (d, *J* = 2.0 Hz, 1H), 7.79 (d, *J* = 8.8 Hz, 1H), 7.56 (dd, *J* = 8.8, 2.0 Hz, 1H), 7.50 (d, *J* = 8.4 Hz, 2H), 7.12 (d, *J* = 8.3 Hz, 2H), 4.37 (s, 2H), 4.10 (s, 2H), 2.64 – 2.34 (m, 3H), 1.73 – 1.38 (m, 2H), 0.86 (t, *J* = 7.3 Hz, 3H).^{13}C NMR (125 MHz, DMSO-d_6) δ 163.95, 163.85, 148.00, 136.38, 135.49, 134.49, 134.47, 127.58, 120.16, 118.21, 117.67, 110.65, 36.75, 35.66, 29.34, 23.08, 12.56. HRMS (ESI) [M-H]$^-$: cald for $C_{20}H_{19}BrN_3O_2S_2$: 476.0108; found 476.0099.

2-Bromo-N-(2-(2-(cyclohexylamino)-2-oxoethylthio)benzo[d]thiazol-6-yl)acetamide (3-14p) white solid (Yield: 86%). ^{1}H NMR (300 MHz, DMSO-d_6) δ

10.67 (s, 1H), 8.38 (d, *J* = 1.5 Hz, 1H), 8.20 (d, *J* = 7.7 Hz, 1H), 7.76 (d, *J* = 8.7 Hz, 1H), 7.53 (dd, *J* = 1.7 Hz, 8.8Hz, 1H), 4.09 (s, 4H), 3.52 (s, 1H), 1.74 – 1.64 (m, 4H), 1.54 – 1.51 (m, 1H), 1.27 – 1.15 (m, 5H); ^{13}C NMR (75 MHz, DMSO-d_6): δ 165.2, 165.1, 164.9, 149.0, 135.4, 135.4, 121.1, 118.7, 111.6, 48.0, 36.9, 32.2, 30.3, 25.1, 24.3. HRMS (ESI) $[M - H]^-$: calcd for $C_{17}H_{19}BrN_3O_2S_2$: 440.0108; found 440.0108.

2-Bromo-N-(2-(2-(3-chlorophenylamino)-2-oxoethylthio)benzo[d]thiazol-6-yl)acetamide (3-14q) white solid (Yield: 80%). ^{1}H NMR (500 MHz, DMSO-d_6) δ 10.60 (s, 2H), 8.38 (s, 1H), 7.89 – 7.74 (m, 2H), 7.53 (dd, *J* = 8.8, 1.4 Hz, 1H), 7.45 (d, *J* = 8.1 Hz, 1H), 7.35 (t, *J* = 8.0 Hz, 1H), 7.13 (d, *J* = 8.0 Hz, 1H), 4.38 (s, 2H), 4.07 (s, 2H); ^{13}C NMR (125 MHz, DMSO-d_6) δ 166.16, 165.40, 165.12, 149.44, 140.64, 136.01, 135.93, 133.64, 131.02, 123.81, 121.66, 119.16, 119.14, 118.06, 112.19, 38.19, 30.79. HRMS (ESI) $[M - H]^-$: calcd for $C_{17}H_{13}BrClN_3O_2S_2$: 467.9248; found 467.9257.

2-Bromo-N-(2-(2-(3-fluorophenylamino)-2-oxoethylthio)benzo[d]thiazol-6-yl)acetamide (3-14r) white solid (Yield: 75%). ^{1}H NMR (300 MHz, DMSO-d_6) δ 8.39 (s, 1H), 7.78 (d, *J* = 8.9 Hz, 1H), 7.59 – 7.51 (m, 2H), 7.40 – 7.30 (m, 2H), 6.90 (t, *J* = 7.5 Hz, 1H), 4.39 (s, 2H), 4.07 (s, 2H); ^{13}C NMR (75 MHz, DMSO-d_6): δ 165.6, 164.9, 164.7, 162.1 (d, *J* = 241.5 Hz, 1C), 148.9, 140.4 (d, *J* = 11.0 Hz, 1C), 135.5, 135.4, 130.5 (d, *J* = 9.3 Hz, 1C), 121.2, 118.7, 114.9, 111.7, 110.1 (d, *J* = 20.9 Hz, 1C), 106.0 (d, *J* = 26.3 Hz, 1C), 37.7, 30.3. HRMS (ESI) $[M - H]^-$: calcd for $C_{17}H_{12}BrFN_3O_2S_2$: 451.9544; found 451.9546.

2-Bromo-N-(2-(2-(3-ethylphenylamino)-2-oxoethylthio)benzo[d]thiazol-6-yl)acetamide (3-14s) white solid (Yield: 82%). ^{1}H NMR (300 MHz, DMSO-d_6) δ 10.69 (s, 1H), 10.39 (s, 1H), 8.39 (d, *J* = 2.0 Hz, 1H), 7.79 (d, *J* = 8.8 Hz, 1H), 7.58 –

7.53 (m, 1H), 7.47 (s, 2H), 7.40 (d, *J* = 8.2 Hz, 1H), 7.21 (t, *J* = 7.8 Hz, 1H), 6.91 (d, *J* = 7.6 Hz, 1H), 4.37 (s, 2H), 4.10 (s, 2H), 2.56 (q, *J* = 7.7 Hz, 2H), 1.15 (t, *J* = 7.6 Hz, 3H).^{13}C NMR (75 MHz, DMSO-d_6) δ 165.11, 164.93, 164.83, 148.97, 144.38, 138.76, 135.47, 135.45, 128.70, 123.10, 121.14, 118.64, 118.51, 116.62, 111.64, 37.76, 30.33, 28.21, 15.47. HRMS (ESI) $[M - H]^-$: calcd for $C_{19}H_{17}BrN_3O_2S_2$: 461.9951; found 461.9956.

2-Bromo-N-(2-(2-(3-methoxyphenylamino)-2-oxoethylthio)benzo[d]thiazol-6-yl)acetamide (3-14t) white solid (Yield: 73%). ^{1}H NMR (300 MHz, DMSO-d_6) δ 10.66 (s, 1H), 10.43 (s, 1H), 8.39 (d, *J* = 2.0 Hz, 1H), 7.78 (d, *J* = 8.7 Hz, 1H), 7.54 (dd, *J* = 8.9 Hz, 2.1 Hz, 1H), 7.29 (d, *J* = 2.0 Hz, 1H), 7.22 (t, *J* = 8.1 Hz, 1H), 7.12 (d, *J* = 8.7 Hz, 1H), 6.65 (dd, *J* = 7.8 Hz, 1H), 4.37 (s, 2H), 4.08 (s, 2H), 3.72 (s, 3H); ^{13}C NMR (75 MHz DMSO-d_6) δ 171.1, 165.3, 164.3, 159.5, 148.7, 139.9, 135.5, 135.3, 129.6, 120.9, 119.2, 111.8, 111.4, 109.0, 105.0, 61.9, 55.0, 37.8. HRMS (ESI) $[M - H]^-$: calcd for $C_{18}H_{15}BrN_3O_3S_2$: 463.9744; found 463.9745.

2-Bromo-N-(2-(2-(4-ethylphenylamino)-2-oxoethylthio)-1H-benzo[d]imidazol-6-yl)acetamide (3-14u) white solid (Yield: 73%). ^{1}H NMR (500 MHz, DMSO-d_6) δ 10.77 (s, 1H), 10.46 (s, 1H), 8.19 (s, 1H), 7.65 (d, *J* = 8.8 Hz, 1H), 7.49 (dd, *J* = 15.3, 5.0 Hz, 3H), 7.14 (d, *J* = 8.3 Hz, 2H), 4.42 (s, 2H), 4.11 (s, 2H), 2.54 (dd, *J* = 15.1, 7.6 Hz, 2H), 1.14 (t, *J* = 7.6 Hz, 3H).^{13}C NMR (125 MHz, DMSO-d_6) δ 165.06, 164.59, 154.22, 149.95, 139.19, 136.19, 135.92, 133.38, 127.98, 119.31, 117.08, 113.81, 102.85, 36.81, 30.29, 27.53, 15.57. HRMS (ESI) $[M - H]^-$: calcd for $C_{19}H_{18}BrN_4O_2S$: 445.0339; found 445.0352.

^{1}H and ^{13}C NMR data of compound 3-1a:

2-(5-(4-Aminophenyl)-4-methyl-4H-1,2,4-triazol-3-ylthio)-N-(2-(2-(benzylamino)-2-oxoethylthio)benzo[d]thiazol-6-yl)acetamide (3-1a1) white solid (Yield: 83%). ^{1}H NMR (500 MHz, DMSO-d_6) δ 10.56 (s, 1H), 8.80 (s, 1H), 8.34 (s, 1H), 7.77 (d, *J* = 8.9 Hz, 1H), 7.52 – 7.23 (m, 8H), 6.65 (d, *J* = 8.2 Hz, 2H), 5.58 (s, 2H), 4.32 (d, *J* = 5.7 Hz, 2H), 4.18 (s, 2H), 4.10 (s, 2H), 3.59 (s, 3H); ^{13}C NMR (125 MHz, DMSO-d_6): δ 166.9, 166.6, 165.1, 156.6, 150.9, 149.5, 149.3, 139.5, 136.1, 136.0, 129.8,128.7, 127.6, 127.3, 121.6, 119.1, 114.1, 113.9, 112.0, 43.0, 38.3, 37.0, 32.2. HRMS (ESI) [M - H]$^{-}$: cald for $C_{27}H_{24}N_7O_2S_3$: 574.1159; found 574.1169.

2-(5-(4-Aminophenyl)-4-methyl-4H-1,2,4-triazol-3-ylthio)-N-(2-(2-(4-fluorobenzylamino)-2-oxoethylthio)benzo[d]thiazol-6-yl)acetamide (3-1a2) white solid (Yield: 71%): ^{1}H NMR (500 MHz, DMSO-d_6) δ 10.59 (s, 1H), 8.78 (t, *J* = 5.7 Hz, 1H), 8.31 (s, 1H), 7.72 (d, *J* = 8.7 Hz, 1H), 7.49 (dd, *J* = 8.8, 1.3 Hz, 1H), 7.38 (d, *J* = 8.5 Hz, 2H), 7.24 (dd, *J* = 8.1, 5.7 Hz, 2H), 7.03 (t, *J* = 8.7 Hz, 2H), 6.73 (d, *J* = 8.4 Hz, 2H), 4.26 (d, *J* = 5.8 Hz, 2H), 4.14 (d, *J* = 2.3 Hz, 4H), 3.62 (s, 3H). ^{13}C NMR (125 MHz, DMSO-d_6) δ 166.49, 165.70, 164.64, 162.12, 160.19, 155.23, 150.58, 150.10, 148.88, 135.57, 135.51, 135.18, 129.77, 129.13, 129.07, 121.15, 118.61, 115.00, 114.83, 114.31, 111.53, 41.87, 40.00, 37.60, 36.52, 32.26. HRMS (ESI) [M - H]$^{-}$: cald for $C_{27}H_{23}FN_7O_2S_3$: 592.1065; found 592.1068.

2-(5-(4-Aminophenyl)-4-methyl-4H-1,2,4-triazol-3-ylthio)-N-(2-(2-(4-methoxybenzylamino)-2-oxoethylthio)benzo[d]thiazol-6-yl)acetamide (3-1a3) white solid (Yield: 76%): ^{1}H NMR (500 MHz, DMSO-d_6) δ 10.86 (s, 1H), 8.81 (s, 1H), 8.38 (s, 1H), 8.03 – 7.31 (m, 5H), 6.99 (m, 7H), 4.21 (br, 6H), 3.68 (br, 6H).^{13}C NMR (125 MHz, DMSO-d_6) δ 166.29, 165.75, 164.60, 158.20, 155.15, 150.49,

149.43, 148.85, 135.68, 135.48, 130.89, 129.81, 128.51, 121.13, 118.55, 114.70, 113.62, 111.43, 55.04, 42.02, 37.62, 36.62, 32.33. HRMS (ESI) $[M - H]^-$: cald for $C_{28}H_{26}N_7O_3S_3$: 604.1265; found 604.1268.

2-(5-(4-Aminophenyl)-4-methyl-4H-1,2,4-triazol-3-ylthio)-N-(2-(2-(benzylamino)-2-oxoethylthio)-1H-benzo[d]imidazol-6-yl)acetamide (3-1a4) white solid (Yield: 63%). ^{1}H NMR (500 MHz, DMSO-d_6) δ 10.68 (s, 1H), 8.89 (s, 4H), 8.10 (s, 2H), 7.59 (d, J = 8.7 Hz, 1H), 7.52 (d, J = 8.1 Hz, 2H), 7.41 (d, J = 8.7 Hz, 1H), 7.24 (tt, J = 14.3, 7.1 Hz, 5H), 6.87 (d, J = 8.1 Hz, 2H), 4.31 (d, J = 5.7 Hz, 2H), 4.26 (s, 2H), 4.22 (s, 2H), 3.72 (s, 3H); ^{13}C NMR (500 MHz, DMSO-d_6) δ 166.64, 165.40, 158.70, 158.41, 151.85, 149.87, 138.81, 135.30, 135.06, 131.87, 130.20, 128.30, 127.21, 126.90, 116.36, 115.14, 114.03, 103.38, 42.70, 37.54, 35.55, 32.68. HRMS (ESI) $[M - H]^-$: cald for $C_{27}H_{25}N_8O_3S_3$: 557.1547; found 557.1543.

2-(5-(4-Aminophenyl)-4-methyl-4H-1,2,4-triazol-3-ylthio)-N-(2-(2-(4-fluorobenzylamino)-2-oxoethylthio)-1H-benzo[d]imidazol-6-yl)acetamide (3-1a5) white solid (Yield: 59%): ^{1}H NMR (500 MHz, DMSO-d_6) δ 10.74 (s, 1H), 8.96 (d, J = 4.8 Hz, 1H), 8.05 (s, 1H), 7.64 – 7.44 (m, 3H), 7.37 (d, J = 8.5 Hz, 1H), 7.33 – 7.21 (m, 2H), 7.07 (t, J = 8.5 Hz, 2H), 6.83 (d, J = 8.1 Hz, 3H), 4.25 (dd, J = 35.0, 4.2 Hz, 6H), 3.68 (s, 3H). ^{13}C NMR (125 MHz, DMSO-d_6) δ 166.94, 165.44, 162.12, 160.20, 154.97, 150.91, 149.69, 149.35, 136.31, 135.15, 134.63, 133.55, 129.96, 129.14, 129.08, 115.49, 115.04, 114.93, 114.87, 114.07, 111.93, 103.50, 41.87, 37.66, 35.37, 32.46. HRMS (ESI) $[M - H]^-$: cald for $C_{27}H_{24}FN_8O_2S_2$: 575.1453; found 575.1448.

2-(5-(4-Aminophenyl)-4-ethyl-4H-1,2,4-triazol-3-ylthio)-N-(2-(2-(benzylamino)-2-oxoethylthio)benzo[d]thiazol-6-yl)acetamide (3-1a6) white solid (Yield: 82%). ^{1}H NMR (500 MHz, DMSO-d_6) δ 10.59 (s, 1H), 8.79 (s, 1H), 8.35 (s, 1H), 7.78 – 7.23

(m, 9H), 6.66 (d, *J* = 7.6 Hz, 2H), 5.55 (s, 2H), 4.33 (d, *J* = 5.1 Hz, 2H), 4.18 (s, 4H), 4.00 (q, *J* = 7.0 Hz, 2H), 1.23 (t, *J* = 7.0 Hz, 3H); ^{13}C NMR (125 MHz, DMSO-d_6): δ 166.8, 166.4, 165.0, 156.0, 150.8, 149.2, 148.9, 139.3, 136.0, 135.9, 129.6, 128.6, 127.5, 127.2, 121.5, 118.9, 114.0 (2C), 111.8, 42.9, 39.8, 38.1, 36.9, 15.5. HRMS (ESI) $[M + Na]^+$: cald for $C_{28}H_{27}N_7NaO_2S_3$: 612.1281; found 612.1282.

2-(5-(4-Aminophenyl)-4-ethyl-4H-1,2,4-triazol-3-ylthio)-N-(2-(2-(4-fluorobenzylamino)-2-oxoethylthio)-1H-benzo[d] thiazol-6-yl)acetamide (3-1a7) white solid (Yield: 60%). ^{1}H NMR (300 MHz, DMSO-d_6) δ 10.58 (s, 1H), 8.81 (t, *J* = 5.9 Hz, 1H), 8.35 (d, *J* = 1.8 Hz, 1H), 7.76 (d, *J* = 8.7 Hz, 1H), 7.52 (dd, *J* = 2.1 Hz, 8.9 Hz, 1H), 7.31 – 7.24 (m, 3H), 7.08 (t, *J* = 8.9 Hz, 2H), 6.65 (d, *J* = 8.6 Hz, 2H), 5.56 (s, 2H), 4.30 (d, *J* = 5.8 Hz, 2H), 4.17 (s, 2H), 3.99 (q, J = 7.2 Hz, 2H), 1.22 (t, J = 7.2, 3H). ^{13}C NMR (125 MHz, DMSO-d_6) δ 166.42, 165.96, 164.52, 162.08, 160.16, 155.63, 150.36, 148.79, 148.53, 135.63, 135.46, 135.18, 135.16, 129.18, 129.11, 129.05, 121.10, 118.54, 114.98, 114.81, 113.63, 113.56, 111.43, 41.82, 37.66, 36.50, 15.09. HRMS (ESI) $[M - H]^-$: calcd for $C_{28}H_{25}FN_7O_2S_3$: 606.1221; found 606.1236.

N-Benzyl-2-(6-(2-(4-methyl-5-phenyl-4H-1,2,4-triazol-3-ylthio)acetamido)benzo[d]thiazol-2-ylthio)acetamide (3-1a8) white solid (Yield: 77%). ^{1}H NMR (500 MHz, DMSO-d_6) δ 10.58 (s, 1H), 8.80 (s, 1H), 8.36 (s, 1H), 7.91 – 7.64 (m, 3H), 7.55 (br, 4H), 7.24 (m, 5H), 4.33 (d, *J* = 4.8 Hz, 2H), 4.18 (m, 4H), 3.64 (s, 3H). ^{13}C NMR (125 MHz, DMSO-d_6) δ 166.89, 166.43, 165.11, 155.88, 150.83, 149.35, 139.46, 136.09, 135.99, 130.45, 129.36, 128.82, 128.69, 127.61, 127.50, 127.27, 121.61, 119.05, 111.97, 43.03, 38.11, 37.04, 32.30. HRMS (ESI) $[M – H]^-$: calcd for $C_{27}H_{23}FN_6O_2S_3$: 559.1050; found 559.1046.

N-(4-Fluorobenzyl)-2-(6-(2-(4-methyl-5-phenyl-4H-1,2,4-triazol-3-ylthio)acetamido)benzo[d]thiazol-2-ylthio)acetamide (3-1a9) light brown solid (Yield: 62%). ^{1}H NMR (300 MHz, DMSO-d_6) δ 10.83 (s, 1H), 8.94 (d, J = 5.8 Hz, 1H), 8.21 (s, 1H), 7.81 – 7.42 (m, 3H), 7.41 – 6.86 (m, 7H), 4.21 (m, 9H). ^{13}C NMR (125 MHz, DMSO-d_6) δ 166.47, 165.96, 164.61, 162.12, 160.19, 155.41, 150.37, 148.85, 135.62, 135.51, 135.22, 129.98, 129.14, 129.07, 128.89, 128.35, 127.01, 121.15, 118.57, 115.01, 114.84, 111.50, 41.86, 37.63, 36.53, 31.82. HRMS (ESI) [M – H]$^-$: calcd for $C_{27}H_{22}FN_6O_2S_3$: 577.0956; found 577.0957.

N-Benzyl-2-(6-(2-(4-ethyl-5-phenyl-4H-1,2,4-triazol-3-ylthio)acetamido)benzo[d]thiazol-2-ylthio)acetamide (3-1a10) white solid (Yield: 64%). ^{1}H NMR (500 MHz, DMSO-d_6) δ 10.89 (s, 1H), 8.89 (s, 1H), 8.38 (s, 1H), 7.76 (d, J = 8.2 Hz, 1H), 7.63 – 7.56 (m, 6H), 7.25 – 7.22 (m, 5H), 4.32 (d, J = 5.7 Hz, 2H), 4.25 (s, 2H), 4.19 (s, 2H), 4.05 (q, J = 6.9 Hz, 2H), 1.22 (t, J = 6.9 Hz, 3H); ^{13}C NMR (125 MHz, DMSO-d_6): δ 166.4, 165.9, 164.5, 154.9, 149.7, 148.8, 139.0, 135.7, 135.4, 130.0, 129.0, 128.3, 128.2, 127.2, 127.1, 126.7, 121.0, 118.5, 111.3, 42.5, 39.6, 37.6, 36.5, 15.0. HRMS (ESI) [M – H]$^-$: calcd for $C_{28}H_{25}N_6O_2S_3$: 573.1207; found 573.1207.

N-Benzyl-2-(6-(2-(5-phenyl-4H-1,2,4-triazol-3-ylthio)acetamido)benzo[d]thiazol-2-ylthio)acetamide (3-1a11) light brown solid (Yield: 60%). ^{1}H NMR (300 MHz, DMSO-d_6) δ 10.60 (s, 1H), 8.80 (t, J = 6.5 Hz, 1H), 8.37 (s, 1H), 7.95 (d, J = 7.4 Hz, 2H), 7.77 (d, J = 9.1 Hz, 1H), 7.56 – 7.47 (m, 4H), 7.29 – 7.21 (m, 4H), 4.32 (d, J = 5.6 Hz, 2H), 4.18 (s, 2H), 4.15 (s, 2H); ^{13}C NMR (125 MHz, DMSO-d_6) δ 166.11, 165.18, 149.87, 138.63, 136.23, 132.90, 129.13, 128.30, 127.28, 127.20, 127.11, 126.95, 117.38, 113.76, 102.78, 42.72, 35.90, 30.33. HRMS (ESI) [M – H]$^-$: calcd for $C_{26}H_{21}N_6O_2S_3$: 545.0894; found 545.0898.

N-(4-Fluorobenzyl)-2-(6-(2-(5-phenyl-4H-1,2,4-triazol-3-ylthio)acetamido)benzo[d]thiazol-2-ylthio)acetamide (3-1a12) white solid (Yield: 64%). ^{1}H NMR (500 MHz, DMSO-d_6) δ 14.40 (s, 1H), 10.53 (s, 1H), 8.79 (s, 1H), 8.38 (s, 1H), 7.95 (d, *J* = 6.3 Hz, 2H), 7.76 (d, *J* = 8.8 Hz, 1H), 7.56 – 7.48 (m, 4H), 7.28 (br, 1H), 7.08 (t, *J* = 8.2 Hz, 1H), 4.30 (d, *J* = 5.0 Hz, 2H), 4.17 (s, 4H); ^{13}C NMR (125 MHz, DMSO-d_6): δ 166.4, 164.4, 162.1, 160.1, 148.7, 135.8, 135.4, 135.2, 135.1, 130.0, 129.1, 129.0, 128.9, 125.9, 121.1, 118.5, 115.0, 114.8, 111.4, 41.8, 36.5, 36.4. HRMS (ESI) $[M - H]^-$: calcd for $C_{26}H_{20}FN_6O_2S_3$: 563.0799; found 563.0806.

N-(4-Methoxybenzyl)-2-(6-(2-(5-phenyl-4H-1,2,4-triazol-3-ylthio)acetamido)benzo[d]thiazol-2-ylthio)acetamide (3-1a13) white solid (Yield: 58%). ^{1}H NMR (500 MHz, DMSO-d_6) δ 10.61 (s, 1H), 8.73 (t, *J* = 5.7 Hz, 1H), 8.40 (d, *J* = 1.7 Hz, 1H), 8.11 – 7.90 (m, 2H), 7.77 (d, *J* = 8.8 Hz, 1H), 7.66 – 7.40 (m, 4H), 7.17 (d, *J* = 8.5 Hz, 2H), 6.82 (d, *J* = 8.6 Hz, 2H), 4.26 (d, *J* = 5.8 Hz, 2H), 4.17 (d, *J* = 3.6 Hz, 4H), 3.70 (s, 3H).^{13}C NMR (125 MHz, DMSO-d_6) δ 166.45, 166.25, 164.46, 158.21, 148.77, 135.81, 135.50, 130.86, 129.93, 128.92, 128.49, 125.92, 121.11, 118.52, 113.61, 111.39, 54.99, 42.03, 36.59, 36.47. HRMS (ESI) $[M - H]^-$: calcd for $C_{27}H_{23}N_6O_3S_3$: 575.0999; found 575.0996.

N-(4-Methylbenzyl)-2-(6-(2-(5-phenyl-4H-1,2,4-triazol-3-ylthio)acetamido)benzo[d]thiazol-2-ylthio)acetamide (3-1a14) white solid (Yield: 63%). ^{1}H NMR (500 MHz, DMSO-d_6) δ 10.56 (s, 1H), 8.76 (t, *J* = 5.7 Hz, 1H), 8.39 (d, *J* = 1.3 Hz, 1H), 7.96 (d, *J* = 6.9 Hz, 2H), 7.76 (d, *J* = 8.8 Hz, 1H), 7.56 (dd, J = 1.9 Hz, 8.8 Hz, 1H), 7.48 (m, 2H), 7.13 (d, *J* = 7.6 Hz, 2H), 7.06 (d, *J* = 8.2 Hz, 2H), 4.27 (d, J = 5.7 Hz, 2H), 4.17 (s, 4H), 2.24 (s, 3H).^{13}C NMR (125 MHz, DMSO-d_6) δ 166.79, 164.98, 149.25, 136.38, 136.33, 136.27, 135.96, 129.47, 129.44, 129.24,

127.63, 126.42, 121.58, 118.99, 111.87, 42.79, 37.05, 21.11. HRMS (ESI) $[M - H]^-$: calcd for $C_{27}H_{23}N_6O_2S_3$: 559.1050; found 559.1058.

N-Benzyl-2-(6-(2-(5-phenyl-4H-1,2,4-triazol-3-ylthio)acetamido)-1H-benzo[d]imidazol-2-ylthio)acetamide (3-1a15) white solid (Yield: 59%). ^{1}H NMR (500 MHz, DMSO-d_6) δ 12.71 (s, 1H), 10.41 (d, J = 1.1 Hz, 1H), 8.83 (s, 1H), 7.98 (s, 3H), 7.72 – 6.98 (m, 9H), 4.80 – 3.88 (m, 6H); ^{13}C NMR (125 MHz, DMSO-d_6) δ 167.37, 165.92, 157.17, 156.94, 149.66, 139.01, 133.52, 133.49, 129.89, 128.94, 128.20, 127.00, 126.70, 125.91, 114.04, 42.43, 36.55, 35.03. HRMS (ESI) $[M - H]^-$: calcd for $C_{26}H_{23}FN_7O_2S_2$: 528.1282; found 528.1289.

N-(4-Fluorobenzyl)-2-(6-(2-(5-phenyl-4H-1,2,4-triazol-3-ylthio)acetamido)-1H-benzo[d]imidazol-2-ylthio)acetamide (3-1a16) white solid (Yield: 56%). ^{1}H NMR (500 MHz, DMSO-d_6) δ 14.42 (s, 1H), 12.55 (s, 1H), 10.31 (s, 1H), 8.78 (s, 1H), 7.97 (br, 3H), 7.74 – 6.80 (m, 8H), 5.10 – 3.76 (m, 6H); HRMS (ESI) $[M - H]^-$: calcd for $C_{27}H_{21}FN_7O_2S_2$: 546.1188; found 546.1208.

N-(4-Methoxybenzyl)-2-(6-(2-(5-phenyl-4H-1,2,4-triazol-3-ylthio)acetamido)-1H-benzo[d]imidazol-2-ylthio)acetamide (3-1a17) white solid (Yield: 65%). ^{1}H NMR (500 MHz, DMSO-d_6) δ 10.44 (s, 1H), 8.70 (s, 1H), 7.97 (d, J = 7.6 Hz, 1H), 7.49 – 7.47 (m, 3H), 7.37 (d, J = 8.2 Hz, 1H), 7.20 (d, J = 7.6 Hz, 1H), 7.14 (d, J = 7.6 Hz, 2H), 4.23 (d, J = 5.0 Hz, 2H), 4.12 (s, 2H), 4.04 (s, 2H), 3.69 (s, 3H); ^{13}C NMR (125 MHz, DMSO-d_6): 167.2, 165.9, 158.1, 157.4, 156.8, 149.6, 133.5, 130.8, 129.7, 128.9, 128.3, 125.8, 114.0, 113.6, 55.0, 41.9, 36.5, 35.1. HRMS (ESI) $[M - H]^-$: calcd for $C_{27}H_{24}N_7O_3S_2$: 558.1388; found 558.1393.

N-Benzyl-N-methyl-2-(6-(2-(5-phenyl-4H-1,2,4-triazol-3-ylthio)acetamido)benzo[d]thiazol-2-ylthio)acetamide (3-1a18) white solid (Yield:

65%). ^{13}C NMR (125 MHz, DMSO-d_6): δ. 167.8, 167.5, 165.8, 149.9, 138.3, 137.9, 136.8, 136.5, 131.1, 130.0, 129.8, 129.5, 128.5, 128.1, 127.9, 127.0, 122.1, 119.6, 112.5, 37.8, 37.5, 36.2, 34.9. HRMS (ESI) [M – H]$^-$: calcd for $C_{27}H_{23}N_6O_2S_3$: 559.1052; found 559.1050.

N-(2-(2-Oxo-2-(phenylamino)ethylthio)benzo[d]thiazol-6-yl)-2-(5-phenyl-4H-1,2,4-triazol-3-ylthio)acetamide (3-1a19) white solid (Yield: 66%). ^{1}H NMR (500 MHz, DMSO-d_6) δ 10.53 (s, 1H), 10.40 (s, 1H), 8.39 (s, 1H), 7.95 (d, J = 6.9 Hz, 2H), 7.78 (d, J = 8.8 Hz, 1H), 7.60 – 7.48 (m, 6H), 7.32 (t, J = 7.6 Hz, 2H), 7.07 (t, J = 7.6 Hz, 1H), 4.37 (s, 2H), 4.15 (s, 2H); ^{13}C NMR (125 MHz, DMSO-d_6): δ 166.5, 165.2, 164.4, 148.7, 138.7, 135.8, 135.5, 130.4, 128.9, 128.8, 125.9, 123.6, 121.1, 119.2, 118.6, 117.6, 111.4, 37.7, 36.3. HRMS (ESI) [M – H]$^-$: calcd for $C_{25}H_{19}N_6O_2S_3$: 531.0737; found 531.0724.

N-(4-Fluorophenyl)-2-(6-(2-(5-phenyl-4H-1,2,4-triazol-3-ylthio)acetamido)benzo[d]thiazol-2-ylthio)acetamide (3-1a20) white solid (Yield: 68%). ^{1}H NMR (300 MHz, DMSO-d_6) δ 10.53 (s, 1H), 10.47 (s, 1H), 10.36 (s, 1H), 8.38 (s, 1H), 7.95 – 7.93 (m, 2H), 7.78 – 7.76 (m, 2H), 7.62 – 7.48 (m, 5H), 7.19 – 7.13 (m, 2H), 4.35 (s, 2H), 4.15 (s, 2H). HRMS (ESI) [M – H]$^-$: calcd for $C_{25}H_{18}FN_6O_2S_3$, 549.0643; found 549.0667; ^{13}C NMR (75 MHz, DMSO-d_6) δ 166.41, 165.16, 164.37, 159.75, 156.57, 148.72, 135.82, 135.48, 135.13, 129.97, 128.93, 127.93, 125.92, 121.10, 121.05, 120.94, 118.58, 115.55, 115.25, 111.45, 37.63, 36.45. HRMS (ESI) [M – H]$^-$: calcd for $C_{25}H_{18}FN_6O_2S_3$: 549.0643; found 549.0641.

N-(4-Chlorophenyl)-2-(6-(2-(5-phenyl-4H-1,2,4-triazol-3-ylthio)acetamido)benzo[d]thiazol-2-ylthio)acetamide (3-1a21) white solid (Yield: 64%). ^{1}H NMR (500 MHz, DMSO-d_6) δ 10.56 (s, 1H), 10.53 (s, 1H), 8.39 (s, 1H),

7.94 (m, 2H), 7.76 (d, *J* = 8.8 Hz, 1H), 7.61 (d, *J* = 8.8 Hz, 1H), 7.53 – 7.37 (m, 6H), 4.37 (s, 2H), 4.13 (s, 2H). HRMS (ESI) $[M - H]^-$: calcd for $C_{25}H_{18}ClN_6O_2S_3$: 565.0347; found 565.0361.

N-(4-Methoxyphenyl)-2-(6-(2-(5-phenyl-4H-1,2,4-triazol-3-ylthio)acetamido)benzo[d]thiazol-2-ylthio)acetamide (3-1a22) white solid (Yield: 67%). ^{1}H NMR (500 MHz, DMSO-d_6) δ 14.46 (s, 1H), 10.53 (s, 1H), 10.34 – 10.20 (m, 2H), 8.39 (s, 1H), 7.96 (s, 2H), 7.78 (d, *J* = 8.2 Hz, 1H), 7.66 (d, *J* = 6.9 Hz, 1H), 7.49 – 7.39 (m, 5H), 6.95 – 6.88 (m, 2H), 4.33 (s, 2H), 4.16 (s, 2H), 3.71 (s, 3H); ^{13}C NMR (125 MHz, DMSO-d_6): δ 166.4, 164.4, 162.1, 160.1, 148.7, 135.8, 135.4, 135.2, 135.1, 130.0, 129.1, 129.0, 128.9, 125.9, 121.1, 118.5, 115.0, 114.8, 111.4, 41.8, 36.5, 36.4. HRMS (ESI) $[M - H]^-$: calcd for $C_{26}H_{21}N_6O_3S_3$: 561.0843; found 561.0847.

N-(2-(2-Oxo-2-(p-tolylamino)ethylthio)benzo[d]thiazol-6-yl)-2-(5-phenyl-4H-1,2,4-triazol-3-ylthio)acetamide (3-1a23) white solid (Yield: 70%). 1H NMR (500 MHz, DMSO-d_6) δ 14.36 (s, 1H), 10.55 (s, 1H), 10.31 (s, 1H), 8.38 (d, *J* = 1.7 Hz, 1H), 8.06 – 7.87 (m, 2H), 7.77 (d, *J* = 8.8 Hz, 1H), 7.51 (m, 6H), 7.13 (t, *J* = 8.9 Hz, 2H), 4.34 (s, 2H), 4.15 (s, 2H), 2.25 (s, 3H).^{13}C NMR (125 MHz, DMSO-d_6) δ 165.38, 163.91, 163.45, 147.72, 135.22, 134.79, 134.45, 131.54, 128.96, 128.32, 128.16, 127.93, 124.90, 120.08, 118.17, 117.56, 110.43, 36.72, 35.43, 19.40. HRMS (ESI) $[M - H]^-$: calcd for $C_{26}H_{21}N_6O_2S_3$: 545.0894; found 545.0896.

N-(4-Ethylphenyl)-2-(6-(2-(5-phenyl-4H-1,2,4-triazol-3-ylthio)acetamido)benzo[d]thiazol-2-ylthio)acetamide (3-1a24) white solid (Yield: 62%). ^{1}H NMR (500 MHz, DMSO-d_6) δ 14.56 (s, 1H), 10.55 (s, 1H), 10.34 (s, 1H), 8.37 (s, 1H), 7.94 (d, *J* = 7.4 Hz, 2H), 7.78 (d, *J* = 8.7 Hz, 1H), 7.51 (m, 6H), 7.14 (m, 2H), 4.33 (s, 2H), 4.15 (s, 2H), 2.53 (q, *J* = 7.5 Hz, 2H), 1.13 (t, *J* = 7.5 Hz, 3H).^{13}C

NMR (125 MHz, DMSO-d_6): δ 166.4, 164.9, 164.4, 148.7, 139.0, 136.4, 135.8, 135.4, 130.0, 128.9, 128.0, 125.9, 121.1, 119.2, 118.6, 111.4, 37.7, 36.4, 27.5, 15.6. HRMS (ESI) $[M - H]^-$: calcd for $C_{27}H_{23}N_6O_2S_3$: 559.1050; found 559.1056.

N-(2-(2-Oxo-2-(4-propylphenylamino)ethylthio)benzo[d]thiazol-6-yl)-2-(5-phenyl-4H-1,2,4-triazol-3-ylthio)acetamide (3-1a25) white solid (Yield: 75%). ^{1}H NMR (500 MHz, DMSO-d_6) δ 10.58 (s, 1H), 10.37 (s, 1H), 8.40 (s, 1H), 7.95 (d, J = 6.9 Hz, 2H), 7.78 (d, J = 8.6 Hz, 1H), 7.52 (m, 5H), 7.13 (d, J = 7.9 Hz, 2H), 4.36 (s, 2H), 4.17 (s, 2H), 2.50 (br, 2H), 1.55 (m, 2H), 0.87 (t, J = 7.1 Hz, 3H). ^{13}C NMR (125 MHz, DMSO-d_6) δ 165.45, 164.01, 163.53, 156.04, 155.97, 147.79, 136.42, 135.51, 134.88, 134.52, 129.06, 127.99, 127.61,126.85, 125.00, 120.14, 118.24, 117.61, 110.46, 36.79, 35.69, 35.50, 23.14, 12.58. HRMS (ESI) $[M - H]^-$: calcd for $C_{28}H_{25}N_6O_2S_3$: 573.1207; found 573.1209.

N-(3-Fluorophenyl)-2-(6-(2-(5-phenyl-4H-1,2,4-triazol-3-ylthio)acetamido)benzo[d]thiazol-2-ylthio)acetamide (3-1a26) white solid (Yield: 69%). ^{1}H NMR (300 MHz, DMSO-d_6) δ 10.81 (s, 1H), 10.64 (s, 1H), 8.38 (d, J = 1.7 Hz, 1H), 7.95 (s, 1H), 7.93 (s, 1H), 7.76 (d, J = 8.7 Hz, 1H), 7.59 – 7.29 (m, 7H), 6.90 (t, J = 8.1 Hz, 1H), 4.38 (s, 2H), 4.10 (s, 2H); ^{13}C NMR (125 MHz, DMSO-d_6): δ 166.4, 165.7, 164.3, 162.1 (d, J = 241.9 Hz, 1C), 157.2, 156.8, 148.7, 140.4 (d, J = 11.0 Hz, 1C), 135.8, 135.5, 130.5 (d, J = 9.2 Hz, 1C), 121.1, 118.6, 115.0, 111.5, 110.0 (d, J = 21.1 Hz, 1C), 106.0 (d, J = 26.6 Hz, 1C), 37.7, 36.5. HRMS (ESI) $[M - H]^-$: calcd for $C_{25}H_{18}FN_6O_2S_3$: 549.0643; found 549.0655.

N-(3-Chlorophenyl)-2-(6-(2-(5-phenyl-4H-1,2,4-triazol-3-ylthio)acetamido)benzo[d]thiazol-2-ylthio)acetamide (3-1a27) white solid (Yield: 73%). ^{1}H NMR (500 MHz, DMSO-d_6) δ 10.84 (s, 2H), 8.39 (s, 1H), 7.97 (s, 2H), 7.79

(d, *J* = 27.3 Hz, 2H), 7.46 (m, 6H), 7.12 (s, 2H), 4.39 (s, 2H), 4.14 (s, 2H). ^{13}C NMR (125 MHz, DMSO-d_6) δ 167.17, 166.24, 164.73, 157.92, 157.16, 149.17, 140.68, 136.39, 135.94, 133.60, 130.98, 130.20, 129.34, 128.86, 126.38, 123.78, 121.58, 119.16, 119.09, 118.10, 111.89, 38.13, 36.93. HRMS (ESI) [M – H]$^-$: calcd for $C_{25}H_{18}ClN_6O_2S_3$: 565.0347; found 565.0347.

N-(3-Methoxyphenyl)-2-(6-(2-(5-phenyl-4H-1,2,4-triazol-3-ylthio)acetamido)benzo[d]thiazol-2-ylthio)acetamide (3-1a28) white solid (Yield: 65%). ^{1}H NMR (300 MHz, DMSO-d_6) δ 10.53 (s, 1H), 10.40 (s, 1H), 8.38 (d, *J* = 1.8 Hz, 1H), 7.95 – 7.93 (m, 2H), 7.77 (d, *J* = 8.9 Hz, 1H), 7.56 – 7.47 (m, 4H), 7.28 – 7.19 (m, 2H), 7.11 (d, *J* = 7.9 Hz, 1H), 6.65 (dd, *J* = 2.4 Hz, 8.1 Hz, 1H), 4.36 (s, 2H), 4.15 (s, 2H), 3.72 (s, 3H). ^{13}C NMR (125 MHz, DMSO-d_6): δ 165.23, 164.38, 159.53, 148.73, 139.86, 135.79, 135.47, 129.59, 128.90, 125.92, 121.07, 118.59, 111.45, 109.04, 105.03, 54.95, 37.79. HRMS (ESI) [M – H]$^-$: calcd for $C_{26}H_{21}N_6O_3S_3$: 561.0843; found 561.0863.

N-(3-Ethylphenyl)-2-(6-(2-(5-phenyl-4H-1,2,4-triazol-3-ylthio)acetamido)benzo[d]thiazol-2-ylthio)acetamide (3-1a29) white solid (Yield: 83%): ^{1}H NMR (500 MHz, DMSO-d_6) δ 10.65 (s, 1H), 10.44 (s, 1H), 8.41 (s, 1H), 8.20 – 7.08 (m, 10H), 6.91 (s, 1H), 4.37 (s, 2H), 4.18 (s, 2H), 2.55 (q, *J* = 6.2 Hz, 2H), 1.14 (s, 3H).^{13}C NMR (125 MHz, DMSO-d_6) δ 166.48, 165.20, 164.51, 148.78, 144.43, 138.81, 135.89, 135.50, 130.04, 128.98, 128.74, 126.00, 123.15, 121.14, 118.61, 118.57, 116.67, 111.46, 37.80, 36.47, 28.27, 15.52. HRMS (ESI) [M – H]$^-$: calcd for $C_{27}H_{23}N_6O_2S_3$: 559.1050; found 559.1064.

N-(4-Ethylphenyl)-2-(6-(2-(5-phenyl-4H-1,2,4-triazol-3-ylthio)acetamido)-1H-benzo[d]imidazol-2-ylthio)acetamide (3-1a30) white solid (Yield: 57%): ^{1}H NMR

(500 MHz, DMSO-d_6) δ 14.52 (s, 1H), 10.41 (s, 1H), 10.34 (s, 1H), 7.96 (br, 3H), 7.45 (m, 6H), 7.24 (d, J = 8.3 Hz, 1H), 7.13 (d, J = 8.2 Hz, 2H), 4.25 (s, 2H), 4.15 (s, 2H), 2.58 – 2.52 (m, 2H), 1.13 (t, J = 7.5 Hz, 3H).^{13}C NMR (125 MHz, DMSO-d_6) δ 165.95, 165.78, 149.73, 138.95, 136.53, 133.86, 128.98, 128.01, 125.95, 119.16, 114.42, 36.30, 27.59, 15.67. HRMS (ESI) [M – H]$^-$: calcd for $C_{27}H_{24}N_7O_2S_2$: 542.1438; found 542.1453.

N-(4-Ethylphenyl)-2-(6-(2-(4-methyl-5-phenyl-4H-1,2,4-triazol-3-ylthio)acetamido)benzo[d]thiazol-2-ylthio)acetamide (3-1a31) white solid (Yield: 80%): ^{1}H NMR (500 MHz, DMSO-d_6) δ 10.58 (s, 1H), 10.35 (s, 1H), 8.37 (s, 1H), 7.96 – 7.32 (m, 8H), 7.15 (s, 2H), 4.35 (s, 2H), 4.17 (s, 2H), 3.63 (s, 3H), 2.54 (br, 2H), 1.14 (br, 3H).^{13}C NMR (125 MHz, DMSO-d_6) δ 165.94, 164.95, 164.64, 155.40, 150.35, 148.84, 139.03, 136.45, 135.64, 135.50, 129.98, 128.88, 128.34, 128.02, 127.00, 121.16, 119.27, 118.60, 111.52, 37.74, 37.61, 31.82, 27.59, 15.67. HRMS (ESI) [M – H]$^-$: calcd for $C_{28}H_{25}N_6O_2S_3$: 573.1207; found 573.1209.

2-(5-(4-Aminophenyl)-4H-1,2,4-triazol-3-ylthio)-N-(2-(2-(4-ethylphenylamino)-2-oxoethylthio)benzo[d]thiazol-6-yl)acetamide (3-1a32) white solid (Yield: 65%): ^{1}H NMR (500 MHz, DMSO-d_6) δ 10.70 (s, 1H), 10.46 (s, 1H), 8.39 (s, 1H), 7.90 (d, J = 7.4 Hz, 2H), 7.77 (d, J = 8.3 Hz, 1H), 7.54 (m, 3H), 7.14 (m, 3H), 4.36 (s, 2H), 4.16 (s, 2H), 2.53 (m, 2H), 1.14 (t, J = 7.0 Hz, 3H).^{13}C NMR (125 MHz, DMSO-d_6) δ 165.52, 163.95, 163.43, 158.22, 147.71, 138.15, 138.02, 135.42, 134.84, 134.45, 126.98, 126.70, 120.08, 118.28, 117.56, 114.68, 110.40, 36.73, 35.34, 26.56, 14.62. HRMS (ESI) [M - H]$^-$: calcd for $C_{27}H_{24}N_7O_2S_3$: 574.1159; found 574.1168.

N-(4-Ethylphenyl)-2-(6-(2-(5-(4-nitrophenyl)-4H-1,2,4-triazol-3-ylthio)acetamido)benzo[d]thiazol-2-ylthio)acetamide (3-1a33) light brown solid

(Yield: 69%): ^{1}H NMR (500 MHz, DMSO-d_6) δ 14.49 (s, 1H), 10.57 (s, 1H), 10.31 (s, 1H), 8.47 – 8.28 (m, 2H), 8.20 (d, *J* = 8.3 Hz, 2H), 7.78 (d, *J* = 8.8 Hz, 1H), 7.60 – 7.40 (m, 3H), 7.15 (d, *J* = 8.4 Hz, 2H), 4.34 (s, 2H), 4.26 (s, 2H), 2.55 (q, *J* = 7.6 Hz, 2H), 1.15 (t, *J* = 7.6 Hz, 3H).^{13}C NMR (75 MHz, DMSO-d_6) δ 166.18, 165.07, 164.68, 148.89, 147.91, 139.19, 136.47, 135.77, 135.57, 128.08, 126.95, 124.34, 121.22, 119.41, 118.72, 111.61, 37.78, 36.77, 27.66, 15.72. HRMS (ESI) $[M - H]^-$: calcd for $C_{27}H_{22}N_7O_4S_3$: 604.0901; found 604.0899.

N-(4-Ethylphenyl)-2-(6-(2-(5-(4-hydroxyphenyl)-4H-1,2,4-triazol-3-ylthio)acetamido)benzo[d]thiazol-2-ylthio)acetamide (3-1a34) white solid (Yield: 60%): ^{1}H NMR (500 MHz, DMSO-d_6) δ 10.55 (s, 1H), 10.35 (s, 1H), 9.96 (s, 1H), 8.39 (s, 1H), 7.77 (d, *J* = 8.2 Hz, 3H), 7.52 (m, 3H), 7.14 (d, *J* = 7.7 Hz, 2H), 6.86 (d, *J* = 8.0 Hz, 2H), 4.35 (s, 2H), 4.12 (s, 2H), 2.54 (q, *J* = 7.4 Hz, 2H), 1.14 (t, *J* = 7.4 Hz, 3H). ^{13}C NMR (125 MHz, DMSO-d_6) δ 166.54, 164.96, 164.45, 159.23, 158.46, 158.16, 156.66, 148.74, 139.06, 136.42, 135.85, 135.48, 128.00, 127.71, 121.10, 119.31, 118.59, 115.70, 111.43, 37.73, 36.36, 27.58, 15.63. HRMS (ESI) $[M - H]^-$: calcd for $C_{27}H_{23}N_6O_3S_3$: 575.0999; found 575.0990.

2-(5-Cyclohexyl-4H-1,2,4-triazol-3-ylthio)-N-(2-(2-(4-ethylphenylamino)-2-oxoethylthio)benzo[d]thiazol-6-yl)acetamide (3-1a35) white solid (Yield: 66%): ^{1}H NMR (500 MHz, DMSO-d_6) δ 10.41 (s, 1H), 10.26 (s, 1H), 8.34 (d, *J* = 1.2 Hz, 1H), 7.77 (d, *J* = 8.8 Hz, 1H), 7.60 – 7.38 (m, 3H), 7.15 (d, *J* = 8.3 Hz, 2H), 4.33 (s, 3H), 4.03 (s, 3H), 2.70 (m, 1H), 2.55 (q, *J* = 7.5 Hz, 2H), 1.98 – 1.82 (m, 2H), 1.77 – 1.68 (m, 2H), 1.64 (dd, *J* = 9.2, 3.4 Hz, 1H), 1.45 (m, 2H), 1.32 (m, 2H), 1.19 – 1.11 (m, 4H). ^{13}C NMR (125 MHz, DMSO-d_6) δ 166.54, 164.94, 164.41, 162.18, 156.85, 148.70, 139.03, 136.42, 135.83, 135.44, 127.98, 121.06, 119.28, 118.54, 111.37,

37.71, 36.19, 35.36, 30.78, 27.57, 25.31, 25.14, 15.62. HRMS (ESI) $[M - H]^-$: calcd for $C_{27}H_{29}N_6O_2S_3$: 565.1520; found 565.1536.

N-(4-Ethylphenyl)-2-(6-(2-(5-propyl-4H-1,2,4-triazol-3-ylthio)acetamido)benzo[d]thiazol-2-ylthio)acetamide (3-1a36) white solid (Yield: 56%): ^{1}H NMR (500 MHz, DMSO-d_6) δ 10.42 (s, 1H), 10.26 (s, 1H), 8.35 (s, 1H), 7.77 (d, *J* = 8.7 Hz, 1H), 7.69 – 7.37 (m, 3H), 7.15 (d, *J* = 8.2 Hz, 2H), 4.34 (s, 2H), 4.03 (s, 2H), 2.62 (t, *J* = 7.4 Hz, 2H), 2.56 (q, *J* = 7.5 Hz, 2H), 1.65 (m, 2H), 1.15 (t, *J* = 7.5 Hz, 3H), 0.88 (t, *J* = 7.3 Hz, 3H); ^{13}C NMR (125 MHz, DMSO-d_6) δ 166.55, 165.00, 164.49, 158.27, 148.74, 139.08, 136.47, 135.85, 135.49, 128.05, 121.12, 119.31, 118.56, 111.40, 37.75, 36.24, 27.79, 27.62, 20.64, 15.70, 13.48. HRMS (ESI) $[M - H]^-$: calcd for $C_{24}H_{25}N_6O_2S_3$: 525.1207; found 525.1199.

N-(4-Ethylphenyl)-2-(6-(2-(5-o-tolyl-4H-1,2,4-triazol-3-ylthio)acetamido)benzo[d]thiazol-2-ylthio)acetamide (3-1a37) white solid (Yield: 79%): ^{1}H NMR (500 MHz, DMSO-d_6) δ 14.14 (s, 1H), 10.46 (s, 1H), 10.27 (s, 1H), 8.37 (s, 1H), 7.77 (d, *J* = 8.7 Hz, 1H), 7.65 (d, *J* = 7.4 Hz, 1H), 7.51 (m, 3H), 7.42 – 7.23 (m, 3H), 7.15 (d, *J* = 8.0 Hz, 2H), 4.34 (s, 2H), 4.15 (s, 2H), 2.55 (q, 7.5 Hz, 2H), 2.46 (s, 3H), 1.15 (t, *J* = 7.5 Hz, 3H); ^{13}C NMR (125 MHz, DMSO-d_6) δ 166.27, 164.83, 164.28, 148.65, 138.95, 136.41, 136.31, 135.75, 135.36, 131.02, 128.71, 127.84, 125.75, 120.97, 119.24, 118.51, 111.33, 37.65, 36.35, 27.45, 20.62, 15.45. HRMS (ESI) $[M - H]^-$: calcd for $C_{28}H_{25}N_6O_2S_3$: 573.1208; found 573.1207.

N-(4-Ethylphenyl)-2-(6-(2-(5-(pyridin-4-yl)-4H-1,2,4-triazol-3-ylthio)acetamido)benzo[d]thiazol-2-ylthio)acetamide (3-1a38) white solid (Yield: 61%): ^{1}H NMR (500 MHz, DMSO-d_6) δ 14.57 (s, 1H), 10.56 (s, 1H), 10.35 (s, 1H), 8.37 (s, 1H), 7.86 (s, 1H), 7.77 (d, *J* = 8.7 Hz, 1H), 7.50 (dd, *J* = 17.9, 8.4 Hz, 3H),

7.14 (d, *J* = 8.2 Hz, 2H), 6.99 (d, *J* = 1.5 Hz, 1H), 6.66 (s, 1H), 4.34 (s, 2H), 4.15 (s, 2H), 2.54 (dd, *J* = 15.0, 7.5 Hz, 2H), 1.14 (t, *J* = 7.5 Hz, 3H); ^{13}C NMR (125 MHz, DMSO-d_6) δ 165.43, 165.01, 149.24, 139.52, 136.91, 136.21, 135.94, 128.49, 121.60, 119.75, 119.05, 111.94, 38.19, 28.05, 16.14. HRMS (ESI) [M – H]$^-$: calcd for $C_{26}H_{23}N_7O_2S_3$: 560.1003; found 560.1001.

2-(5-(4-Aminophenyl)-4-methyl-4H-1,2,4-triazol-3-ylthio)-N-(2-(2-(4-ethylphenylamino)-2-oxoethylthio)benzo[d]thiazol-6-yl)acetamide (3-1a39) white solid (Yield: 57%): ^{1}H NMR (500 MHz, DMSO-d_6) δ 10.63 (s, 1H), 10.35 (s, 1H), 8.36 (s, 1H), 7.78 (d, *J* = 8.6 Hz, 1H), 7.59 – 7.44 (m, 4H), 7.16 (t, *J* = 9.4 Hz, 2H), 6.82 (d, *J* = 8.1 Hz, 1H), 4.35 (s, 3H), 4.22 (s, 2H), 3.69 (s, 3H), 2.55 (dd, *J* = 15.1, 7.8 Hz, 2H), 1.15 (t, *J* = 7.3 Hz, 3H). HRMS (ESI) [M – H]$^-$: calcd for $C_{28}H_{26}N_7O_2S_3$: 588.1316; found 588.1316.

N-Cyclohexyl-2-(6-(2-(5-phenyl-4H-1,2,4-triazol-3-ylthio)acetamido)benzo[d]thiazol-2-ylthio)acetamide (3-1a40) white solid (Yield: 59%). ^{1}H NMR (300 MHz, DMSO-d_6) δ 10.52 (s, 1H), 8.38 (s, 1H), 8.18 (d, *J* = 7.9 Hz, 1H), 7.93 (m, 2H), 7.76 (d, *J* = 8.7 Hz, 1H), 7.53 – 7.51 (m, 4H), 4.13 (br, 2H), 4.08 (s, 2H), 3.53 (m, 1H), 1.74 – 1.63 (m, 4H), 1.54 – 1.51 (m, 1H), 1.27 – 1.11 (m, 5H); ^{13}C NMR (125 MHz, DMSO-d_6): δ 166.4, 165.2, 164.7, 159.3, 155.2, 148.8, 135.7, 135.4, 130.3, 129.0, 126.8, 125.9, 121.0, 118.5, 111.4, 48.0, 36.9, 36.3, 32.1, 25.1, 24.3. HRMS (ESI) [M – H]$^-$: calcd for $C_{25}H_{25}N_6O_2S_3$: 537.1207; found 537.1215.

Chapter 4

Synthesis, *In Vitro* Evaluation and Docking Studies of (-)-4-Benzoyl-3-hydroxy-1-(5-mercapto-1,3,4-thiadiazol-2-yl)-5-phenyl-1H-pyrrol-2(5H)-ones as Potent Inhibitor of WNV NS2B-NS3 Protease

4.1 Synthesis of analogues of the lead compound

The general synthetic strategies of compounds **4-1a1** and **4-7** are shown in Scheme 4.1. An appropriate methyl aryl ketone **4-3** was reacted with diethyloxalate in the presence of sodium ethoxide to produce 2,4-diketo ethyl ester **4-4**, which was subsequently hydrolyzed to the target 2,4-diketoacids **4-5** with NaOH in a one pot reaction.[112] Using this one pot reaction, without isolation of the ester **4-4**, compound **4-5** was obtained in higher yield than that with the isolation of the intermediate **4-4**. On the other hand, compound **4-2** was synthesized from 5-sulfanyl-1,3,4-thiadiazol-2-ylamine, which was reacted with different alkyl and benzyl bromide in ethanol at room temperature and in the presence of KOH.[113] With **4-2** and **4-5** in our hands, we proceeded to synthesize the amide compound **4-6** which was obtained in a one pot procedure by first treating the acid **4-5** in dimethyl acetamide (DMA) with thionyl chloride and then reacting the intermediate with stoichiometric amounts of amine **4-2** to give **4-6**. DMA was used as it offers the rate and stability advantages over dimethylformamide (DMF).[114,115] The cyclization reaction for forming the racemic compound **4-1a** was performed either by the reaction of compound **4-6** and aryl aldehyde[115] or by a three components reaction using 2,4-diketo ethyl ester **4-4**, amine **4-2** and the corresponding aldehyde.[116] The reaction of **4-6** with aldehyde was investigated with various catalysts, solvents and at different temperature. A

Scheme 4.1 Synthesis of **4-1a** and **4-7**

Reagents: (a) R^3X, KOH, EtOH, rt, 2h; (b) $(COOEt)_2$, NaOEt, ethanol, rt, 14h; (c) NaOH, H_2O, rt, 4h; (d) $SOCl_2$, DMA, 0 °C, 15min; (e) Compound **4-2**, rt, 4h; (f) R^2CHO, toluene, 20 mol% piperidine/acetic acid (1:1), 70 °C, 12h; (g) R^2CHO, **4-2**, toluene, 20 mol% piperidine/acetic acid (1:1), 70 °C, 12h (h) R^4NH_2, dioxane, reflux, (i) $SnCl_2.H_2O$, EtOH, reflux; (j) m-CPBA, DCM, 0-5 °C, 2.5 h; (k) MeOH, PPh_3, DIAD, 0 °C-rt, 15 h.

combination of piperidine/AcOH (entry 10) was found to give better yield (60%) in toluene at 70 °C. Alternatively, the synthesis of compound **4-1a** in a three component reaction, at 70 °C in 1,4-dioxane gave better yield than in a two component reaction (amide **4-6** and aldehyde). Compound **4-1a30** i.e 4-aminophenyl group at R^1 was

Table 4.1 Optimization of cyclization reaction to prepare compound **4-1a**

Entry	Catalysis	Solvent	Time (h)	Temperature	Yield
1	NaOEt	Ethanol	12	rf[a]	NA
2	DBU	Toluene	12	rf	NA
3	TMSCl	DMF	12	rf	NA
4	Pyridine	Toluene	12	rf	NA
5	Piperidine	Ethanol	12	rf	NA
6	Piperidine/AcOH	Ethanol	12	rf	NA
7[b]	Piperidine/AcOH	ACN	0.5	110 °C	NA
8	Piperidine/AcOH	THF	12	rf	Trace
9	Piperidine/AcOH	Toluene	12	rf	25%
10	Piperidine/AcOH	Toluene	12	70 °C	60%

[a] rf: reflux; [b] Microwave heating

synthesized by reduction of the 4-itrophenyl group of compounds **4-1a29** with stannous chloride in ethanol under reflux condition (Scheme 4.1B). Since the best inhibitor of the WNV NS2B-NS3 protease reported till date are several sulphone derivatives, therefore the sulfide group in **4-1a16** was oxidized to the corresponding sulphone to yield compound **4-1a33** (Scheme 4.1C). To explore the importance of the enolic hydrogen on the compound's biological activity, we replaced hydrogen in **4-1a16** with methyl group by Mitsunobu reaction.[117] To increase the diversity of compound **4-1a**, the enolic hydroxyl was replaced with 2-hydroxyethylamino group

Scheme 4.2 Synthesis of compounds **4-8** and **4-9**

by the reaction of 2-aminoethanol and **4-1a** in refluxing anhydrous dioxane[118] to obtain the desired product **4-7** (Scheme 4.1A). To investigate the importance of the thiadiazole ring in compound **4-1a** on inhibition activity, structural modifications that replaced the enol moiety on the thiadiazole ring with different substituted amine groups were achieved using the synthetic strategy shown in Scheme 4.2. To obtain compound **4-8**, a three-component reaction was applied starting from alkyl oxalacetate **4-4** with several amines and aldehydes at room temperature and further modification was achieved by replacing the enolic hydroxyl group in compound **4-8** with various amine to obtain compound **4-9**.

4.2 Structure-activity relation studies

A representative set of 39 analogs of compound **4-1a** was synthesized and tested in a WNV NS2B-NS3 protease assay at 200 μM concentration to identify potential inhibitors. Inhibitors exhibiting more than 50% inhibition were further evaluated for their effects at different concentrations and the IC_{50} values of each compound were calculated using the Graphpad Prism software (Table 4.1). The fluorogenic peptide Pyr-RTKR-AMC was used as a substrate for the WNV NS2B-NS3 protease and the K_m value was determined, using the protocol from the SensoLyte® 440 West Nile Virus Protease Assay Kit, to be 3.45±0.41 μM.

In our preliminary SAR study, R^1, R^2 and R^3 in compound **4-1a1** were replaced with substituted phenyl groups having electron donating and withdrawing characters (Table 1. cpds **4-1a2** to **4-1a13**). Although, these changes did not provide any significant improvement in the biological activity, the presence of *p*-Cl-phenyl group at R^1 and R^2 positions and a phenyl group at R^3 position (Table 1, cpd **4-1a13**)

showed relatively better activity compared to the other changes. Therefore, we proceeded to screen the inhibitory activity of compounds by varying the substituent on the R^3 position whilst keeping the substituents on R^1 and R^2 unchanged. This was achieved by decorating the R^3 position with different sizes of alkyl chains as well as alkyl chains with functional groups of ethylester, cyanide and alcohol. The best inhibition was observed in compound **4-1a16** which contains an *n*-Pr group at the R^3 position. Further tuning of compound **4-1a16** by varying with halide through different position on phenyl ring (Table 1, cpd **4-1a23** to **4-1a28**) did not result in further improvement of the inhibitory activity confirming the importance of the *p*-Cl-phenyl group in the compound's inhibitory activity. In addition, biological screening result of compound **4-1a16** with an electron donating or withdrawing functional group containing phenyl ring at R^1 and R^2

Table 4.2 IC_{50} values of compounds [a] 4-1a, 4-7, 4-8 and 4-9

Cpd	R^1	R^2	R^3	R^4	IC_{50}
4-1a2	4-Cl-Ph	3,4-C$PhCl_2$Ph	4-F-$PhCH_2$	-	118±8.4
4-1a3	Ph	Ph	$PhCH_2$	-	151±21.6
4-1a4	Ph	Ph	4-F-$PhCH_2$	-	44.8±5.7
4-1a5	Ph	4-MeS-Ph	4-F-$PhCH_2$	-	26.8±4.5
4-1a6	3-MeO-Ph	Ph	4-F-$PhCH_2$	-	79.6±6.2
4-1a7	Ph	4-F-Ph	$PhCH_2$	-	24.5±4.0
4-1a8	Ph	4-F-Ph	4-MeO-$PhCH_2$	-	41.3±3.7
4-1a9	Ph	4-MeS-Ph	4-MeO-$PhCH_2$	-	31.1±2.5
4-1a10	4-Cl-Ph	Ph	$PhCH_2$	-	35.5+4.1
4-1a11	4-Cl-Ph	2-Furyl	$PhCH_2$	-	38.3±5.1
4-1a12	4-Cl-Ph	4-MeO-Ph	$PhCH_2$	-	34.4±3.4
4-1a13	4-Cl-Ph	4-Cl-Ph	$PhCH_2$	-	21.4±3.1
4-1a14	4-Cl-Ph	4-Cl-Ph	CH_3	-	124±5.1
4-1a15	4-Cl-Ph	4-Cl-Ph	$CH(CH_3)_2$	-	42.5±5.5
4-1a16	4-Cl-Ph	4-Cl-Ph	$CH_2CH_2CH_3$	-	6.1±1.9
4-1a17	4-Cl-Ph	4-Cl-Ph	$(CH_2)_3CH_3$	-	11.4±2.6
4-1a18[b]	4-Cl-Ph	4-Cl-Ph	$CH(CH_2)_4$	-	11.9±1.5
4-1a19	4-Cl-Ph	4-Cl-Ph	$(CH_2)_4CH_3$	-	70.0±7.1
4-1a20	4-Cl-Ph	4-Cl-Ph	CH_2CH_2OH	-	>200

4-1a21	4-Cl-Ph	4-Cl-Ph	CH_2COOEt	-	>200
4-1a22	4-Cl-Ph	4-Cl-Ph	CH_2CH_2CN	-	>200
4-1a23	4-Cl-Ph	4-F-Ph	$CH_2CH_2CH_3$	-	24.5±3.4
4-1a24	4-Cl-Ph	4-Br-Ph	$CH_2CH_2CH_3$	-	30.6±0.8
4-1a25	4-Cl-Ph	3-Cl-Ph	$CH_2CH_2CH_3$	-	51.5±2.3
4-1a26	4-F-Ph	4-Cl-Ph	$CH_2CH_2CH_3$	-	32±2.08
4-1a27	4-Br-Ph	4-Cl-Ph	$CH_2CH_2CH_3$	-	58.6±7.3
4-1a28	4-I-Ph	4-Cl-Ph	$CH_2CH_2CH_3$	-	NA
4-1a29	4-NO_2-Ph	4-Cl-Ph	$CH_2CH_2CH_3$	-	32.6±11.1
4-1a30	4-NH_2-Ph	4-Cl-Ph	$CH_2CH_2CH_3$	-	38.8±7.5
4-1a31	4-Cl-Ph	4-NO_2-Ph	$CH_2CH_2CH_3$	-	19.7±5.3
4-1a32	2Benzofuryl	4-Cl-Ph	$CH_2CH_2CH_3$		21.3±0.6
4-1a33	4-Cl-Ph	4-Cl-Ph	$SO_2CH_2CH_2C$		NA[c]
4-1a34	4-Cl-Ph	4-Cl-Ph	$CH_2CH_2CH_3$	CH_3	NA
4-7	4-Cl-Ph	4-F-Ph	4-F-$PhCH_2$	CH_2CH_2OH	NA
4-8a	CH_3	Ph	CH_3	-	NA
4-8b	CH_3	Ph	$PhCH_2$	-	NA
4-9a	CH_3	Ph	$PhCH_2$	H	NA
4-9b	CH_3	Ph	$PhCH_2$	CH_3	NA
4-9c	CH_3	Ph	$PhCH_2$	CH_2CH_2OH	NA

[a] Data represent the concentrations required to inhibit the WNV NS2B-NS3 protease activity by 50% and are the mean±SE of triplicate experiments; compounds used are ≥95% pure. [b] R^3= cyclopentyl. [c] NA = no activity.

positions did not result in further improvement of the biological activity. However, replacement of R^1 group with benzofuryl showed moderate activity (Table 1, cpd **4-1a32**). To investigate the effect of the enolic hydrogen, we replaced it with methyl group and oxidized the bonded to R^3 in compound **4-1a16** to a sulphone (Table 1, cpd **4-1a33**). However these compounds did not show any biological activity. Next, we examined the importance of the hydroxyl group on inhibition potency against WNV NS2B-NS3 protease by replacing the enolic hydroxyl with 2-hydroxyethylamino group (Table 1, cpd **4-7**). However, this compound completely lost its inhibitory activity against WNV protease. Finally, we investigated the importance of the thiadiazole ring for inhibiting the protease activity. A series of compounds (**4-8** and **4-9**) where the thiadiazole ring was replaced by simple amine groups were synthesized

and tested for their inhibition activities. Unfortunately, these compounds also showed no inhibitory activity against the WNV NS2B-NS3 protease. The stabilities of compounds **4-1a13**, **4-1a16** and **2-1a17** in pH 8 buffer were determined by analyzing the amount of compound remaining with time using LCMS-IT-TOF detection. Quantization of the compounds was determined by Shimadzu's LCsolution software. Compounds **4-1a13**, **4-1a16** and **4-1a17** showed excellent stability in a pH 8 buffer.

Considering that the compounds tested thus far were always racemate, we proceeded to investigate the influence of stereochemistry on the compounds' biological activities. Compounds **4-1a13**, **4-1a16** and **4-1a17** which showed comparatively better inhibition results were selected for chiral separation. **Table 4.3** showed that the inhibition results of the (-) and (+) enantiomers of compound **4-1a13**, **4-1a16**, **4-1a17**.

Table 4.3, The inhibition results of enantiomers from selected racemic compounds

Entry	cpd	Optical rotation	IC_{50}(μM)	K_i (μM)
1	**4-1a13**	racemic - +	21.4±9.1 16.6±0.4 62.8±6.1	13.76±0.33
2	**4-1a16**	racemic - +	6.1±1.9 2.2±0.7 90.4±28.3	1.82±0.58
3	**4-1a17**	racemic - +	11.4±2.6 7.2±0.3 22.3±0.5	5.97±0.25

The results show that the (-) enantiomer demonstrated much better inhibition potency than the corresponding (+) enantiomer. Among these enantiomers, the (-) enantiomer of compound **4-1a16** exhibited the best inhibition activity with an IC_{50} value of 2.2±0.7 μM.

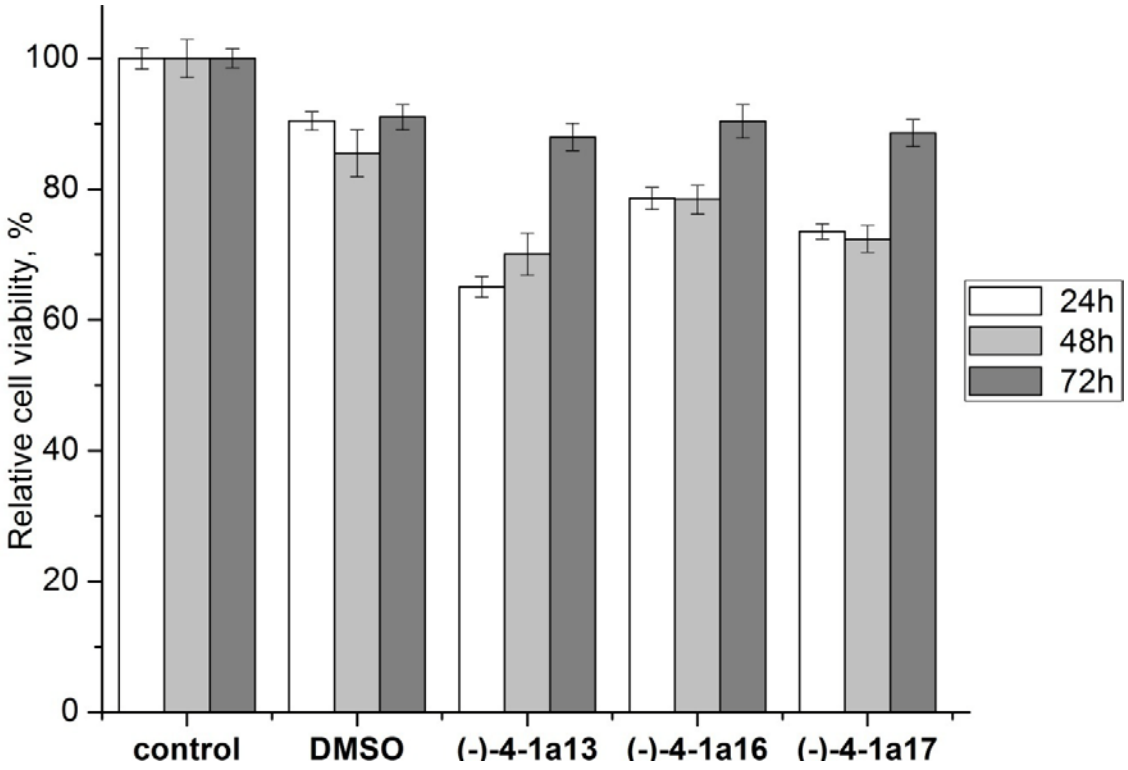

Figure 4.1 MTS assay results obtained at incubation times of 24 h ( ), 48 h ( ) and 72 h ( ) with the BHK21 cell line. Compounds were added at a final concentration of 25 μM.

Next we evaluated the cytotoxicities of compounds **(-)-4-1a13**, **(-)-4-1a16** and **(-)-4-1a17** against baby hamster kidney fibroblast (BHK21 cells) at three different incubation timings. Vehicular control, dimethyl sulfoxide (DMSO), was also included to serve as control as the test compounds were dissolved in DMSO. The amount of DMSO used in the assay was controlled at 0.1% of the total volume. This is to ensure that DMSO does not result in cytotoxicity of cells. From the results obtained (Figure 4.1), compounds **(-)-4-1a13**, **(-)-4-1a16** and **(-)-4-1a17** were shown to be non-cytotoxic to BHK21 cells.

To determine the mode of inhibition of the WNV NS2B-NS3 protease activity by the (-) enantiomer of compound **4-1a16**, we performed the kinetics of inhibition using

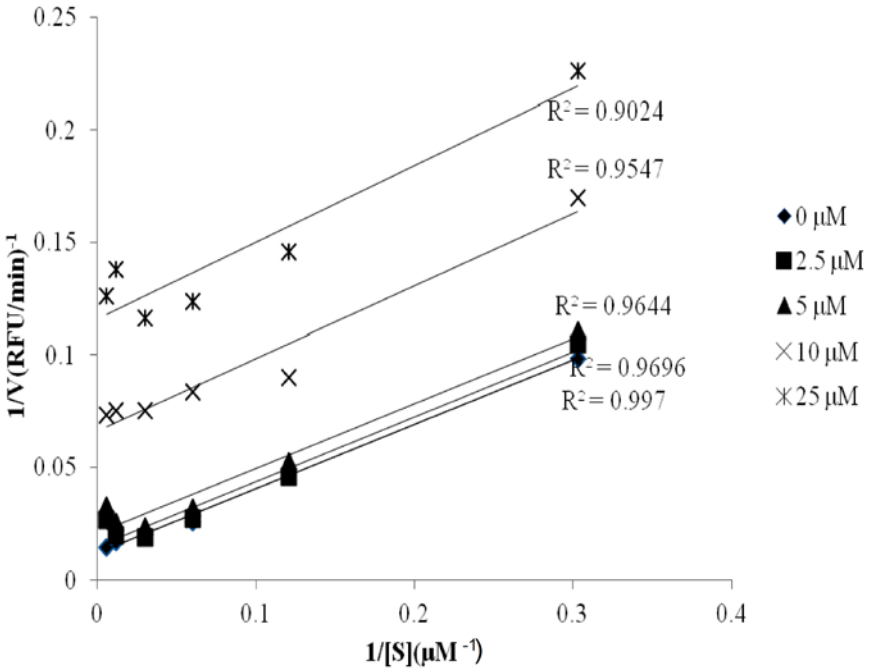

Figure 4.2 Uncompetitive inhibition of **(-)-4-1a16** with WNV NS2B-NS3 protease**.** WNV protease assays were performed at various concentrations of **(-)-4-1a16** (0, 2.5, 5.0, 10, and 25μM) and substrate concentrations (3.3, 8.3, 16.7, 33.3, 83.3, 166.7μM). Double reciprocal plots of 1/V versus 1/[S] for **(-)-4-1a16** at each inhibitor concentration were plotted using the Microsoft excel 2007.

Pyr-RTKR-AMC as substrate. Four different inhibitor concentrations and a no-inhibitor control (0 to 25 μM) were each assayed at six or more substrate concentrations ranging from 3.3 μM to 166.7 μM. In each assay, the enzyme and inhibitor were incubated at 37 °C temperature for 15 min, followed by the addition of the substrate to start the kinetic measurement. The rate of substrate cleavage (v) was monitored using an Infinite F200 microplate reader. To illustrate the inhibition mechanism, double reciprocal plots of 1/V versus 1/[S] at each inhibitor concentration were plotted using Microsoft Excel (Figure 4.2). The parallel lines for the control data and the plus inhibitor data in the double reciprocal plots of 1/V versus 1/[S] at each inhibitor concentration were consistent with an uncompetitive mechanism of

inhibition of the WNV NS2B-NS3 protease. K_i values were calculated from the IC_{50} values according to the equation, $K_i = IC_{50} / (1+ K_m /[S])$[119] for uncompetitive inhibition (Table 4.3). The experiments were repeated three times with similar results. Further investigation of the inhibition mechanism of (-) enantiomer of compound **4-4-1a17** was found to be uncompetitive inhibitor in absence of charge on the inhibitor that prefers active site of the protease.

4.3 Docking analysis

A docking study was performed to rationalize the inhibition and kinetics result as well as to identify possible binding site of compound **4-1a16** on NS2B-NS3 protease. The crystal structure of the WNV NS2B-NS3 protease in complex with peptide Bz-Nle-Lys-Arg-Arg-H (pdb 2fp7) has been reported earlier.[74] We performed *in silico* docking study with Molecular Operating Environment (MOE) using this reported crystal structure coordinates. Since compound (-)-**4-1a16** is an uncompetitive inhibitor of the WNV NS2B-NS3 protease, we focussed our analysis on regions beyond the substrate binding sites. Earlier studies have shown that the integration of residues 78-87 of NS2B into the protease-cofactor complex affected the formation of the catalytic active sites.[74,75,105] Deletion or mutagenesis of these residues produced an inert enzyme. Therefore, the region on the NS3 protease, where key interactions with the NS2B cofactor (residues 78-87) occur, is important for the NS2B-NS3 protease activity and particularly attention was paid to this region during our docking studies.

Since compound **4-1a16** contains a chiral centre, the R- and S-enantiomers were separately analyzed for their interactions with the WNV NS2B-NS3 protease. Our

docking analysis suggested that both enantiomers bind to NS3 protease with

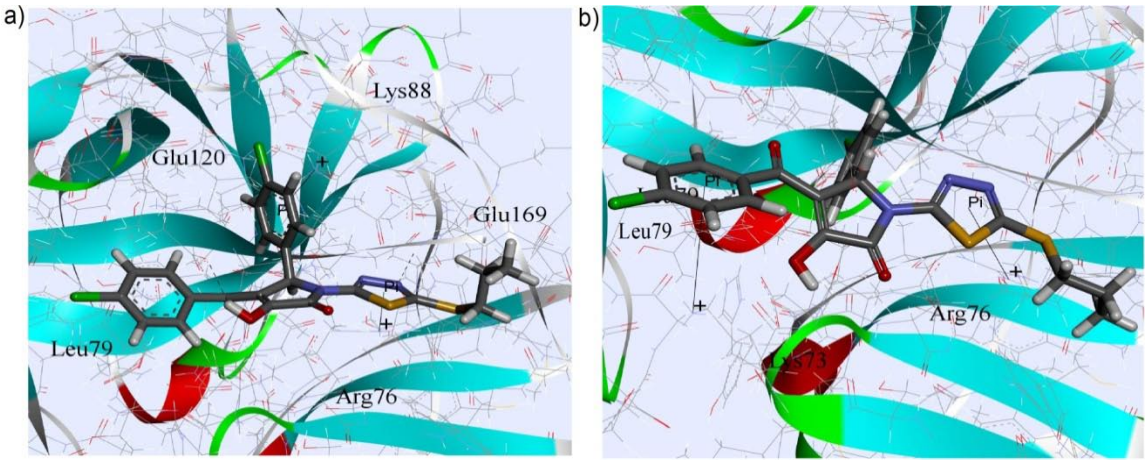

Figure 4.3 Molecular docking of compound **4-1a16** onto WNV NS2B-NS3 protease. The WNV protease crystal structure coordinates (pdb 2fp7)[74] were used for the molecular docking. The NS2B-NS3 protease and the enantiomers of compound **4-1a16** are shown as a wireframe and flat ribbon model generated using Discovery Studio 3.1 client. (a) R-enantiomer; (b) S-enantiomer.

good shape and complementarities. The amino acid residues that are in close proximity (less than 5 Å) to the atoms of the R-enantiomer include Arg78, Leu79 and Phe85 of NS2B; Trp69, Lys73, Glu74, Arg76, Lys88, Thr118, Pro119, Glu120, Gly121, Glu122, Ile123, Gln167, Gly168 and Glu169 of the NS3 protease. Amino acid residues that are in close proximity (less than 5 Å) to the atoms of the S-enantiomer are Val77, Arg78, Leu79 and Phe85 of NS2B; Trp69, Lys73, Glu74, Arg76, Trp83, Lys88, Thr118, Pro119, Glu120, Ile123, Val166, Gln167, Gly168 and Glu169 of the NS3 protease. The guanidine group in Arg76 of the NS3 protease is bound to the thiodiazole group of both enantiomers via π-cation type of interaction. In addition, the R-enantiomer could potentially form hydrogen bonds with residue Glu169 and Glu120 as well as π-cation type of interactions with Lys88 on the NS3 protease (Figure 4.3a). On the other hand, a π-cation type of interaction was also

observed between acetophenyl group of S-enantiomer and protonated amino group from Lys73 on NS3 protease (Figure 4.3b). Bound enantiomers very closely interact with amino acid residue Leu-79 of NS2B and that might thus interfere with the productive associations of NS2B with NS3protease. However, docking analysis predicted that the dock score of the R- enantiomer (-28.56 kJ/mol) is higher than the S-enantiomer (-24.04 kJ/mol). This indicates that the R-enantiomer is a preferred isomer for the inhibition of the WNV NS2B-NS3 protease which is in agreement with the experimental inhibition result obtained for **(-)-4-1a16**.

4.4 Conclusion

In this study, a primary screening of 110 compounds has led to the discovery of an initial "hit" compound with promising therapeutic indices and activity against WNV NS2B-NS3 protease. Based on this initial "hit" compound, we have designed and developed a focused chemical library to further evaluate the initial "hit" and gain insight into the requirements for activity. In the evaluation, compound **(-)-4-1a16** with K_i value of 1.82±0.58 μM was identified to be an uncompetitive inhibitor of the WNV NS2B-NS3 protease.

4.5 Experimental section

4.5.1 Chemistry

All chemical reagents were obtained from Aldrich, Merck, Lancaster or Fluka and used without further purification. Analytical TLC was carried out on pre-coated plates (Merck silica gel 60, F254) and visualized with UV light or stained with ninhydrin.

Flash column chromatograph was performed with silica (Merck, 70-230 mesh). Final compounds for biological assay were purified on a Gilson preparative HPLC system with a Waters C_{18} column (250 x 10.0 mm, 5 μm). Detection was conducted at 254 nm, The mobile phase was a gradient with solvent B increasing from 5% to 100% over 40 min and a flow rate of 5.0ml/min. Solvent A was 0.1% trifluoroacetic acid in water, and solvent B was 0.1% trifluoroacetic acid in acetonitrile. The purities of the compounds were determined via analytical HPLC using a Shimadzhu LCMS-IT-TOF system with a Phenomenex Luma C_{18} column (50 x 3.0 mm, 5 μm). Detection was conducted at 254 nm, and integration was obtained with a Shimadzhu LCMS solution software. The mobile phase was a gradient with solvent B increasing from 0% to 100% over 7 min and a flow rate of 0.8 ml/min. Compounds used in biological assay has purities of at least 95%. Racemic compound separation was performed on a Shimadzhu HPLC system with a Chiralpak AD-H column (250 x 4.6 mm, 5 μm), eluted with hexanes/iPrOH (80:20) or Chiralpak IC column (250 x 4.6 mm, 5 μm), eluted with 100% $CHCl_3$ with 0.1% TFA at 1.0 ml/min, γ =254 nm. ^{1}H NMR and ^{13}C NMR spectra were measured at 298 K on a Bruker ACF 300 or AMX 500 Fourier Transform spectrometer. Chemical shifts were reported in δ (ppm) relative to the residual undeuterated solvent which was used as internal reference. The signals observed were described as: s (singlet), d (doublet), t (triplet), m (multiplet). The number of protons (n) for a given resonance was indicated as nH. Mass spectra were performed on Finnigan MAT 95/XL-T spectrometer under electron impact (EI and electrospray ionization (ESI) techniques. Optical rotations were determined with a JASCO DCP-1000 digital polarimeter and were the average of at least 10 measurements with an RSD value of less than -100%.

General procedure for the synthesis of 4-2

5-Amino-1,3,4-thiadiazole-2-thiol (2.664 g, 20 mmol) was dissolved in a mixture of KOH (2.64 g, 40 mmol) in absolute ethanol (20 mL). After 10 min, the corresponding benzyl or alkyl bromide (20 mmol) was added drop wise with vigorous stirring. The reaction progress was monitored by TLC and was completed within 2 hours; the reaction mixture was concentrated under rotary evaporator. The organic compound was extracted with EtOAc/H_2O and the combined organic layer was dried over anhydrous Na_2SO_4, concentrated, purified by column chromatography using EtOAc/hexane as an eluent and dried in a vacuum oven (at 50 °C) to afford **4-2** as a solid in 69-95% yield.

General procedure for the synthesis of 4-4

To a mixture of the corresponding acetophenone **4-3** (10 mmol) and diethyloxalate (2.03 mL, 15 mmol) in anhydrous ethanol (40 mL) was added 21% sodium ethoxide solution in ethanol (11.33 mL, 30 mmol). The resulting mixture was stirred at room temperature for 12 hours. After that, the reaction mixture was neutralized with 4M HCl and solvent was removed under rotary evaporation. The resultant brown solid residue obtained was extracted with EtOAc/H_2O solvent system and combined organic layer was dried over Na_2SO_4, concentrated and purified by column chromatography using ethyl acetate/hexane (starting from 1:20 to 1:9) solvent system and dried under vacuum at 50 °C temperature to yield compound **4-4** in 70-85% yield.

General procedure for the synthesis of 4-5

To a mixture of the corresponding acetophenone **4-3** (10 mmol) and diethyloxalate (2.03 mL, 15 mmol) in anhydrous ethanol (40 mL) was added 21% sodium ethoxide

solution in ethanol (11.33 mL, 30 mmol). The resulting mixture was stirred at room temperature for 12 hours. After that, the solvent was removed on a rotary evaporator; a solution of 1M NaOH (50 mL, 50 mmol) in water was added into the crude mixture. The hydrolysis reaction was stirred at room temperature for 4 hours. The basic solution was extracted 3 times with ethyl acetate; the water phase was collected and then acidified with 4N HCl solution to pH 1-2. The resulting solution was again extracted 3 times with ethyl acetate and the combined organic layer was dried over anhydrous Na_2SO_4, filtered, concentrated by evaporation and dried under vacuum at 50 °C temperature to yield compound **4-5**. The crude yield of the reaction is 80-90% which was directly coupled with various amines without further purification to obtain compound **4-6**.

General procedure for the synthesis of 4-6

A solution of the respective acid **4-5** (2.21 mmol) in anhydrous dimethylacetamide (10 mL) was stirred at 0-5 °C for 10min. Thereafter, thionyl chloride (160 µL, 2.21 mmol) was added over 10 min. The reaction mixture was stirred for next 20 min and the corresponding amine **4-2** (2.21 mmol) was added to the solution very slowly at same temperature. Upon completion of addition, the mixture was warmed to room temperature and stirred for another 4 hours. After that, 60 mL of water was added into the reaction mixture and the resultant precipitate formed **4-6** was recovered by filtration and copiously washed with water (3x20 mL) followed by cold ether (2x10 mL). This product was used without further purification as the impurities present did not affect the reaction. The overall yield of the reaction over the last two steps is 45-61%.

General procedure for the synthesis of 4-1a

To an amide **4-6** (0.8 mmol) in toluene (10 mL) was added 20 mol% of acetic acid (9.2 μL, 0.16 mmol) and piperidine (15.8 μL, 0.16 mmol) followed by the corresponding benzaldehyde (81.5 μL, 0.8 mmol). The mixture was stirred at 70°C for 14 hours then cooled to room temperature for 1 hour. The precipitate that formed was filtered by suction then washed with water and cold ether. This crude product was purified by preparative HPLC using a Gilson preparative HPLC system with a Waters C_{18} column (250 x 10.0 mm, 5 μm). Detection was set up at 254 nm and the mobile phase was a gradient with solvent B increasing from 5% to 100% over 40 min and a flow rate of 5.0ml/min. Solvents A and B were prepared with 0.1% trifluoroacetic acid in water and acetonitrile respectively. Fractions containing the pure product were combined, concentrated and dried overnight under vacuum at 50 °C to give compound **4-1a** in 35-60% yield.

General procedure for the synthesis of 4-1a and 4-8

To a suspension of 2,4-diketo ethyl ester **4-4** (1.0 mmol), the corresponding amine (1 mmol), and the aldehyde (1.0 mmol) in 1,4-dioxane (8 mL) was stirred at 70 °C temperature for 18h. After which, the reaction mixture was concentrated under rotary evaporator and wash with water and cold diethyl ether. Residual crude product was purified either by column chromatography (EtOAc:DCM = 1:1) or by reverse phase preparative HPLC using solvent A with 0.1% TFA in water, and solvent B was 0.1% TFA in acetonitrile as the mobile phase. Detection was conducted at 254 nm, the mobile phase was a gradient with solvent B increasing from 5% to 95% over 30 min and a flow rate of 8.0ml/min. Fractions containing the pure product were combined,

concentrated and dried overnight under vacuum at 50 °C to give compound **4-1a** in 54-75% yield and compound **4-8** in 45-60% yield.

Synthesis of 4-(4-aminobenzoyl)-5-(4-chlorophenyl)-3-hydroxy-1-(5-(propylthio)-1,3,4-thiadiazol-2-yl)-1H-pyrrol-2(5H)-one (4-1a30)

To a solution of compound **4-1a29** (26 mg, 0.05 mmol) in absolute ethanol (8 mL) was added $SnCl_2.H_2O$ (57 mg, 0.25 mmol). The mixture was stirred under reflux condition and checked by TLC for reaction completion. When the reaction has completed, the mixture was concentrated and extracted with EtOAc/H_2O mixture and combined organic layer was concentrated under rotary evaporator, purified by column chromatography using ethyl acetate/hexane (3:1) solvent system and dried under vacuum at 50 °C temperature to yield compound **4-1a30** in 87% yield.

Synthesis of 4-(4-chlorobenzoyl)-5-(4-chlorophenyl)-3-hydroxy-1-(5-(propylsulfonyl)-1,3,4-thiadiazol-2-yl)-1H-pyrrol-2(5H)-one (4-1a32)

A solution of the compound **4-1a16** (150 mg, 0.29 mmol) in DCM (10 mL) at 0 °C was treated with m-CPBA (110 mg, 0.64 mmol) and the mixture was stirred at 0-5 °C for 2.5 hrs. The reaction mixture was diluted with another 10 ml of DCM and wash with saturated Na_2CO_3 solution three times. The organic layer was dried over Na_2SO_4 and concentrated under rotary evaporator to get the crude product **4-1a32**. The crude product was purified by reverse phase preparative HPLC using solvent A with 0.1% TFA in water, and solvent B was 0.1% TFA in acetonitrile as the mobile phase. Detection was conducted at 254 nm, the mobile phase was a gradient with solvent B increasing from 5% to 95% over 30 min and a flow rate of 8.0ml/min. Fractions containing the pure product were combined, concentrated and dried overnight under vacuum at 50 °C to give compound **4-1a32** in 76% yield.

Synthesis of 4-(4-chlorobenzoyl)-5-(4-chlorophenyl)-3-methoxy-1-(5-(propylthio)-1,3,4-thiadiazol-2-yl)-1H-pyrrol-2(5H)-one (4-1a33)

To a solution of starting materials **4-1a16** (100 mg, 0.2 mmol) in THF (5 mL) at 0 °C was added triphenylphosphine (0.3 mmol) and DIAD (0.3 mmol). The mixture was stirred for 15 min at 0 °C then methanol (12 µL, 0.3 mmol)) was added. The resulting reaction mixture was stirred at room temperature for the next 15 h and then the solvent was removed with a rotary evaporator. The crude mixture was dissolved in EtOAc (30 mL), washed with 1M NaOH followed by saturated sodium chloride solution. The resultant organic layer was dried over Na_2SO_4, concentrated under vacuum, purified by flash chromatography using ethyl acetate/hexane (starting from 1:1 to 3:1) as the eluent and dried under vacuum at 50 °C temperature to yield compound **4-1a33** in 83% yield.

Synthesis of 4-(4-chlorobenzoyl)-1-(5-(4-fluorobenzylthio)-1,3,4-thiadiazol-2-yl)-5-(4-fluorophenyl)-3-(2-hydroxyethylamino)-1H-pyrrol-2(5H)-one (4-7). To a solution of 1-(5-(4-fluorobenzylthio)-1,3,4- thiadiazol-2-yl)-3-amino-4-(4-chlorobenzoyl)-5-(4-fluorophenyl)-1H-pyrrol-2(5H)-one (55.5 mg, 0.1 mmol,) in anhydrous 1,4-dioxane (10 mL) was added 2-aminoethanol (12 µL, 0.2 mmol). The mixture was stirred under reflux condition and checked by TLC for reaction completion. When the reaction has completed, the mixture was concentrated and extracted with ethyl acetate/H_2O mixture and the combined organic layer was concentrated under rotary evaporation and purified by column chromatography using EtOAc/hexane (3:1) as the eluent to get product **4-1a34** in 40% yield.

General procedure for the synthesis of 4-9

To a solution of **4-8** (0.3 mmol, 92.2 mg) in dioxane (10 mL) was added the corresponding amine (0.3 mmol). The reaction mixture was stirred at reflux condition until TLC monitoring showed that the reaction has completed. After which, the mixture was concentrated under rotary evaporator and purified by column chromatography by (EtOAc:DCM = 1:1) and dried under vacuum at 50 °C temperature to yield compound **4-9** in 70-90% yield. For **4-9c**, AcOH was used as solvent.

4.5.2 Biology

All the compounds used in the biological testing were at least 95% pure. Compounds were tested against the WNV NS2B-NS3 protease using the SensoLite® 440 WNV protease assay kit (Catalog # 72079) and the active recombinant WNV protease (Calalog # 72081) which were purchased from Anaspec (USA). This protease assay kit uses a fluorogenic peptide Pyr-RTKR-AMC as substrate. Eight different substrate concentrations ranging from 1 μM to 80 μM were incubated in 96-well plates with 0.3 μg/mL recombinant WNV protease at 37 °C in the buffer provided. The increase in fluorescence intensity was monitored using an Infinite F200 microplate reader (Tecan, Switzerland) at an excitation wavelength of 354 nm (±10 nm) and emission wavelength of 442 nm (±15 nm). The initial velocity was determined from the linear portion of the progress curve, and the value of K_m was determined using the Michaelis-Menten equation, i.e. $v = V_{max}[S] / ([S] + K_m)$ to be 3.45±0.41 μM. Triplicate measurements were taken at each data point and the data were reported as mean±SE. In the preliminary WNV NS2B-NS3 protease inhibition assay, analogs of **4-1a** were screened at a fixed concentration of 50 μM to filter out potential inhibitors.

Compounds which showed more than 50% inhibition were further investigated for their IC_{50} determination.

Determination of IC_{50}

For the IC_{50} calculations, recombinant WNV protease concentration of 0.3 µg/mL and seven different concentrations of the inhibitor ranging from 10 nM to 200 µM were used. For each experiment, the protease was pre-incubated with the inhibitor at 37 ^{o}C for 15 min in separate wells and the enzyme kinetics was initiated by adding substrate Pyr-RTKR-AMC to a final concentration 16.7 µM. The increase in fluorescence intensity was monitored continuously using an Infinite F200 microplate reader at an excitation wavelength of 354 nm and emission wavelength at 442 nm. Fluorescence values obtained from the positive control (no inhibitor) were considered as 100% complex formation and those values obtained in the presence of inhibitors were calculated as the percentage of inhibition of the control. Triplicate measurements were obtained at each data point. The IC_{50} values were calculated using a sigmoidal dose-response using the Graphpad prism 3.0 software (San Diego, USA). Triplicate measurements were recorded as the mean±SE.

Determination of inhibition mechanism

Three different inhibitor concentrations and a no-inhibitor control (0 to 25 µM) were each assayed at five substrate concentrations ranging from 3.3 µM to 83.3 µM. In each assay, the enzyme and inhibitor were incubated at 37 °C for 15 min, followed by the addition of the substrate to start the kinetic measurement. The rate of substrate cleavage (v) was monitored using the F200 microplate reader. To illustrate the inhibition mechanism, 1/V versus 1/[S] was plotted for at each inhibitor concentration using OriginPro8.

MTS Assay

The baby hamster kidney fibroblast (BHK21) cells were cultured in Roswell Park Memorial Institute (RPMI) 1640 medium containing 10% fetal bovine serum (FBS). The 1500 cells were placed in each well of three 96-well plates with a cell density of $1.66x10^4$ cells/mL and incubated for 24 h at 37 °C with 5% CO_2. Thereafter, the compound of interest or DMSO was added into each well at 25 µM. Wells containing plain DMSO served as a vehicular control. The plate was then placed in the incubator for 24, 48 and 72 h of incubation at 37 °C with 5% CO_2. At the end of each individual incubation time point, MTS reagent solution (20 µL) was added into each sample well. The plate was then incubated again in the dark for 2 h, gently shaken using a vortemp machine for 5 min to ensure equal mixing and absorbance at 492 nm was taken using a spectrometer.

4.5.3 Docking

All docking studies were performed using the Molecular Operating Environment (MOE 2009.10) software system designed by the Chemical Computing Group. The program operated under the 'Windows Vista' operating system installed on an Intel Core™2 Duo PC with a 2.4 MHz processor and 4.0 GB RAM. Docked compounds were built using the MOE builder and subjected to energy minimization with the MMFF94x force field. The active site of the WNV protease was prepared using the crystal structure of the WNV NS2B-NS3 protease in complex with peptide Bz-Nle-Lys-Arg-Arg-H (pdb 2fp7). The structure was stripped of all water molecules and bound ligand followed by the addition of valance hydrogen atoms to the protein. By keeping in mind the amino acid residues in NS2B which are responsible for the activation of the catalytic triad, the active site in NS2B (NS2B-NS3) was identified

using the Alpha site finder tool. Docking simulations were performed at default settings with placement at triangle matcher, rescoring at London DG, refinement at force field and the geometry of resulting complex was studied using the Discovery Studio 3.1 client.

4.6 ^{1}H and ^{13}C NMR data of all compounds synthesized

^{1}H and ^{13}C NMR data of compound 4-2:

5-(Benzylthio)-1,3,4-thiadiazol-2-amine (4-2a). (Yield 90%). ^{1}H NMR (500 MHz, DMSO-d_6) δ 7.36-7.24 (m, 7H), 4.30 (s, 2H); ^{13}C NMR (125 MHz, DMSO-d_6): δ 169.8, 149.5, 137.0, 128.9, 128.4, 127.4, and 38.5. HRMS-EI [M] calcd for $C_9H_9N_3S_2$: 223.0238, found: 223.0245.

5-(4-Fluorobenzylthio)-1,3,4-thiadiazol-2-amine (4-2b). (Yield 88%). ^{1}H NMR (500 MHz, DMSO-d_6): δ 7.40-7.37 (m, 2H), 7.28 (s, 2H), 7.16-7.13 (m, 2H), 4.29 (s, 2H). ^{13}C NMR (125 MHz, DMSO-d_6): δ 169.9, 149.1, 133.4, 131.0, 130.9, 115.3, 1115.1, 37.5. HRMS-EI [M] calcd for $C_9H_8FN_3S_2$: 241.0144, found: 241.0146.

5-(4-Methoxybenzylthio)-1,3,4-thiadiazol-2-amine (4-2c). (Yield 89%). ^{1}H NMR (500 MHz, DMSO-d_6): δ 7.29-6.86 (m, 6H), 4.24 (s, 2H), 3.72 (s, 3H). ^{13}C NMR (125 MHz, DMSO-d_6): δ 169.8, 158.6, 149.6, 130.2, 128.7, 113.8, 55.0, 38.0. HRMS-EI [M] calcd for $C_{10}H_{11}N_3OS_2$: 253.0344, found: 253.0349.

5-(Methylthio)-1,3,4-thiadiazol-2-amine (4-2d). (Yield 85%). ^{1}H NMR (500 MHz, DMSO-d_6): δ 3.34 (s, 3H). ^{13}C NMR (125 MHz, DMSO-d_6): δ 169.3, 152.4, 17.1. HRMS-EI [M] calcd for $C_3H_5N_3S_2$: 146.9925, found: 146.9930.

5-(Propylthio)-1,3,4-thiadiazol-2-amine (4-2e). (Yield 83%). ^{1}H NMR (500 MHz, $CDCl_3$): δ 5.62 (s, 2H), 3.11-3.08 (t, *J* = 7.6 Hz, 2H), 1.78-1.73 (m, 2H), 1.03-1.01 (t, *J* = 7.3 Hz, 3H). ^{13}C NMR (125 MHz, $CDCl_3$): δ 168.8, 154.8, 36.9, 22.8, 13.2. HRMS-EI [M] calcd for $C_5H_9N_3S_2$: 175.0238, found: 175.0238.

5-(Isopropylthio)-1,3,4-thiadiazol-2-amine (4-2f). (Yield 85%). ^{1}H NMR (500 MHz, $CDCl_3$): δ 6.05 (s, 2H), 3.64-3.56 (m, 1H), 1.38-1.37 (d, *J* = 7.0 Hz, 6H). ^{13}C NMR (125 MHz, $CDCl_3$): δ 170.1, 152.9, 40.8, 22.2. HRMS-EI [M] calcd for $C_5H_9N_3S_2$: 175.0238, found: 175.0248.

5-(Butylthio)-1,3,4-thiadiazol-2-amine (4-2g). (Yield 80%). ^{1}H NMR (500 MHz, $CDCl_3$): δ 6.02 (s, 2H), 3.10-3.08 (t, *J* = 7.6 Hz, 2H), 1.72-1.66 (m, 2H), 1.46-1.39 (m, 2H), 0.92-0.89 (t, *J* = 7.3 Hz, 3H). ^{13}C NMR (125 MHz, $CDCl_3$): δ 169.3, 154.5, 34.8, 31.4, 21.7, 13.5. HRMS-EI [M] calcd for $C_6H_{11}N_3S_2$: 189.0394, found: 189.0397.

5-(Pentylthio)-1,3,4-thiadiazol-2-amine (4-2h). (Yield 78%). ^{1}H NMR (500 MHz, $CDCl_3$): δ 6.62 (s, 2H), 3.04-3.01 (t, *J* = 6.9 Hz, 2H), 1.68-1.64 (m, 2H), 157-1.26 (m, 4H), 0.87-0.83 (t, *J* = 6.7 Hz, 3H). ^{13}C NMR (125 MHz, $CDCl_3$): δ 169.8, 154.1, 35.2, 30.6, 30.0, 22.1 13.8. HRMS-EI [M] calcd for $C_7H_{13}N_3S_2$: 203.0551, found: 203.0550.

5-(Cyclopentylthio)-1,3,4-thiadiazol-2-amine (4-2i). (Yield 95%). ^{1}H NMR (500 MHz, $CDCl_3$): δ 5.47 (s, 2H), 3.81 (b, 1H), 2.11-1.63 (m, 8H). ^{13}C NMR (125 MHz, $CDCl_3$): δ 168.8, 154.9, 48.1, 33.6. 24.7. HRMS-EI [M] calcd for $C_7H_{11}N_3S_2$: 201.0394, found: 201.0397.

2-(5-Amino-1,3,4-thiadiazol-2-ylthio)ethanol (4-2j). (Yield 69%). ^{1}H NMR (500 MHz, MeOD): δ 4.84 (s, 2H), 3.81-3.78 (t, *J* = 6.3 Hz, 2H), 3.22-3.20 (t, *J* = 6.3 Hz,

2H), 1.03-1.01 (t, *J* = 7.3 Hz, 3H). ^{13}C NMR (125 MHz, MeOD): δ 172.1, 154.4, 61.6, 38.2. HRMS-EI [M] calcd for $C_4H_7N_3OS_2$: 177.0031, found: 177.0030.

3-(5-Amino-1,3,4-thiadiazol-2-ylthio)propanenitrile (4-2k). (Yield 71%). ^{1}H NMR (500 MHz, MeOD): δ 4.83 (s, 2H), 3.37-3.32 (m, 2H), 2.94-2.92 (t, *J* = 6.9 Hz, 2H). ^{13}C NMR (125 MHz, MeOD): δ 172.6, 151.9, 119.3, 31.1, 19.1. HRMS-EI [M] calcd for $C_5H_6N_4S_2$: 186.0034, found: 186.0027.

Ethyl 2-(5-amino-1,3,4-thiadiazol-2-ylthio)acetate (4-2l). (Yield 82%). ^{1}H NMR (500 MHz, $CDCl_3$): δ 6.02 (s, 2H), 4.21-4.17 (m, 2H), 3.88 (s, 2H), 1.27-1.24 (t, *J* = 7.0 Hz, 3H). ^{13}C NMR (125 MHz, $CDCl_3$): δ 169.7, 168.4, 152.0, 62.1, 36.3, 14.0. HRMS-EI [M] calcd for $C_6H_9N_3O_2S_2$: 219.0136, found: 219.0135.

^{1}H and ^{13}C NMR data of compound 4-4:

Ethyl 4-(4-bromophenyl)-2,4-dioxobutanoate (4-4a). ^{1}H NMR (500 MHz, $CDCl_3$): δ 7.85 (d, *J* = 8.6 Hz, 2H), 7.64 (d, *J* = 8.5 Hz, 2H), 7.02 (s, 1H), 4.40 (q, *J* = 7.1 Hz, 2H), 1.41 (t, *J* = 7.2 Hz, 3H). ^{13}C NMR (125 MHz, $CDCl_3$): δ 189.74, 170.37, 162.29, 133.97, 132.52, 129.56, 129.29, 97.99, 62.99, 14.35.

Ethyl 4-(4-iodophenyl)-2,4-dioxobutanoate (4-4b)

^{1}H NMR (500 MHz, $CDCl_3$): δ 15.25 (s, 1H), 7.87 (d, *J* = 8.1 Hz, 2H), 7.70 (d, *J* = 8.1 Hz, 2H), 7.02 (s, 1H), 4.40 (dd, *J* = 14.2, 7.1 Hz, 2H), 1.41 (t, *J* = 7.1 Hz, 3H). ^{13}C NMR (125 MHz, $CDCl_3$): δ 189.91, 170.54, 162.32, 138.53, 134.52, 129.41, 102.09, 97.93, 63.00, 14.36.

Ethyl 4-(benzofuran-2-yl)-2,4-dioxobutanoate (4-4c) ^{1}H NMR (500 MHz, $CDCl_3$) δ 7.62 (ddd, *J* = 52.0, 27.2, 7.8 Hz, 4H), 7.36 (t, *J* = 7.4 Hz, 1H), 7.14 (s, 1H), 4.44 (dd, *J* = 14.1, 7.0 Hz, 2H), 1.45 (t, *J* = 7.1 Hz, 3H). ^{13}C NMR (125 MHz, $CDCl_3$): δ 181.16, 168.93, 162.11, 156.48, 151.18, 128.94, 127.56, 124.46, 123.53, 114.16, 112.65, 99.35, 62.96, 14.36.

^{1}H and ^{13}C NMR data of compound 4-6:

(Z)-N-(5-(Benzylthio)-1,3,4-thiadiazol-2-yl)-2-hydroxy-4-oxo-4-phenylbut-2-enamide (4-6a). (Yield 52%). ^{1}H NMR (500 MHz, DMSO-d_6): δ 8.10-7.10 (m, 11H), 4.52 (s, 2H). HRMS-EI [M] calcd for $C_{19}H_{14}FN_3O_3S_2$: 415.0461, found: 415.0464.

N-(5-(4-Fluorobenzylthio)-1,3,4-thiadiazol-2-yl)-2,4-dioxo-4-phenylbutanamide (4-6b). (Yield 52%). ^{1}H NMR (500 MHz, DMSO-d_6): δ 8.10-7.14 (m, 10H), 4.52 (s, 2H). HRMS-EI [M] calcd for $C_{19}H_{15}N_3O_3S_2$: 397.0555, found: 397.0558.

N-(5-(4-Methoxybenzylthio)-1,3,4-thiadiazol-2-yl)-2,4-dioxo-4-phenylbutanamide (4-6c). (Yield 54%).^{1}H NMR (500 MHz, DMSO-d_6): δ 8.11-6.89 (m, 10H), 4.48 (s, 2H), 3.73 (s, 3H). HRMS-ESI *m/z* [M - H] calcd for $C_{20}H_{16}N_3O_4S_2$: 426.0582, found: 426.0597.

N-(5-(Benzylthio)-1,3,4-thiadiazol-2-yl)-4-(4-chlorophenyl)-2,4-dioxobutanamide (4-6d). (Yield 57%). ^{1}H NMR (500 MHz, $CDCl_3$): δ 7.89-7.13 (m, 10H), 4.45 (s, 2H). HRMS-ESI *m/z* [M - H] calcd for $C_{19}H_{13}ClN_3O_3S_2$: 430.0087, found: 430.0085.

4-(4-Chlorophenyl)-N-(5-(4-fluorobenzylthio)-1,3,4-thiadiazol-2-yl)-2,4-dioxobutanamide (4-6e). (Yield 61%). ^{1}H NMR (500 MHz, DMSO-d_6): δ 8.07-7.14

(m, 9H), 4.52 (s, 2H). HRMS-ESI *m/z* [M - H] calcd for $C_{19}H_{12}ClFN_3O_3S_2$: 447.9993, found: 447.9998.

4-(4-Chlorophenyl)-N-(5-(methylthio)-1,3,4-thiadiazol-2-yl)-2,4-dioxobutanamide (4-6f). (Yield 54%). ^{1}H NMR (500 MHz, DMSO-d_6): δ 8.10-7.61 (m, 4H), 7.08 (s, 1H), 2.74 (s, 2H). HRMS-ESI *m/z* [M - H] calcd for $C_{13}H_9ClN_3O_3S_2$: 364.0556, found: 364.0566.

4-(4-Chlorophenyl)-2,4-dioxo-N-(5-(propylthio)-1,3,4-thiadiazol-2-yl)butanamide (4-6g). (Yield 48%). ^{1}H NMR (500 MHz, DMSO-d_6): δ 8.12-7.62 (m, 4H), 7.08 (s, 1H), 3.26-3.00 (m, 2H), 1.75-1.62 (m, 2H), 1.01-1.94 (m, 3H). HRMS-ESI *m/z* [M - H] calcd for $C_{15}H_{13}ClN_3O_3S_2$: 382.0087, found: 382.0089.

Ethyl 2-(5-(4-(4-chlorophenyl)-2,4-dioxobutanamido)-1,3,4-thiadiazol-2-ylthio) acetate (4-6h). (Yield 45%). ^{1}H NMR (500 MHz, DMSO-d_6): δ 8.08-7.61 (m, 4H), 7.08 (s, 1H), 2.57-2.50 (m, 2H), 1.19-1.16 (m, 3H). HRMS-ESI *m/z* [M - H] calcd for $C_{16}H_{13}ClN_3O_5S_2$: 425.9985, found: 425.9990.

N-(5-(4-Fluorobenzylthio)-1,3,4-thiadiazol-2-yl)-4-(3-methoxyphenyl)-2,4-dioxobutanamid (4-6i). (Yield 56%). ^{1}H NMR (500 MHz, DMSO-d_6): δ 7.10-7.15 (m, 10H), 4.53 (s, 2H), 3.86 (s, 3H). HRMS-ESI *m/z* [M - H] calcd for $C_{20}H_{15}FN_3O_4S_2$: 444.0488, found: 444.0495.

4-(4-Nitrophenyl)-2,4-dioxo-N-(5-(propylthio)-1,3,4-thiadiazol-2-yl)butanamide (4-6j). (Yield 45%). ^{1}H NMR (500 MHz, DMSO-d_6): δ 8.37-8.15 (m, 4H), 7.11 (s, 1H), 3.25-3.00 (m, 2H), 1.76-1.60 (m, 2H), 1.01-0.93 (m, 3H). HRMS-ESI *m/z* [M - H] calcd for $C_{15}H_{13}N_4O_5S_2$: 393.0327, found: 393.0332.

^{1}H and ^{13}C NMR data of compound 4-1a:

4-(4-Chlorobenzoyl)-5-(3,4-dichlorophenyl)-1-(5-(4-fluorobenzylthio)-1,3,4-thiadiazol-2-yl)-3-hydroxy-1H-pyrrol-2(5H)-one (4-1a2). (Yield 35%). ^{1}H NMR (500 MHz, DMSO-d_6) δ 7.76-7.12(m, 12H), 6.15 (s, 1H), 4.52-4.43 (m, 2H). ^{13}C NMR (125 MHz, DMSO-d_6): δ 187.6, 164.8, 162.5, 160.5, 159.2, 155.8, 149.6, 137.7, 136.3, 135.0, 132.6, 131.1, 129.8, 128.3, 128.2, 120.8, 115.4, 115.2, 61.5, 36.4. HRMS-ESI *m/z* [M - H] calcd for $C_{26}H_{14}Cl_3FN_3O_3S_2$: 603.9526, found: 603.9531.

4-Benzoyl-1-(5-(benzylthio)-1,3,4-thiadiazol-2-yl)-3-hydroxy-5-phenyl-1H-pyrrol-2(5H)-one (4-1a3). (Yield 50%). ^{1}H NMR (500 MHz, DMSO-d_6): δ 7.74-7.19 (m, 13H), 6.19 (s, 1H), 4.52-4.44 (m, 2H). ^{13}C NMR (125 MHz, DMSO-d_6): δ 189.0, 164.9, 159.4, 155.8, 148.1, 137.4, 136.4, 135.5, 133.0, 129.0, 128.8, 128.5, 128.2, 128.1, 127.7, 127.6, 122.2, 62.4, 37.3. HRMS-ESI *m/z* [M - H] calcd for $C_{26}H_{18}N_3O_3S_2$: 484.0790, found: 484.0801.

1-(5-(4-Fluorobenzylthio)-1,3,4-thiadiazol-2-yl)-4-benzoyl-3-hydroxy-5-phenyl-1H-pyrrol-2(5H)-one (4-1a4). (Yield 49%). ^{1}H NMR (500 MHz, DMSO-d_6): δ 7.74-7.11(m, 14H), 6.18 (s, 1H), 4.51-4.42 (m, 2H). ^{13}C NMR (125 MHz, DMSO-d_6): δ 188.75, 165.4, 160.5, 159.1, 156.0, 137.8, 136.2, 132.8, 136.2, 132.8, 132.7, 131.1, 131.0, 128.8, 128.1, 128.0, 127.7, 115.4, 115.2, 62.3, 36.4. HRMS-ESI *m/z* [M - H] calcd for $C_{26}H_{17}FN_3O_3S_2$: 502.0695, found: 502.0700.

1-(5-(4-Fluorobenzylthio)-1,3,4-thiadiazol-2-yl)-4-benzoyl-3-hydroxy-5-(4-(methylthio)phenyl)-1H-pyrrol-2(5H)-one (4-1a5). (Yield 47%). ^{1}H NMR (500 MHz, DMSO-d_6): δ 7.74-7.12(m, 13H), 6.13 (s, 1H), 4.52-4.44 (m, 2H), 2.40 (s, 3H).

^{13}C NMR (125 MHz, DMSO-d_6): HRMS-ESI *m/z* [M - H] calcd for $C_{27}H_{19}FN_3O_3S_3$: 548.0573, found: 548.0551.

1-(5-(4-Fluorobenzylthio)-1,3,4-thiadiazol-2-yl)-3-hydroxy-4-(3-methoxybenzoyl)-5-phenyl-1H-pyrrol-2(5H)-one (4-1a6). (Yield 48%).^{1}H NMR (500 MHz, $CDCl_3$): δ 7.48-7.12(m, 13H), 6.15 (s, 1H), 4.52-4.43 (m, 2H), 3.77 (s, 3H). HRMS-ESI *m/z* [M - H] calcd for $C_{27}H_{19}FN_3O_4S_2$: 532.0801, found: 532.0791.

4-Benzoyl-1-(5-(benzylthio)-1,3,4-thiadiazol-2-yl)-5-(4-fluorophenyl)-3-hydroxy-1H-pyrrol-2(5H)-one (4-1a7). (Yield 46%). ^{1}H NMR (500 MHz, DMSO-d_6): δ 7.77-7.06 (m, 14H), 6.20 (s, 1H), 4.54-4.43 (m, 2H). ^{13}C NMR (125 MHz, DMSO-d_6): δ 189.1, 164.8, 163.4, 160.2, 159.4, 155.8, 148.4, 137.5, 136.4, 133.0, 131.8, 130.1, 130.0, 129.0, 128.8, 128.5, 128.2, 127.6, 121.8, 115.2, 114.9, 61.7, 37.2. HRMS-ESI *m/z* [M - H] calcd for $C_{26}H_{17}FN_3O_3S_2$: 502.0695, found: 502.0708.

1-(5-(4-Methoxybenzylthio)-1,3,4-thiadiazol-2-yl)-4-benzoyl-5-(4-fluorophenyl)-3-hydroxy-1H-pyrrol-2(5H)-one (4-1a8). (Yield 35%). ^{1}H NMR (500 MHz, DMSO-d_6): δ 7.74-6.86 (m, 13H), 6.14 (s, 1H), 4.46-4.39 (m, 2H), 3.73 (s, 3H). ^{13}C NMR (125 MHz, DMSO-d_6): δ 188.3, 162.5, 160.6, 159.3, 158.7, 155.8, 138.1, 132.4, 130.3, 130.0, 129.9, 128.8, 128.6, 128.1, 128.0, 115.0, 114.8, 114.0, 61.5, 55.0, 36.9. HRMS-ESI *m/z* [M - H] calcd for $C_{27}H_{19}FN_3O_4S_2$: 532.0801, found: 532.0796.

1-(5-(4-Methoxybenzylthio)-1,3,4-thiadiazol-2-yl)-4-benzoyl-3-hydroxy-5-(4-(methylthio)phenyl)-1H-pyrrol-2(5H)-one (4-1a9). (Yield 41%). ^{1}H NMR (500 MHz, DMSO-d_6): δ 7.56-6.59(m, 13H), 5.64 (s, 1H), 4.41-4.30 (m, 2H), 3.76 (s, 3H), 2.41 (s, 3H). ^{13}C NMR (125 MHz, DMSO-d_6): δ168.9, 165.8, 163.4, 161.1, 159.2, 156.3, 138.1, 135.2, 134.0, 131.3, 130.3, 129.9, 129.6, 128.8, 128.4, 128.3, 127.7,

125.7, 114.1, 108.2, 61.5, 55.2, 37.7, 23.4, 15.4. HRMS-ESI *m/z* [M - H] calcd for $C_{28}H_{22}N_3O_4S_3$: 560.0772, found: 560.0769.

1-(5-(Benzylthio)-1,3,4-thiadiazol-2-yl)-4-(4-chlorobenzoyl)-3-hydroxy-5-phenyl-1H-pyrrol-2(5H)-one (4-1a10). (Yield 60%). ^{1}H NMR (500 MHz, DMSO-d_6): δ 7.76-7.19(m, 14H), 6.17 (s, 1H), 4.53-4.44 (m, 2H). ^{13}C NMR (125 MHz, DMSO-d_6): δ 187.8, 164.7, 159.4, 155.8, 148.7, 137.9, 136.4, 136.2, 135.5, 130.7, 129.0, 128.5, 128.4, 128.2, 128.1, 127.8, 127.6, 121.7, 62.3, 37.3. HRMS-ESI *m/z* [M - H] calcd for $C_{26}H_{17}ClN_3O_3S_2$: 518.0400, found: 518.0387.

1-(5-(Benzylthio)-1,3,4-thiadiazol-2-yl)-4-(4-chlorobenzoyl)-5-(furan-2-yl)-3-hydroxy-1H-pyrrol-2(5H)-one (4-1a11). (Yield 40%). ^{1}H NMR (500 MHz, $CDCl_3$): δ 7.52-5.98(m, 12H), 5.8 (s, 1H), 4.51-4.38 (m, 2H). ^{13}C NMR (125 MHz, DMSO-d_6): δ 187.8, 164.4, 159.6, 155.8, 149.2, 147.4, 142.9, 137.9, 136.5, 136.2, 130.7, 129.1, 128.6, 128.5, 127.6, 118.6, 110.8, 110.5, 56.0, 37.3. HRMS-ESI *m/z* [M - H] calcd for $C_{24}H_{15}ClN_3O_4S_2$: 508.0193, found: 508.0189.

1-(5-(Benzylthio)-1,3,4-thiadiazol-2-yl)-4-(4-chlorobenzoyl)-3-hydroxy-5-(4-methoxyphenyl)-1H-pyrrol-2(5H)-one (4-1a12). (Yield 45%).^{1}H NMR (500 MHz, DMSO-d_6): δ 7.77-6.80 (m, 13H), 6.11 (s, 1H), 4.53-4.44 (m, 2H), 3.67 (s, 3H). HRMS-ESI *m/z* [M - H] calcd for $C_{27}H_{19}ClN_3O_4S_2$: 548.0506, found: 548.0520.

1-(5-(Benzylthio)-1,3,4-thiadiazol-2-yl)-4-(4-chlorobenzoyl)-5-(4-chlorophenyl)-3-hydroxy-1H-pyrrol-2(5H)-one (4-1a13). (Yield 59%). ^{1}H NMR (500 MHz, DMSO-d_6): δ 7.77-7.25 (m, 13H), 6.16 (s, 1H), 4.52-4.44 (m, 2H). ^{13}C NMR (125 MHz, DMSO-d_6): δ 187.7, 164.7, 159.5, 155.7, 149.3, 137.8, 136.4, 136.2, 134.8, 132.7, 130.7, 129.8, 129.0, 128.5, 128.4, 128.2, 127.6, 121.0, 61.6, 37.3. HRMS-ESI *m/z* [M

- H] calcd for $C_{26}H_{16}Cl_2N_3O_3S_2$: 552.0010, found: 552.0001. **(-)-4-1a13**, $[\alpha]^{25}$ -48.4° $degmLg^{-1}dm^{-1}$ (*c* 3.2 x 10^{-3} g/mL, CH_2Cl_2); **(+)-4-1a13**, $[\alpha]^{25}$ +84.7° (*c* 3.0 x 10^{-3} g/mL, CH_2Cl_2).

4-(4-Chlorobenzoyl)-5-(4-chlorophenyl)-3-hydroxy-1-(5-(methylthio)-1,3,4-thiadiazol-2-yl)-1H-pyrrol-2(5H)-one (4-1a14). (Yield 53%). ^{1}H NMR (500 MHz, DMSO-d_6): δ 7.75-7.20 (m, 8H), 6.2 (s, 1H), 2.68 (s, 3H). ^{13}C NMR (125 MHz, DMSO-d_6): δ 189.0, 164.8, 161.5, 155.2, 148.1, 137.4, 135.6, 133.0, 128.8, 127.7, 122.1, 62.3, 15.9. HRMS-ESI *m/z* [M - H] calcd for $C_{20}H_{12}C_{l2}N_3O_3S_2$: 475.9697, found: 475.9701.

4-(4-Chlorobenzoyl)-5-(4-chlorophenyl)-3-hydroxy-1-(5-(isopropylthio)-1,3,4-thiadiazol-2-yl)-1H-pyrrol-2(5H)-one (4-1a15). (Yield 55%). ^{1}H NMR (500 MHz, DMSO-d_6): δ 7.78-7.26 (m, 8H), 6.0 (s, 1H), 3.78-3.72 (m, 1H), 1.35-1.32(t, *J* =6.0 Hz, 6H). HRMS-ESI *m/z* [M - H] calcd for $C_{22}H_{16}C_{l2}N_3O_3S_2$: 504.0010, found: 504.0011.

4-(4-Chlorobenzoyl)-5-(4-chlorophenyl)-3-hydroxy-1-(5-(propylthio)-1,3,4-thiadiazol-2-yl)-1H-pyrrol-2(5H)-one (4-1a16). (Yield 55%). ^{1}H NMR (500 MHz, DMSO-d_6): δ 7.77-7.30 (m, 8H), 6.1 (s, 1H), 3.23-3.14 (m, 2H), 1.71-1.64 (m, 2H), 0.96-0.94 (t, 3H, C*H*$_3$, *J* =4.9Hz). ^{13}C NMR (125 MHz, DMSO-d_6): δ 186.6, 160.0, 155.6, 137.2, 137.1, 136.8, 136.4, 136.4, 136.4, 132.2, 130.6, 129.7, 118.6, 61.4, 35.3, 22.3, 12.9. HRMS-ESI *m/z* [M - H] calcd for $C_{22}H_{16}Cl_2N_3O_3S_2$: 504.0010, found: 504.0004. **(-)-4-1a16**, $[\alpha]^{25}$ -42.9° (*c* 11.2 x 10^{-3} g/mL, CH_2Cl_2); **(+)-4-1a16**, $[\alpha]^{25}$ +13.1° (*c* 12.1 x 10^{-3} g/mL, CH_2Cl_2).

1-(5-(Butylthio)-1,3,4-thiadiazol-2-yl)-4-(4-chlorobenzoyl)-5-(4-chlorophenyl)-3-hydroxy-1H-pyrrol-2(5H)-one (4-1a17). (Yield 49%). ^{1}H NMR (500 MHz, DMSO-

d_6): δ 7.76-7.31 (m, 8H), 6.1 (s, 1H), 3.26-3.15 (m, 2H), 1.67-1.61 (m, 2H), 1.41-1.34 (m, 2H), 0.88-0.85(t, *J* =4.8 Hz, 3H). ^{13}C NMR (125 MHz, DMSO-d_6): δ. 210.6, 187.3, 165.1, 160.1, 155.5, 137.4, 136.6, 135.5, 132.5, 130.6, 129.8, 128.2, 128.1, 120.1, 61.5, 33.1, 30.9, 21.1, 13.3. HRMS-ESI *m/z* [M - H] calcd for $C_{23}H_{18}Cl_2N_3O_3S_2$: 518.0167, found: 518.0167. **(-)-4-1a17**, $[\alpha]^{25}$ -9.2° (*c* 11.0 x 10^{-3} g/mL, CH_2Cl_2); **(+)-4-1a13**, $[\alpha]^{25}$ +41.9° (*c* 2.6 x 10^{-3} g/mL, CH_2Cl_2).

4-(4-Chlorobenzoyl)-5-(4-chlorophenyl)-1-(5-(cyclopentylthio)-1,3,4-thiadiazol-2-yl)-3-hydroxy-1H-pyrrol-2(5H)-one (4-1a18). (Yield 45%). ^{1}H NMR (500 MHz, DMSO-d_6): δ 7.79-7.25 (m, 8H), 5.96 (s, 1H), 3.90-3.87 (t, *J* =6.3 Hz, 2H), 3.01-3.00 (m, 2H), 2.11-2.08 (m, 2H), 1.68-1.54 (t, *J* =6.27 Hz, 4H). ^{13}C NMR (125 MHz, DMSO-d_6): δ 183.7, 169.2, 162.9, 158.9, 156.1, 140.1, 139.4, 134.3, 131.1, 130.5, 129.3, 127.4, 126.9, 112.4, 60.9, 46.7, 43.7, 33.3, 24.2, 24.1. HRMS-ESI *m/z* [M - H] calcd for $C_{24}H_{18}C_{l2}N_3O_3S_2$: 530.0167, found: 530.0177.

4-(4-Chlorobenzoyl)-5-(4-chlorophenyl)-3-hydroxy-1-(5-(2-hydroxyethylthio)-1,3,4-thiadiazol-2-yl)-1H-pyrrol-2(5H)-one (4-1a20), (Yield 48%). ^{1}H NMR (500 MHz, DMSO-d_6): δ 7.77-7.31 (m, 8H), 6.14 (s, 1H), 3.67-3.64 (t, *J* =6.3 Hz, 2H), 3.35-3.25 (m, 2H). HRMS-ESI *m/z* [M - H] calcd for $C_{21}H_{14}Cl_2N_3O_4S_2$: 505.9803, found: 505.9805.

5-(4-Chlorophenyl)-4-(4-fluorobenzoyl)-3-hydroxy-1-(5-(propylthio)-1,3,4-thiadiazol-2-yl)-1H-pyrrol-2(5H)-one (4-1a23). (Yield 54%). ^{1}H NMR (300 MHz, DMSO) δ 7.84 (dd, *J* = 8.6, 5.6 Hz, 2H), 7.53 (d, *J* = 8.4 Hz, 2H), 7.39 – 7.17 (m, 4H), 6.16 (s, 1H), 3.31 – 3.05 (m, 2H), 1.80 – 1.53 (m, 2H), 0.95 (t, *J* = 7.3 Hz, 3H); ^{13}C NMR (75 MHz, DMSO) δ 186.50, 165.61, 163.75, 162.28, 159.19, 154.48, 147.84, 133.88, 133.12, 133.09, 131.74, 130.93, 130.80, 128.90, 127.27, 120.29,

114.54, 114.25, 60.68, 34.30, 21.29, 11.90. HRMS-ESI *m/z* [M - H] calcd for $C_{22}H_{17}ClFN_3O_3S_2$-H: 488.0306, found: 488.0306.

5-(4-Bromophenyl)-4-(4-chlorobenzoyl)-3-hydroxy-1-(5-(propylthio)-1,3,4-thiadiazol-2-yl)-1H-pyrrol-2(5H)-one (4-1a24). (Yield 64%). ^{1}H NMR (500 MHz, DMSO) δ 7.75 (d, *J* = 8.5 Hz, 2H), 7.53 (d, *J* = 8.5 Hz, 2H), 7.49 – 7.39 (m, 4H), 6.12 (s, 1H), 3.24 – 3.14 (m, 4H), 1.81 – 1.58 (m, 2H), 0.96 (t, *J* = 7.4 Hz, 3H); ^{13}C NMR (125 MHz, DMSO) δ 187.69, 164.76, 160.19, 155.44, 149.55, 137.79, 136.26, 135.42, 131.13, 130.67, 130.17, 128.38, 121.30, 120.82, 61.64, 35.31, 22.26, 12.86. HRMS-ESI *m/z* [M - H] calcd for $C_{22}H_{16}ClBrN_3O_3S_2$: 547.9510, found: 547.9509; HRMS-ESI *m/z* [M - H] calcd for $C_{22}H_{16}Cl^{81}BrN_3O_3S_2$: 549.9490, found: 549.9491.

3-(4-Chlorobenzoyl)-4-(3-chlorophenyl)-2-hydroxy-5-(5-(propylthio)-1,3,4-thiadiazol-2-yl)cyclopent-2-enone (4-1a25). (Yield 57%). ^{1}H NMR (500 MHz, DMSO) δ 7.76 (dd, *J* = 6.3, 4.6 Hz, 2H), 7.59 (s, 1H), 7.53 (dd, *J* = 8.6, 1.9 Hz, 2H), 7.44 (dt, *J* = 7.0, 1.8 Hz, 1H), 7.35 – 7.23 (m, 2H), 6.14 (s, 1H), 3.29 – 3.10 (m, 2H), 1.76 – 1.61 (m, 2H), 0.96 (t, *J* = 7.3 Hz, 3H); ^{13}C NMR (125 MHz, DMSO) δ 187.73, 164.76, 160.27, 155.51, 149.68, 138.48, 137.86, 136.25, 132.75, 130.71, 130.08, 128.39, 128.22, 128.06, 126.46, 120.72, 61.71, 35.34, 22.28, 12.87. HRMS-ESI *m/z* [M - H] calcd for $C_{22}H_{16}Cl_2N_3O_3S_2$: 504.0016, found: 504.0024.

4-(4-Bromobenzoyl)-5-(4-chlorophenyl)-3-hydroxy-1-(5-(propylthio)-1,3,4-thiadiazol-2-yl)-1H-pyrrol-2(5H)-one (4-1a27). (Yield 61%). ^{1}H NMR (500 MHz, DMSO) δ 7.69 (s, 4H), 7.52 (d, *J* = 8.3 Hz, 2H), 7.33 (d, *J* = 8.4 Hz, 2H), 6.16 (s, 1H), 3.27 – 3.15 (m, 2H), 1.75 – 1.62 (m, 2H), 0.97 (t, *J* = 7.3 Hz, 3H); ^{13}C NMR (125 MHz, DMSO) δ 187.84, 164.77, 160.17, 155.44, 149.63, 136.62, 134.99, 132.67, 131.30, 130.74, 129.83, 128.20, 126.88, 120.80, 61.54, 35.31, 22.25, 12.85. HRMS-

ESI *m/z* [M - H] calcd for $C_{22}H_{16}ClBrN_3O_3S_2$: 547.9510, found: 547.9511; HRMS-ESI *m/z* [M - H] calcd for $C_{22}H_{16}Cl^{81}BrN_3O_3S_2$: 549.9490, found: 549.9496.

5-(4-Chlorophenyl)-3-hydroxy-4-(4-iodobenzoyl)-1-(5-(propylthio)-1,3,4-thiadiazol-2-yl)-1H-pyrrol-2(5H)-one (4-1a28). (Yield 59%). ^{1}H NMR (500 MHz, DMSO) δ 7.85 (d, *J* = 8.2 Hz, 2H), 7.50 (d, *J* = 7.9 Hz, 4H), 7.32 (d, *J* = 8.3 Hz, 2H), 6.13 (s, 1H), 3.21 (m, 3H), 1.68 (dd, *J* = 14.4, 7.2 Hz, 2H), 0.96 (t, *J* = 7.3 Hz, 3H). HRMS-ESI *m/z* [M - H] calcd for $C_{22}H_{16}ClIN_3O_3S_2$: 595.9372, found: 595.9394.

5-(4-Chlorophenyl)-3-hydroxy-4-(4-nitrobenzoyl)-1-(5-(propylthio)-1,3,4-thiadiazol-2-yl)-1H-pyrrol-2(5H)-one (4-1a29). (Yield 54%). ^{1}H NMR (500 MHz, DMSO) δ 8.27 (d, *J* = 8.4 Hz, 2H), 7.94 (d, *J* = 8.4 Hz, 2H), 7.57 (d, *J* = 8.1 Hz, 2H), 7.34 (d, *J* = 8.1 Hz, 2H), 6.17 (s, 1H), 3.31 – 3.04 (m, 2H), 1.66 (dt, *J* = 14.0, 7.0 Hz, 2H), 0.93 (t, *J* = 7.2 Hz, 3H); ^{13}C NMR (125 MHz, DMSO) δ 187.57, 164.64, 160.43, 155.41, 151.32, 149.55, 142.96, 135.06, 132.79, 130.00, 129.94, 128.27, 123.41, 120.13, 61.48, 35.32, 22.30, 12.92. HRMS-ESI *m/z* [M - H] calcd for $C_{22}H_{17}ClN_4O_5S_2$: 515.0256, found: 515.0265.

4-(4-Aminobenzoyl)-5-(4-chlorophenyl)-3-hydroxy-1-(5-(propylthio)-1,3,4-thiadiazol-2-yl)-1H-pyrrol-2(5H)-one (4-1a30). (Yield 87%). ^{1}H NMR (500 MHz, DMSO) δ 7.53 (d, *J* = 8.3 Hz, 2H), 7.41 (d, *J* = 7.9 Hz, 2H), 7.30 (d, *J* = 8.0 Hz, 2H), 6.51 (d, *J* = 8.2 Hz, 2H), 6.13 (s, 1H), 3.30 – 3.07 (m, 2H), 1.67 (dd, *J* = 14.3, 7.1 Hz, 2H), 0.95 (t, *J* = 7.2 Hz, 3H); ^{13}C NMR (125 MHz, DMSO) δ 185.73, 165.02, 159.85, 155.59, 154.38, 144.85, 134.70, 132.67, 132.05, 129.64, 128.31, 124.47, 124.24, 112.31, 62.06, 35.31, 22.32, 12.92. HRMS-ESI *m/z* [M - H] calcd for $C_{22}H_{18}ClN_4O_3S_2$: 485.0514, found: 485.0531.

4-(Benzofuran-2-carbonyl)-5-(4-chlorophenyl)-3-hydroxy-1-(5-(propylthio)-1,3,4-thiadiazol-2-yl)-1H-pyrrol-2(5H)-one (4-1a32). (Yield 75%). ^{1}H NMR (500 MHz, DMSO) δ 8.11 (s, 1H), 7.85 (d, *J* = 7.7 Hz, 1H), 7.69 (d, *J* = 8.2 Hz, 1H), 7.53 (t, *J* = 9.0 Hz, 3H), 7.34 (dd, *J* = 20.1, 7.6 Hz, 3H), 6.27 (s, 1H), 3.37 – 3.09 (m, 2H), 1.68 (dd, *J* = 14.2, 7.1 Hz, 2H), 0.95 (t, *J* = 7.2 Hz, 3H); ^{13}C NMR (125 MHz, DMSO) δ 176.60, 165.06, 160.78, 155.90, 155.46, 152.19, 149.89, 135.28, 133.31, 130.45, 129.26, 128.73, 127.16, 124.55, 124.37, 121.38, 116.82, 112.61, 61.96, 35.84, 22.78, 13.37. HRMS-ESI *m/z* [M - H] calcd for $C_{24}H_{17}ClN_3O_4S_2$: 510.0354, found: 510.0370.

4-(4-Chlorobenzoyl)-5-(4-chlorophenyl)-3-hydroxy-1-(5-(propylsulfonyl)-1,3,4-thiadiazol-2-yl)-1H-pyrrol-2(5H)-one (4-1a33). (Yield 76%) ^{1}H NMR (500 MHz, DMSO) δ 7.78 (d, *J* = 8.5 Hz, 2H), 7.56 (dd, *J* = 23.5, 8.4 Hz, 4H), 7.34 (d, *J* = 8.5 Hz, 2H), 6.22 (s, 1H), 3.77 – 3.61 (m, 2H), 1.85 – 1.59 (m, 2H), 0.95 (t, *J* = 7.4 Hz, 3H). HRMS-ESI *m/z* [M - H] calcd for $C_{22}H_{16}Cl_2N_3O_5S_2$: 535.9914, found: 535.9917.

4-(4-Chlorobenzoyl)-5-(4-chlorophenyl)-3-methoxy-1-(5-(propylthio)-1,3,4-thiadiazol-2-yl)-1H-pyrrol-2(5H)-one (4-1a34). (Yield 83%). ^{1}H NMR (500 MHz, DMSO) δ 7.92 – 7.82 (m, 2H), 7.60 (dd, *J* = 6.2, 4.5 Hz, 2H), 7.56 – 7.44 (m, 2H), 7.34 (dd, *J* = 6.2, 4.5 Hz, 2H), 6.18 (s, 1H), 4.02 (s, 3H), 3.21 (ddd, *J* = 19.4, 11.1, 4.5 Hz, 2H), 1.69 (dd, *J* = 14.5, 7.3 Hz, 2H), 0.97 (t, *J* = 7.4 Hz, 3H).

4-(4-Chlorobenzoyl)-1-(5-(4-fluorobenzylthio)-1,3,4-thiadiazol-2-yl)-5-(4-fluorophenyl)-3-(2-hydroxyethoxy)-1H-pyrrol-2(5H)-one (4-7a). (Yield 40%). ^{1}H NMR (500 MHz, DMSO-d_6): δ 7.56-6.36 (m, 12H), 5.75 (s, 1H), 4.45-4.33 (m, 2H), 3.79-3.77 (t, *J* = 6.5 Hz, 2H), 3.36-3.35 (b, 2H). ^{13}C NMR (125 MHz, DMSO-d_6): δ 173.9, 166.5, 163.3, 162.9, 161.2, 161.0, 155.9, 136.8, 132.9, 131.5, 130.9, 130.8,

129.5, 129.4, 128.4, 115.7, 115.5, 115.1, 115.0, 108.9, 61.0, 60.0, 47.6, 37.4, 29.8. HRMS-ESI *m/z* [M - H] calcd for $C_{28}H_{20}ClF_2N_4O_3S_2$: 597.0633, found: 597.0633.

4-Acetyl-3-hydroxy-1-methyl-5-phenyl-1H-pyrrol-2(5H)-one (4-8a). (Yield 45%). ^{1}H NMR (500 MHz, DMSO-d_6): δ 7.34-7.16 (m, 5H), 5.12 (s, 1H), 2.63(s, 3H), 2.27 (s, 3H). ^{13}C NMR (125 MHz, DMSO-d_6): δ 191.3, 165.1, 154.8, 136.8, 128.5, 128.0, 127.5, 120.0, 61.8, 29.7, 27.2. HRMS-ESI *m/z* [M - H] calcd for $C_{13}H_{12}NO_3$: 230.0817, found: 230.0814.

4-Acetyl-1-benzyl-3-hydroxy-5-phenyl-1H-pyrrol-2(5H)-one (4-8b). (Yield 60%). ^{1}H NMR (500 MHz, DMSO-d_6): δ 7.33-7.06 (m, 10H), 4.94 (s, 1H) 4.86-4.82 (d, *J* = 15.8 Hz, 1H), 3.61-3.58 (d, *J* = 15.2 Hz, 1H), 2.27 (s, 3H). ^{13}C NMR (125 MHz, DMSO-d_6): δ 191.3, 165.3, 154.7, 136.4, 136.3, 128.7, 128.6, 128.1, 127.7, 127.6, 127.4, 120.2, 59.9, 43.6, 40.3, 29.7. HRMS-ESI *m/z* [M - H] calcd for $C_{19}H_{16}NO_3$: 306.1130, found: 306.1124.

4-Acetyl-3-amino-1-benzyl-5-phenyl-1H-pyrrol-2(5H)-one (4-9a). (Yield 85%). ^{1}H NMR (500 MHz, $CDCl_3$): δ 7.37-7.11 (m, 10H), 5.21-5.18 (d, *J* = 15.1 Hz 1H), 4.86 (s, H), 3.47-3.44 (d, *J* = 15.1 Hz, 1H), 1.69 (s, 3H). ^{13}C NMR (125 MHz, $CDCl_3$): δ 191.3, 165.3, 154.7, 136.4, 136.3, 128.7, 128.6, 128.1, 127.7, 127.6, 127.4, 120.2, 59.9, 43.6, 40.3, 29.7. HRMS-ESI *m/z* [M - H] calcd for $C_{19}H_{17}N_2O_2$: 305.1290, found: 305.1290.

4-Acetyl-1-benzyl-3-(methylamino)-5-phenyl-1H-pyrrol-2(5H)-one (4-9b). (Yield 70%). ^{1}H NMR (500 MHz, $CDCl_3$): δ 11.05 (b, H), 7.28-7.04 (m, 10H), 5.17-5.14 (d, *J* = 14.5 Hz, 1H), 4.78 (s, H), 3.37-3.34 (d, *J* = 15.1 Hz 1H), 2.92-2.91 (d, *J* = 5.7 Hz, 1H), 1.58 (s, 3H). ^{13}C NMR (125 MHz, $CDCl_3$): δ 177.7, 165.1, 164.3, 138.1, 136.5,

129.0, 128.6, 128.5, 128.1, 127.6, 108.9, 58.8, 43.9, 29.9, 14.9. HRMS-ESI *m/z* [M - H] calcd for $C_{19}H_{19}N_2O_2$: 319.1447, found: 319.1447.

4-Acetyl-1-benzyl-3-(2-hydroxyethylamino)-5-phenyl-1H-pyrrol-2(3H)-one (4-9c). (Yield 90%). ^{1}H NMR (500 MHz, $CDCl_3$): δ 11.31 (b, H), 7.28-7.03 (m, 10), 5.04-5.01 (d, *J* = 15.2 Hz, 1H), 4.76 (s, 1H), 4.50 (b, 1H), 3.81-3.79 (t, *J* = 5.7 Hz, 2H), 3.50-3.42 (b, 2H), 3.39-3.36 (d, *J* = 15.2 Hz, 1H), 1.62 (s, 3H). ^{13}C NMR (125 MHz, $CDCl_3$): δ 176.4, 165.5, 164.5, 137.7, 136.3, 128.9, 128.6, 128.3, 128.1, 127.5, 106.9, 66.9, 60.6, 59.1, 45.9, 43.9, 15.4. HRMS-ESI *m/z* [M - Na] calcd for $C_{21}H_{22}N_2O_3Na$: 373.1528, found: 373.1536.

4.7 Chiral Chromatogram of compounds 4-1a13, 4-1a16 and 4-1a17

a) Chiral chromatogram of compound 4-1a13 using AD-H column

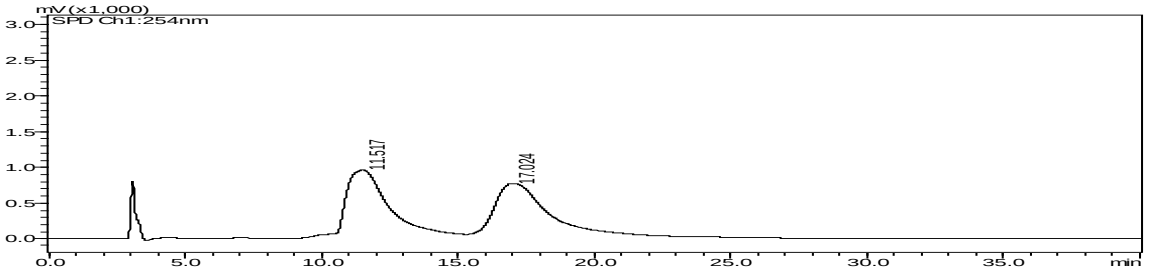

b) Chiral chromatogram of compound 4-1a16 using IC column

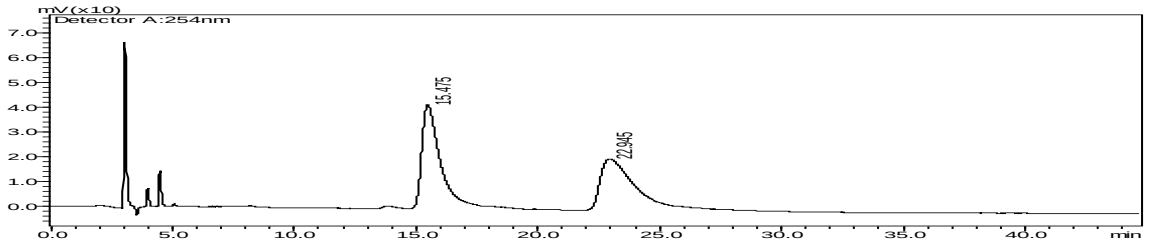

c) Chiral chromatogram of compound 4-1a17 using AD-H column

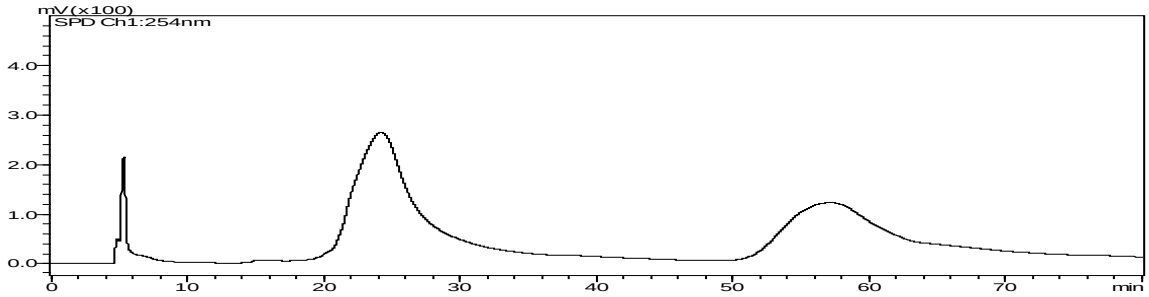

Figure 4.4 Chiral chromatograms of compounds **4-1a13, 4-1a16** and **4-1a17** at 254 nm.

References

1. Martina, B. E.; Koraka, P.; Osterhaus, A. D., West Nile Virus: is a vaccine needed? *Curr. Opin. Investig. Drugs.* **2010,** *11*, 139-146.

2. Barrett, A. D. T., Current Status of Flavivirus Vaccines. *Ann. N. Y. Acad. Sci.* **2001,** *951*, 262-271.

3. Mansfield, K. L.; Horton, D. L.; Johnson, N.; Li, L.; Barrett, A. D. T.; Smith, D. J.; Galbraith, S. E.; Solomon, T.; Fooks, A. R., Flavivirus-induced antibody cross-reactivity. *J. Gen. Virol.* **2011,** *92*, 2821-2829

4. Smithburn, K. C.; Hughes, T. P.; Burke, A. W.; Paul, J. H., A Neurotropic Virus Isolated from the Blood of a Native of Uganda. *Am. J. Trop. Med. Hygi.* **1940,** *s1-20*, 471-492.

5. Lanciotti, R. S.; Ebel, G. D.; Deubel, V.; Kerst, A. J.; Murri, S.; Meyer, R.; Bowen, M.; McKinney, N.; Morrill, W. E.; Crabtree, M. B.; Kramer, L. D.; Roehrig, J. T., Complete genome sequences and phylogenetic analysis of West Nile virus strains isolated from the United States, Europe, and the Middle East. *Virology* **2002,** *298*, 96-105.

6. www.cdc.gov/ncidod/dvbid/westnile/index.htm.

7. Gubler, D. J., The Continuing Spread of West Nile Virus in the Western Hemisphere. *Clin. Infect. Dis.* **2007,** *45*, 1039-1046.

8. Hall, D. A.; Tyler, K. L.; Frey, K. L.; Kozora, E.; Arciniegas, D. B., Persistent neurobehavioral signs and symptoms following West Nile fever. *J. Neuropsychiatry Clin. Neurosci.* **2008,** *20*, 122-123.

9. Diamond, M. S.; Brinton, M. A., Molecular Biology of West Nile Virus Encephalitis Virus Infection. *Springer New York.* 2009; pp 97-136.

10. Gubler, D. J., Kuno, G., and Markoff, J, Flaviviruses. In "Fields Virology. *Lippincott Williams and Wilkins.* **2007**, pp. 1153-1252.

11. a) Gould, L. H.; Fikrig, E., West Nile virus: a growing concern? *J. Clin. Invest.* **2004,** *113*, 1102-1107; b) http://www.arlingtonva.us/Departments/Human Services /services/health/envhealth/HumanServicesmosquitocontrol5.aspx.

12. Modis, Y.; Ogata, S.; Clements, D.; Harrison, S. C., A ligand-binding pocket in the dengue virus envelope glycoprotein. *Proc. Natl. Acad. Sci.* **2003,** *100*, 6986-6991.

13. Murphy, F. A., *New York, Academic Press.* **1980**, pp.241-316.

14. Mukhopadhyay, S.; Kim, B. S.; Chipman, P. R.; Rossmann, M. G.; Kuhn, R. J., Brevia: Structure of West Nile virus. *Science.* **2003,** *302*, 248.

15. Beasley, D. W. C.; Barrett, A. D. T., Identification of Neutralizing Epitopes within Structural Domain III of the West Nile Virus Envelope Protein. *J. Virol.* **2002,** *76*, 13097-13100.

16. Zhang, Y.; Corver, J.; Chipman, P. R.; Zhang, W.; Pletnev, S. V.; Sedlak, D.; Baker, T. S.; Strauss, J. H.; Kuhn, R. J.; Rossmann, M. G., Structures of immature flavivirus particles. *EMBO. J.* **2003,** *22*, 2604-2613.

17. Brinton, M. A.; Fernandez, A. V.; Dispoto, J. H., The 3'-nucleotides of flavivirus genomic RNA form a conserved secondary structure. *Virology* **1986,** *153*, 113-121.

18. Allison, S. L.; Schalich, J.; Stiasny, K.; Mandl, C. W.; Kunz, C.; Heinz, F. X., Oligomeric rearrangement of tick-borne encephalitis virus envelope proteins induced by an acidic pH. *J. Virol.* **1995,** *69*, 695-700.

19. Zhang, Y.; Corver, J.; Chipman, P. R.; Zhang, W.; Pletnev, S. V.; Sedlak, D.; Baker, T. S.; Strauss, J. H.; Kuhn, R. J.; Rossmann, M. G., Structures of immature flavivirus particles. *EMBO. J.* **2003,** *22*, 2604-2613.

20. Heinz, F. X.; Auer, G.; Stiasny, K.; Holzmann, H.; Mandl, C.; Guirakhoo, F.; Kunz, C., The interactions of the flavivirus envelope proteins: implications for virus entry and release. *Arch. Virol. Suppl.* **1994,** *9*, 339-348.

21. Brinton, M. A., The molecular biology of West Nile virus: a new invader of the Western hemisphere. *Annu. Rev. Microbiol.* **2002,** *56*, 371-402.

22. Lindenbach, B. D.; Rice, C. M., Molecular biology of flaviviruses. *Adv. Virus. Res.* **2003,** *59*, 23-61.

23. a) Elshuber, S.; Allison, S. L.; Heinz, F. X.; Mandl, C. W., Cleavage of protein prM is necessary for infection of BHK-21 cells by tick-borne encephalitis virus. *J. Gen. Virol.* **2003,** *84*, 183-191; b) http://www.microbiologytext.com/index.php?module=Book&func=displayarticle&art_id=492.

24. Lindenbach, B. D.; Rice, C. M., Unravelling hepatitis C virus replication from genome to function. *Nature* **2005,** *436*, 933-938.

25. Schalich, J.; Allison, S. L.; Stiasny, K.; Mandl, C. W.; Kunz, C.; Heinz, F. X., Recombinant subviral particles from tick-borne encephalitis virus are fusogenic and provide a model system for studying flavivirus envelope glycoprotein functions. *J. Virol.* **1996,** *70*, 4549-4557.

26. Chambers, T. J.; Hahn, C. S.; Galler, R.; Rice, C. M., Flavivirus genome organization, expression, and replication. *Annu. Rev. Microbiol.* **1990,** *44*, 649-688.

27. Shiryaev, S. A.; Cheltsov, A. V.; Gawlik, K.; Ratnikov, B. I.; Strongin, A. Y., Virtual Ligand Screening of the National Cancer Institute (NCI) Compound Library Leads to the Allosteric Inhibitory Scaffolds of the West Nile Virus NS3 Proteinase. *Assay Drug. Dev. Technol.* **2011,** *9*, 69-78.

28. Westaway, E. G.; Mackenzie, J. M.; Kenney, M. T.; Jones, M. K.; Khromykh, A. A., Ultrastructure of Kunjin virus-infected cells: colocalization of NS1 and NS3 with

double-stranded RNA, and of NS2B with NS3, in virus-induced membrane structures. *J. Virol.* **1997,** *71*, 6650-6661.

29. Nowak, T.; Färber, P. M.; Wengler, G.; Wengler, G., Analyses of the terminal sequences of west nile virus structural proteins and of the *in vitro* translation of these proteins allow the proposal of a complete scheme of the proteolytic cleavages involved in their synthesis. *Virology* **1989,** *169*, 365-376.

30. Speight, G.; Coia, G.; Parker, M. D.; Westaway, E. G., Gene Mapping and Positive Identification of the Non-structural Proteins NS2A, NS2B, NS3, NS4B and NS5 of the Flavivirus Kunjin and Their Cleavage Sites. *J. Gen. Virol.* **1988,** *69*, 23-34.

31. Falgout, B.; Markoff, L., Evidence that flavivirus NS1-NS2A cleavage is mediated by a membrane-bound host protease in the endoplasmic reticulum. *J. Virol.* **1995,** *69*, 7232-7243.

32. Stadler, K.; Allison, S. L.; Schalich, J.; Heinz, F. X., Proteolytic activation of tick-borne encephalitis virus by furin. *J. Virol.* **1997,** *71*, 8475-8481.

33. Lin, C.; Amberg, S. M.; Chambers, T. J.; Rice, C. M., Cleavage at a novel site in the NS4A region by the yellow fever virus NS2B-3 proteinase is a prerequisite for processing at the downstream 4A/4B signalase site. *J. Virol.* **1993,** *67*, 2327-2335.

34. Amberg, S. M.; Nestorowicz, A.; McCourt, D. W.; Rice, C. M., NS2B-3 proteinase-mediated processing in the yellow fever virus structural region: *in vitro* and in vivo studies. *J. Virol.* **1994,** *68*, 3794-3802.

35. Chambers, T. J.; Weir, R. C.; Grakoui, A.; McCourt, D. W.; Bazan, J. F.; Fletterick, R. J.; Rice, C. M., Evidence that the N-terminal domain of nonstructural protein NS3 from yellow fever virus is a serine protease responsible for site-specific cleavages in the viral polyprotein. *Proc. Natl. Acad. Sci. U S A.* **1990,** *87*, 8898-8902.

36. Nestorowicz, A.; Chambers, T. J.; Rice, C. M., Mutagenesis of the Yellow Fever Virus NS2A/2B Cleavage Site: Effects on Proteolytic Processing, Viral Replication, and Evidence for Alternative Processing of the NS2A Protein. *Virology* **1994,** *199*, 114-123.

37. a) Amberg, S. M.; Nestorowicz, A.; McCourt, D. W.; Rice, C. M., *J. Virol.* **1994,** *68*, 3794-3802.; b) Mackenzie, J. M.; Jones, M. K.; Young, P. R., Immunolocalization of the Dengue Virus Nonstructural Glycoprotein NS1 Suggests a Role in Viral RNA Replication. *Virology* **1996,** *220*, 232-240.

38. Miller, S.; Sparacio, S.; Bartenschlager, R., Subcellular Localization and Membrane Topology of the Dengue Virus Type 2 Non-structural Protein 4B. *J. Biol. Chem.* **2006,** *281*, 8854-8863.

39. Wengler, G.; Wengler, G., The NS 3 Nonstructural Protein of Flaviviruses Contains an RNA Triphosphatase Activity. *Virology* **1993,** *197*, 265-273.

40. Koonin, E. V., Computer-assisted identification of a putative methyltransferase domain in NS5 protein of flaviviruses and λ2 protein of reovirus. *J. Gen. Virol.* **1993,** *74*, 733-740.

41. Kofler, R. M.; Heinz, F. X.; Mandl, C. W., Capsid Protein C of Tick-Borne Encephalitis Virus Tolerates Large Internal Deletions and Is a Favorable Target for Attenuation of Virulence. *J. Virol.* **2002,** *76*, 3534-3543.

42. Dokland, T.; Walsh, M.; Mackenzie, J. M.; Khromykh, A. A.; Ee, K.-H.; Wang, S., West Nile Virus Core Protein: Tetramer Structure and Ribbon Formation. *Structure* **2004,** *12*, 1157-1163.

43. Stocks, C. E.; Lobigs, M., Signal Peptidase Cleavage at the Flavivirus C-prM Junction: Dependence on the Viral NS2B-3 Protease for Efficient Processing Requires Determinants in C, the Signal Peptide, and prM. *J. Virol.* **1998,** *72*, 2141-2149.

44. Jones, C. T.; Ma, L.; Burgner, J. W.; Groesch, T. D.; Post, C. B.; Kuhn, R. J., Flavivirus Capsid Is a Dimeric Alpha-Helical Protein. *J. Virol.* **2003,** *77*, 7143-7149.

45. Kiermayr, S.; Kofler, R. M.; Mandl, C. W.; Messner, P.; Heinz, F. X., Isolation of Capsid Protein Dimers from the Tick-Borne Encephalitis Flavivirus and *In Vitro* Assembly of Capsid-Like Particles. *J. Virol.* **2004,** *78*, 8078-8084.

46. Lindenbach, B. D.; Prágai, B. M.; Montserret, R.; Beran, R. K. F.; Pyle, A. M.; Penin, F.; Rice, C. M., The C Terminus of Hepatitis C Virus NS4A Encodes an Electrostatic Switch That Regulates NS5A Hyperphosphorylation and Viral Replication. *J. Virol.* **2007,** *81*, 8905-8918.

47. Mandl, C. W.; Guirakhoo, F.; Holzmann, H.; Heinz, F. X.; Kunz, C., Antigenic structure of the flavivirus envelope protein E at the molecular level, using tick-borne encephalitis virus as a model. *J. Virol.* **1989,** *63*, 564-571.

48. Allison, S. L.; Schalich, J.; Stiasny, K.; Mandl, C. W.; Heinz, F. X., Mutational Evidence for an Internal Fusion Peptide in Flavivirus Envelope Protein E. *J. Virol.* **2001,** *75*, 4268-4275.

49. Falgout, B.; Chanock, R.; Lai, C. J., Proper processing of dengue virus nonstructural glycoprotein NS1 requires the N-terminal hydrophobic signal sequence and the downstream nonstructural protein NS2a. *J. Virol.* **1989,** *63*, 1852-1860.

50. Winkler, G.; Randolph, V. B.; Cleaves, G. R.; Ryan, T. E.; Stollar, V., Evidence that the mature form of the flavivirus nonstructural protein NS1 is a dimer. *Virology* **1988,** *162*, 187-196.

51. Winkler, G.; Maxwell, S. E.; Ruemmler, C.; Stollar, V., Newly synthesized dengue-2 virus nonstructural protein NS1 is a soluble protein but becomes partially hydrophobic and membrane-associated after dimerization. *Virology* **1989,** *171*, 302-305.

52. Grun, J. B.; Brinton, M. A., Characterization of West Nile virus RNA-dependent RNA polymerase and cellular terminal adenylyl and uridylyl transferases in cell-free extracts. *J. Virol.* **1986,** *60*, 1113-1124.

53. Falgout, B.; Markoff, L., Evidence that flavivirus NS1-NS2A cleavage is mediated by a membrane-bound host protease in the endoplasmic reticulum. *J. Virol.* **1995,** *69*, 7232-7243.

54. Lee, J. M.; Crooks, A. J.; Stephenson, J. R., The synthesis and maturation of a non-structural extracellular antigen from tick-borne encephalitis virus and its relationship to the intracellular NS1 protein. *J. Gen. Virol.* **1989,** *70*, 335-343.

55. Schlesinger, J. J.; Brandriss, M. W.; Monath, T. P., Monoclonal antibodies distinguish between wild and vaccine strains of yellow fever virus by neutralization, hemagglutination inhibition, and immune precipitation of the virus envelope protein. *Virology* **1983,** *125*, 8-17.

56. Kummerer, B. M.; Rice, C. M., Mutations in the yellow fever virus nonstructural protein NS2A selectively block production of infectious particles. *J. Virol.* **2002,** *76*, 4773-4784.

57. Chambers, T. J.; Nestorowicz, A.; Amberg, S. M.; Rice, C. M., Mutagenesis of the yellow fever virus NS2B protein: effects on proteolytic processing, NS2B-NS3 complex formation, and viral replication. *J. Virol.* **1993,** *67*, 6797-6807.

58. Falgout, B.; Miller, R. H.; Lai, C. J., Deletion analysis of dengue virus type 4 nonstructural protein NS2B: identification of a domain required for NS2B-NS3 protease activity. *J. Virol.* **1993,** *67*, 2034-2042.

59. Brinkworth, R. I.; Fairlie, D. P.; Leung, D.; Young, P. R., Homology model of the dengue 2 virus NS3 protease: putative interactions with both substrate and NS2B cofactor. *J. Gen. Virol.* **1999,** *80*, 1167-1177.

60. Clum, S.; Ebner, K. E.; Padmanabhan, R., Cotranslational membrane insertion of the serine proteinase precursor NS2B-NS3(Pro) of dengue virus type 2 is required for efficient *in vitro* processing and is mediated through the hydrophobic regions of NS2B. *J. Biol. Chem.* **1997,** *272*, 30715-30723.

61. Bazan, J. F.; Fletterick, R. J., Detection of a trypsin-like serine protease domain in flaviviruses and pestiviruses. *Virology* **1989,** *171*, 637-639.

62. Nall, T. A.; Chappell, K. J.; Stoermer, M. J.; Fang, N. X.; Tyndall, J. D. A.; Young, P. R.; Fairlie, D. P., Enzymatic Characterization and Homology Model of a Catalytically Active Recombinant West Nile Virus NS3 Protease. *J. Biol. Chem.* **2004,** *279*, 48535-48542.

63. Borowski, P.; Mueller, O.; Niebuhr, A.; Kalitzky, M.; Hwang, L. H.; Schmitz, H.; Siwecka, M. A.; Kulikowsk, T., ATP-binding domain of NTPase/helicase as a target for hepatitis C antiviral therapy. *Acta. Biochim. Pol.* **2000,** *47*, 173-180.

64. Bartelma, G.; Padmanabhan, R., Expression, purification, and characterization of the RNA 5'-triphosphatase activity of dengue virus type 2 nonstructural protein 3. *Virology* **2002,** *299*, 122-132.

65. Lindenbach, B. D.; Rice, C. M., Genetic interaction of flavivirus nonstructural proteins NS1 and NS4A as a determinant of replicase function. *J. Virol.* **1999,** *73*, 4611-4621.

66. Mackenzie, J. M.; Khromykh, A. A.; Jones, M. K.; Westaway, E. G., Subcellular localization and some biochemical properties of the flavivirus Kunjin nonstructural proteins NS2A and NS4A. *Virology* **1998,** *245*, 203-215.

67. Cahour, A.; Falgout, B.; Lai, C. J., Cleavage of the dengue virus polyprotein at the NS3/NS4A and NS4B/NS5 junctions is mediated by viral protease NS2B-NS3,

whereas NS4A/NS4B may be processed by a cellular protease. *J. Virol.* **1992,** *66*, 1535-1542.

68. Tan, B. H.; Fu, J.; Sugrue, R. J.; Yap, E. H.; Chan, Y. C.; Tan, Y. H., Recombinant Dengue Type 1 Virus NS5 Protein Expressed inEscherichia coliExhibits RNA-Dependent RNA Polymerase Activity. *Virology* **1996,** *216*, 317-325.

69. Koonin, E. V., Computer-assisted identification of a putative methyltransferase domain in NS5 protein of flaviviruses and lambda 2 protein of reovirus. *J. Gen. Virol.* **1993,** *74*, 733-740.

70. Khromykh, A. A.; Kenney, M. T.; Westaway, E. G., trans-Complementation of flavivirus RNA polymerase gene NS5 by using Kunjin virus replicon-expressing BHK cells. *J. Virol.* **1998,** *72*, 7270-7279.

71. Buckley, A.; Gaidamovich, S.; Turchinskaya, A.; Gould, E. A., Monoclonal antibodies identify the NS5 yellow fever virus non-structural protein in the nuclei of infected cells. *J. Gen. Virol.* **1992,** *73*, 1125-1130.

72. Kapoor, M.; Zhang, L.; Ramachandra, M.; Kusukawa, J.; Ebner, K. E.; Padmanabhan, R., Association between NS3 and NS5 proteins of dengue virus type 2 in the putative RNA replicase is linked to differential phosphorylation of NS5. *J. Biol. Chem.* **1995,** *270*, 19100-19106.

73. Chappell, K. J.; Nall, T. A.; Stoermer, M. J.; Fang, N. X.; Tyndall, J. D. A.; Fairlie, D. P.; Young, P. R., Site-directed Mutagenesis and Kinetic Studies of the West Nile Virus NS3 Protease Identify Key Enzyme-Substrate Interactions. *J. Biol. Chem.* **2005,** *280*, 2896-2903.

74. Erbel, P.; Schiering, N.; D'Arcy, A.; Renatus, M.; Kroemer, M.; Lim, S. P.; Yin, Z.; Keller, T. H.; Vasudevan, S. G.; Hommel, U., Structural basis for the activation of

flaviviral NS3 proteases from dengue and West Nile virus. *Nat. Struct. Mol. Biol.* **2006,** *13*, 372-373.

75. Aleshin, A. E.; Shiryaev, S. A.; Strongin, A. Y.; Liddington, R. C., Structural evidence for regulation and specificity of flaviviral proteases and evolution of the Flaviviridae fold. *Protein Sci.* **2007,** *16*, 795-806.

76. Malet, H.; Masse, N.; Selisko, B.; Romette, J. L.; Alvarez, K.; Guillemot, J. C.; Tolou, H.; Yap, T. L.; Vasudevan, S.; Lescar, J.; Canard, B., The flavivirus polymerase as a target for drug discovery. *Antiviral Res.* **2008,** *80*, 23-35.

77. Malet, H.; Egloff, M. P.; Selisko, B.; Butcher, R. E.; Wright, P. J.; Roberts, M.; Gruez, A.; Sulzenbacher, G.; Vonrhein, C.; Bricogne, G.; Mackenzie, J. M.; Khromykh, A. A.; Davidson, A. D.; Canard, B., Crystal structure of the RNA polymerase domain of the West Nile virus non-structural protein 5. *J. Biol. Chem.* **2007,** *282*, 10678-10689.

78. Zhou, Y.; Ray, D.; Zhao, Y.; Dong, H.; Ren, S.; Li, Z.; Guo, Y.; Bernard, K. A.; Shi, P. Y.; Li, H., Structure and function of flavivirus NS5 methyltransferase. *J. Virol.* **2007,** *81*, 3891-3903.

79. Chappell, K. J.; Stoermer, M. J.; Fairlie, D. P.; Young, P. R., Insights to Substrate Binding and Processing by West Nile Virus NS3 Protease through Combined Modeling, Protease Mutagenesis, and Kinetic Studies. *J. Biol. Chem.* **2006,** *281*, 38448-38458.

80. Ganesh, V. K.; Muller, N.; Judge, K.; Luan, C. H.; Padmanabhan, R.; Murthy, K. H. M., Identification and characterization of nonsubstrate based inhibitors of the essential dengue and West Nile virus proteases. *Bioorg. Med. Chem.* **2005,** *13*, 257-264.

81. Ekonomiuk, D.; Su, X. C.; Ozawa, K.; Bodenreider, C.; Lim, S. P.; Yin, Z.; Keller, T. H.; Beer, D.; Patel, V.; Otting, G.; Caflisch, A.; Huang, D., Discovery of a Non-Peptidic Inhibitor of West Nile Virus NS3 Protease by High-Throughput Docking. *PLoS Neg.l Trop. Dis.* **2009,** *3*, e356.

82. Luzhkov, V. B.; Selisko, B.; Nordqvist, A.; Peyrane, F.; Decroly, E.; Alvarez, K.; Karlen, A.; Canard, B.; Qvist, J., Virtual screening and bioassay study of novel inhibitors for dengue virus mRNA cap (nucleoside-2'O)-methyltransferase. *Bioorg. Med. Chem.* **2007,** *15*, 7795-7802.

83. Dong, H.; Zhang, B.; Shi, P. Y., Flavivirus methyltransferase: A novel antiviral target. *Antiviral Res.* **2008,** *80*, 1-10.

84. Mueller, N. H.; Yon, C.; Ganesh, V. K.; Padmanabhan, R., Characterization of the West Nile virus protease substrate specificity and inhibitors. *Int. J. Biochem. Cell Biol.* **2007,** *39*, 606-614.

85. Yusof, R.; Clum, S.; Wetzel, M.; Murthy, H. M.; Padmanabhan, R., Purified NS2B/NS3 serine protease of dengue virus type 2 exhibits cofactor NS2B dependence for cleavage of substrates with dibasic amino acids *in vitro*. *J. Biol. Chem.* **2000,** *275*, 9963-9969.

86. Jordan, I.; Briese, T.; Fischer, N.; Lau, J. Y. N.; Lipkin, W. I., Ribavirin Inhibits West Nile Virus Replication and Cytopathic Effect in Neural Cells. *J. Infect. Dis.* **2000,** *182*, 1214-1217.

87. Shi, P. Y.; Kauffman, E. B.; Ren, P.; Felton, A.; Tai, J. H.; Dupuis, A. P.; Jones, S. A.; Ngo, K. A.; Nicholas, D. C.; Maffei, J.; Ebel, G. D.; Bernard, K. A.; Kramer, L. D., High-Throughput Detection of West Nile Virus RNA. *J. Clin. Microbiol.* **2001,** *39*, 1264-1271.

88. Leung, D.; Schroder, K.; White, H.; Fang, N. X.; Stoermer, M. J.; Abbenante, G.; Martin, J. L.; Young, P. R.; Fairlie, D. P., Activity of recombinant dengue 2 virus NS3 protease in the presence of a truncated NS2B co-factor, small peptide substrates, and inhibitors. *J. Biol. Chem.* **2001,** *276*, 45762-45771.

89. Leung, D.; Schroder, K.; White, H.; Fang, N. X.; Stoermer, M. J.; Abbenante, G.; Martin, J. L.; Young, P. R.; Fairlie, D. P., Activity of Recombinant Dengue 2 Virus NS3 Protease in the Presence of a Truncated NS2B Co-factor, Small Peptide Substrates, and Inhibitors. *J. Biol. Chem.* **2001,** *276*, 45762-45771.

90. Knox, J. E.; Ma, N. L.; Yin, Z.; Patel, S. J.; Wang, W. L.; Chan, W. L.; Ranga Rao, K. R.; Wang, G.; Ngew, X.; Patel, V.; Beer, D.; Lim, S. P.; Vasudevan, S. G.; Keller, T. H., Peptide Inhibitors of West Nile NS3 Protease: SAR Study of Tetrapeptide Aldehyde Inhibitors. *J. Med. Chem.* **2006,** *49*, 6585-6590.

91. Stoermer, M. J.; Chappell, K. J.; Liebscher, S.; Jensen, C. M.; Gan, C. H.; Gupta, P. K.; Xu, W. J.; Young, P. R.; Fairlie, D. P., Potent Cationic Inhibitors of West Nile Virus NS2B/NS3 Protease With Serum Stability, Cell Permeability and Antiviral Activity. *J. Med. Chem.* **2008,** *51*, 5714-5721.

92. Shiryaev, S. A.; Ratnikov, B. I.; Chekanov, A. V.; Sikora, S.; Rozanov, D. V.; Godzik, A.; Wang, J.; Smith, J. W.; Huang, Z.; Lindberg, I.; Samuel, M. A.; Diamond, M. S.; Strongin, A. Y., Cleavage targets and the D-arginine-based inhibitors of the West Nile virus NS3 processing proteinase. *J. Biochem.* **2006,** *393*, 503-511.

93. Lim, H. A.; Joy, J.; Hill, J.; San Brian Chia, C., Novel agmatine and agmatine-like peptidomimetic inhibitors of the West Nile virus NS2B/NS3 serine protease. *Eur. J. Med. Chem.* **2011,** *46*, 3130-3134.

94. Mueller, N. H.; Pattabiraman, N.; Ansarah-Sobrinho, C.; Viswanathan, P.; Pierson, T. C.; Padmanabhan, R., Identification and Biochemical Characterization of Small-Molecule Inhibitors of West Nile Virus Serine Protease by a High-Throughput Screen. *Antimicrob. Agents Chemother.* **2008,** *52*, 3385-3393.

95. Lipinski, C. A., Lead- and drug-like compounds: the rule-of-five revolution. *Drug Discovery Today: Technol.* **2004,** *1*, 337-341.

96. Ezgimen, M.; Lai, H.; Mueller, N. H.; Lee, K.; Cuny, G.; Ostrov, D. A.; Padmanabhan, R., Characterization of the 8-hydroxyquinoline scaffold for inhibitors of West Nile virus serine protease. *Antiviral Res.* **2012,** *94*, 18-24.

97. Dou, D.; Viwanathan, P.; Li, Y.; He, G.; Alliston, K. R.; Lushington, G. H.; Brown-Clay, J. D.; Padmanabhan, R.; Groutas, W. C., Design, Synthesis, and *In Vitro* Evaluation of Potential West Nile Virus Protease Inhibitors Based on the 1-Oxo-1,2,3,4-tetrahydroisoquinoline and 1-Oxo-1,2-dihydroisoquinoline Scaffolds. *J. Comb. Chem.* **2010,** *12*, 836-843.

98. Johnston, P. A.; Phillips, J.; Shun, T. Y.; Shinde, S.; Lazo, J. S.; Huryn, D. M.; Myers, M. C.; Ratnikov, B. I.; Smith, J. W.; Su, Y.; Dahl, R.; Cosford, N. D.; Shiryaev, S. A.; Strongin, A. Y., HTS identifies novel and specific uncompetitive inhibitors of the two-component NS2B-NS3 proteinase of West Nile virus. *Assay. Drug. Dev. Technol.* **2007,** *5*, 737-750.

99. Sidique, S.; Shiryaev, S. A.; Ratnikov, B. I.; Herath, A.; Su, Y.; Strongin, A. Y.; Cosford, N. D. P., Structure-activity relationship and improved hydrolytic stability of pyrazole derivatives that are allosteric inhibitors of West Nile Virus NS2B-NS3 proteinase. *Bioorg. Med. Chem. Lett.* **2009,** *19*, 5773-5777.

100. Doleschall, G.; Lempert, K., 1,2,4-Triazine und kondensierte derivate-XII : Die reaktion von 3-alkylthio-6-(2-aminophenyl)-1,2,4--triazin-5(2H)-onen mit oxoverbindungen, Schiffschen basen und orthoestern. *Tetrahedron* **1973,** *29*, 639-649.

101. Doleschall, G.; Lempert, K., 1,2,4-triazines and condensed derivatives--XIV : Thermal and acid catalysed degradations of 3-alkylthio-6,7-dihydro-[1.2.4]Triazino[1.6-c]quinazolin-5-ium-1-olates. *Tetrahedron* **1974,** *30*, 3997-4012.

102. Lai, Y.; Ma, L.; Huang, W.; Yu, X.; Zhang, Y.; Ji, H.; Tian, J., Synthesis and biological evaluation of 3-[4-(amino/methylsulfonyl)phenyl]methylene-indolin-2-one derivatives as novel COX-1/2 and 5-LOX inhibitors. *Bioorg. Med. Chem. Lett.* **2010,** *20*, 7349-7353.

103. Polychronopoulos, P.; Magiatis, P.; Skaltsounis, A. L.; Myrianthopoulos, V.; Mikros, E.; Tarricone, A.; Musacchio, A.; Roe, S. M.; Pearl, L.; Leost, M.; Greengard, P.; Meijer, L., Structural Basis for the Synthesis of Indirubins as Potent and Selective Inhibitors of Glycogen Synthase Kinase-3 and Cyclin-Dependent Kinases. *J. Med.Chem.* **2004,** *47*, 935-946.

104. Ma, L. J.; Li, X. X.; Kusuyama, T.; El-Sayed, I. E. T.; Inokuchi, T., Synthetic Access to Poly-Substituted 6-Alkoxyindoles from 1,3-Cyclohexanediones and Nitroolefins through Facile Aromatization Reaction. *J. Org. Chem.* **2009,** *74*, 9218-9221.

105. Radichev, I.; Shiryaev, S. A.; Aleshin, A. E.; Ratnikov, B. I.; Smith, J. W.; Liddington, R. C.; Strongin, A. Y., Structure-based mutagenesis identifies important novel determinants of the NS2B cofactor of the West Nile virus two-component NS2B-NS3 proteinase. *J. Gen. Virol.* **2008,** *89*, 636-641.

106. Shacklady-McAtee, D. M.; Dasgupta, S.; Watson, M. P., Nickel(0)-Catalyzed Cyclization of N-Benzoylaminals for Isoindolinone Synthesis. *Org. Lett.* **2011,** *13*, 3490-3493.

107. Li, L.; Zhu, L.; Chen, D.; Hu, X.; Wang, R., Use of Acylhydrazine- and Acylhydrazone-Type Ligands to Promote CuI-Catalyzed C-N Cross-Coupling Reactions of Aryl Bromides with N-Heterocycles. *Eur. J. Org. Chem.* **2011,** 2692-2696, S2692/1-S2692/34.

108. Rostamizadeh, S.; Mollahoseini, K.; Moghadasi, S., A one-pot synthesis of 4,5-disubstituted-1,2,4-triazole-3-thiones on solid support under microwave irradiation. *Phosphorus, Sulfur Silicon Relat. Elem.* **2006,** *181*, 1839-1845.

109. Rivera, N. R.; Balsells, J.; Hansen, K. B., Synthesis of 2-amino-5-substituted-1,3,4-oxadiazoles using 1,3-dibromo-5,5-dimethylhydantoin as oxidant. *Tetrahedron Lett.* **2006,** *47*, 4889-4891.

110. Smith, A. B.; Savinov, S. N.; Manjappara, U. V.; Chaiken, I. M., Peptide−Small Molecule Hybrids via Orthogonal Deprotection−Chemoselective Conjugation to Cysteine-Anchored Scaffolds. A Model Study. *Org. Lett.* **2002,** *4*, 4041-4044.

111. Smith, A. M. R.; Rzepa, H. S.; White, A. J. P.; Billen, D.; Hii, K. K., Delineating Origins of Stereocontrol in Asymmetric Pd-Catalyzed α-Hydroxylation of 1,3-Ketoesters. *J. Org. Chem.* **2010,** *75*, 3085-3096.

112. Bevan, P. S.; Ellis, G. P., Benzopyrones. Part 19. Synthesis and some reactions of ethyl 3-bromo-4-oxochromen-2-carboxylate. *J. Chem. Soc., Perkin Trans. 1* **1983**, 1705-1709.

113. Clerici, F.; Pocar, D.; Guido, M.; Loche, A.; Perlini, V.; Brufani, M., Synthesis of 2-Amino-5-sulfanyl-1,3,4-thiadiazole Derivatives and Evaluation of Their Antidepressant and Anxiolytic Activity. *J. Med. Chem.* **2001,** *44*, 931-936.

114. Cvetovich, R. J.; DiMichele, L., Formation of Acrylanilides, Acrylamides, and Amides Directly from Carboxylic Acids Using Thionyl Chloride in Dimethylacetamide in the Absence of Bases. *Org. Process Res. Dev.* **2006,** *10*, 944-946.

115. Cui, T.; Chum, M. P.; Lam, Y.; Gao, Y. Compounds for use as anti-viral agents. SG162629A1, **2010**.

116. Ma, K.; Wang, P.; Fu, W.; Wan, X.; Zhou, L.; Chu, Y.; Ye, D., Rational design of 2-pyrrolinones as inhibitors of HIV-1 integrase. *Bioorg. Med. Chem. Lett.* **2011,** *21*, 6724-6727.

117. Zou, D.; Zhai, H. X.; Eckman, J.; Higgins, P.; Gillard, M.; Knerr, L.; Carre, S.; Pasau, P.; Collart, P.; Grassi, J., Novel, Acidic CCR2 Receptor Antagonists: From Hit to Lead. *Lett. Drug Des. Discov.* **2007,** *4*, 185-191.

118. Jourdan, F.; Kaiser, J.; Lowe, D., Synthesis of new N-(2-oxo-2,5-dihydropyrrol-3-yl)glycines and their esters. *Synth. Commun.* **2005,** *35*, 2453-2466.

119. Burlingham, B. T.; Widlanski, T. S., An intuitive look at the relationship of *Ki* and IC_{50}: a more general use of the Dixon plot. *J. Chem. Educ.* **2003,** *80*, 214-218.

Appendix

1) ^{1}H and ^{13}C NMR spectra of 2-1a23

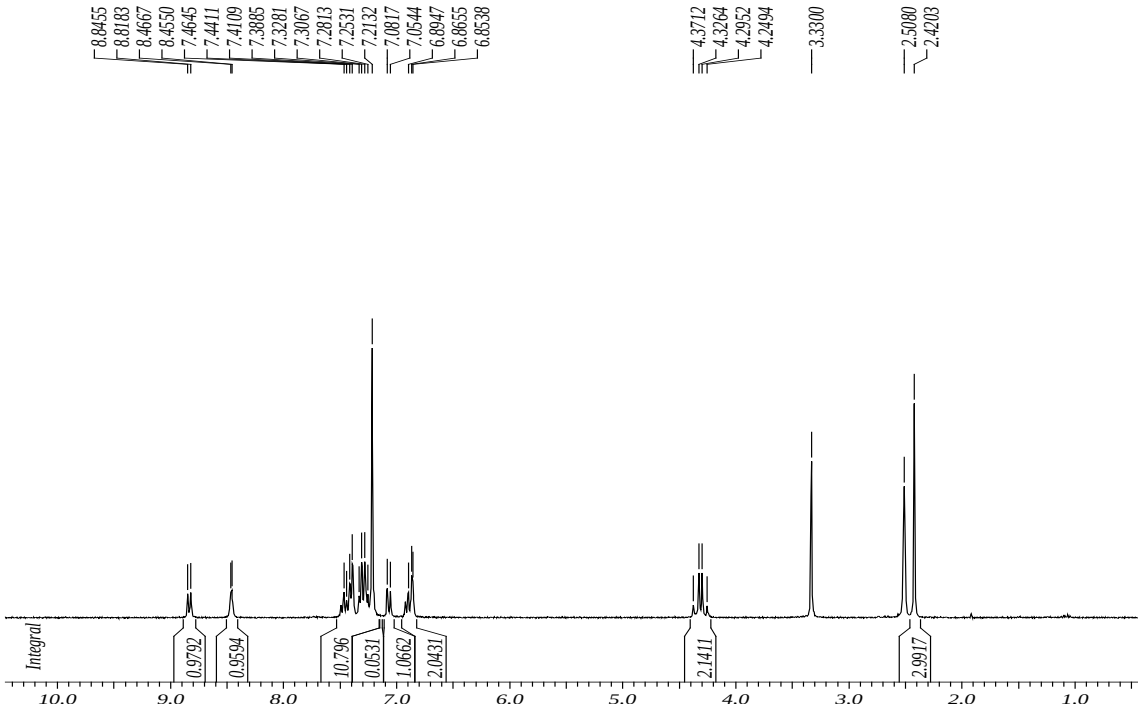

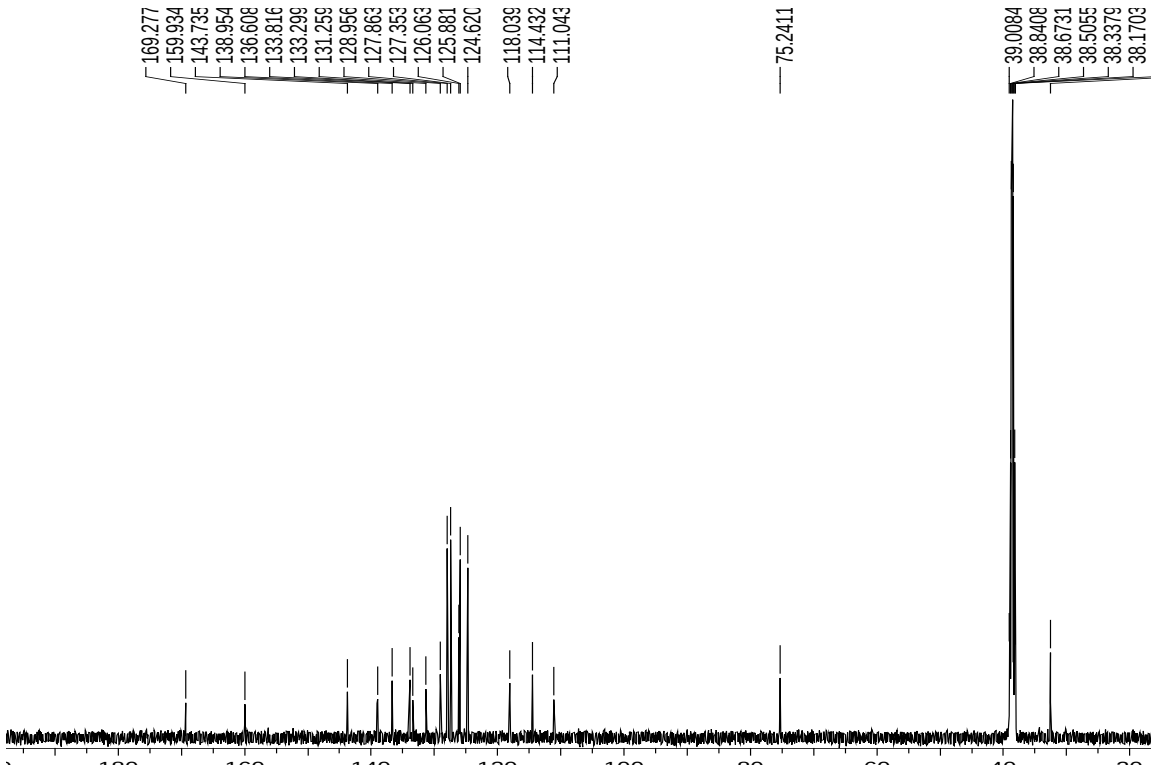

2) ^{1}H and ^{13}C NMR spectra of 2-1a40

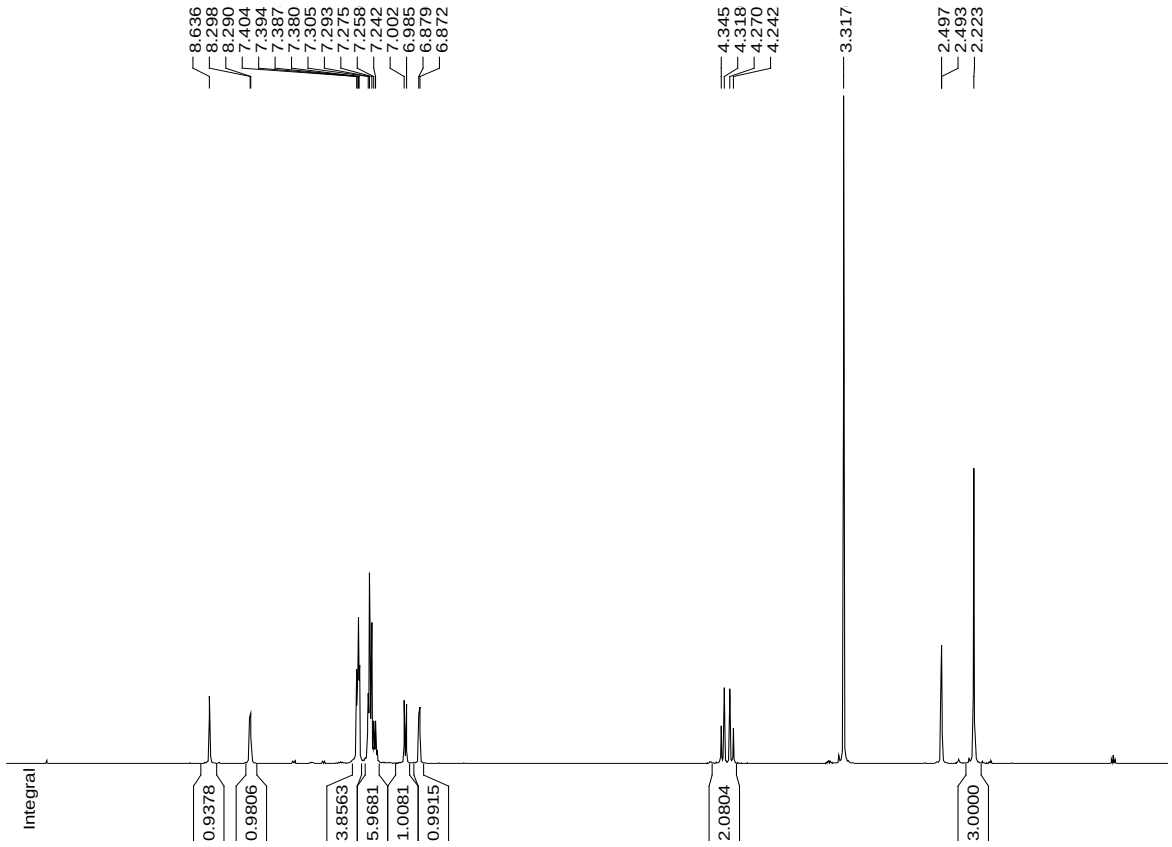

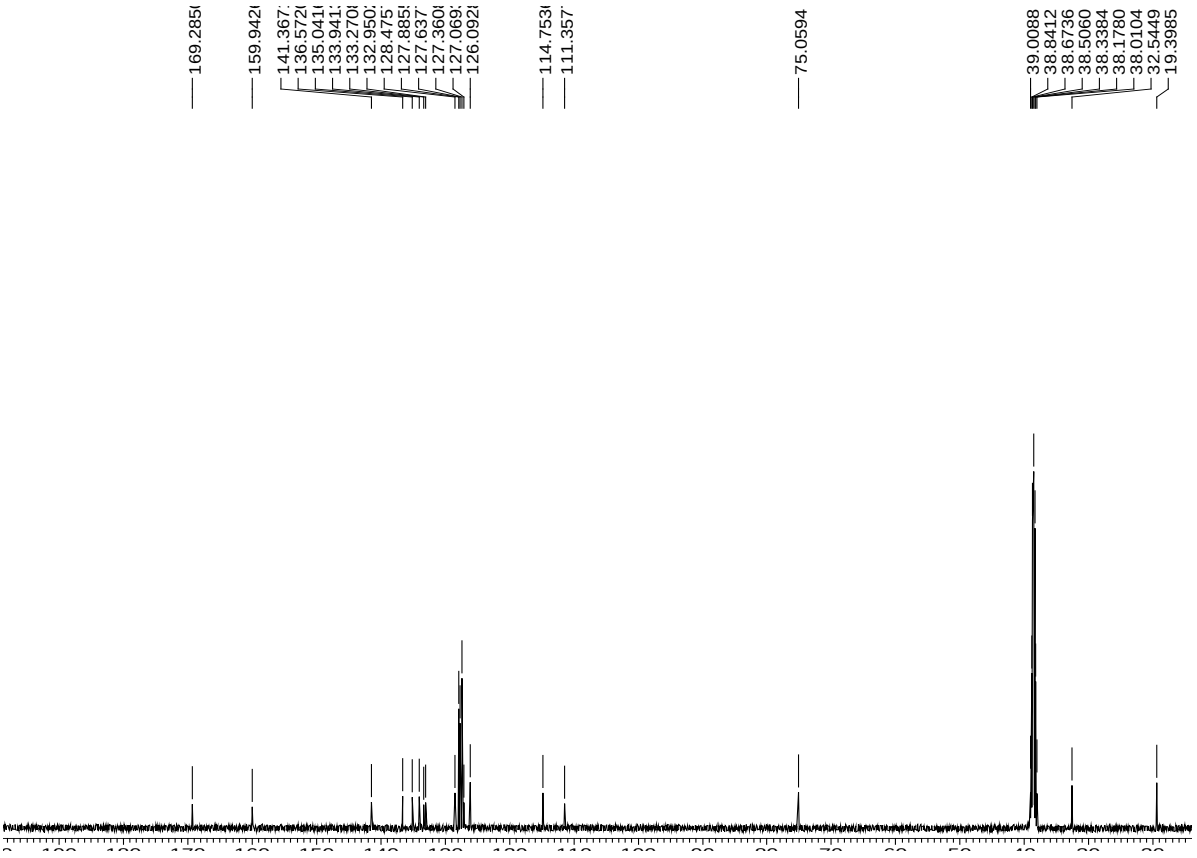

3) ^{1}H and ^{13}C NMR spectra of 2-1a53

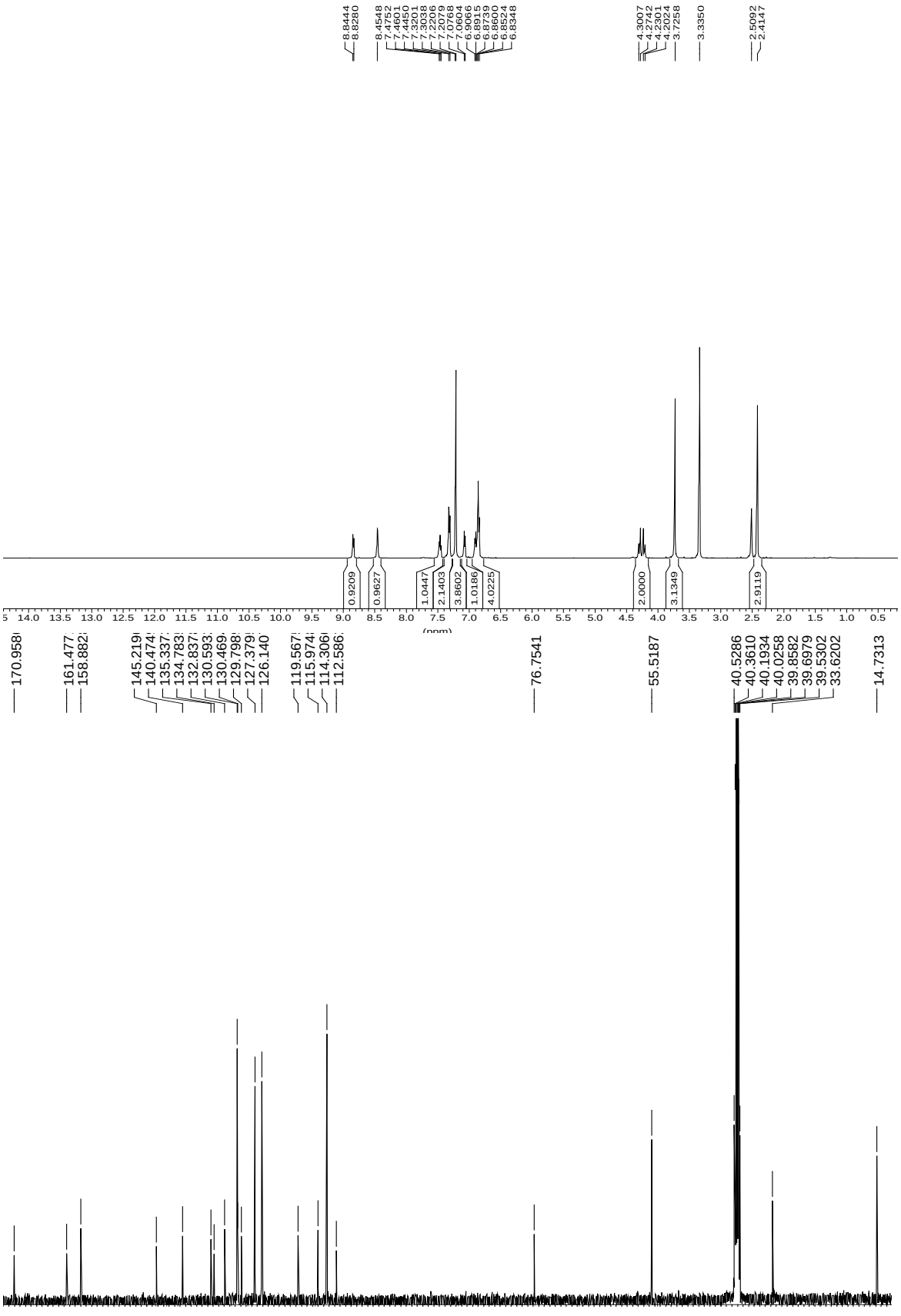

4) ^{1}H and ^{13}C NMR spectra of 3-1a23

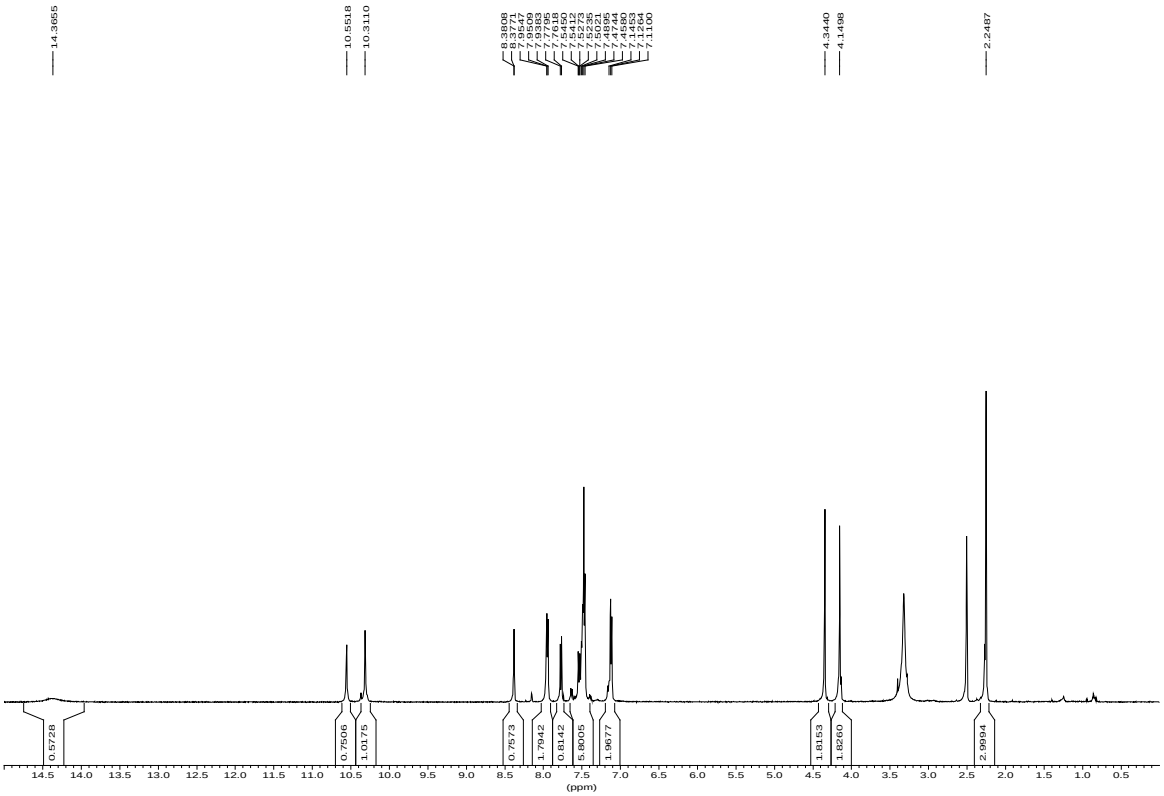

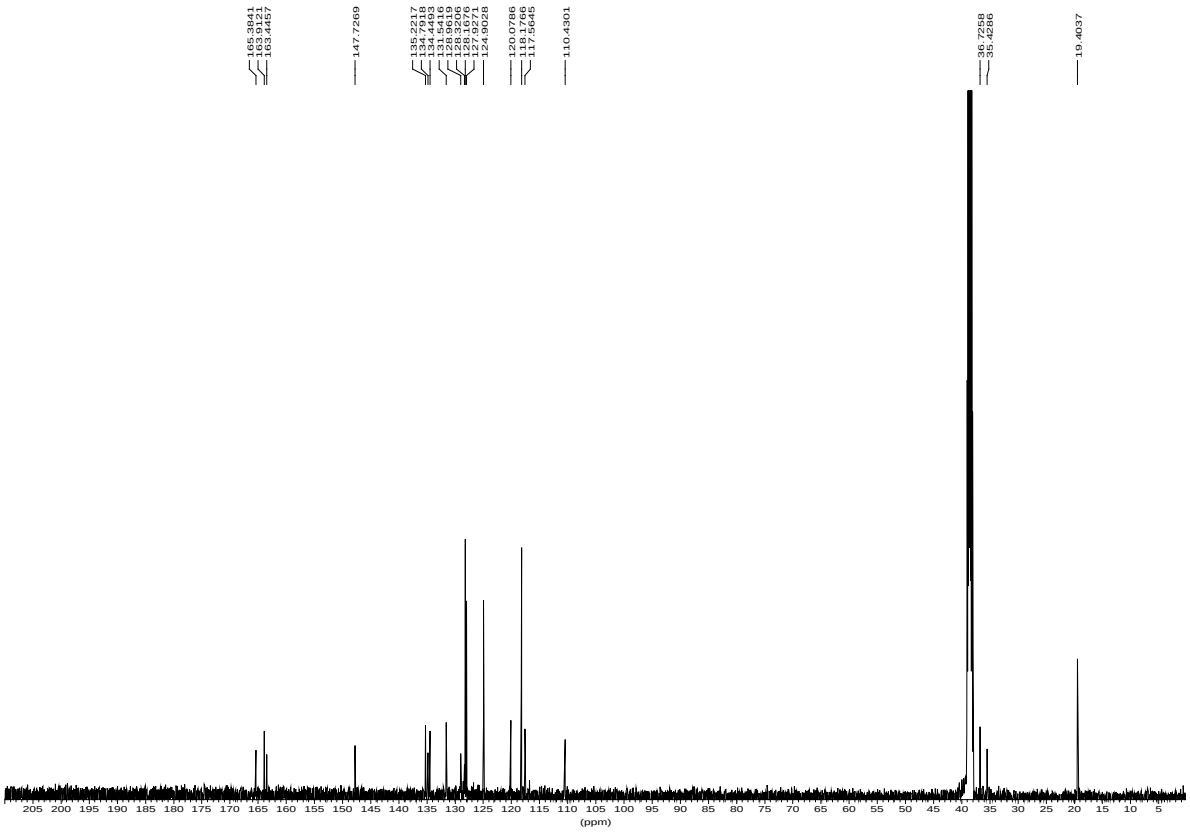

5) ^{1}H and ^{13}C NMR spectra of 3-1a24

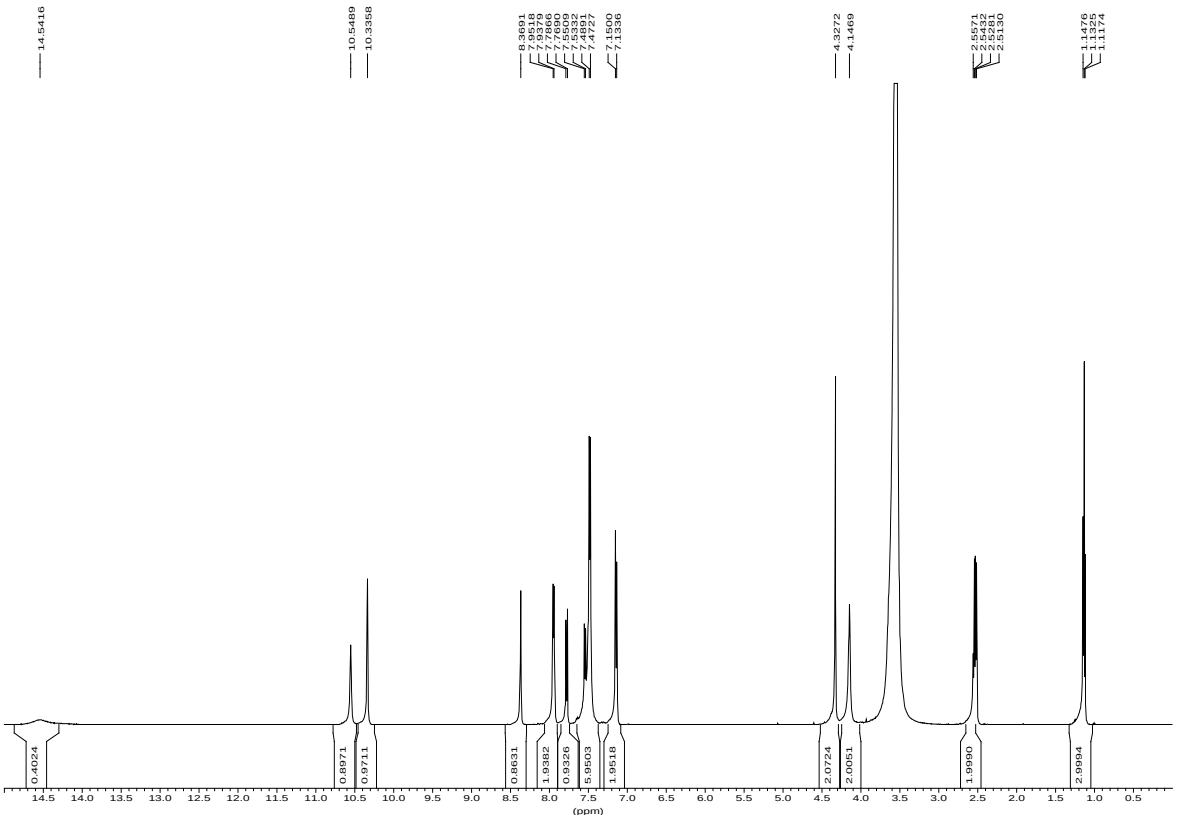

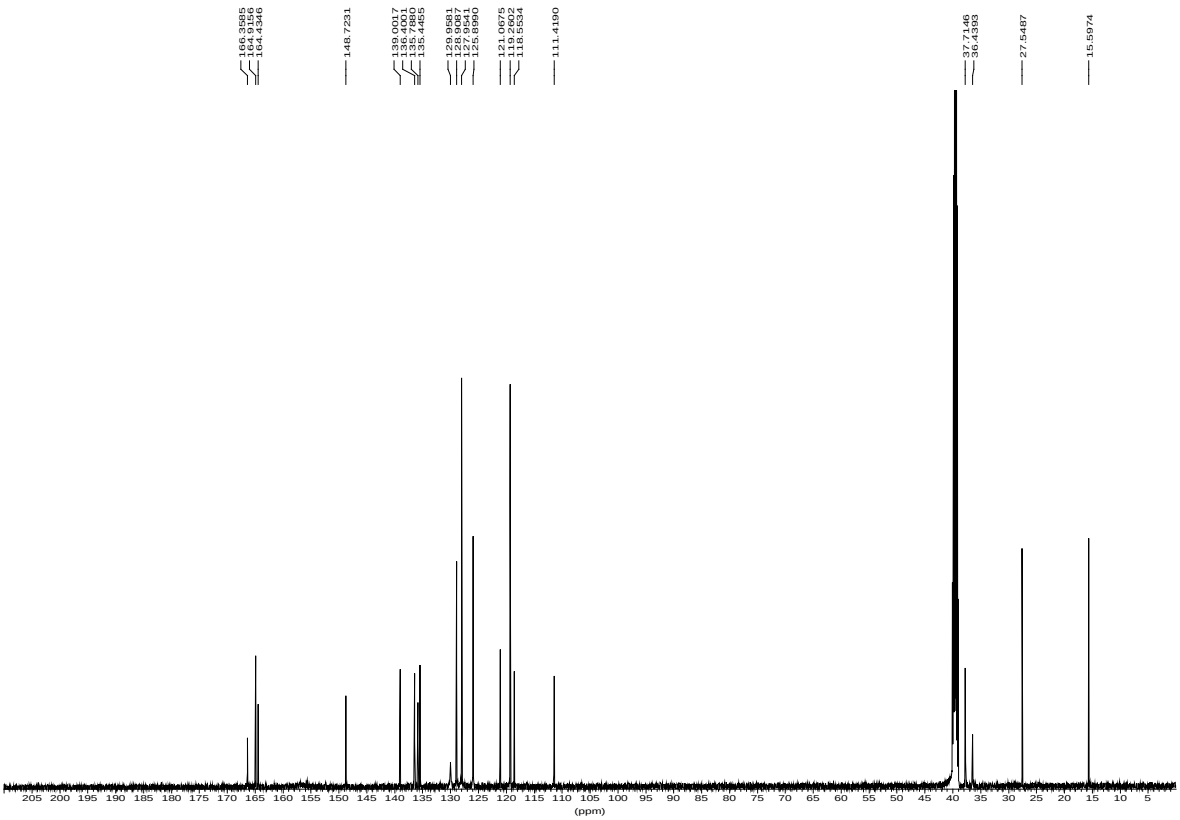

6) ^{1}H and ^{13}C NMR spectra of 3-1a25

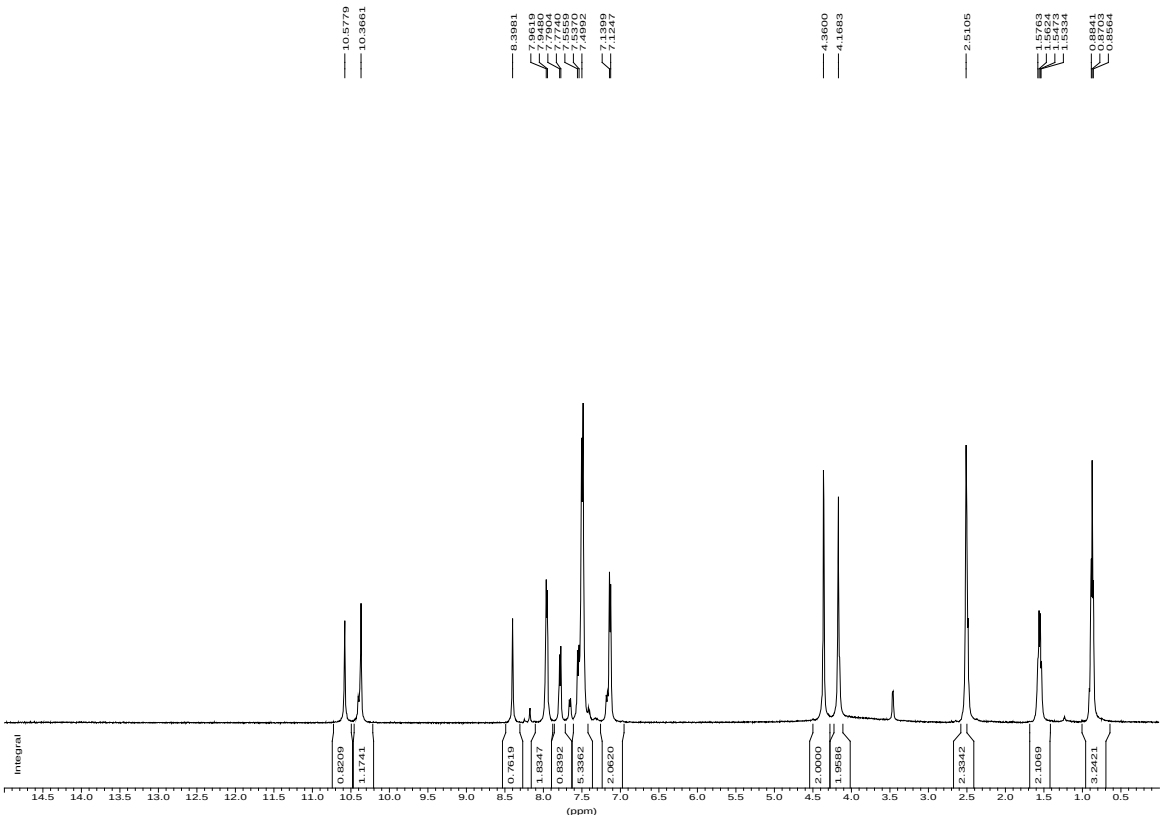

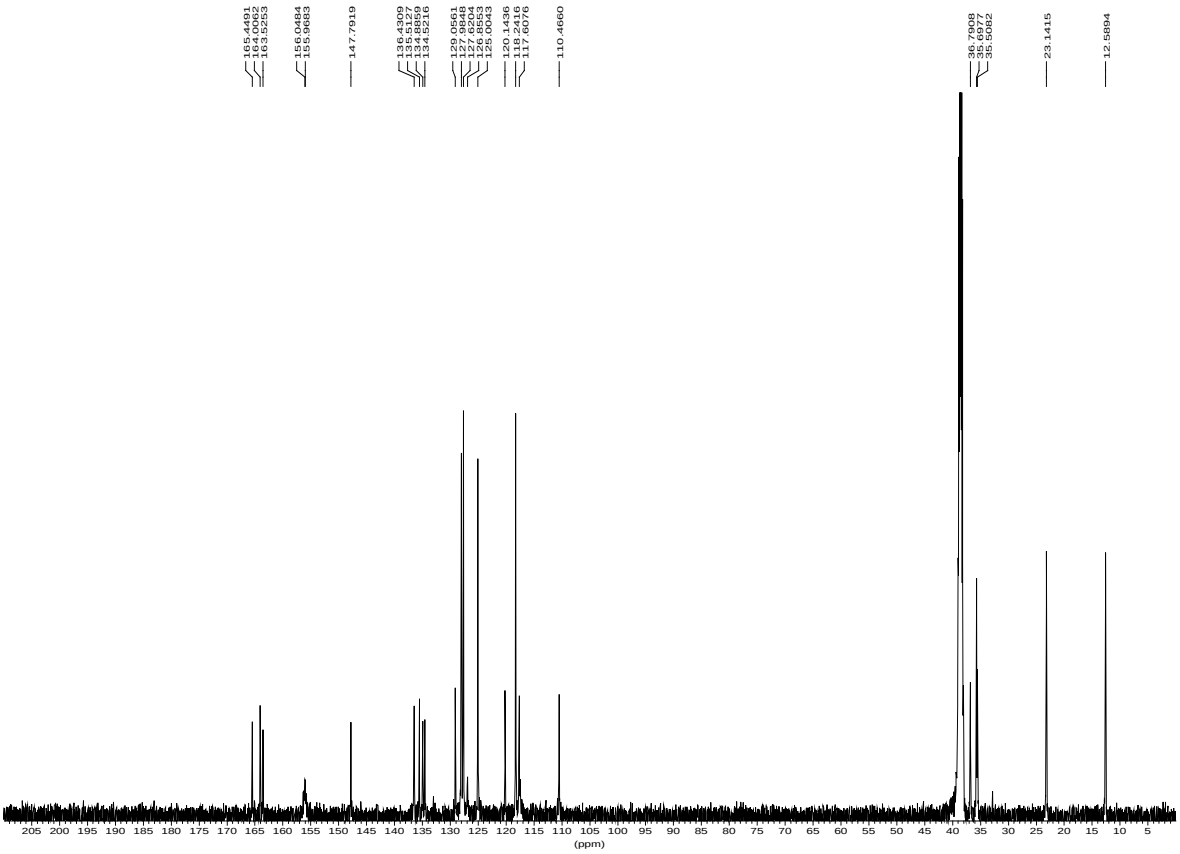

7) ^{1}H and ^{13}C NMR spectra of 3-1a37

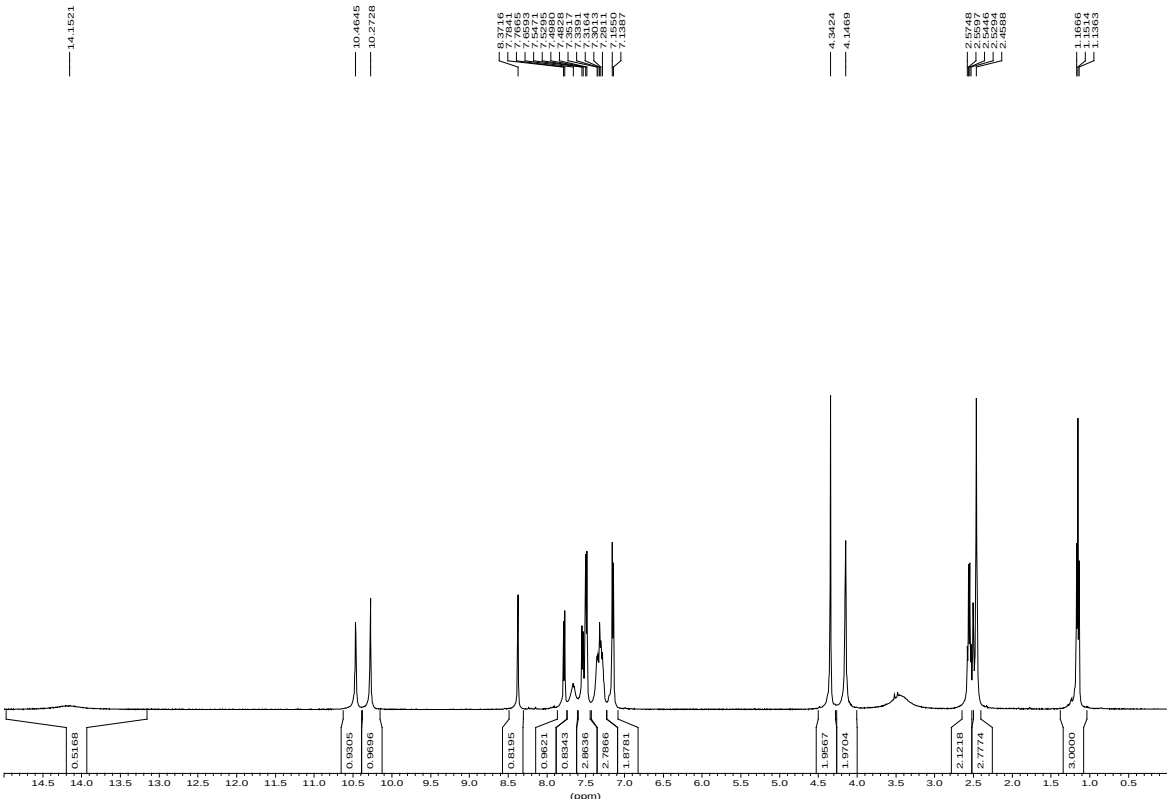

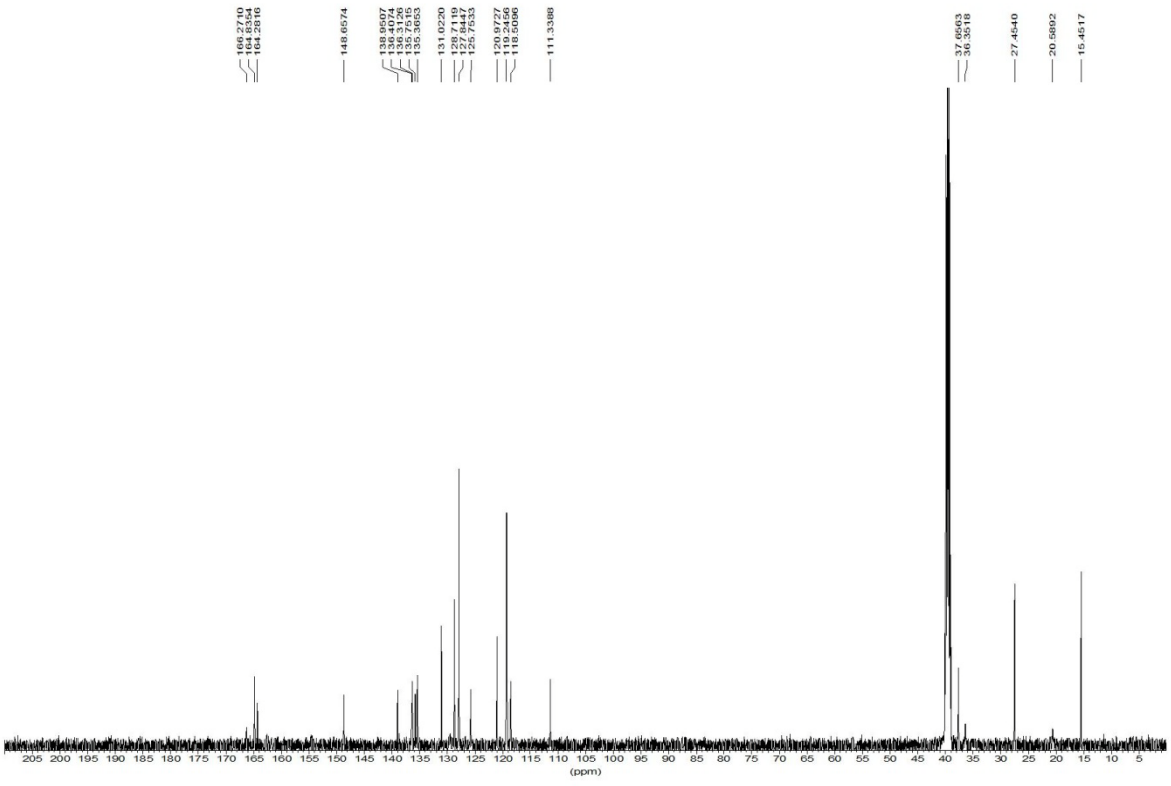

8) ^{1}H and ^{13}C NMR spectra of 4-1a13

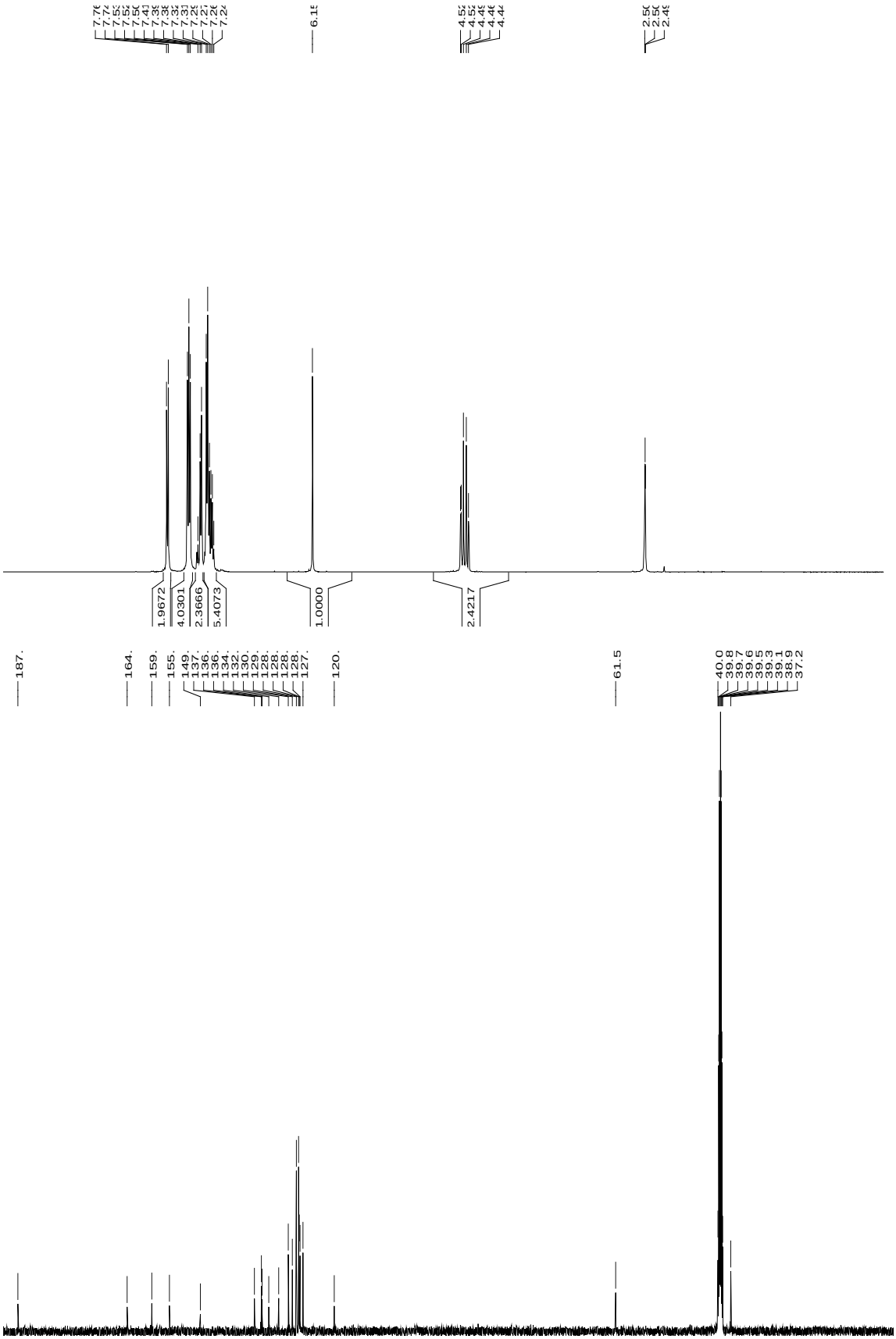

9) ^{1}H and ^{13}C NMR spectra of 4-1a16

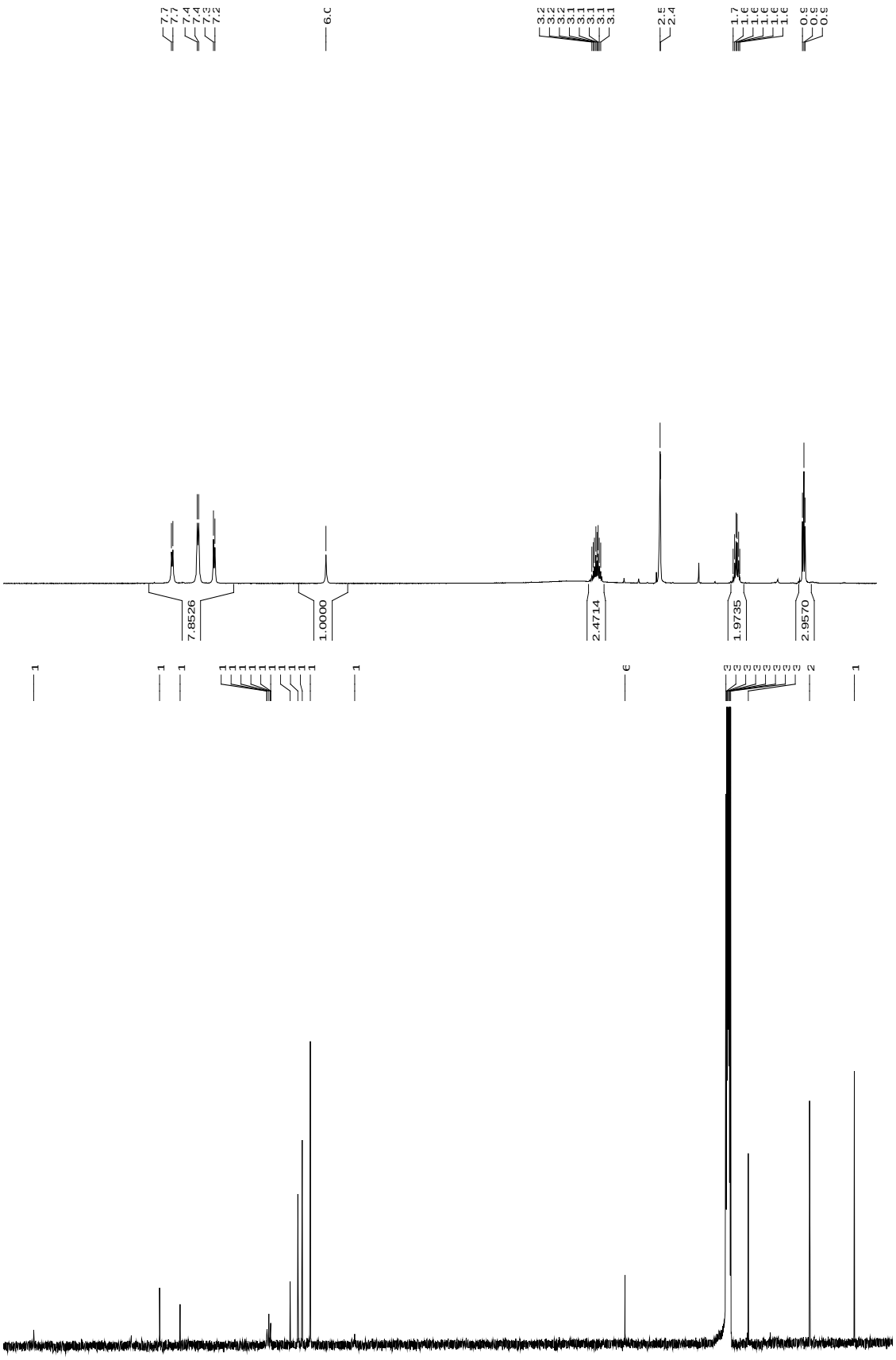

10) ^{1}H and ^{13}C NMR spectra of 4-1a17